VAPOR EXPLOSIONS IN LIGHT WATER REACTORS: A REVIEW OF THEORY AND MODELING

M. L. CORRADINI, B. J. KIM and M. D. OH

University of Wisconsin, Nuclear Engineering Department, Madison, WI 53706-1687, U.S.A.

Abstract - A vapor explosion is a physical event in which a hot liquid (fuel) rapidly fragments and transfers its internal energy to a colder, more volatile liquid (coolant); in so doing, the coolant vaporizes at high pressures and expands, doing work on its surroundings. In present day fission reactors, if complete and prolonged failure of normal and emergency coolant flow occurs, fission product decay heat would cause melting of the reactor materials. In postulated severe accident analyses vapor explosions are considered if this molten "fuel" contacts residual water in-vessel or ex-vessel, because these physical explosions have the potential of contributing to reactor vessel failure and possibly containment failure and release of radioactive fission products. Vapor explosions are also a real concern in industrial processes where a hot fluid can contact a colder volatile fluid, e.g., foundries for aluminum and steel, paper pulping mills, LNG operations. The vapor explosion is commonly divided into four phases of heat transfer: (1) quiescent mixing of fuel and coolant, (2) triggering of the explosion, (3) explosion escalation and propagation, and (4) expansion and work production. This work provides a comprehensive review of vapor explosion theory and modeling in these four areas. Current theories and modeling have led to a better understanding of the overall process, although some specific fundamental issues are either not well understood or require experimental verification of theoretical hypotheses. These key issues include the extent of fuel-coolant mixing under various contact modes, the basic fuel fragmentation mechanism, and the effect of scale on the mixing process coupled to the explosion propagation and efficiency. Current reactor safety concerns with the vapor explosion are reviewed in light of these theories and models.

1. INTRODUCTION

An explosion involves the rapid conversion of energy from one form to another. Before the explosion is initiated, the energy must be stored in a form that exists for some time without significant dissipation of available energy or conversion to other forms of energy, i.e. a metastable state. The explosion may then be triggered when some relatively small amount of activation energy initiates the rapid conversion of the system energy into some form that can do work on the surroundings, e.g., kinetic energy (Fig. 1). In an explosion the usual vehicle for explosion is such a process in which a hot liquid (fuel) transfers its internal energy to a colder, more volatile liquid (coolant); in doing so the coolant vaporizes at high pressures and expands, doing work on its surroundings.

Consider a qualitative description of the mechanistic path by which the stored fuel internal energy is converted to produce work by a high pressure vapor. In a typical vapor explosion when the two liquids first come into contact, the coolant begins to vaporize at the fuel-coolant liquid interface as a vapor film separates the two liquids. The system remains in this nonexplosive metastable state for a delay period ranging from a few milliseconds up to a few seconds. During this time the fuel and coolant liquid intermix due to density and velocity differences as well as vapor production.

Then vapor film destabilization occurs, triggering fuel fragmentation. This rapidly increases the fuel surface area, vaporizing more coolant liquid and increasing the local vapor pressure. This 'explosive" vapor formation spatially propagates throughout the fuel-coolant mixture causing the macroscopic region to become pressurized by the coolant vapor. Subsequently, the high pressure coolant vapor expands against the inertial constraint of the surroundings and the mixture itself. The vapor explosion process is now complete, transforming the fuel internal energy into the kinetic energy of the mixture and its surroundings. This kinetic energy takes two forms. At early stages shock waves can be generated in the fuel-coolant mixture and at later times the overall mixture is accelerated by the expanding coolant vapor. The high pressure vapor produced, the dynamic liquid phase shock waves, and the slug kinetic energy can all do destructive work on the surroundings.

To be more precise the vapor explosion can be considered as a subset of a fuel-coolant interaction in which the timescale for heat transfer between the liquids is smaller than the timescale for pressure wave propagation and expansion in a local region of the fuel-coolant mixture. Therefore, the rise in pressure locally forms a shock wave, which spatially propagates with a velocity which is greater than the characteristic speed of sound in the mixture ahead of the shock front (Mach No. > 1). A significant fraction of the thermal energy initially stored in the fuel could be transferred to the coolant as the fuel is fragmented. The key feature of the vapor explosion is that the shock wave propagation through the mixture directly contributes to the rapid fuel fragmentation and associated heat transfer to the coolant; i.e. analogous to shock heating in a chemical detonation.

A "non-vapor explosion" is a fuel-coolant interaction which does not exhibit these shock wave characteristics. Thus fuel fragmentation is not necessarily linked to shock wave propagation and the rapid boiling phenomena does not spatially propagate on a timescale equal to pressure wave propagation. A large amount of coolant vapor may be produced in this process and the fuel may still become finely fragmented, yet the character of the fuel-coolant interaction is not explosive. One should note that analogous to a deflagration such an event might still be destructive under certain conditions.

In the past (e.g., Board et al., 1976) the vapor explosion process has been conceptually subdivided into these four phases of (1) mixing, (2) triggering, (3) explosion propagation and (4) expansion. These phases can possibly occur in three geometrical arrangements (Fig. 2), (a) fuel pouring into coolant, (b) coolant injected into fuel or (c) fuel and coolant as

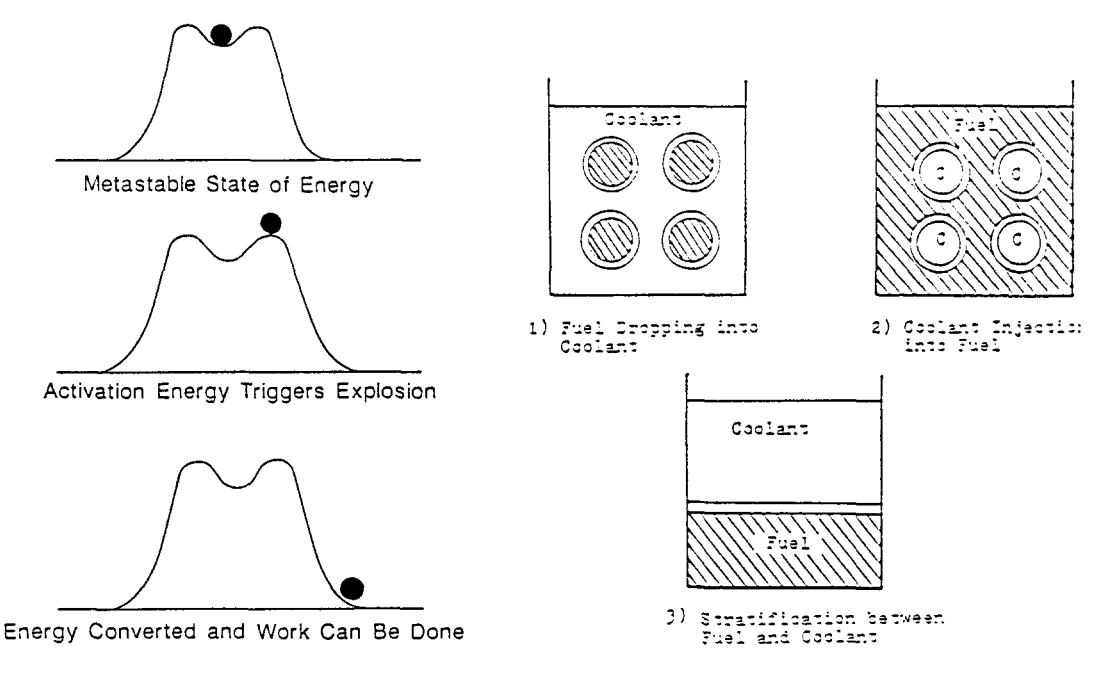


Fig. 1. Conceptual stages of an explosion Fig. 2. Descriptive illustration of fuel-coolant contact modes

stratified layers. Depending on the industrial application any one of these geometrical arrangements may occur. Although the details of these four stages may change with the contact mode, each would be present during the explosion.

The work done on the surroundings can be destructive and this has raised safety questions in a number of industries. Industrial processes which involve hot molten materials (e.g., "fuels" such as steel, aluminum, smelt, slag) have reported a number of accidents in which hot material inadvertently mixes with water (coolant) and a vapor explosion results causing structural damage to the plant, injuries and sometimes fatalities to workers (e.g., P. Hess and K. Brondyke, 1969; W. Nelson and E.H. Kennedy, 1956; H. Tetzner, 1959). These vapor explosions can be especially damaging because the fuel may be metallic and chemically reactive with the coolant Because of this possibility the fuel may exothermically react with the coolant causing the subsequent energy release and formation of high pressure coolant vapor to be larger and the subsequent expansion blast wave to be more destructive. In certain accidents it is felt the triggering and propagation are affected by these chemical reactions.

The transport of liquified natural gas (LNG) has raised safety questions. If an LNG spill occurs on water (fuel), the LNG (coolant) may become involved in a vapor explosion between these stratified liquid layers, which would vaporize and disperse the natural gas in the surrounding air. The concern is not only the work potential from the vapor explosion, but also the possible ignition and combustion of the vaporized natural gas mixed with the air (T. Enger, 1972).

In certain volcanic activity where water is present it is believed that the energetic release that accompanies such geophysical events is related to hydromagnetic volcanic eruptions in which water and the hot magma come into contact and a vapor explosion occurs; rapidly fragmenting and quenching the hot magma (Wohletz, 1984). In this situation the major interest is the destructive work potential that might be derived from the water and molten magma coming into contact.

In some combustion designs it has been proposed that water be emulsified with the fuel and injected into the combustion chamber. Upon injection the fuel-water droplets will heat up in the surrounding air. The water heats up beyond its boiling point and explosively vaporizes, fragmenting the fuel (F.L. Dryer, 1976) it is mixed with. This small-scale vapor explosion rapidly fragments the fuel to very small sizes causing the subsequent fuel combustion to be more complete, reducing unwanted pollutants.

In present day nuclear fission reactors if complete and prolonged failure of normal and emergency coolant flow occurs fission product decay heat could cause melting of the reactor fuel. If a sufficiently large mass of molten fuel mixes with the coolant and a vapor explosion results, the subsequent vapor expansion might cause a breach in the containment of the radioactive fission products by dynamic or static pressurization or missile generation caused by the slug kinetic energy. These radioactive fission products could then be released to the environment threatening the safety of the general public. Although this type of severe accident is considered remote, the health consequences are large enough that it is considered in safety studies. In fact vapor explosions have occurred in accidents and destructive tests involving experimental reactors (e.g., W.E. Loewe, 1958; R.W. Miller, 1964). A comprehensive risk assessment effort in the Reactor Safety Study, WASH-1400 (1975), was the first study to estimate the likelihood of this event and its effect on a power reactor. The major concern from the vapor explosion was determined to be a direct failure of the containment caused by missile generation (designated alpha-mode failure). Since the accident at Three Mile Island, a number of investigators (e.g., Theofanous et al., 1986; Corradini et al., 1979, 1981a, b; Fauske et al., 1981; W. Bohl et al., 1986) have reexamined this phenomenon as applied to reactor safety. This research is motivated by this application and research in this area is continuing.

In this work we review the important basic theoretical concepts of the fundamental understanding of the vapor explosion. To aid in this review we examine the individual phases of the vapor explosion and the key models proposed for each phase: Section 2 - fuel-coolant mixing, Section 3 - fuel fragmentation and triggering, Section 4 - explosion propagation and expansion. Finally, we briefly review the application of these theories and models to the current assessment of containment failure (i.e., alpha-mode failure) in a core melt accident in a light water reactor. For a more detailed discussion of this specific application the reader is referred to the Steam Explosion Expert Review Group Report (see Steam Explosion Review Group, Ginsberg et al., 1985) and associated detailed reactor studies on this issue (e.g., Berman et al., 1984; et al., 1986; Swenson et al., 1981: Theofanous et al., 1986).

This review of vapor explosion theories and models is based on the following four criteria:

a) For each complete model, what approximations (assumptions, simplifications) are made and how

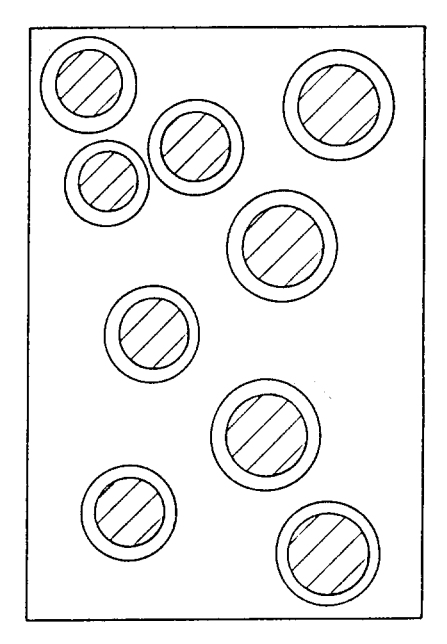
may they affect the models' results?

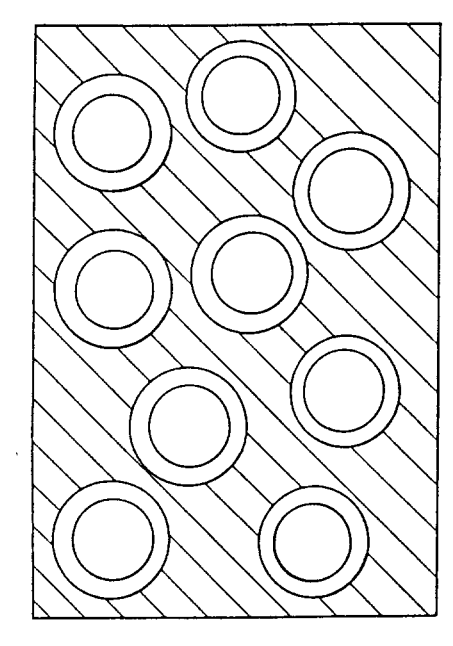
- b) What is the range of validity for each model and what are its inherent limitations that may affect the results compared to experimental data?
- c) In comparing models for describing the same phenomenon what are the areas of commonality and difference, and can these differences be resolved?
- d) Given these models what is their applicability to the reactor situation, and can they be made more applicable?

Throughout this review the models are contrasted with available data to help in determining their usefulness and limitations in regard to the stated criteria.

2. MIXING

The concept of mixing is vague and not well-defined. Qualitatively it could be described as the condition where the fuel and coolant liquids disperse within one another (e.g., discrete fuel liquid surrounded by continuous coolant liquid or vice versa, Fig. 3) as





(a) Fuel within coolant liquid

(b) Coolant with fuel liquid

Fig. 3. Conceptual pictures of fuel-coolant mixing

the heat transfer rate remains relatively small (e.g., film boiling). The importance of this mixing process is that the fuel-coolant system remains in this nonexplosive metastable state for a dwell time which allows for the fuel-coolant exposed surface area to increase. If this area can be allowed to increase in this quiescent period and still maintain the fuel and coolant liquids in close proximity (i.e., without fluidization, Fig. 3) the subsequent explosion could become more efficient. In the following discussion we describe models which primarily consider the contact mode of fuel pouring into the coolant, therefore Fig. 2.a is more applicable for current safety issues. In general this does not have to be the case.

One should note that this qualitative description of mixing as shown in Fig. 2 has not included the case of discrete fuel and coolant liquid masses dispersed in a continuous vapor phase. The reason is that it is not clear that such a geometry can sustain an explosion because (1) such a geometry implies that the liquids have been fluidized and would not remain in a local mixture region (e.g., see Fauske, 1981), and (2) this dispersed mixture would be very difficult to pressurize from the fuel-coolant heat transfer during the interaction, because the vapor produced could be relieved from the mixture to the surroundings (i.e., no inertial constraint). Therefore, a fuel-coolant interaction might occur in this geometry, but it would not be explosive in nature. These points are detailed in the following discussion.

Past research into mixing (sometimes called premixing or coarse-mixing) has focused on understanding the transient fluid dynamics and heat transfer between fuel and coolant in the absence of the explosion, and on predicting the physical limits for which mixing can occur.

Fauske (1974) and Henry and Fauske (1976) originally proposed that the fuel/coolant interface temperature upon liquid-liquid contact must exceed the spontaneous nucleation temperature to allow premixing of the fuel and coolant in a vapor explosion. The spontaneous nucleation temperature is equal to the homogeneous nucleation temperature for a perfectly wetted system (see Sections 3 and 4 for a detailed discussion of the spontaneous nucleation temperature and theory). The physical picture was that stable film boiling is established above this limit for a liquid-liquid system, and this allows the fuel time to penetrate and mix within the coolant. For light water reactor safety issues and most industrial applications involving water, the fuel and coolant easily satisfy this criterion. Thus the criterion is a necessary but not a sufficient criterion for premixing.

Cho et al. (1976) considered the energy requirements for fuel fragmentation for both the premixing phase and the rapid fuel fragmentation phase during a steam explosion. The analysis indicated that the fuel during fragmentation must overcome surface energy, kinetic energy, and frictional dissipation to break up to smaller diameters and mix with the surrounding coolant. In situations of practical interest, Cho pointed out that the mixing energy requirements are primarily due to frictional dissipation, and other contributions may be ignored. They then derived two models to estimate this mixing. The physical picture considered was similar to Fig. 3a although one could derive it for the other case. If the fuel mass were to be mixed in one step with the surrounding coolant, the required mixing energy

$$E_{m \mid one \ step} = \frac{3}{8} C_{D} \frac{\rho V_{f}^{2}}{t_{m}^{2} R_{f}} , \qquad (1)$$

where:

was given by

 V_f = initial volume of the fuel mass to be mixed

p = average density of the surrounding fluid

 $\begin{array}{l} t_m = \mbox{mixing time} \\ C_D = \mbox{local drag coefficient} \\ R_f = \mbox{final radius of the fuel after mixing has occurred.} \end{array}$

If the fuel mass were to be mixed in a series of progressive mixing steps so as to minimize the required mixing energy, the resultant expression was

$$E_{m|min} = 1.81 C_{D} \rho V_{f} \left(1 - \frac{V_{f}^{2/3}}{t_{-}^{2}}\right) \left(\frac{R_{f}^{2}}{V_{f}^{2/3}}\right) \ln \left(\frac{V_{f}^{1/3}}{R_{f}}\right). \tag{2}$$

In a sense these two models bound the amount of energy required for fuel-coolant mixing.

The two major assumptions of the model were that the density of the coolant (vapor and liquid) remained constant through the mixing process and that one had some prior knowledge of initial fuel size and its final size after mixing. Given that this model was the first attempt to quantitatively estimate the energy requirements for mixing the assumptions seem reasonable. However, the analysis is limited to a parametric assessment of mixing energy requirements because one must always specify the initial and final fuel sizes (i.e., $R_{\rm f}$), and the environmental conditions surrounding the fuel.

One also notes that the difference in these two estimates is essentially proportional to the ratio of the final fuel radius to its initial size

$$\frac{E_{m}|_{\min n}}{E_{m}|_{\text{one step}}} = \frac{R_{f}}{V_{f}^{1/3}} \ln \left(\frac{V_{f}^{1/3}}{R_{f}} \right) . \tag{3}$$

and can be large if the ratio of the final fuel radius to the initial volume is small. From this analysis, Cho et al. made the following observations. First, the mixing energy required for fuel fragmentation must be considered in relation to the ultimate source of energy in this system, i.e. the internal energy of the fuel, E_{f0} . For the fuel/coolant system, one requires $E_{m} < E_{f0}$. Second, for a given mixing energy, Eqs. (1) and (2) define the maximum volume of fuel that could mix with coolant as a function of t_{m} and R_{f} . For light water reactor safety issues, the energy for premixing E_{m} is very small compared to the internal energy of the fuel E_{f0} , since film boiling exists between the fuel and coolant liquids. This allows for larger t_{m} and smaller

Two mixing analysis concepts were developed at about the same time in the course of the probabilistic risk assessment for the Zion nuclear power plant. They are based on two different, but not mutually exclusive points of view. The model of Henry and Fauske (1981a) assumes that the fuel is premixed with water (Fig. 3a) and considers the physical limitations to the mass of fuel and its diameter that can exist in such a configuration without liquid fluidization. Theofanous et al. (1982) assumed that the molten fuel enters a coolant pool (Fig. 4) as a jet of arbitrary diameter and considers limitations to mixing due to the hydrodynamics of the jet breakup process. Subsequently Corradini et al. (1982, 1983, 1985, 1986) and Bankoff, et al. (1984a, b) have refined these concepts and considered them to be mutually complementary. Each of these original concepts and associated further developments are discussed below.

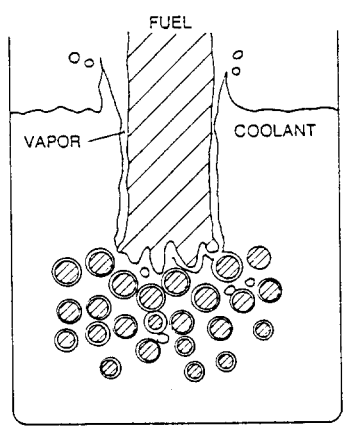


Fig. 4. Conceptual picture of fuel jet into coolant pool

2.1. Fluidization Limits

Henry and Fauske (1981a, b) proposed the physical concept that for the fuel to exist in a premixed configuration with the coolant, the conceptual picture of Fig. 3a must be achieved and sustained. If this configuration breaks down, one would revert to a situation where fuel and coolant droplets are in a continuum of vapor as the vapor drives the coolant away from the molten fuel by fluidization. Discrete fuel particles would coalesce into larger particles and reverse the fragmentation mixing process. Therefore, the film boiling heat flux can be equated to the capability of the water to stay mixed with fuel under the imposed steam flow. Henry and Fauske estimated this capability from the pool boiling critical heat flux (CHF). They equated the energy lost by the fuel with the maximum energy that could be removed by the steam flow (i.e., $q_{\mathrm{CHF}}^{\mathrm{c}}$) and estimated the minimum fuel diameter during mixing D_{min} , below which the steam flow would fluidize and drive the coolant out of the mixture.

$$D_{\min n} = \frac{6 \, m_f q_{\text{drop}}^n}{\rho_f^A_{\text{cham}} q_{\text{CHF}}^n} , \tag{4}$$

where: m_f = fuel mass in the mixture

Acham = cross-sectional area of the chamber of the density

 $q_{d\,rop}^h$ = heat flux from the fuel droplet given by blackbody radiation and film boiling heat transfer.

We have

$$q_{drop}^{"} = \sigma_{T}(T_{f}^{4} - T_{sat}^{4}) + h_{film}(T_{f} - T_{sat})$$
, (5)

where: I_f = fuel temperature

 T_{sat}^T = coolant saturation temperature σ_T = Stephan-Boltzmann constant

hfilm = film boiling heat transfer coefficient.

Henry and Fauske also pointed out that this steady-state model can be used to estimate the maximum mass of fuel that could mix with the water coolant assuming some premixing diameter, D_{mix} :

$$m_{f_{max}} = \frac{{}^{\rho} f^{A} cham^{D} mi x^{q} \ddot{C} HF}{6 q^{d}_{q} rop}.$$
 (6)

For in-vessel reactor safety considerations [pressurized water reactor (PWR) specifically], Henry and Fauske point out that no more than 100 kg of fuel could mix with the water coolant for saturated water at a pressure of 1 bar and $D_{\rm mix} = 10$ mm. The assumption that a one-dimensional steady-state CHF model is applicable under these conditions deserves further discussion.

The model prediction that only a minuscule fuel mass, 100 kg, can mix to a small fuel diameter, 10 mm (or conversely a large fuel mass mixed, 10,000 kg, implies an enormous fuel mixing diameter, 1 m), is due to two fundamental assumptions. First, the model assumes that the coolant liquid entering the mixture is entering from above in countercurrent flow to the coolant vapor being generated, and second that this countercurrent flooding phenomenon can be predicted by the pool boiling CHF limit. For a contact mode of fuel pouring into a coolant pool the more realistic case is the fuel falls from above as the coolant liquid enters from below with the vapor generated flowing out through the top of the pool. The concept of coolant liquid fluidization is quite reasonable although the model was simplified to be one-dimensional and steady-state. In the real world situation the fuel entry in a coolant pool would be multidimensional (Fig. 2) and transient with the coolant entering the mixture from the sides as well as below, and the fuel mass breaking up as time progresses. The fuel breakup will also allow for fuel fluidization as well as coolant liquid.

Corradini et al. (1985) subsequently used the same concept of coolant fluidization as suggested by Fauske under one-dimensional steady-state conditions, but corrected for the two assumptions previously mentioned. In the analysis one calculates the mass of fuel that could mix with a given mass of coolant up to the point of coolant fluidization or fuel fluidization given a fuel mixing diameter. By using a first principles fluidization model instead of the pool boiling CHF heat transfer limit one must consider coolant droplet breakup during fluidization. Therefore, there is a range of values for the fuel mass mixed that one could calculate given a fuel mixing diameter. The coolant droplet diameter would range from the initial to the final diameter stable under Weber breakup considerations. The results of the analysis (Fig. 5) indicated for the light water reactor application a range of fuel masses as mixed with coolant from 1000-10,000 kg for a range of fuel mixing diameters of 10 mm to 100 mm; $D_{\rm mix} = 10$ mm represents the size assumed by Fauske while $D_{\rm mix} = 100$ mm represents that conservatively used by Theofanous in his analysis. The other model results shown in the figure are discussed blow.

More recently, Corradini (1982) and Corradini and Moses (1983) have attempted to analyze the Sandia National Laboratories FCI experiments (Berman, Mitchell et al., 1981; Mitchell and Evans, 1982) designated as the fully instrumented test series (FITS).

The fuel/coolant mixing in the FITS experiments was observed by viewing high-speed movies of the interaction. These tests involved pouring a fuel simulant (5 to 20 kg of Fe-Al $_2$ 0 $_3$ at 3000 K) into a water pool (40 to 250 kg of water at 283 to 367 K) to simulate FCIs in a pouring contact mode. The conceptual picture of the mixture zone was one where the fuel enters the water pool as a single discrete mass (an elongated ellipsoidal shape) in film boiling and begins to fragment. As it continues to fall through the pool, it continues to break apart into smaller pieces and mix with the surrounding water while in film boiling. These smaller fuel particles may subdivide further as the steam produced in film boiling flows out through the top of the fuel/coolant mixture and escapes the water pool, and water flows in from the sides. The mixture grows radially as the fuel, now mixed with water and steam, falls to the chamber base (Fig. 6). At the time of or near base contact, two possible events occur: an energetic vapor explosion is triggered, or the premixed molten fuel settles on the chamber base and eventually quenches.

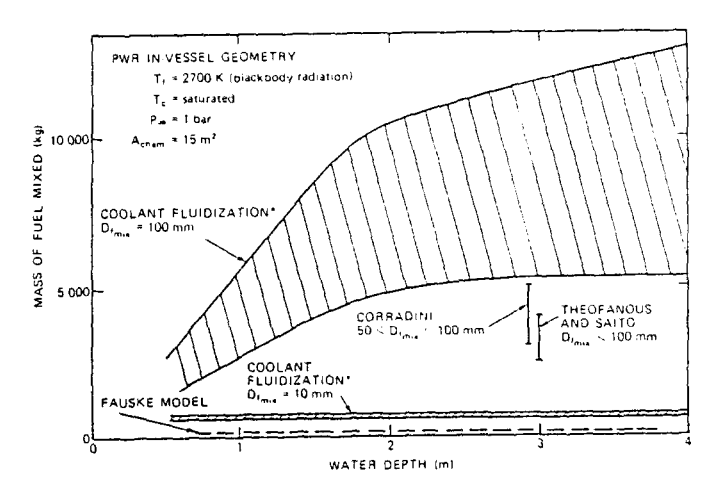


Fig. 5. Limits to fuel/coolant mixing based on Fauske's concepts of coolant fluidization. The asterisk indicates the range of values designated by the shaded area, which is due to two different coolant characteristic diameters. One is related to the fuel diameter (higher value) andthe other to the critical Weber number diameter (lower value) (Corradini 1985)

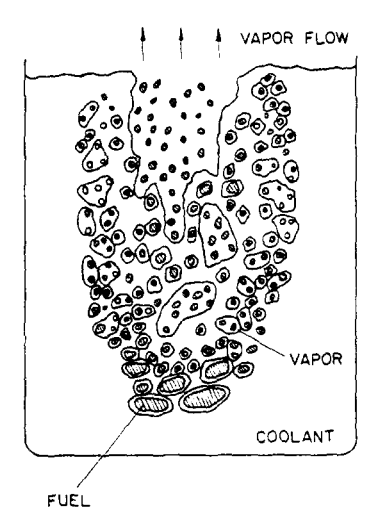


Fig. 6. Conceptual picture of fuel coolant mixing as observed in FITS experiment

Corradini analyzed the observed mixing process with a characteristic dimensionless time derived from hydrodynamic considerations and was able to correlate the available mixing data (i.e., MD and MDC test series) so that one could find the time history of the mixing volume, the displaced water volume, and visual observation of fuel fragment sizes. From these correlations, one could estimate the integral fuel, vapor, and liquid coolant volume fractions as a function of time. In addition, based on simple fluidization arguments, Corradini developed a simple steady-state model that predicted the minimum fuel diameter that could exist in the mixture before the liquid fuel or coolant would be fluidized by the steam flow. In all cases of interest, coolant fluidization occurred first as compared to the fuel, so the minimum fuel mixing diameter was given by

$$D_{\min} = (\frac{3}{4})^{1/3} \left(\frac{\alpha_f}{\alpha_c}\right)^{2/9} \left(\frac{\alpha_f}{\alpha_v}\right)^{2/3} \left(\frac{6q_{\text{drop}}^{"}}{\rho_v^{"}f_{\alpha}}\right)^{2/3} \left(\frac{C_0 H_c^2}{g}\right)^{1/3} \left(\frac{\rho_v}{\rho_c}\right)^{1/3} , \qquad (7)$$

where: α = volume fraction for fuel f, vapor v, and liquid coolant c, respectively

= density for fuel f, vapor v, and liquid coolant c, respectively

 i_{fg} = latent heat of vaporization H_{c} = depth of the water pool.

The values q_{drop}^{n} and C_{D} are previously defined. To use this model, one must know the volume fraction of the fuel, vapor, and liquid coolant at a given point in time; this was obtained by using the empirically correlated values for α_{f} , α_{v} , and α_{c} from the FITS data (Corradini, 1982). This latter point is an important limitation of this particular model. The reason is that the Sandia experiments at that time, although intermediate scale, were not conducted over a large range of fuel masses and coolant masses, temperature and depths; e.g., one should note that the coolant depth is a determinant in the fuel mixing size. Therefore, the correlations for fuel and coolant volume fractions are not universal and should not be extrapolated without

further experimental data. One should also be aware of the similar assumption of a one-

2.2 Transient Jet Breakup

dimensional system.

Theofanous and Saito (1982) also addressed the question of a limit to fuel/coolant mixing but took a different approach. Instead of investigating steady-state limits to mixing, they concluded that the mixing process would be driven by the hydrodynamics of transient jet breakup as the fuel pours into a water coolant pool. Corresponding to this conceptual picture (Fig. 7), they identified three regions where mixing may progressively occur: vertical jetting, horizontal jetting, and vertical rise and fallback. Jet and surface instabilities in each one of these phases would produce fuel breakup and mixing. Gravitational settling due to density differences, on the other hand, would promote separation and retard mixing.

Owing to the confined geometry, the time available for instabilities to develop is governed by the coolant depth, H_C , as well as the jet diameter, D_{jet} . Various modes of instability were examined: (1) Kelvin-Helmholtz instabilities on the surface of the fuel jet, (2) Rayleigh

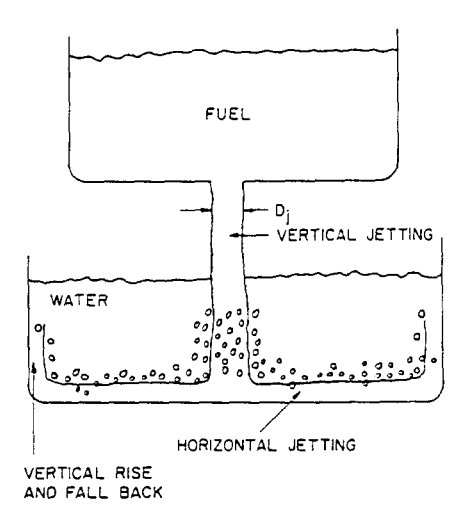


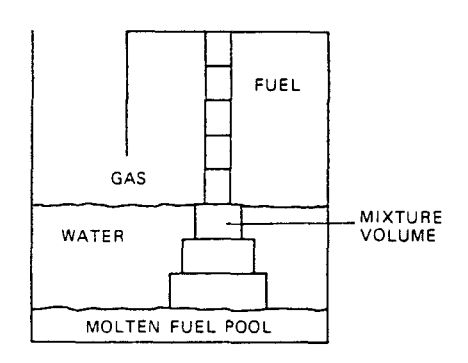
Fig. 7. Geometry of fuel pouring into the lower plenum of the vessel (Theofamous 1982)

breakup of the jet into discrete fuel masses, and (3) Taylor instabilities breaking up the discrete fuel masses. For a jet below a certain diameter ($0_{\rm jet} < 10$ -20 cm for the in-vessel case) it was estimated that Rayleigh jet breakup into discrete masses followed by hydrodynamic instabilities droplet breakup would mix the fuel with the coolant. However, if the jet diameter

was much greater than this diameter there was insufficient time for the jet to form discrete masses due to Rayleigh breakup, and the jet would take on the appearance of a largely undisturbed jet body and hydrodynamic breakup and fuel mixing would occur only at the leading edge of the jet (Fig. 3). This concept of a mixing limitation due to transient jet breakup is quite useful. However, based on subsequent analysis by Fauske (1985) and Ginsberg (1985) a Rayleigh jet breakup mechanism may not be correct. This will be discussed below.

Theofanous and Saito then quantitatively considered the effect of jet sizes from small pour streams to jet diameters approaching the size of the fuel volume. Their order-of-magnitude calculations indicated that only a few percent of the available fuel mass could mix with the water coolant for in-vessel reactor safety core melt situations. This represents 2500 to 4000 kg of fuel that could mix to characteristic mixing diameters less than 100 mm (see Fig. 5). The major reason that more mixing could not occur was because the available time for hydrodynamic mixing was limited because the water depth in the lower plenum of the reactor vessel (PWR for these example cases) was relatively limited. For ex-vessel fuel/coolant mixing, they estimated that ~ 10% of the available molten fuel mass could mix (13,000 kg for a PWR system).

In addition to the simple model for the minimum mixing diameter, Corradini and Moses (1983) developed a dynamic mixing model (MEDICI-MI) that predicts the fuel breakup as it falls through the gas atmosphere into the water pool, eventually reaching the chamber base and quenching or undergoing a steam explosion (Fig. 8). The model considers the fuel to fragment due to



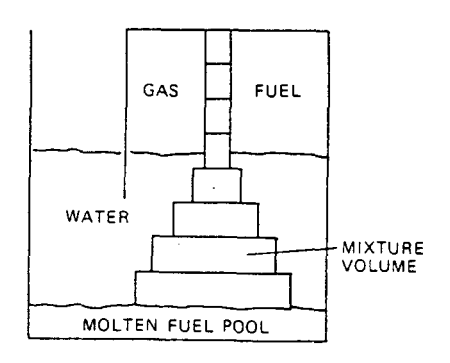


Fig. 8. The M1 model for fuel/cooling mixing in a coolant pool.

primarily hydrodynamic forces, and the fuel diameter is taken to be

$$D_f = D_{f0} \exp(-T^+) , \qquad (8)$$

based on the theoretical work of Buchanan (1973) where

$$T^{+} \equiv \frac{v_{f}t}{D_{f0}} \left(\frac{\rho_{c}}{\rho_{f}}\right)^{1/2} \tag{9}$$

t = time $v_f = fuel fall velocity$ $D_{f0} = initial fuel diameter.$

The mechanism for breakup was considered to be Helmholtz and Taylor instabilities. Now, within this context of dynamic mixing, coolant fluidization, which would limit mixing, was not applied. This limit in the dynamic model is a function of the fuel temperature, the water depth (since $\rm H_C=v_{ft}$) the fuel initial size $\rm D_{f0}$, and the mixing phenomena from the FITS tests as empirically correlated. If one combines these factors, one can solve for the fuel diameter after mixing as a function of $\rm H_C$ and $\rm D_{f0}$ (Fig. 9). One can also plot the fluidization limit for for different fuel temperatures assuming a blackbody radiative heat flux from the fuel surface. All the diameters to the left of the fluidization mixing limit for a given fuel temperature can mix without fluidization, while those diameters to the right of the limit for a given $\rm H_C$ and $\rm D_{f0}$ will begin to fluidize. This dynamic model for mixing and mixing limit only

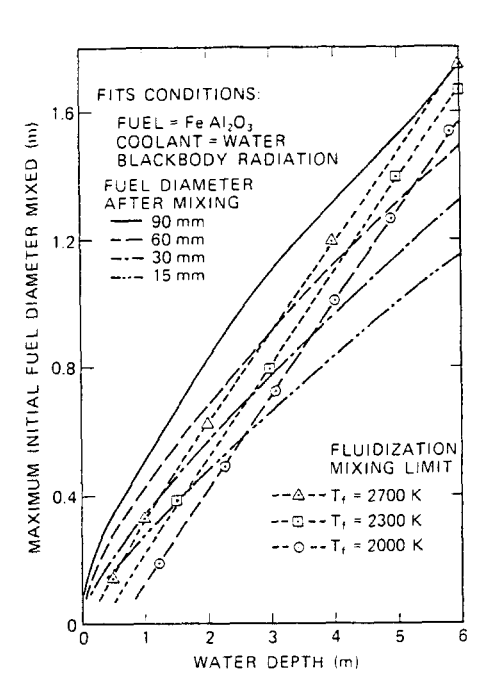
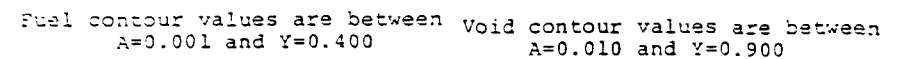


Fig. 9. Limits to fuel/cooling mixing based on fluidization model with transient jet breakup.

considers the leading edge (i.e., an equivalent spherical volume) of the entering fuel jet to be capable of mixing. The fuel mass behind this leading edge can also mix but must first undergo jet breakup into discrete fuel masses based on mechanisms such as those proposed by Theofanous (1982).

Based on this work for light water reactor safety issues, it was estimated that a maximum of 3000-5000~kg of fuel could mix with water to a diameter of 50-100~kg mm within the reactor vessel (see Fig. 4). Once again the major limitation of this approach is that it relies on the empirical data of fuel-coolant volume fractions from the Sandia FITS tests. It also does not include the multidimensional effects of mixing.

Two-dimensional transient effects were first considered as an extension of these concepts by Bankoff et al. (1984a, b). Bankoff and his coworkers used the PHOENICS two-fluid, twodimensional computer code to model the transient mixing of an array of fuel droplets as they enter a coolant pool. Their analysis indicated for in-vessel conditions (Fig. 10) that substantial liquid coolant fluidization and sweepout occurred as the coolant vapor volume fraction exceeded 50% in the majority of the fuel-coolant mixture. This also suggests the lack of an inertial constraint for a subsequent explosion. However, because of computer code limitations, the coolant (steam and water) was considered as a single homogeneous fluid (i.e., equal velocities, temperatures and pressures) and the fuel was considered to be the other fluid, prefragmented to a user-specified diameter <u>before</u> entry into the coolant pool. Under saturated coolant conditions Bankoff considered these to be reasonable approximations because it was proposed that the fuel would rapidly fragment at the coolant pool surface due to high impact velocities and initial steam generation. However, visual as well as flash x-ray high-speed photographs from the FITS tests (Berman, et al., 1984) do not support this assumption, and this is not considered likely as scale increases. Therefore, one might consider this analysis technique to be parametric with the fuel "prefragmented" size as the key parameter. The assumption that the coolant liquid and vapor can be treated as a homogeneous fluid is also suspect because for these larger void fractions it would unphysically enhance the coolant liquid expulsion (i.e., fluidization and sweepout) from the fuel-coolant mixture region. assumptions tend to oppose mixing and therefore can cause one to underpredict the amount of fuel and coolant mixed. Fletcher (1984, 1985a, b) has also reviewed the development of this model and the more general case of fuel jet mixing. The work involves an Eulerian formulation similar to PHOENICS with the fuel and coolant considered as searate fluids.



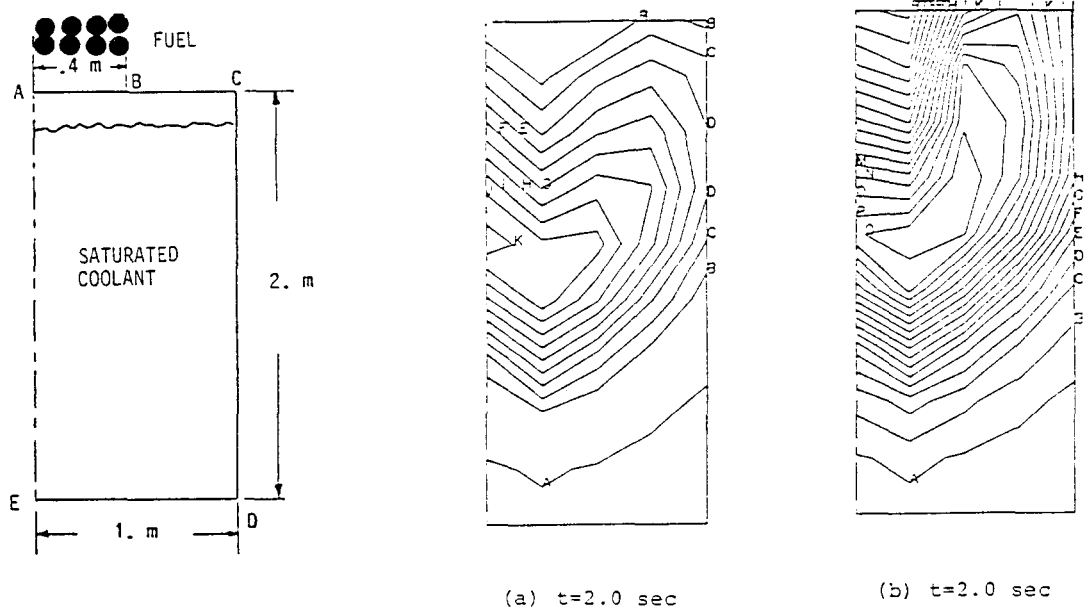


Fig. 10. Simulation of pre-fragmented fuel particles mixing with a coolant pool for an invessel reactor case (Bankoff et al. 1984)

Recently, Theofanous et al., (1987) have also developed a two-dimensional model for fuel-coolant mixing that employs the K-FIX computer model with substantial modifications of the constitutive relations. The basic simplifying assumptions of the computer analysis are exactly the same as those of Bankoff:

- The coolant liquid and vapor are considered to be a homogeneous fluid;
- (2) The fuel is modelled as a collection of droplets at a user-specified prefragmented size.

Thus the overall results are similar. There are interesting differences that should be noted. Bankoff had difficulty obtaining a stable solution at higher ambient pressures. Theofanous analysis indicates that mixing is significantly enhanced at higher ambient pressures. In addition Theofanous uses a technique to define the mass of fuel mixed similar to that employed by Chu (1986), in which the fuel is considered mixed when it is in a regime of coolant liquid ($\alpha_{\rm C} > .5$). Based on this definition little of the fuel is found to mix with coolant under atmospheric pressure conditions in the LWR.

Recently, Epstein and Fauske (1985) have taken another look at the concept of fuel jet breakup and mixing. In particular they considered the effect of film boiling on jet breakup. In their analysis they estimated the breakup length of a fuel jet entering a coolant pool under two bounding conditions: (1) a thin coolant vapor film that could be neglected, and (2) a thick coolant vapor film that must be considered. Also, they provided a criterion to determine when the vapor film was thick or thin as well as quantitative estimates for light water reactor safety issues. The fundamental assumptions in their analysis were that they considered steady-state jet breakup and that the dominant mechanism for jet breakup under these conditions was jet atomization as given by Levich's model (1962). The assumption of steady-state conditions for jet breakup neglects the fuel mixing that would occur as the fuel jet first enters the coolant pool; i.e., leading edge effects are ignored. This would underestimate fuel-coolant mixing upon jet entry as first considered by Theofanous (1982). This is discussed further below. The second assumption that a jet atomization mechanism is operative is quite reasonable and points out that the Rayleigh jet breakup regime is not likely to be operative. As Fig. 11 indicates, four regimes of jet breakup have been identified. Under most conditions of interest for large scale systems the Weber number and fluid properties (e.g., Ohnesorge No.) put the fuel jet within the atomization regime or the transition to it. The velocity or jet diameter would have to be quite small for Rayleigh breakup to be operative. In fact if one uses Levich's model one would tend to overpredict fuel jet mixing in the Wind Induced Breakup regime (Windquist, 1986) during the transition to atomization.

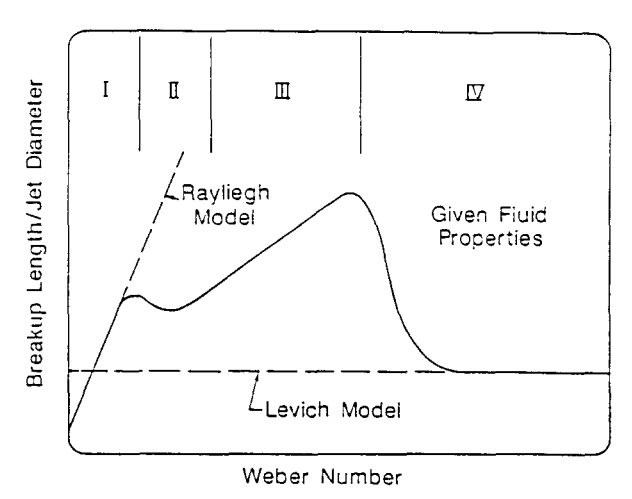


Fig. 11. Jet breakup regimes

I. Rayleigh

III. Second wind induced IV. Atomization

II. First wind induced

In this analysis the fuel jet is separated from the coolant by a stable vapor film (Fig. 12). The surface instabilities (i.e., Kelvin-Helmholtz instabilities) will grow rapidly due

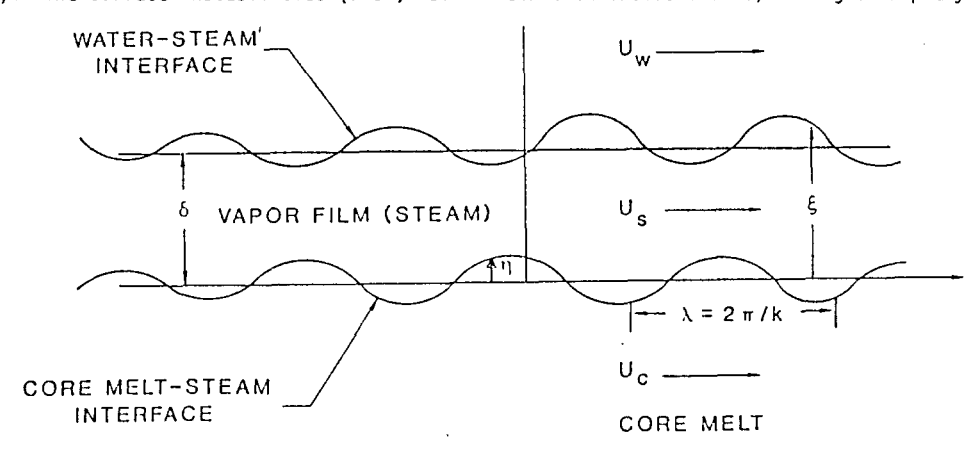


Fig. 12. Schematic of stability model (Fauske et al. 1985)

to relative fuel-coolant velocities to a maximum amplitude equal to their wavelength and are assumed to be stripped off the jet surface. Any liquid fuel mass which is separated from the main jet could be considered mixed with the coolant. The size of the fuel droplet which is mixed is proportional to the fastest growing wavelength, $D_{\rm f}=\lambda_{\rm m}$, where

$$K = \frac{2\pi}{\lambda_{\rm m}} = \frac{2\rho_{\rm f} \rho_{\rm i} U^2_{\rm rel}}{3(\rho_{\rm f} + \rho_{\rm i})\sigma_{\rm f}}$$
 (10)

is the fuel surface tension where

is the fuel density

 ρ_f is the fuel density U_{rel} is the fuel-coolant vapor relative velocity, U_f - U_v is the continuous fluid density, either liquid coolant for a thick film.

thin film or vapor for a thick film.

These simplifying assumptions tend to overestimate the extent of fuel jet breakup and thus could be considered an upper bound to the extent of jet mixing under steady-state conditions. The characteristic time for the instability growth is

$$\tau = \frac{5}{2} \frac{(\rho_f + \rho_i)\sigma_f}{(\rho_f \rho_i)^{3/2} u_{rel}^3}$$
 (11)

and therefore the rate of breakup is given by $V_b \equiv \lambda_m/\tau$. Combining these conditions one finds the fuel jet breakup length, L_B , to be given by

$$L_{B} = V_{b}t_{b} = \frac{0 \text{ jet } \tau}{2 \text{ } \lambda_{m}}$$
 (12)

$$\frac{L_B}{D_{jet}} = \frac{\sqrt{3}}{4\pi} \left(\frac{U_f}{U_{rel}}\right) \left(\frac{\rho_f}{\rho_i}\right)^{1/2} \left(1 + \frac{\rho_i}{\rho_f}\right) . \tag{13}$$

In the original analysis by Epstein and Fauske the relative velocity was approximated by the jet velocity, U_f ; in general though one should retain this term. The analysis also suggested a simple estimate to decide if a thick film or thin film approximation should be used by comparing the vapor film thickness, δ , to the instability wavelength [Eq. (2.10)]; i.e. $K\delta >> 0$ implies a thick film and $K\delta \rightarrow 0$ implies a thin film.

For light water reactor applications of in-vessel jet mixing the analysis indicates that for large scale jets (> 0.1 m) the vapor film is considered thick and the jet breakup length is much larger than the coolant pool depth (at least an order of magnitude); therefore, fuel-coolant mixing by this mechanism is insignificant. One should note though that since the rate of jet breakup is essentially constant one finds that the jet mass is being stripped away and mixed with the surrounding coolant pool linearly with distance. Therefore, as the fuel jet diameter decreases the percentage mixed goes up linearly. Conversely, the actual mass mixed decreases with the jet area, $D_{\rm fet}^{\gamma}$, and thus for smaller jets (<< 10 cm) one computes a short breakup length (~ 1 m) but an insignificant amount of mass mixed. The original analysis assumed that $U_{\rm rel}^{\gamma} \sim U_{\rm f}$, but Windquist (1986) has extended the analysis and verified that the thick vapor film limit is still maintained for large jets when one considers the actual relative velocity.

As noted previously, the one assumption in the Epstein-Fauske model that would underestimate mixing upon initial jet entry is that the jet breakup of the leading edge is neglected. Recently, a transient, multifluid, one-dimensional model has been developed that would allow one to consider the mixing between fuel and coolant and can account for leading edge effects. Chu et al. (1985, 1986) based this model on the TEXAS code (Young, 1981), a Lagrangian-Eulerian hydrodynamics code that was originally used for design and analysis of fuel-coolant interaction experiments for LMFBR safety. Two Eulerian fields (coolant vapor and liquid) and one Lagrangian particle field (fuel) are employed in the model. The model is currently limited to nonexplosive fuel-coolant interactions, although this restriction could be relaxed. Chu (1985) developed a complete set of constitutive relations for interfacial mass, momentum and energy transport; e.g., a virtual mass model for rapid acceleration. The key constitutive relation is a fuel fragmentation model based on Rayleigh-Taylor instabilities (Chu, 1984). This constitutive model considers the fuel to be dynamically fragmented from its initial entry diameter to smaller sizes. This is an improvement over the PHOENICS analysis and other similar analyses in which the fuel was assumed to be prefragmented and does not dynamically fragment. In the model parallel velocity shear forces (e.g., Kelvin-Helmholtz instabilities) The model for fuel breakup as used in TEXAS was simplified from the detailed model (Chu, 1984) to a linear time-independent form (Chu, 1986) where

$$D_f^{n+1} = D_f^n (1 - C_0 \Delta T^+ We^{0.25})$$
 (14)

where: n, n + 1 designates the old and new timestep values We is the fuel Weber number ΔT^{\dagger} is a dimensionless timestep

$$We = \rho V_{rel}^2 D_f^n / \sigma_f$$
 (15)

$$\Delta T^{+} = \frac{V_{rel}(t^{n+1} - t^{n})}{D_{f}^{n}} \left(\frac{\rho_{c}}{\rho_{f}}\right)^{1/2}$$
 (16)

$$C_0 = 0.108 - 0.0785 \left(\frac{{}^{\circ}_{c}}{{}^{\circ}_{f}}\right)^{1/2}$$
 (17)

This model has been applied to analysis of fuel-coolant mixing in the Sandia FITS tests (Chu, 1986). In particular a group of experiments was conducted in which no vapor explosions occurred and the fuel simulant quenched in the water. In these cases the post-test debris size distribution gives one a rough indication of the fuel mixing size during the fuel-coolant interaction. Table I presents the results of the analysis and it indicates the results of the model developed by Chu as well as other predictions.

Table 1. Measured and predicted particle sizes for non-explosive FITS experiments

										
TEST	FUEL	COOL.	SAUTER	UENRY-	Erstein	CORR	CORR	CHU-	CUU-	PILCH.
NAME	MASS		/MASS	FAUSER	-FAUSEE	FLUID-	WOSES	CORR.	CORR.	
	*	COOF-			THIN	IZATION		EXPON.		
		ING	DIA.		TRICK	20/11/20/		u	D 11	
		1110	DLA.	1981	1986	1982.85	1983	1985	1985	1985
	11	/F1								
	(kg)	(K)	(mm)	(mm)	(mm)	(mm)	(mm)	(mm)	(mm)	(mm)
FITSIA		84	1.8/4.1		0.052/ 66.	8.9	0.40	13.	20.	48.
FITS 4A	4.3	166	2.8/5.4	8.7	0.041/ 5.9	110.	0.18	12.	16.	68.
FITS5A	5.4	160	3.0/5.2	11.	0.072/ 9.6	75.	0.026	12.	?	?
FITSGB	14.5	0	5.9/11.	200.	0.010/ 40.	84.	24.	25.	94.	150.
FITSEB		ō	1.7/12.	380.	0.047/ 68.	85.	20.	37.	130.	180.
FITSOD	17.8	0	1.5/4.6	210.	0.059/ 73.	N.W.	97.	100.	130.	170.
(BC)					0.059/ 73.	25.	27.	38.	79.	150.
FITS2D		168		86.	0.088/ 5.0		28.	28.	БО.	140.
FITSED	19.5	0	0.81/3.4	520.	0.048/ 58.	N.W.	140.	160.	?	200.
(BC)					0.048/ 58.	м.ж.	115.	130.	?	200.
SEALS (S	SAT) BO	(8,	= 1.5 m)	(2000	kg iron-alu	mina)				
Yfuel=			N.A.	2190.	•	1020.	340.	999.		
SEALS (S	SAT) BO	· (II.	= 1.4 m)	(2000	kg iron-alu	n(nn)				
Vfuel=			N.A.	2190.	0.083/100.		370.	440.		
· tref -	, .				, 100.					_
BC - 1	COTTOL	CONT	ACT	·	Not Availab		N.W	N- WI-1		
DU - 1		1 0001	401		HOC WANTING	1 T .	17.50	no wixi	ng freq	ircred.

BC - BOTTOM CONTACT N.A. - Not Available. N.W. - No Mixing Predicted.
- - PRELIMINARY CALCULATIONS USING THE TEXAS COMPUTER CODE WITH HEAT TRANSFER

When the TEXAS model is applied to the breakup of a fuel jet in a coolant for conditions similar to those considered by Fauske, it also predicts that under steady-state conditions the fuel jet breakup and mixing is small (Chu, 1986). However, for the initial fuel jet entry the leading edge can mix with the coolant. As the leading edge of the jet breaks up and is decelerated in the coolant, the fuel upstream of this mass becomes the leading edge and can break up due to Taylor instabilities. If the coolant depth is shallow relative to the jet diameter ($H_{\rm c}/D_{\rm jet} < 10$), then the jet length has only time to break up a couple of jet diameters. In a light water reactor safety application, consider an in-vessel situation of a corium fuel jet with a flow rate of 5000 kg/s at a velocity of 5 m/s falling into a saturated water pool of 3 m depth and 4.2 m diameter at 1 atm. These conditions are similar to those considered by Bankoff (1984). The vapor void fraction and mixed fuel mass were plotted in Fig. 15 at different times after the fuel jet falls into the water pool. It is seen that less than 20% of the available submerged fuel mass (3000 kg as the fuel jet falls onto the pool base at approximately 0.523 s) mixes with the water. Also, one-third of the water pool has a vapor volume fraction of about 0.5 and the highest vapor void fraction is about 0.65 near the middle of the water pool. If one correlates the location of the fuel stripped off the main jet and this void fraction one finds that about 50% of this total mass stripped is in a region where $\alpha_{\rm V} > 0.5$. Thus, according to the original concept of Fig. 2 even less fuel mass is mixed with a continuum of liquid coolant. Rather the fuel is mixed with liquid coolant in a vapor rich region (i.e., lack of inertial constraint). The fuel particle diameter is predicted to be about 10 mm near the pool base and about 1 mm near the top part of the fuel-coolant mixture as the fuel jet falls onto the water pool. This indicates that the potential for a finely mi

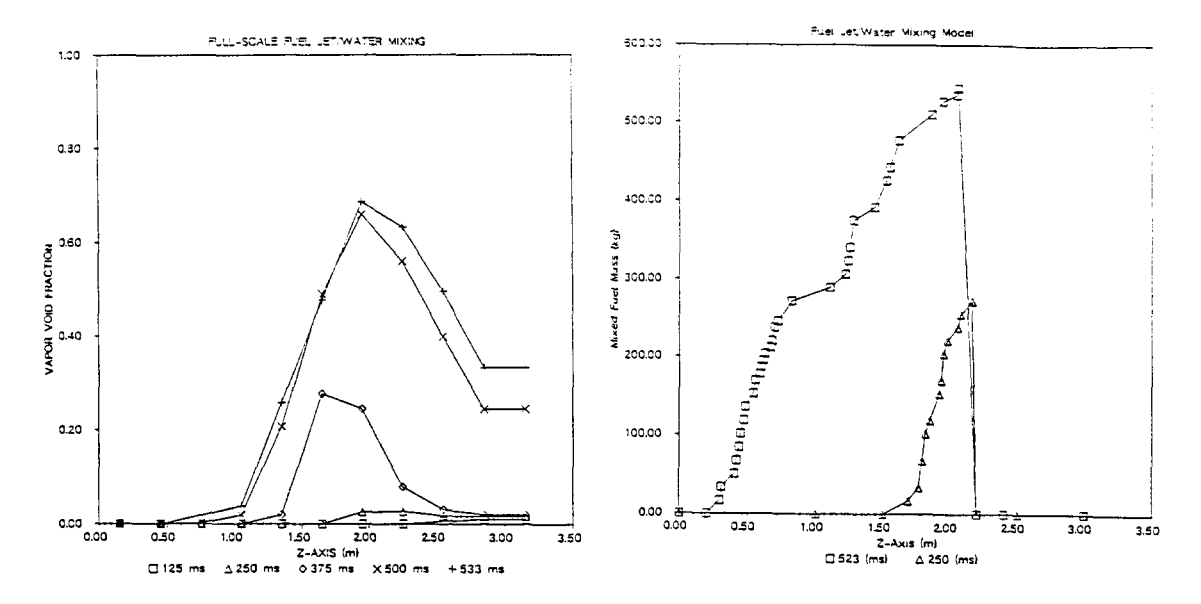


Fig. 13. Vapor void fraction within coolant pool. (Chu 1986)

Fig. 14. Fuel mass mixed within the (Chu, 1986)

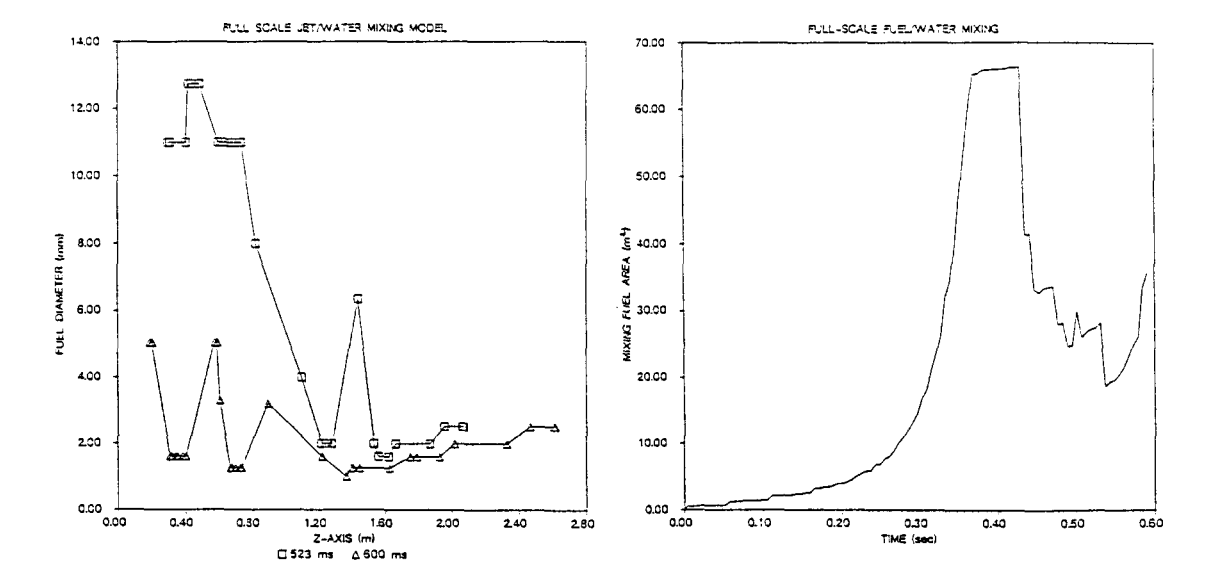


Fig. 15. Diameter distribution of fuel mixed in coolant pool (Chu 1986)

Fig. 16. Overall exposed surface area for fuel mixed (Chu 1986)

This mixing model incorporates all the insights of past analyses; however it is still severely limited by a one-dimensional treatment. A one-dimensional model neglects multidimensional circulation patterns that would allow coolant to enter from sides of the fuel jet enhancing mixing. Conversely, the 1-D model homogenizes the vapor void over the cross-sectional area. A 2-D model would concentrate this void near the fuel jet and this would aid fluidization and sweepout of the coolant and the fragmented fuel from the mixing region, thus retarding local mixing.

Quite recently, Young (1987) has taken the concept of dynamic mixing from Chu's analysis and separate dynamic mixing investigations by Pilch (1987) and developed a two-dimensional model for fuel-coolant mixing analysis, IFCI. This represents an advance in modelling the mixing prior to a vapor explosion because 1) it is multi-dimensional, 2) it allows for three separate fluids to be considered with different temperatures and velocities (fuel, coolant liquid, and coolant vapor) and 3) it employs a model for dynamic fuel fragmentation instead of a user-specified pre-fragmented size as in PHOENICS and K-FIX analysis. The results published to date are quite preliminary, but the capabilities of the tool seem to be quite promising. In our opinion if one is to investigate the fundamentals of fuel-coolant mixing an approach similar to that employed by IFCI is needed. One point that should be considered are the advantages and disadvantages of using an Eulerian approach rather than a Lagrangian approach to tracking the fuel transport. TEXAS employs a Lagrangian technique in difference to IFCI, and the superiority of either method has not been demonstrated.

2.3 Other Considerations

In all the previous mixing models a common assumption has been that the radiative energy transfer from the fuel through the coolant vapor film is deposited at the coolant liquid-vapor interface, and thus directly contributes to vapor generation. This approximation was examined by Kim (1985) by performing detailed EMR transport calculations through the vapor film. The radiative energy is actually deposited volumetrically within the coolant liquid in an exponential fashion and the cumulative energy deposited at a given depth is a function of the fuel surface temperature. One can only accurately consider the energy deposited in the coolant liquid boundary layer to be directly contributing the vapor formation. Therefore, for light water reactor safety applications one must be careful to correctly partition the portion of radiative energy to the interface and that to the bulk liquid, because it will affect fuel-coolant mixing calculations indirectly by the vapor generation rate.

Fuel-coolant mixing can also be induced by external dispersive forces. For example in the Sandia experiments by Mitchell et al. (1985) it was sometimes observed that when a fuel mass first entered the coolant pool a surface explosion occurred. This event partially ruptured the coolant chamber, but it also helped in fragmenting the fuel remaining in the coolant liquid and in mixing the fuel and coolant together. This repeatedly occurred in a number of experiments and suggests that multiple explosions must be considered as a mechanism for mixing. Let us consider the two fundamental concepts of physical mixing limits, transient jet breakup and fluidization limits, in light of multiple explosions. The former limit would govern the normal circumstances of fuel entering a coolant pool. The latter, however, is more general in its application and could be used in estimating the limit to mixing given multiple explosions. The use of this limit was first suggested by members of the Steam Explosion Review Group (Ginsberg et al., 1985). One should note that in this context one would again seek the minimum mixing diameter given a fuel and coolant mass and geometry (or conversely the maximum fuel mass given its diameter and coolant geometry Eq. (2.4) or Fig. 3). One would find that if explosion-induced mixing were too efficient the coolant and fuel fluidization would be accompanied by the reduction of the inertial constraint.

When explosion triggering is considered in the following section, one observes that the vapor explosion is quite frequently triggered when the fuel comes into contact with solid structure; e.g., chamber base or internal structures. In the absence of a trigger upon contact the structure may also be considered (Berman, 1984) as a possible external source for enhanced fuel-coolant mixing (Fig. 14). Internal structure could break up the jet by splashing or flow through the holes causing finer jet breakup. Qualitatively this seems quite possible, but one must again consider the concept of a fluidization limit. In this case one would again expect the coolant liquid to be more rapidly swept out of regions between the jets where the fuel jet would be fragmenting to smaller sizes.

The subject of fuel-coolant mixing and the two proposed concepts of limitations to mixing have been discussed primarily for the contact mode of fuel pouring into a coolant pool. Many of the analyses can be extended to the case of coolant injection into a fuel pool, however, the situation of stratified layers of fuel and coolant has not been widely considered. This geometry can occur in a number of industrial safety applications (e.g., paper pulping or LNG spills) as well as reactor safety situations. Fuel-coolant mixing in such a configuration would probably be caused by the initial entry of the liquids and the subsequent film boiling that separates them. In particular one would expect that the excess vapor generated at the interface would leave as bubbles from the vapor film, and this would cause local circulation patterns to develop, mixing the fuel into the coolant liquid (likewise the coolant in the fuel liquid). Fauske (1985) has suggested that fluidization considerations may again limit mixing, but no detailed theoretical analysis has been advanced nor experimental data been analyzed for this

3. TRIGGERING AND LOCAL FUEL FRAGMENTATION BEHAVIOR

3.1 Fragmentation Mechanisms

Since fragmentation seems to be the key to the enhanced heat transfer rate in a vapor explosion, investigations into the fragmentation phenomena as well as the mechanisms that trigger fragmentation have been conducted in several industries. Indeed there are many fragmentation concepts, which are often mechanistically quite different. Likewise, certain fragmentation concepts may be consistent with one proposed path for explosive interaction but not with others.

Generally, fragmentation models have been classified depending upon the source of the driving force for fragmentation or the mode of contact between the hot liquid and the cold In this discussion fragmentation mechanisms were categorized into two broad classes: namely, those due to pure hydrodynamics or thermal effects. Thermal effects were further divided into boiling effects, internal pressurization effects, and solidification effects. However, these categories are not always clearly separable. A summary of the proposed fragmentation mechanisms is given in Table 2.

- 3.1.1 $\underline{\text{Hydrodynamic Effects}}$ $\underline{\text{Hydrodynamic fragmentation occurs when a molten droplet is subjected to external surface forces sufficient to overcome the cohesive forces of drop surface$ tension. Droplet fragmentation occurs in two integral ways:
- Acceleration of a drop in a flow: The drop enters another liquid medium and experiences rapid acceleration or deceleration until it reaches the fluid velocity. The relative velocity induced surface force causes the deformation and breakup of the drop.
- Fragmentation upon impact: For a free contact mode of fuel into coolant, the drop of hot liquid falls freely into the cold liquid pool. Breakup is due to the impact of drop upon the liquid surface where the inertial force is high enough to overcome the cohesive forces of drop surface tension. The potential to cause the breakup of drop in both ways can be expressed in terms of the ratio of inertial to surface tension forces. This was recognized in early work on liquid droplet oscillations and breakup (Bohr, 1923, Weber, 1931). The Weber number is an expression of this ratio

$$We = \frac{\rho_c U_{rel}^2 D_d}{\sigma_{dc}}$$
 (18)

where:

p: the density of the cold liquid

Urel: the relative velocity between the liquids D_d: the diameter of the drop σ_{dc} : interfacial surface tension.

Table 2. Summary of proposed fragmentation mechanisms

Hithdrodynamic Effects P:Boiling Effects I:Internal Pressurication Effects B:Boild:Fication Effects

Author	egons Proposed Fragmentation Mechanisms	Remarks
Anderson, Arastrong (1972)	B - Local collapse of vapor layer acts as	
Anderson, Armstrong (1973)	8 Dinamic impact heating model	Cannot explain soontaneous explosion
Bankoff,Fausta (1974)	3 Spontaneous nucleation and generation	of For the experiment of Na drop injected
	§ spherical compression	into UO2
Benz et al. (1977)	B. Transmittance of bubble energy to fue	No explanation for the break-up mechanism
Bjornard et al. (1974)	8 Pressure oscillation induced fuel fra	qmentation
Board, Hall (1974)	H Frag. due to MH or RT instabilities a	
	interaction front/large pressure wave)
Brauer et al. (1967)	I Encapsulation of cold liquid in fuel	Alusinum bubble formation on the fuel surface
Bradley, Witte (1970)	Enitiation of fragmentation is tied to	o Explosion becames violent with I(melt).
	S instantaneous cooling rate of fuel	
Buchanan (1974)	B Breakup of fuel upon penetration of c	oolant jet
Buxton, Nelson (1977)	I Regid growth of gas bubble in fuel	A large quantity of gas should be dissolved.
Caldarola, Kastenberg 1974)	B impact of coolant jet on feel surface	in the defendance of the succession of the succe
Coloate et al. (1973)	H Miring by RT or KH instabilities.	
Corradini, Todreas (1979)	3 Propagation of cracks at Kickic	Constant properties
Coffield, Wattlet (1970)	8 Pressurization due to the thermal exp	
	3 heated sodium layer in contact with t	
Gromenberg et al. (1974)	S Pressurization and thermal stress and	
Oreaheller (1979)	Empact of coolant to fuel upon bubble	
Epstain (1974a)	I Violent release of dissolved gas upon	
Fauske (1972)	8 Pagid vaporitation at apontaneous nuc	
Fauske (1973)	B Entrainment, watting, and superheatin	
	3 cold liquid dres in fuel	,
Flory at al (1969)	Entrainment of cold liquid by KH inst	ability. Formation of thin-shelled bubbles of Al
Heas,Brandoka (1959)		pressurization.Crust formation at the interface provide
	<u>.</u>	some constraint more violent explosion.
Heary, Cho (1972)	8 Flashing of liquid at spontaneous tem	perature Extensive fragmentation at T(hn)(T(Melt)(T(f)
Hsiao at al. (1972)	9 Pressure and thermal stress upon soli	
lvins (1967)	Suppose of the Sup	
	3 More extensive fragmentation at higher	
Karimi (1973)	I Cavitation induced fraggentation	Imprities in the melt help bubble inception.
Kja (19 85)	I coolant jet formation upon vapor film	
	I and genetration into fuel	fuel breakup
rnapp,Todreas (1975)	6 Pressure and thermal stress due to te	ap. gradient limited to semi-brittle or brittle materials.
Long (1957)	I Entrappment of lig. between welt and	
Makanishi,Reid (1971)	B Superheating of cryogen and flashing	
Ochiai, Bankoff (1976)	8 Splash model	Self-mixing theory
Paoli,Mesler (1968)	I Entrainment of cold liquid by KH inst	
Schins (1973)	I Rapid vaporization of entrained cools	
Segev et al. (1979)	H Hydroeffects-Impact	Shock-tube analysis
Sharon, Bankoff (1979a)	H Fragmentation of fuel by RT instabili	
Sharon, Bankoff (1979b)	f Fragmentation of fuel by boundary lay	er stripping.
Swift,Baker (1965)	B Violent bailing induced fuel breakup	Frag. only if T(leidenfrost)>T(melt)
Swift, Pavlik (1966)	B Frag, due to turbulence caused by vio	
Witte et al. (1973)	B Impact of coolant on the melt drop or	
	phenomenon upon liqliq. contact fra	
Zyszkowski (1975)	S Change of intercrystal structure upon	

If the Weber number exceeds a critical value, the inertial force overcomes the surface tension and the drop fragments into a smaller more stable size as demonstrated by Hinze (1948a, 1948b). In the early experiments by Swift and Baker (1965), stainless steel was dropped from different heights into water. However, the violence and the extent of fragmentation did not

appear to be affected by the difference in these drop falling distances. Therefore, the impact velocity was not assumed to be a critical parameter. Ivins (1967) performed experiments on impact fragmentation, where low-melting point metals (tin, lead, bismuth, mercury) were dropped into water at room temperature. The results, as shown in Fig. 17, indicate that a critical

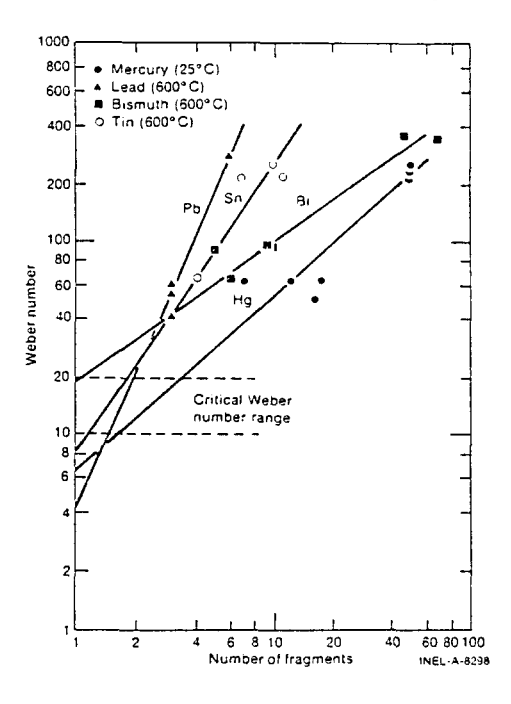


Fig. 17. Plot of Weber number versus number of fragments for molten metals dropped into room-temperature water (Cronenberg 1978)

Weber number for fragmentation lies between 10-20 which corresponds to that suggested by Hinze (1948b). However, in experiments with gallium (Ivins, 1967), two fragmentation mechanisms were suggested, a dynamic breakup at the lower fuel temperature which is proportional to the Weber number and fragmentation in the violent boiling regime where a striking change in the extent of fragmentation is evident independent of Weber number (Fig. 18). Armstrong (1970b) conducted similar experiments for tin/water interactions while varying the temperature of molten tin and water. Generally the extent of fragmentation increased with increasing entrance velocity or Weber number. Figure 19. shows that for a given entrance velocity the extent of fragmentation differs with initial tin temperature. For a certain range of tin temperature fragmentation was significantly enhanced. The temperature range of enhanced fragmentation appears to correspond to the maximum-heat-flux region of nucleate boiling. The temperature range was little affected by the entrance velocity. Bradley and Witte (1972) performed injection experiments, where hot molten metal jets were injected into subcooled distilled water. They observed some breakup of mercury jets at room temperature but more extensive breakup of the heated metal jet. Even though the disruptive forces of impact and viscous drag may contribute to breakup, it appeared that thermal effects play a more important role in the fragmentation of these molten materials.

Frohlich et al. (1976) reported that the low entrance velocity and spherical shape of a submerged melt intensified the thermal interactions. In their baseline experiments, Nelson and Duda (1981) showed that the drops at lower drop fall height underwent spontaneous explosions, while those at larger fall height than a certain value required external triggering to cause explosions. This was interpreted by Corradini (1981) and Kim and Corradini (1984) in terms of the amount of the noncondensable gas (air) carried in with the drop into the cold liquid, which increased with drop fall height and inhibited the molten drop from liquid-liquid contact with the cold liquid and triggering the event.

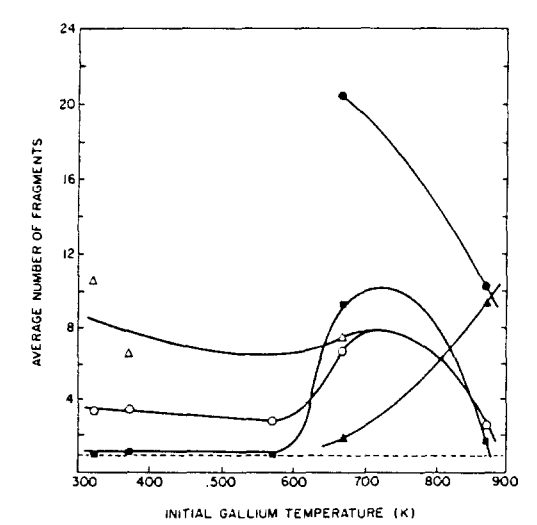


Fig. 18. Fragmentation of molten gallium in water (Witte 1973)

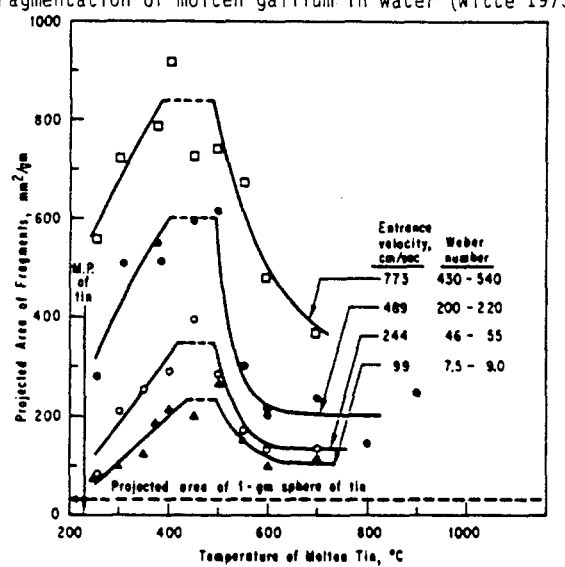


Fig. 19. Effect of entrance velocity on fragmentation of molten tin quenched in 22°C water (Armstrong 1970b)

For the case of extensive breakup of ${\rm UO}_2$ in sodium, Cronenberg and Grolmes (1974) investigated the experimental conditions of the work of Armstrong et al. (1971), where the dropping experiments were conducted at a Weber number of about 100. To quantitatively estimate the fragmentation size, the kinetic energy of the droplet at impact is compared with the work required to create new surface area. The results showed that the significant portion of the kinetic energy should be converted to mechanical breakup energy to result in the debris size observed in the experiments.

There are several kinds of hydrodynamic-related fragmentation mechanisms which are believed to cause the breakup of drops. Rayleigh-Taylor instabilities, Kelvin-Helmholtz instabilities, and boundary layer stripping are fundamental ways to fragment the fuel and may be involved in all of the breakup observed in experiments.

If two different fluids having a common plan boundary are accelerated in the direction from the lighter liquid to the heavier liquid perpendicular to the boundary, the irregularities of the interface will tend to grow. This effort is known as a Rayleigh-Taylor instability (Taylor). Rayleigh-Taylor instabilities are thought to be involved in the forced liquid/liquid contact experiments, such as shock tube experiments, reported by Wright and Humberstone (1966), Hillary et al. (1972), Darby et al. (1972), and Segev et al. (1979). Board and Hall (1974a) came

to the idea, based on their experiments, that explosion propagation can occur through pressuredriven vapor blanket collapse; i.e. a local interaction increases the pressure in the surrounding liquid sufficiently to collapse the vapor blanket in a large area of the adjacent material, and hence trigger the explosion. One of the fragmentation mechanisms, presented by Board and Hall (1974b), was Rayleigh-Taylor or Kelvin-Helmholtz instabilities which could occur in the explosion pressure fields. Cooper and Dienes (1978) investigated the growth of Rayleign-Taylor instabilities following the deceleration of fuel by a less dense coolant using the method of generalized coordinates, which allows one to study the nonlinear late time aspects of the problem as well as the possibility of fuel freezing at the surface. They considered the liquid coolant in contact with three possible states of fuel -- pure liquid, pure solid, and liquid fuel freezing at the interface -- and treat three acceleration mechanisms -- drag deceleration, pressure pulse and thermal gradient impulses due to the expansion of the coolant layer heated $u\dot{p}$ (Coffield and Wattelet, 1970). Sharon and Bankoff (1978b) showed that the Taylor instability alone is too slow to support a thermal detonation wave if the dimensionless breakup time is calculated based on the experimental correlation given by Simpkins and Bales (1972) and Reinecke and Waldman (1970). The dimensionless breakup time is given as

$$T_b^* = \frac{Ut_b(\frac{\rho}{\rho_d})^{1/2}}{r_d(\frac{\rho}{\rho_d})^{1/2}} \tag{19}$$

$$\approx 2 \text{ F Bo}^{-1/4}$$
 (20)

where Bo is Bond number given by

$$Bo = \frac{\rho_d a r_d^2}{\sigma} \tag{21}$$

and r_d : the radius of the drop

 $\bar{\rho_d}$: the density of the drop

tb: breakup time a: acceleration

22 (Simpkins and Bales) 68 (Reinecke and Waldman)

1.5 (Patel and Theofanous) based on a different breakup definition.

If the correlations of Patel and Theofanous (1978) were used, a detonation wave might be supported under a specific set of assumptions such as dimensionless breakup depending only on the relative velocity at the shock front. Theofanous et al. (1979) considered Taylor instabilities as a relevant mechanism of hydrodynamic fragmentation in propagating thermal explosions with molten metals based on their experimental and analytical work. Pilch (1980) derived a mechanistic model for droplet breakup for We < 50 and the general concept of multistage breakup at higher Weber numbers. Chu (1984, 1985, 1986) used this general concept and developed a mechanistic droplet breakup model based on Taylor instabilities and boundary layer stripping.

The interface between two different liquids becomes unstable when there exists a parallel relative velocity between the liquids. This phenomenon, a Kelvin-Helmholtz instability, can be observed on a lake when the wind blows over it. Paoli and Mesler (1968) indicated, in their experiments of lead/water interactions, the formation of ripples on the metal surface was due to the Kelvin-Helmholtz instabilities induced by the relative velocities. Flory et al. (1969) observed similar instability growth in tin/water and mercury/water interactions. In injection experiments, Bradley and Witte (1972) observed hydrodynamic instabilities in the form of a wavy jet. However, it is pointed out that no extensive breakup of the jet was caused by these hydrodynamic effects. Colgate and Sigurgeirsson (1973) have interpreted lava/water interactions as involving both Kelvin-Helmholtz and Rayleigh-Taylor instabilities. It is considered that the Kelvin-Helmholtz instability has a significant effect during volcanic crater formation as well as during entrainment.

In boundary layer stripping, the tangential components of flow at the drop surface exert a shearing force, which sets the layer at the edge of the drop, i.e. the boundary layer into motion. When a specific relative velocity is exerted, the boundary layer detaches itself and breaks up into a fine mist of droplets. The mechanism for this process is still not clearly understood. Benz and Schriewer (1978) explained the mechanism could be the centrifugal forces exerted on the boundary layer due to its motion or unstable growth of capillary waves triggered at the stagnation point. Sharon and Bankoff (1978a) used boundary layer stripping mechanism in their modeling of propagation of shock waves through a fuel/coolant mixture. Schriewer et al. (1979) investigated the fragmentation of single drops struck by a stationary shock wave. They studied the effects of deformation as well as fragmentation due to pure boundary layer stripping and surface instabilities. It was suggested that pure boundary layer stripping without additional effects, such as surface waves, is not effective enough to be an important fragmentation mechanism. Both Taylor instabilities and unstable capillary waves may cause fragmentation of drops in a very short period of time $(T^* < 5)$, thus speeding up the stripping process. Baines et al. (1980) applied this hydrodynamic fragmentation mechanism to their large-scale fuel coolant interaction modeling and found hydrodynamic fragmentation is efficient over a wide range of conditions. They expected large velocity differences between fuel and coolant behind the steep pressure rise of the shock front in their tests. In the experimental investigations they found the dimensionless breakup time, T_0^* was in the range of 3 to 5. Their data suggested that the boundary layer stripping was dominant at We = 100 to 2000.

Besides those hydrodynamic fragmentation models, various hydrodynamic-type fragmentation-intermixing models have been developed. Robert (1972) considered the exponential increase of liquid-liquid interface with time when one liquid is entrained in the other as a result of spiral vortices. Under the estimation of the turbulent velocity which is considered to be proportional to the square root of the energy content of the vortex, the increase in surface area becomes

$$A = \frac{A_0}{\left(1 - BT/A_0\right)^2} \tag{22}$$

where Ao is the initial surface area, and B is a constant dependent on a number of scaling factors concerning the kinematics of turbulence and associated energy dissipation process. However, it is not certain how the constant B is to be evaluated. The assumption of vortex-type geometry for the intermixing of two dissimilar liquids may not be valid for the case where rapid heat transfer and phase change occur, with vaporization of the cold fluid and solidification of the hot material. In addition the source of energy for the initiation of vortices was not clear. Bruckner and Unger (1973) developed a somewhat similar turbulent mixing model. They coupled the kinetic energy of the turbulent field with the heat flux between the hot and cold liquid. It was assumed that a certain portion of heat was converted into mechanical energy. However, the same problems still remained to be solved.

The hydrodynamic effects, usually identified as Weber number effects, definitely tend to cause fragmentation of molten materials. However, since the breakup of the hot molten material often occurs in small velocity differentials for dropping experiments, the fragmentation process is not likely to be controlled by hydrodynamic effects alone, although such effects may enhance breakup. As the scale of interaction increases the potential exists for the relative velocity to become large (see Board and Hall's (1972) detonation model), and these hydrodynamic instabilities could become dominant. However, at large scales one of the key issues becomes escalation to this state where hydrodynamic effects dominate. The question to be considered here is whether the rate of fragmentation is sufficient to account for the short energy release times required for an explosion escalation as well as propagation. The consequence of the hydrodynamic-induced fragmentation should be studied further in relation to the properties of materials involved and the contact mode of the systems in the interactions.

- 3.1.2 <u>Thermal Effects</u> Thermally initiated fragmentation mechanisms were categorized as being due to either boiling effects, internal pressurization effects, or solidification effects depending upon the source of energy for fragmentation. However, the processes of fuel-coolant interactions cannot be easily categorized into any single subclass, but may span more than one category.
- 3.1.2.1 <u>Boiling Effects</u> When a molten material is introduced into the cold liquid, it undergoes a quenching process. The quenching process can be explained in terms of the conventional boiling curve as shown in Fig. 20.

As soon as molten material submerges into the cold liquid a continuous vapor film blankets the surface of hot material if the temperature difference is high enough. The major resistance to heat transfer in film boiling is confined to this vapor film. Film boiling is hydrodynamically "quiet", i.e. there is little turbulence attributed to the boiling process. Vapor is removed from the layer in the form of bubbles released regularly both in time and space. As the temperature of the molten material drops from 1 to 2, the heat transfer rate decreases.

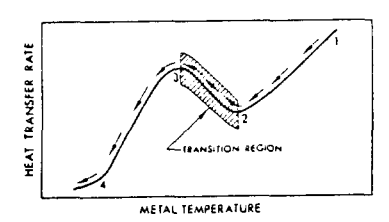


Fig. 20. Heat transfer behavior for quenching high-temperature molten metal. (Witte 1973)

At point 2 the vapor film becomes unstable and collapses toward the surface of the material. However, the material is still above the boiling point of the liquid and the film is reestablished. In this transition region, liquid periodically contacts the heating surface. The transition can be very violent, hydrodynamically, and continuous until the nucleate boiling regime is attained at point 3.

In the nucleate boiling regime from point 3 to 4, bubbles form at specific sites on the surface. This regime is somewhat turbulent due to the growth and collapse of bubbles adjacent to the surface. However, the level of violence is generally lower than that of the transition regime. The surface temperature decreases very slowly for a relatively large change in surface heat flux. Below point 4, the temperature of the material has decreased to the saturation temperature of the cold liquid. The heat transfer mechanism no longer involves phase change but is simply ordinary natural or forced convection.

In their experiments, Swift and Baker (1965) suggested that the driving force for breakup might be the violent growth and collapse of vapor bubbles which are the characteristics of subcooled boiling in the transition and nucleate boiling regimes. This mechanism suggests that fragmentation cannot occur unless the melting temperature of the hot liquid lies below the Leidenfrost point of the boiling curve for the system. Moreover, fragmentation cannot occur when the hot liquid temperature exceeds the critical temperature of the cold liquid. The difference in the interaction behavior between water and sodium -- fragmentation of the molten metal in sodium but not in water -- was attributed to the difference in the temperature region of violent boiling between them. This mechanism was shown not to be universal for the platinum/mercury system by Swift and Pavlik (1966), where a sample of platinum at 1900°C suffered from fragmentation when dropped into mercury (critical point 1450°C). Even though they did not consider that there is an important problem about wetting and contact temperature with mercury, the mechanism approximately holds for a number of other materials in contact with liquid sodium, water, or liquid nitrogen.

Witte et al. (1973) indicated that the violent boiling hypothesis was not valid because of the time scales involved. In their experiments they found that the entire interaction occurred in a slightly longer time period than the oscillation time for vapor collapse and reformation around small spheres found by Stevens (1971). Therefore, if transition has any effects upon fragmentation initiation, it must occur in the initial collapse of the vapor film. The violence caused by collapse and reformation of vapor was not thought to be significant since there is insufficient time for its development. In turn they suggested the impact pressure upon vapor collapse, reduction in interfacial surface tension upon liquid-liquid contact, and thermally controlled phenomena such as the superheating of the cold liquid as fragmentation mechanisms either individually or collectively.

Cho and Gunther (1973) performed a series of experiments with varying water and molten metal temperatures. Figure 21. shows the effects of water subcooling on the extent of fragmentation for molten bismuth, silver chloride, and tin, where the extent of fragmentation decreases with the water temperature. In an attempt to understand the subcooling effects, Cho et al. (1974) considered the Swift and Baker (1965) hypothesis where the violence of bubble growth and collapse was supposed to increase with water subcooling to comply with the experimental results. An indication of violence might be the liquid kinetic energy associated with the bubble growth and collapse. Bankoff and Mikesell (1959) analyzed Gunther's data (1951) of bubble growth and collapse, considering only the effects of liquid inertia and came up with two parameters, the mean effective pressure difference between the surroundings and the bubble given as

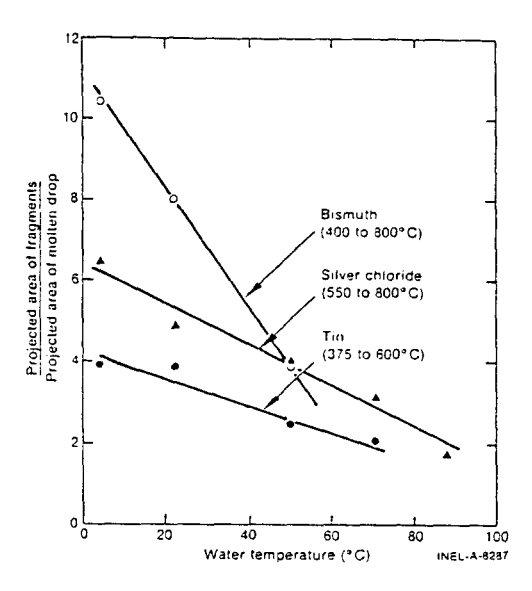
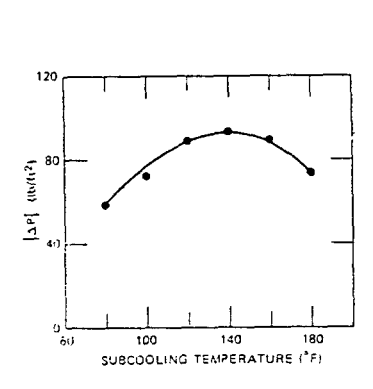


Fig. 21. Fragmentation of molten metals dropped into water illustrating effect of coolant sub cooling

$$W = \frac{4}{3} \pi R_{\rm m}^2 \left| \Delta P \right| \tag{23}$$

where R_{m} is the maximum bubble radius and ΔP may be considered as the driving force for bubble collapse. This work represents the potential energy of the liquid at the instant of maximum bubble size which can be equated to the kinetic energy of the liquid when the bubble size is very small. Figures 22 and 23 show the effects of the water subcooling. At high



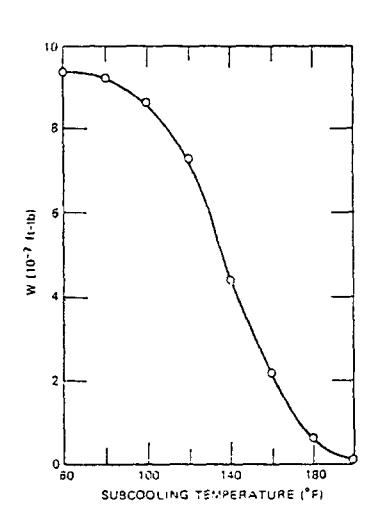


Fig. 22 Fig. 23

Bankoff's and Midesell's Interpretation

subcooling $|\Delta P|$ passes through a maximum and then decreases as subcooling increases. In Fig. 21 the bubble energy decreases strongly as the subcooling increases. These results seem to contradict the observed trends of fragmentation data. However, Cho et al. pointed out that Gunther's data pertain to boiling from a solid surface whereas the process of fragmentation presumably involves boiling from a liquid surface. The nature of bubble nucleation from a liquid surface could be quite different from that for a solid surface. Another question that still remained concerns what would happen to the molten tin samples rest on the filter paper in water. The initial temperature of tin was high enough to cause film boiling upon liquid-liquid contact. The molten material should have gone through the transition and nucleate boiling regimes as the material cooled down and fragmented according to the violent boiling hypothesis. However, the experimental data showed that they eventually solidified without further fragmentation. The absence of fragmentation could be interpreted as a result of the lowering of minimum film boiling point due to the local heating of water surrounding the hot material. Even in this case the violent boiling criteria does not provide a complete explanation for the apparent nonfragmentation of tin samples that rest on the filter paper.

Several variations of the bubble growth and collapse models have been developed to describe the fragmentation process. Usually such modeling has been performed in conjunction with small-scale experiments of a free-contact mode. Anderson and Armstrong (1974) suggested the dynamic impact heating model based on the experiments (NaCl-H $_2$ O and UO $_2$ -Na). The model considers the dynamics in the initial contact between liquids and assumes a sequence of events to occur:

- Initial mixing of liquids -- one liquid will become entrapped in the other liquid with a gas and/or vapor layer separating the two.
- 2. Collapse of gas/vapor layer due to an external force.
- 3. High heat transfer and vaporization of cold liquid upon liquid/liquid contact.
- 4. Subsequent behavior of the system is determined by the fraction of cold liquid vaporization during a single contact. Large vaporization fractions can cause an explosion with one liquid/liquid contact. Smaller vaporization fractions require multiple liquid/liquid contacts with each contact generating vapor and driving the remaining cold liquid back into the surrounding hot liquid.

The crucial assumption in the sequence proposes that two liquids, driven together, can transfer large quantities of heat in the short periods.

Caldarola and Kastenberg (1974) presented a mathematical model for the fragmentation of UO during the molten UO $_2$ /sodium thermal interactions. Assuming spherical symmetry, bubble growth is described by the Rayleigh equation:

$$\ddot{R}R + 1.5 \dot{R}^2 = (P_b - P_{\infty})/\rho_C$$
 (24)

where:

R : bubble radius $P_b\colon$ bubble pressure $P_{\varpi}\colon$ ambient pressure.

The initial conditions for the vapor growth were those of unstable film boiling shown in Fig. 24. The bubble was assumed to grow up to the time the inertial force from the surrounding

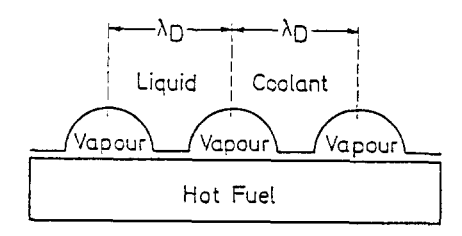


Fig. 24. Idealized model for film boiling on a hot surface. (Caldarola 1974)

liquid becomes zero and begin to collapse. Due to the asymmetric bubble collapse, instabilities in the form of microjets are produced at the vapor/liquid interface. It is the impingement of

these microjets upon the fuel surface which produces fuel fragmentation. As a result of local impingement an elastic wave is assumed to be generated in the molten fuel. From acoustic approximation the transmitted energy due to jet impact is given by

$$E_{tr} = 2\pi R_{jet}^{2} t_{st} \frac{P_{st}(P_{st} - P_{w})}{\rho_{f} C_{o}} \left[1 + \frac{C_{o} t_{st}}{R_{jet}}\right]$$
 (25)

where:

 R_{jet} : radius of jet P_{st} : stagnation pressure upon impact tst : duration of the stagnation pressure C_{o} : speed of sound in the fuel ρ_{f} : density of fuel

The ratio of transmitted energy to the available potential energy of bubble then becomes

$$\varepsilon = \frac{\varepsilon_{tr}}{\varepsilon_{b}} = 1.92 \frac{\rho_{c}}{\rho_{f}}. \tag{26}$$

The energy dissipation in the fuel due to impingement is only a small fraction of the bubble work and much less than that required to account for fine-scale fragmentation. Therefore, this mechanism cannot completely explain the fragmentation process and the acoustic energy deposited in the fuel usually gives a larger predicted fuel radius than those found in experiments.

Buchanan (1973) proposed a cyclic process of fuel fragmentation, where the interaction is divided into five stages: an initial perturbation which triggers the interaction and causes a vapor bubble to form at the fuel/coolant interface; bubble expansion and collapse with jetting; penetration of the fuel by the liquid jet; heat transfer from the fuel to the jet; the formation of new bubble. The process then repeats itself from the second stage (see Section 3.3 for details). This mechanism was accepted to be one of those leading to a fine fragmentation of fuel by Board and Hall (1974b) in large scale explosions. Board et al. (1974) argued that this mechanism can account for both the time scale and energy transfer rate characteristic of thermal explosions, including those in a shock tube geometry.

Vaughan et al. (1976) criticized Buchanan's model because it suffered from the lack of an initial perturbation which allows for entry into the cyclic process. They suggested that the triggering had two well-defined stages. First, direct contact between two liquids, without an insulating layer of vapor, occurs; secondly some phenomenon takes place which provides the entry into the cyclic process of bubble growth and collapse. This unknown phenomenon was claimed to be initially connected with the breakdown of film boiling.

Benz et al. (1977) proposed a "steam bubble collapse" model to describe the course of fragmentation of liquid melt in water. Two preconditions which were deduced from their preliminary experiments were used for the development of the SBC model: (a) the melt fragments in the liquid state; (b) vapor-film collapse proceeds fragmentation. Hence they assumed no partial vapor film, but bubbles on the surface of the molten metal, although the liquid surface with great superheating is present. Basically the approach taken is to calculate the heat removal rate from the molten surface assuming a nucleate boiling heat transfer mode. The growth in a bubble radius was described as a function of time as given by Beer (1969),

$$r_b(t) \frac{1}{2} \left[0.234 \left(\frac{\kappa_c}{\rho_c i_{fg}}\right) \left(\frac{\rho_c \sigma_c}{\mu_c^2 \Delta \psi}\right)^{0.55} Pr_c^{1/3}\right]^{0.58} \left(T_s - T_c\right)^{0.69} t^{0.69}$$
 (27)

 $T_s\colon$ is the surface temperature of hot liquid $K_c^s\colon$ is the conductivity of the cold liquid $i_{fg}\colon$ is the latent heat for vaporization of coolant

 $(\frac{\sigma}{\Delta M})$: is the change of surface tension with bubble central angle

Some of the bubbles grow to such an extent, reaching a certain size, that they separate from the melt surface; the rest of the bubbles collapse. The collapse of the bubble and the increase of surface area of hot liquid continues until the molten material solidifies. The model assumed that the work required for surface formation comes from the energy released in the collapse of a steam bubble. Only a certain fraction of the bubble energy was allowed to be transferred to the molten metal. An iterative calculation was made for each bubble growth-collapse period, during which time an assessment was made of the heat transfer process associated with solidification of the molten metal. This parametric model showed that the higher the tin temperature, the sooner fragmentation begins, and the greater was the surface area attained. The degree of fragmentation increased with increasing melt mass. However, the effects of water subcooling contradicted the experiments. The fraction of bubble energy transferred to the fuel for fragmentation, number of bubbles to be collapsed, and the heat transfer coefficient from the fuel to the cold liquid assumed in the modeling were quite arbitrary.

Another fragmentation model by the coolant impact was presented by Drumheller (1979). By using the variational method, he coupled the heat transfer process of film boiling with the motion of the vapor film surrounding the molten metal drop. In his model complete symmetrical film collapse and the impact of coolant onto the fuel drop were initiated by applying a disturbance to the system. By using a one-dimensional wave propagation code the pressure behavior in the interior of the drop was calculated. His model showed that even modest impact velocities of coolant can produce a large pressure in the interior of the drop. As the wave front reflects at the drop center, large pressure gradients are generated behind the wave front that eventually drive the material in the center of the drop toward the boundary of the drop. This outward motion of material causes a sharp decrease of pressure at the centerline of the drop. The pressure in the core of drop then falls to zero, resulting in extensive fragmentation of the drop within the region. The existence of the vapor film apparently enhances the fragmentation process and the vapor film must completely collapse to initiate fragmentation in his model. The impact pressure was found to be suppressed by the elevated pressure due to the increased stiffness of the vapor film. This model explained only the criteria for the fuel fragmentation due to the pressure gradient, not the microscopic process of surface area increase during fragmentation. Also the time over which the pressure within the fuel remains negative is quite short and may not be sufficient to allow for fragmentation. Finally, the behavior of the film vapor pressure, which remains relatively low during the entire process of film collapse, seems doubtful theoretically, based on the subsequent analysis of others (Corradini, 1981; Kim, 1984, 1985).

Vaughan (1979) made an attempt to develop theoretical arguments to determine the size of the debris from energy considerations, where the kinetic energy of the drop is used to account for the formation of new surface area, frictional dissipation as the debris is separated from the parent drop, and kinetic energy of the debris. By estimating the breakup time from the Simpkin and Bales correlation, the lower limit for the uniform size of the particle is given by

$$r_{d} = \frac{\left[\frac{3}{\rho_{d}} + \frac{8}{\rho_{c}} + \frac{(6c_{D})^{3/4}}{(\rho_{c}\rho_{d})^{1/2}}F\right] \sigma_{dc}M_{d}}{0.5 M_{d}V^{2} + S\sigma_{dc}}$$
(28)

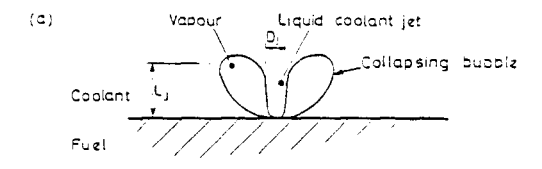
where M_{d} is the initial mass of the drop and S is the initial surface area of the molten metal. He applied this general debris size theory to Buchanan's model as shown in Fig. 25. The energy given up in the rapid vaporization and expansion of the dispersed coolant drop entrapped in the fuel is transferred as kinetic energy to the fuel slugs above it. In estimating the energy transferred, it was assumed that once the fuel slug has moved a distance equal to its own length, d_{D} , the vapor vents and does no more work. From adiabatic expansion of the vapor, the debris size is given as

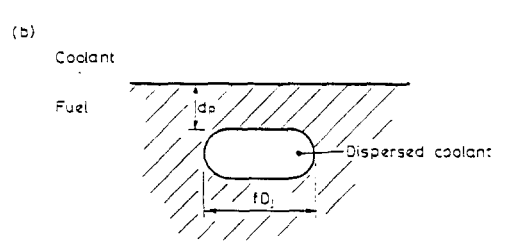
$$r_{d} = \frac{(\gamma - 1) \left[\frac{3}{8} \frac{\rho_{d}}{\rho_{c}} \frac{(6C_{0})^{3/4}}{(\rho_{c}\rho_{d})^{1/2}} F\right] f^{2} (\rho_{c}\rho_{d})^{1/2} \sigma_{dc}}{\rho_{I} \left[1 - \left(\frac{1}{1 + f^{2} (\rho_{c}/\rho_{d})^{1/2}}\right)^{\gamma - 1}\right]}$$
(29)

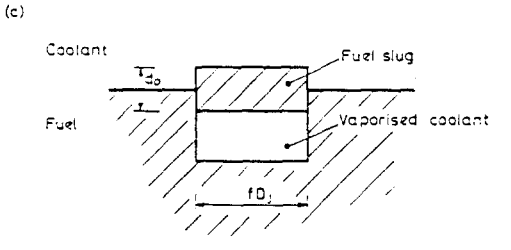
where: γ is the ratio of gas specific heats P_{T} is the initial pressure of vapor $f \ge 1$ since the jet spreads as it moves into the fuel.

The minimum size of the slug below which it solidifies before the breakup under the influence of inertial forces was also derived. These calculations were preliminary and numerous assumptions were involved. The model shows interesting aspects of fragmentation of fuel upon jet penetration and gives reasonable agreement with those experiments considering the approximations used.

Limit-of-superheat theory (spontaneous nucleation) was also considered as the driving force for the fuel fragmentation. For the liquid/liquid contact, because of the lack of nucleation sites, the temperature of the cold liquid can be raised well above the normal boiling temperature. There exists a point where the superheated liquid can no longer remain in a liquid







- (a) Formation of jet
- (b) Heating of coolant / fuel mixture
- (c) Ejection of fuel slug by expanding vapour

Fig. 25. Schematic view of the jet penetration model. (Vaughn, 1979)

state. At this temperature, the spontaneous nucleation temperature, vaporization occurs very rapidly. The spontaneous nucleation rate J per unit volume of liquid due to statistical density fluctuations can be calculated from

$$J = wN \exp[-W/K_bT]$$
 (30)

where: N is the number of molecules per unit volume of liquid

w is the collision frequency

K_B is the Boltzmann constant

W^D is the reversible work of formation of the critical embryo given by

$$W = \frac{16 \pi \sigma^3}{3(P_V - P_C)^2} \tag{31}$$

and P, is the pressure in the vapor.

Fauske felt that vapor explosions would only occur when the interfacial liquid-liquid contact temperature was at or above this spontaneous nucleation threshold. In particular, Fauske (1973) presented a mechanism considered to be responsible for the explosive vapor growth observed in Armstrong's (1971, 1972) experiments where liquid sodium was injected into a molten $\rm U0_2$ pool. Basically the liquid sodium globule was entrapped and wets the liquid $\rm U0_2$ surfaces. The postulated lack of nucleation sites in liquid-liquid-like systems would result in the overheating of the liquid sodium. When the superheat limit is reached vaporization is rapid enough to produce shock waves. The shock wave then fragments the fuel. However, this mechanism could not explain the extensive fragmentation observed in Armstrong's experiments (1970a, 1970b, and 1970c) of a small amount of $\rm U0_2$ dropped into a large sodium bath since the $\rm U0_2$ -Na contact temperature was found to be well below that for spontaneous nucleation. The assumption of lack of nucleation sites is in contrast with the experimental observation of violent boiling. The existence of gas or impurities in the cold liquid might promote the boiling prior to reaching the threshold for spontaneous nucleation. In addition, Anderson and Armstrong (1977) reported data in which the contact interface temperature for a R-22/water system was below that for homogeneous nucleation (53°C), yet violent interactions occurred. Henry and Fauske (1976, 1979) proposed a drop capture model, which was a modification of the original spontaneous nucleation model based on the stability criterion of the cold liquid drop, as the mechanism leading to explosive boiling in the free contacting mode (see Section 3.3 for details).

Ochiai and Bankoff (1976) proposed a "splash" model which was a self-mixing theory for the initiation and early propagation stages of vapor explosions. Random local contacts were assumed to occur between the two liquids, which are separated by a vapor film, due to capillary instability of the vapor film. The contact above the spontaneous nucleation temperature then leads to the growth of a large number of bubbles which coalesce into a high pressure vapor layer at the liquid-liquid contact area. This amounts to an impact pressure applied to the free surface and results in a certain velocity distribution in the liquid. As the impulse provided by this pressure is transmitted to the fuel an annular jet forms around the initial contacting tongue of the solid liquid and crosses the vapor space. Subsequent impact of an annular jet on the opposite liquid promotes further liquid-liquid contact and the propagation step can lead to exponential growth of the interaction zone provided that the splash velocity is above the threshold value and the contact is made over an area at least equal to the original contact area. The evidence of this mechanism is quite sparse. The model lacks the effect of solidification, and energetic triggers, such as the acceleration of the two liquids toward each other on the arrival of a strong pressure pulse. The model cannot explain the occurrence of explosions at the contact temperature well below the spontaneous nucleation temperature.

Coffield and Wattelet (1971) suggested a fragmentation mechanism, which is due to the acoustic pressure pulse generation in the cold liquid, as a consequence of the heating and thermal expansion of the coolant layer at the fuel-coolant interface for UO2/Na interactions. The conservative assumption made was that when the average pressure of the entire pulse over the unheated sodium layer, from the interface to the location of the pressure leading edge, falls below saturation pressure corresponding to the interface temperature coolant boiling begins. Hence the maximum energy available for breakup was evaluated from the energy contained in the pulse. In addition, a completely rigid system with perfect contact had to be assumed to induce a significant sodium pressurization. Even with these assumptions Cronenberg (1972) found the maximum energy associated with the postulated thermally induced acoustic pulse was approximately three times smaller than the estimated surface energy of the UO2-Na interface. Thus he concluded that this mechanism could not account for the observed fuel breakup.

The mechanism of violent vapor bubble growth and collapse has the advantage of potentially being the one mechanism able to account for both the fragmentation and pressure pulse for molten fuel/coolant interactions. It can describe the spatial propagation of the interactions very clearly since the increase in pressure from a local interaction may cause the collapse of adjacent vapor regions. The role of spontaneous nucleation, in general, is not completely understood. Spontaneous nucleation seems to result in the rapid vapor formation rather than the suppression of vapor bubble growth with enhanced heat fluxes. Vapor bubble-growth-and-collapse alone does not seem to account for the violent, extensive fragmentation. It might provide more potential for the explosion if violent boiling of the cold liquid results in the certain fine fuel/coolant mixtures and spontaneous nucleation of the cold liquid then occurs with some constraints supporting the nucleation process. Nevertheless this review indicates that most of the models proposed were found lacking in the microscopic process of fine fragmentation of the molten fuel. A detailed physical picture of the fragmentation process would be necessary to evaluate the validity of any proposed hypothesis.

3.1.2.1 <u>Internal Pressurization Effects</u> For hydrodynamic and boiling effects, the driving force for the fuel fragmentation is exerted on the surface of the molten fuel and this can be called externally driven fragmentation. It is also possible that internally generated pressures cause the breakup of the surrounding molten fuel. Internal pressurization can be induced by

coolant entrapment, coolant encapsulation, acoustic cavitation, and release of dissolved gas.

Long (1957) introduced the entrapment fragmentation concept based on the experiments of dropping a large quantity of molten aluminum in water. The fragmentation was claimed to be induced by the evaporation of water entrapped between the hot molten metal and a solid surface. This mechanism could explain the breakup of the molten metal in a relatively shallow pool of the cold liquid. It was experimentally shown that when entrapment of water was made difficult by greasing or painting the bottom of the water container, fragmentation of aluminum was prevented. Hess and Brondyke (1969) supported Long's hypothesis and described three types of explosions: moderate, violent and catastrophic explosions depending upon the extent of the violence. Witte et al. (1971) confirmed the entrapment theory; however, a somewhat different hypothesis concerning the initiation mechanism resulted. The alternate hypothesis concerns the "bonding" characteristics between the metal and the surface of the container. If, when the molten metal encounters the bottom of the container, a good bond between the metal and the surface forms, the vapor formed from the entrapped layer of the cold liquid under the metal cannot be relieved and high pressures are generated and break up the molten metal. Evidence of this was seen when aluminum samples were dropped into a glass dish filled with water. The sample penetrated to the bottom was observed to "dance" around on the bottom. Perhaps the addition of oil-base or other coatings prevents bonding rather than prevents wetting as suggested by Long. Similar entrapment was observed by Sallack (1955) when molten smelt was poured into water or green liquor.

Brauer et al. (1968) observed the growth and rupture of large bubbles formed from a molten metal during the quenching of the moiten aluminum in water. Usually molten lead formed a "spongy" like quenched debris and did not show the evidence of boiling, which was not in accordance with a violent boiling hypothesis. From these observations, they suggested the following mechanisms: The molten metal drop, upon contact with the quenched liquid or shortly after, forms a solid shell due to rapid heat transfer from the metal surface. Somehow, some of the cold liquid is trapped inside this shell. The trapped liquid is rapidly vaporized and produces a large internal pressure in trying to escape. The interior molten metal, due to this internal pressure, breaks through the weakest part of the material shell and is dispersed. The method of quench-liquid entrainment was not clearly understood. A possible explanation was that the cold liquid was forced through a porous solid metal due to the voids formed by an increase in the interior metal density.

Paoli and Mesler (1968) tested the hypothesis of Brauer et al. (1968). A particular effort was made to investigate the manner in which liquid encapsulation occurred and to link the eruption of molten metal with the explosion. They observed the formation of ripples by the Kelvin-Helmholtz instability on the molten metal surface. These ripples were suggested as one method of water encapsulation beneath the molten metal surface. Flory et al. (1969) observed similar trends of surface instabilities. They found the presence of the cold liquid sealed inside the solid metal in some nonfragmentation experiments, and the water bubble formed in polyethylene. However, at high temperature, the explosions occur so soon after entry into the cold liquid that it is difficult to conceive that there would be sufficient time for the ripples of the hot molten metal to entrap the cold liquid.

Caldarola and Kastenberg (1973) proposed a schematic diagram for the fragmentation process which contains five transients:

- 1. Initial liquid-liquid direct contact.
- 2. Superheated coolant boils and bubble growth occurs.
- 3. Entrapment of coolant droplets into fuel.
- 4. Explosive vaporization of these droplets produces fragmentation of the surrounding fuel.

However, the detailed descriptions of each stage and mathematical modeling were not given.

Schins (1973) proposed a sequence of events which might lead to such encapsulation and fragmentation, which is called the consistent boiling model for fragmentation in mild thermal interactions:

- Liquid-liquid contact which imparts a rapid temperature increase in the adjacent coolant layer.
- 2. Bubble and film generation.
- 3. Asymmetric collapse of bubbles in the transition boiling region. Though the collapsing pressure is 1 atm at the utmost, the collapsing force is considerable because it acts for far more time than the film generation transient. So there will result a definite impact accompanied by entrainment.
- Entrainment of coolant into the fuel caused by the asymmetric collapse and its cavitating resultant force.

5. Fragmentation. Instead of fuel surrounded by coolant, one has now the reverse situation of coolant droplet surrounded by fuel.

This sequence of transients is given in Fig. 26. Two important adaptions in this model are:

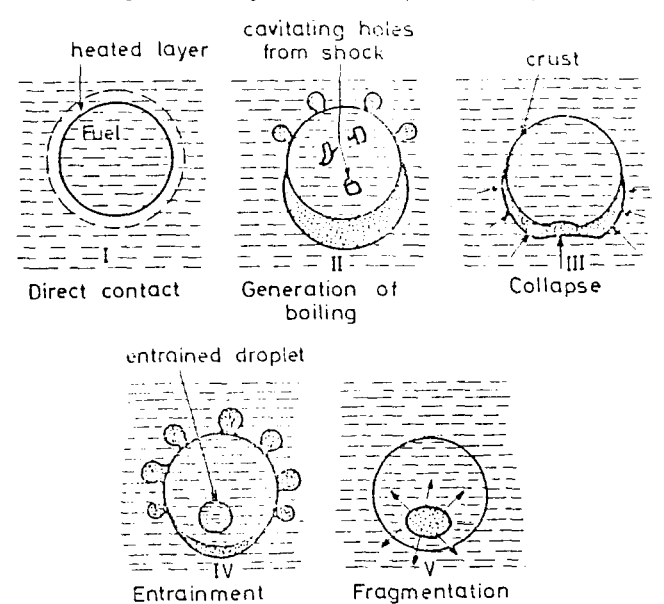


Fig. 26. Consistent boiling model for natural fragmentation

- 1. The temperature of the heating surface is not the fuel temperature, but the contact temperature.
- The coolant temperature is far lower than the saturation temperature. The result of this situation is that all the bubbles and films which grow in the thermal layer of the cold liquid will collapse after a short time.

Even though a mechanistic description is proposed, no quantitative analysis of the fragmentation process is given. Therefore it is not clear if this mechanism is energetic enough to cause fine fragmentation of the molten metal and can simulate the overall phenomena found in the experiments.

Kim (1985) studied the modeling of small-scale fuel-coolant interactions based on the experiments performed by Nelson and Duda (1982). The modeling of small-scale single droplet fuel-coolant interactions was conceptually divided into four phases, the last three of which could occur cyclically:

- 1. Film boiling around a molten fuel droplet in coolant;
- Film collapse due to an external pressure pulse and coolant jet formation due to Rayleigh-Taylor instability in a spherical geometry;
- 3. Jet penetration into the molten fuel and encapsulation in the fuel;
- 4. Expansion of the molten fuel surface due to the rapid evaporation of the encapsulated coolant and fragmentation of this fuel surface.

Figure 27. shows the schematic diagram of the process which is similar to that given by Schins. This model, though similar to past qualitative models, is unique in that it provides a complete mathematical description to predict the behavior of single droplet fuel-coolant interactions (see Section 3.3 for detail).

Kazimi (1973) proposed a cavitation-induced fragmentation process. The pressure at the molten surface due to the growth and collapse of a vapor film would exhibit positive and negative fluctuations about the initially uniform pressure in the molten drop-coolant system. A rapidly changing pressure at the surface of a molten material gives rise to pressure waves within the molten drop. As the pressure fluctuations created at the surface of a spherical particle travel toward the center of the particle, the pressure fluctuations are expected to be magnified. Therefore, subatmospheric pressures obtained at the surface can momentarily reach

very large negative values near the drop center, thus facilitating internal cavitation in the molten material which leads to the observed fragmentation. The theoretical negative threshold pressures required to create cavitation in molten material are estimated using an expression developed by Bernath (1951).

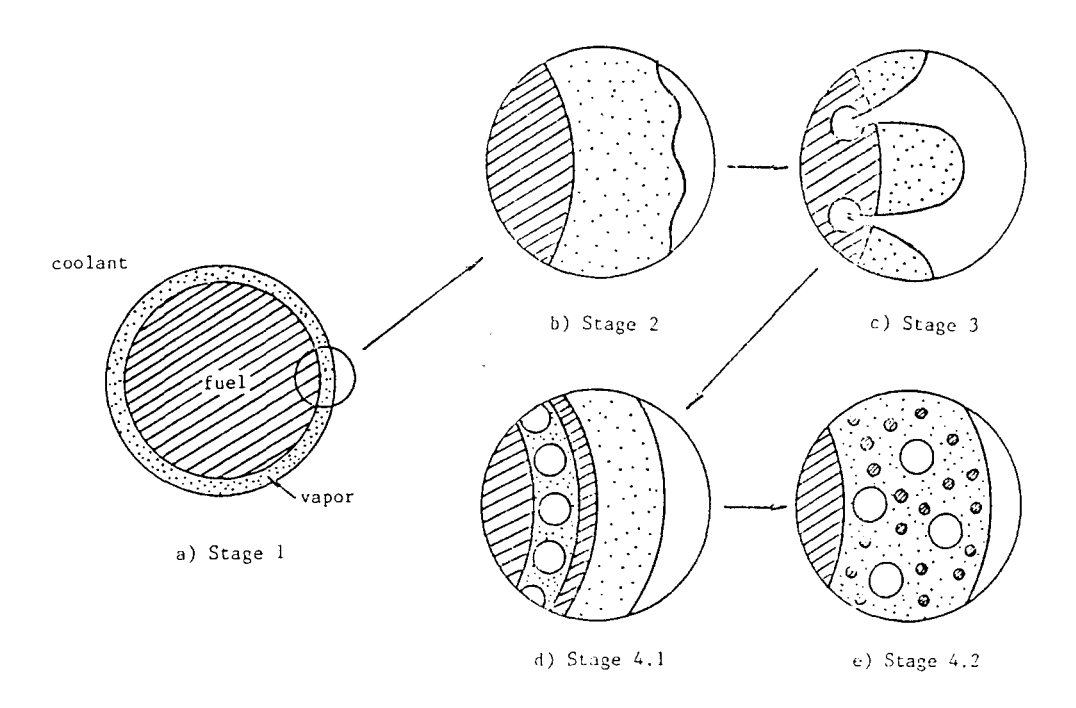


Fig. 27. Conceptual pictures of a small-scale single-droplet fuel-coolant interaction. (Kim, 1985)

$$P_{th} = \left[\frac{9.06 \, \sigma^3 / K_B T}{\ln \left(\frac{1.45 \, \rho N^2 \sigma^2}{P_{+b} M^3 / 2_R T} \right) - \frac{i_{fq}}{K_B T}} \right]^{1/2}$$
(32)

where:

K_B: Boltzmann's constant N: Avogadro's number M: Molecular weight R: Gas constant

The theoretical negative threshold values required for cavitation were found to be too large to be available in the molten metal/coolant system. However, cavitation may be obtained at smaller values of negative pressure if the molten material contains impurities or dissolved gases. Flynn (1964) estimated the threshold negative pressure by considering the presence of small amounts of gas in the molten droplet, which is given as

$$P_{th} = \Delta P + \frac{4\sigma}{3\sqrt{3} R_g} (1 + \Delta P \frac{R_g}{2\sigma})^{-1/2}$$
 (33)

where: $\Delta P\colon$ difference between system and vapor pressure $R_\alpha\colon$ radius of gas nuclei.

Even if such a cavitated bubble could nucleate in the molten metal, it must continue to grow in

an oscillating pressure field. Thus the rates of bubble growth must be greater than the rates of bubble collapse to achieve a sufficient buildup of energy to induce the fragmentation of the molten metal. Since no assessment of either the work potential or the growth kinetics was made, the validity of the model is difficult to assess. Further studies into the dynamics of cavitation bubble growth and its potential energy buildup in the fluctuating pressure field seem to be necessary to test the hypothesis as a mechanism of fuel fragmentation. Nevertheless, Kazimi claimed that this mechanism seemed particularly suitable to explain the internal cavities produced in aluminum in the experiments of Flory et al. (1969), and the expansion in the size of the molten jet prior to the fragmentation in the experiments of Bradley and Witte (1972). However, Bjonard (1974) tested Kazimi's hypothesis and concluded that the acoustic cavitation could not explain his observations in similar experiments with tin. Further work by Bjorkquist (1975) using tin, bismuth and lead confirmed Bjornard's conclusions.

Rapid gas release from a metastable superheated solution has been proposed as a mechanism for fragmentation in metals. Epstein (1974a, 1974b) proposed the violent release of dissolved gas within the molten metal as the mechanism of fragmentation based on simple thermodynamic calculations and existing experimental observations. Initially dissolved gases are assumed to be present in the molten metal. During quenching the liquid becomes super-saturated such that the gas coming out of solution exerts extremely high pressures causing fragmentation. If the quenching rate is great enough and if the molten sample is sufficiently superheated above its melting point, violent dissolved gas evolution will occur just below the surface of the melt (within the thermal boundary layer) and tear the liquid surface layer from the sample. A fresh liquid surface is then exposed to the quenched liquid and the breakup process repeats causing a fragmentation wave to propagate through the melt and dividing the sample into small particles. This mechanism was believed to account for the observed time scale of extensive fragmentation. Under conditions of small dissolved-gas concentrations or low quenching rates, gas release will not be initiated just below the surface of the melt. Instead, the growing region of cold melt or solidified crust will expel the dissolved gas, so the concentration of the dissolved material in the hotter core region of the sample increases. Violent gas evolution, therefore, may occur at a relatively large distance from the sample surface. It was pointed out by Epstein that the main criticism of this mechanism is that the homogeneous nucleation of a gas bubble requires extremely high pressures because of the very large surface tension of the molten metal. In addition, to account for breakup by this mechanism requires that the molten metal be capable of dissolving gas without forming a stable phase, and the solubility of the gas in the molten metal must increase with increasing temperature. These are true for some low-melting-point materials; however, extensive fragmentation still occurred in some experiments performed by Zyszkowski (1975a) and Bjorkquist (1975), where metal/water systems were in an inert atmosphere. Gunnerson and Cronenberg (1975) demonstrated that the solubility characteristics of $\mathrm{U0}_2$ in the gases present in a reactor environment was unlikely to favor this mechanism.

A mechanism similar to that of Epstein in the other application field is the homogeneous bubble nucleation model proposed by Nelson (1965) and Meyer and Nelson (1970). In their experiments, explosions of falling zirconium droplets occurred as they burned at high temperatures (3000-4300 K) in nitrogen/oxygen mixture at 625 torr. The major observations were: (i) the intensity of explosion could be varied by changing the percentage of N_2 in O_2 ; (ii) no explosion occurred during combustion in pure O_2 when nitrogen was alloyed with zirconium prior to ignition; (iv) the solidified droplet quenched in liquid argon after burning partially in an N_2/O_2 mixture showed the presence of zirconium oxide, zirconium nitride, and several zirconium oxy-nitrides. In addition they noticed the physical appearance of the micro-bubbles with nitrogen inside at a threshold N_2/O_2 ratio and the retention of the entire original mass of metal in the droplet after inflation. With these observations, they concluded that the inflation and explosion were associated with the release of nitrogen gas in the superheated liquid. However, the required excess critical pressure for the homogeneous bubble nucleation was found to be unusually high based on the estimated values for the surface tensions of Zr-O-N systems. Levine (1971) showed that a simple bubble nucleation process alone was inadequate to account for the initiation stage of the Zr droplet explosion process. He claimed the existence of chemisorbed species on the surface of the embryos leads to a decrease in the required critical pressure to more reasonable values.

Buxton and Nelson (1977) proposed an impulse-initiated gas release mechanism primarily based on the results observed for steam explosion triggering experiments (Nelson and Buxton, 1977) in which the system was subjected to impulsive pressure transients. They considered the internal bubble nucleation process to be impulse initiated. The four basic steps required for the postulated impulse-initiated fragmentation process are:

- 1. The achievement of a large quantity of dissolved gas in the melt.
- The achievement of a supersaturation of dissolved gases in the melt as the melt cools due to the boiling of coolant on its surface.

- 3. Nucleation of the supersaturated gases by the applied transient.
- 4. The rapid growth of the gas bubbles in the melt interior causing fragmentation of the melt.

In the impulse initiated process, the applied impulse is assumed to be actually transmitted into the fuel interior, and reflects at the fuel/coolant interface as a tension pulse which then assists the dissolved gas latent pressures in nucleating a bubble against surface tension forces. Therefore only modest, and not extremely large, latent gas pressures are required for nucleation in this mechanism. Impurities in the molten metal also help initiate a nucleation process. However, many experiments were conducted in an inert or evacuated environment with short heating times, in the absence of known impulse triggers, yet violent interactions occurred. In addition, Nelson and Duda (1982) indicated that the gas released during the interactions was too small to account for the fine fragmentation observed. Although such a mechanism may be possible, no quantitative calculations were made on the energy associated with such gas release nor what was necessary to fragment the material.

In summary, in the encapsulation theory, if the encapsulted cold liquid droplets are heated up to the homogeneous nucleation temperature, the resultant pressurization might be energetic enough to cause fine fragmentation of the molten fuel. Besides, the cooling or the solidification of the molten fuel might provide some constraints for the pressurization, which would lead to more violent fragmentation. However, most of the models (e.g., gas release) are lacking in the detailed fragmentation processes, where the history of gas release or bubble growth kinematics, the pressure buildup, and required energy for the formation of new surface area are necessary. Since internal pressurization effects may account for the extensive fragmentation of the molten fuels and the appearance of the spongy-like particles observed for some of the fragmented materials, further studies on microscopic fragmentation processes in addition to the potential of fragmentation are needed. In fact a causal relationship is needed between the internal pressurization and an external initiator.

- 3.1.2.3 <u>Solidification Effects</u> In the fragmentation mechanisms described previously it was generally assumed that prior to and during fragmentation the quenched materials remained in the molten state. However, as the molten fuel cools in the cold liquid it solidifies. Such rapid quenching and solidification of the fuel may lead to the development of thermal stresses in the fuel. When the resultant thermal stress is greater than the yielding stress of the material fissures may develop in the outer frozen shell. Zyszkowski (1973) has observed the solidification of the molten metal in the form of a broken or empty shell and small jets of molten metal from the interior of the molten drop which solidifies in the form of a horn. Zyszkowski (1975b) interpreted the expulsion of jets of melt from the main particle as being due to the pressurization of the molten metal in a shrinking shell and the induced thermal stresses. He suggested that the "sharp-change" of the crystalline structure and the occurrence of the intercrystal forces during the solidification of the molten metal were the cause of the explosive fragmentation. Later Zyszkowski (1976) proposed a hypothesis based on the experiments of copper/water interactions, in which thermal explosion is divided into six phases:
- Initial phase -- the molten metal drop is surrounded by vapor film in the cold liquid.
- 2. Pressurization of the molten metal due to the solidification.
- 3. Expulsion of jets of small molten mass.
- Fast cooling of these metal jets, which establishes a liquid-liquid contact between the molten metal and the cold liquid.
- 5. Fast phase transformation followed by the growth and rupture of the metal particles.
- A vapor explosion occurs if the amounts of the heat transferred to the cold liquid is sufficiently large.

Pressure from shrinking of the solidifying outer layer of the fuel seems to force it out and cause bursting of the shell. However, in the experiments performed by Witte et al. (1971), bismuth, which expands 3% upon freezing, fragmented in similar fashion to tin and lead. Thus, this provided one good example of violent fragmentation in the absence of shrinkage. The breakup of mercury also shows evidence of fragmentation without solidification of the material.

One of the principal concerns of the shell solidification concept is whether or not crystallization occurs at the quenching surface for the short times of interest in thermal interactions, which are on the order of several milliseconds. Basically the freezing process is essentially a reordering of molecules from the less structured liquid state to the more ordered crystalline structure and as such involves both energy exchange and molecular movement, which are accomplished over a finite period of time. Cronenberg and Fauske (1974) investigated the kinetics of crystal formation and growth and compared with the heat transfer controlled solidification rate to determine whether or not the surface of $\rm UO_2$ can remain molten if contact is established during quenching in sodium coolant. The criterion for the liquid to nucleate into a solid is proportional to the product of the embryo density and the collision frequency. The rate of nucleation-site activation is given by Volmer (1945) and Turnbell (1950) such that

$$J = 10^{33} \exp\left[\frac{16 \pi \sigma_{s1}^{3} T_{E}^{2}}{3\rho^{2} L_{f}^{2} \Delta T_{R}^{2} T_{E}^{3}}\right]$$
 (34)

where: σ_{s1} : interfacial energy

 T_F : melting temperature

ΔT: T_E - T

K_R: Boltzman constant Lf: latent heat of fusion.

The rate of solidification as a function of temperature is determined by predicting the likelihood for a molecule to cross the liquid-solid surface as developed by Jackson and Chalmer (1951). The rate of crystallization is expressed in terms of the interface velocity, which is given by

$$R (cm/s) = VNGV [A_L e^{-Q(f)/RT} - A_S e^{-Q(m)/RT}]$$
 (35)

where: V: molecular volume of the solid

N: the number of molecules per unit area

G: geometric factor

v: Debye frequency.

 $\rm Q(f)$ and $\rm Q(m)$ are activating energies for freezing and melting; $\rm A_f$ and $\rm A_m$ are accomodation coefficients for freezing and melting. To determine whether the molten fuel droplet will freeze, the heat transfer process was studied with an instantaneous boundary condition. For the case of ${\rm UO}_2$ and sodium, the contact temperature is well below the homogeneous crystallization temperature and the estimated rate of crystal growth is greater than the heat transfer controlled solidification velocity for times greater than 1 ms. As shown in Fig. 28, the

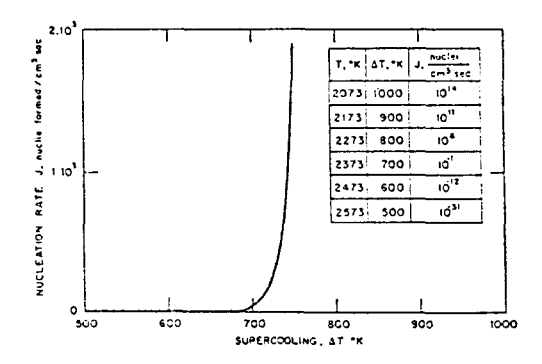


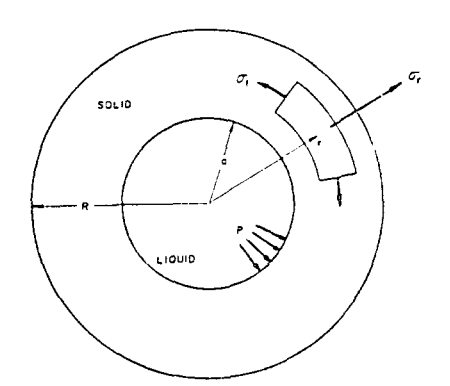
Fig. 28. Homogeneous nucleation rate of UO2 crystal formation in its melt as a function of temperature (Cronenberg 1978)

solidification commences immediately after contact and is limited by the heat transport process rather than molecular reordering. Cronenberg and Coats (1976) extended the crystallization kinetics to UC and UN. They confirmed the results of Cronenberg and Fauske (1974).

Hsiao et al. (1972) also investigated this effect. The total tangential stress is far greater than the total radial stress and is the dominant factor in the rupture of the solidifying shell. Failure is imminent if the total tangential stress exceeds the ultimate stress locally and the location of the maximum stress coincides with the external surface where failure probably occurs. If rupture occurs the failure is likely to occur immediately after solidification occurs, since high values of stresses occur at the surface when the solidified

crust is very thin and stresses decrease as solidification proceeds. Rupture of the solidifying shell may simply be a split at the surface. His work, however, does not predict the sequence of events following the rupture.

Cronenberg et al. (1974) extended the analysis to the $80_2/Na$ system (Fig. 29) by considering the temperature-dependent mechanical properties and the compressibility of the inner core as well as the effects of the surface heat transfer conditions. He derived the transient numerical solutions for the temperature distributions in the drop and the propagation rate of the solidification front. The assumption of the solidification is based on the crystallization kinetics. This indicates that the time for molecular ordering to form a solid from the melt is short compared to the time constant for heat transfer. Generally they confirmed the results of Hsiao et al. They indicated that the solidification process in the UO₂/Na system is limited by the low conductivity of UO₂ rather than by the surface heat transport process. In contrast the solidification process for highly conductive aluminum is strongly dependent upon the surface heat transfer process as shown in Fig. 30. In contrast dropping experiments of molten aluminum the contact temperature between the two materials tends to take on a value nearer the more conductive medium, the thermal gradient in the UO2 shell in sodium is higher than that for aluminum in water, resulting in a much greater thermal stress in the former case as shown in Fig. 31. These results are in qualitative agreement with the dropping experiment performed by by Swift and Baker (1965); molten ${\tt UO_2}$ exposed to subcooled sodium undergoes fragmentation while Al in water usually results in a little breakup. An increase in the fragmentation with decreasing coolant temperature is also in qualitative agreement with a thermal stress-induced fragmentation mechanism.



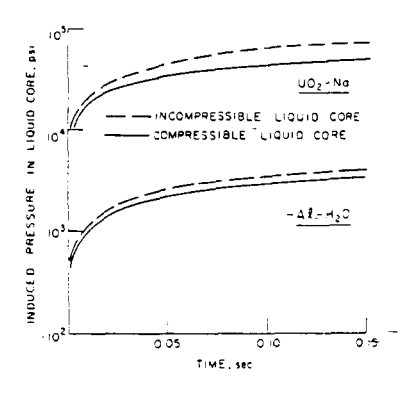
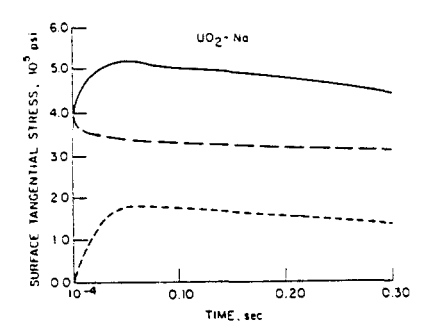


Fig. 29 Fig. 30
Effect of liquid compressibility on the induced pressure within the unsolidified portion of the droplet (Cronenberg, 1978)

Board (1974) claimed that, for both $\rm UO_2$ in Na and Na in $\rm UO_2$, the interactions may be understood in terms of the single hypothesis of $\rm UO_2$ shell freezing. Since the interface temperature estimated under experimental conditions is lower than the melting temperature of the $\rm UO_2$, a frozen shell must form for both cases, which prevents the liquid-liquid contact. It was proposed, however, that such processes are likely to act only as a trigger mechanism for coherent large scale explosions, since release through frozen shell bursting, as with the superheated drop nucleation, could only occur for very special initial conditions, e.g., as

Fauske had proposed for sodium injection into a UO2 pool for Armstrong's tests (1970).

Knapp and Todreas (1975) used a fracture mechanics approach to assess whether or not the solidifying $\rm IO_2$ would fracture under the thermally induced stresses, since the fracture stresses developed in the solid are likely to be intensified when the solid has surface cracks or flaws. It is reasonable that such flaws or cracks could exist on the solid spherical surface



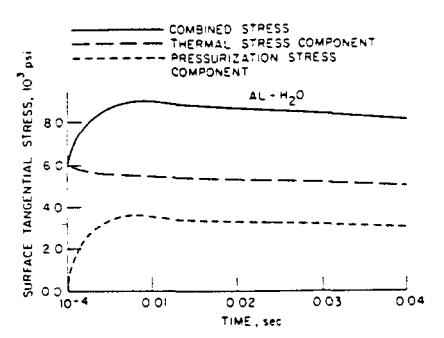


Fig. 31. Comparison of the outer surface tangential stress components versus time for both $\rm UO_2$ in Na and Al in $\rm H_2O$ (Cronenberg 1978)

caused by voids due to fission gas release or pores in the microstructure. A steady-state approximation was used for the heat transfer process and the requirement for fracture was such that the local stress intensity factor $(K_{\rm I})$ should be greater than the facture toughness $(K_{\rm IC})$ of a material. They included a first order estimate for the change in density from liquid to solid during solidification. They reconfirmed that the stresses generated in the solidifying shell in a UO_2/Na system were sufficient to result in the fracture from anticipated inherent flaws. It was found that rapid instantaneous fracture is to be expected with an initial fissure, where the remaining thermal stresses are strong enough to lead to the multiple cracking. However, they pointed out that this mechanism would not be applicable to ductile materials such as tin, lead or aluminum since the use of a local intensity factor is no longer valid as the plastic zone develops with crack propagation.

Ladish et al. (1977) commented that the first solidified shell is unlikely to form at once on the whole surface of the sphere. Rather "islands" of the solidified material will develop at different sites. Therefore, pressure generation in a solidifying sphere is very improbable. It was also suggested that the first thin skin breaks immediately as it solidifies and that fuel not yet solidified reaches the surface via the gaps formed. In addition they claimed that fissure formation does not necessarily imply fragmentation in the sense that a new heat transfer area is generated. The specific elastic energy ($E_{\rm E}$) is compared to the specific surface energy ($E_{\rm S}$) of fragments and the specific energy for mixing ($E_{\rm mix}$); these are given by

$$E_{s} = 3\sigma/r_{f} \tag{36}$$

$$E_{\rm F} = 0.5 \, \sigma_{\rm B}^2 / \Upsilon \tag{37}$$

$$E_{mix} = 0.375 \, \rho V/t^2 \, r_f$$
 (38)

where: r_f : radius of fragments (100 μm for illustration

σ: surface tension σ_B: breaking stress Y: Young's modulus

V: volume

t: mixing time (1 ms for illustration).

It was concluded that the breakup by the thermal stress is possible only if the conversion of elastic energy into surface energy has high efficiency, but the energy provided by thermal

stresses does not seem sufficient to intermix the fuel fragments with the coolant.

Corradini and Todreas (1979) performed an analytical study to determine the minimum UO2 particle size that could survive fragmentation induced by thermal stress in UO2/Na fuel-coolant interactions based on a brittle fracture mechanics approach. This is an extension of the work of Knapp and Todreas (1975). Basic assumptions used are almost the same as those used by Hsiao et al. (1972) except the droplet surface is subjected to constant heat transfer rates or specified temperatures. They evaluated the local stress intensity factor as a function of the surface heat transfer coefficient and the size of fuel, where, once $K_{\rm I}$ exceeds $K_{\rm IC}$, the fuel breaks up or crack propagation occurs. They found the bound on the minimum size of a UO2 particle was within the range of experimental findings. At large surface heat transfer coefficients and at a larger radius of a molten metal droplet, $K_{\rm I} > K_{\rm IC}$ and surface flaws could propagate through the solid. If $K_{\rm I} >> K_{\rm IC}$, it is then likely that the crack propagates into the ductile zone of UO2, resulting in complete rupture of the solid particles and liquid particles being released from the shell. Since the analysis is based on an approximation fracture model of the phenomena with assumptions employed, this model can be considered only as a first order approximation to predict the phenomena.

Even though Lazarrus et al. (1973), Mizuta (1974), and Zyszkowski (1975a, 1975b) suggested that this solidification effect was a fragmentation mechanism in their experimental observations, most molten metals undergo plastic rather than brittle deformation. Therefore, many of the metal-water fragmentation experiments cannot be accounted for by a thermal stress mechanism only in contrast to the brittle fracture of oxides (e.g., UO2). However, the role of solidification as an initiation mechanism (trigger) of thermal interaction cannot be completely neglected. It is possible that the molten metal is expelled by internal stresses into the cold liquid, or the cold liquid penetrates through the cracks into the molten core, or that boiling occurs within these cracks resulting in fragmentation of the metal. The thermal stress models proposed were able to predict the possibility of fragmentation, but subsequent processes of thermal interactions were not studied at all. What has not been shown in whether the whole process of solidification, fuel fracture and breakup and subsequent melt freezing is fast enough to completely account for the violent interactions observed. The timescale for such events may be too short. Post-test debris also does not indicate that the majority of the fuel debris that is small is angular or of irregular shape. Rather much of it is smooth and spherical or spongy in character when the interaction is very violent. Therefore, solidification probably occurred for the majority of the fuel after fragmentation. It is recommended that the thermal stress model be coupled with a violent boiling model which could provide more reasonable surface heat transfer conditions, and solidification would play a proper role in the processes. Consequently the overall procedure of the thermal interaction could be better understood.

3.2 Triggering Mechanisms

Triggering is a local small-scale phenomenon which initiates the fragmentation of the fuel. Most of the experimentation that has been performed to understand fuel-coolant interactions applies primarily to the triggering process rather than the explosivity of the interaction. Trigger requirements are directly related to the stability of the vapor film for the fuel/coolant system. If the system is quite stable a strong trigger is needed to produce interactions. If the initial configuration is only marginally stable, an interaction can be triggered quite easily, perhaps spontaneously by the system's own fluctuations. Nelson and Duda (1981, 1982) clearly demonstrated the triggerability of a fuel-coolant interaction as a function of initial conditions in their experiments of molten iron oxide in water, where an FCI was classified into spontaneous and triggered explosions. The triggerability of any system is of importance. If very energetic triggers are required, this could reduce the explosion hazard considerably. The knowledge of the triggering process could be essential in devising preventive measures to protect against damaging explosions.

Buxton and Nelson (1975) considered three separate areas of triggering: triggering due to vaporization of the cold liquid, triggering due to mechanical actions of fuel and coolant, and in some instances chemical interactions between the molten metal and the cold liquid. Basically all of these areas result in the generation of a pressure disturbance which sets the fuel/coolant vapor film into an unstable situation. Most fuel-coolant interactions appear to be initiated by the collapse of the vapor film layer or bubble in a localized region. This may arise spontaneously, or it could be triggered by an external pressure pulse. The external pressure pulse can be induced by a mechanical device such as a detonator in a controlled test or simply by contact of the fuel with the solid wall. The precipitous collapse of the vapor layer in the cold bulk liquid adjacent to the interaction region can produce a pressure disturbance spontaneously, which can lead to the breakup of the molten fuel. Oscillatory motion of the vapor film, which occurs during the onset of transition boiling, can also result in the initiation of interactions.

Numerous experimental and theoretical work has been performed to study the characteristics of the destabilization of the film boiling process. In this section studies on the violent boiling process of cold liquid in contact with a hot solid or hot liquid surface will be reviewed as a possible triggering mechanism in relation to fuel-coolant interactions.

Walford (1969) studied the rapidly changing modes of boiling in his experiments of a solid nickel sphere propelled through water at constant velocity. He classified seven types of boiling: laminar film, fine turbulent film, coarse turbulent film, violent nucleate, nucleate, convective, and explosive cavity mode. For the explosive cavity boiling regime, a local spherical cavity was produced around the sphere. The sphere progressed through this cavity until the sphere neared the vapor-liquid interface, when another cavity was rapidly formed. The newly formed cavity grew to be as large as the preceding one; the cycle was repeated with a period of 5-10 ms.

By recognizing that the enhancement of heat transfer area by the dispersal of the molten material is necessary for fuel-coolant interaction to occur, Board et al. (1971) studied the energy transfer process of heated metal foils with water. They observed oscillating vapor films in the kilohertz frequency range between nucleate boiling and stable film boiling regimes. Their experiments show that under certain conditions dependent upon water temperature, the vapor film can collapse extremely rapidly, probably on the order of 40 to 50 microseconds or less.

Stevens and Witte (1971) showed in their experiments for a solid copper sphere in water that the transition from film to nucleate boiling occurs as a pulsating phenomenon. Transition begins with a relatively slow pulsation of the vapor film at the sphere surface. The frequency of the vapor pulsations was observed to increase as transition proceeded. In later studies of silver sphere in water, Stevens and Witte (1973) noted a similar behavior. Under suitable water and sphere temperatures they found that a stable vapor film surrounding the sphere underwent a precipitous violent film collapse. They suggested two types of behavior in the destabilization of the vapor film: (1) a precipitous instability, referred to as a "transplosion," and (2) a progressive instability controlled by bubble-like irregularities on the liquid-vapor interface, which is much slower than the "transplosion." Both types of instability-triggered pulsational boiling were followed by a three-region boiling phenomenon; i.e. a situation where nucleate, pulsational and meta-stable film boiling occurs simultaneously on the sphere surface.

The experiments of Farahat et al. (1974) in which a hot sphere of tantalum was cooled in a pool of liquid sodium showed that bubble growth and collapse in the transition boiling regime may be very energetic. Large vapor bubbles were formed, producing pressure pulses reaching a maximum of 5 bar at a sodium temperature of 750° C. The "transplosion" phenomenon was also confirmed by Zyszkowski (1976) in the molten copper/water system. He claimed that this "transplosion" has a random characteristic and is affected by the nature and roughness of the surface, its temperature, wettability of the hot surface, and subcooling the cold liquid.

Anderson and Bova (1971) investigated the effects of collapsing vapor film around the explosive interaction of molten salt and water. They injected water into hot molten sodium chloride. He noted the following sequence of events: As the water jet penetrated in molten salt, a region of vapor separated the liquid jet from the salt. This behavior persisted until the jet had penetrated to the bottom of the container; then, the vapor region collapsed and a violent interaction resulted. Anderson and Armstrong (1972) hypothesized that a localized collapse of the vapor film layer acts as an initiating trigger though the experimental observations were not fine enough to follow the individual steps of the vapor layer breakdown.

Bjornard et al. (1974) observed, in tin drop-water interactions, that the qualitative pressure behavior consisted of a period of high-frequency (about 15 kHz), low-amplitude pressure oscillations followed by a lower frequency (about 1 kHz), higher amplitude oscillation that accompanied the fragmentation event. The duration, frequencies and magnitudes of these two distinct portions of the waveform were influenced by the initial tin and water temperature. This oscillatory pressure behavior indicates that the fragmentation mechanism is linked to the dynamics of the vapor film surrounding the droplet. Further, the two distinct regimes evidenced by the pressure signature are strongly suggestive of film boiling, possibly followed by film collapse, which is in turn followed by the fragmentation event itself. These observations appear to us to be quite important, because the behavior of an oscillating vapor film is likely to be quite general. Such overall behavior is not highly specific to any one geometric situation (although the details will be) or combination of materials; rather only film boiling is needed to allow for initial fuel/coolant interpenetration.

Kim and Corradini (1984) claimed that the oscillatory behavior of vapor film is responsible for the initiation of fuel-coolant interactions. They showed for the particular case of an iron-oxide fuel droplet in the water coolant that the oscillation of vapor film could be induced spontaneously during the initial growth period of vapor film under certain initial conditions,

or mechanically by applying an external pressure pulse to stable film boiling around a molten droplet. They explained the triggerability of FCI in the single-droplet experiments of Nelson and Duda (1981, 1982) in terms of the fluctuation of the vapor film in their dynamic film boiling model; higher oscillation and pressure fluctuation of the vapor film in their model qualitatively predicts the easier triggering of fuel-coolant interaction in Nelson and Duda's experiments.

Generally, the presence of a vapor film will delay the interaction, but the oscillation or the collapse of the vapor film will lead to the fragmentation of fuel. Under some circumstances the vapor film may collapse rapidly enough to act as the event that triggers fragmentation and perhaps the explosion. The nature of precipitous vapor film collapse is one of the key steps to the initiation of the vapor explosion.

3.3 Review of Selected Fragmentation Models

In this section three models are discussed in more detail. These three models are the Drop Capture model of Henry and Fauske (1976, 1979), Buchanan's (1973) model of violent bubble growth and collapse, and Kim's (1985) model of rapid evaporation of encapsulated coolant droplets in fuel. These models are specifically chosen because they have a physical picture coupled with a relatively complete mathematical model to allow for direct comparison to data.

3.3.1 The Capture Model Henry and Fauske (1976, 1979) propsed a model based on spontaneous nucleation, which described the triggering and initial propagation mechanisms for a vapor explosion in the free contact mode of fuel into coolant, although the basic concepts are not restricted to this geometry. The model considers that fuel enters the coolant in a film boiling regime. Locally at the fuel-coolant interface the film oscillates and the coolant liquid continually attempts to wet the fuel surface by establishing direct liquid/liquid contact. Under these conditions of a liquid-liquid system only spontaneous nucleation is possible. Thus, the establishment of the film or liquid/liquid contact and explosive vaporization depends on spontaneous nucleation. The spontaneous nucleation bubble cannot begin to grow until the thermal boundary layer is sufficiently thick, criteria (point A) for the vapor (Fig. 32) bubble. Also the maximum diameter can grow to Point B in a stable manner. Even though the nucleation rate is very large when the interface temperature upon contact is larger than the minimum spontaneous nucleation value, the pressurization due to the additional nuclei formation suppresses the nucleation rate and slows down the bubble growth. The maximum site density, which results in the mutual pressurization, is determined from the compressibility of the liquid phase. Pressure increase in the liquid is then related to the increase in vapor volume, the increase in the density of liquid, and sonic velocity within the

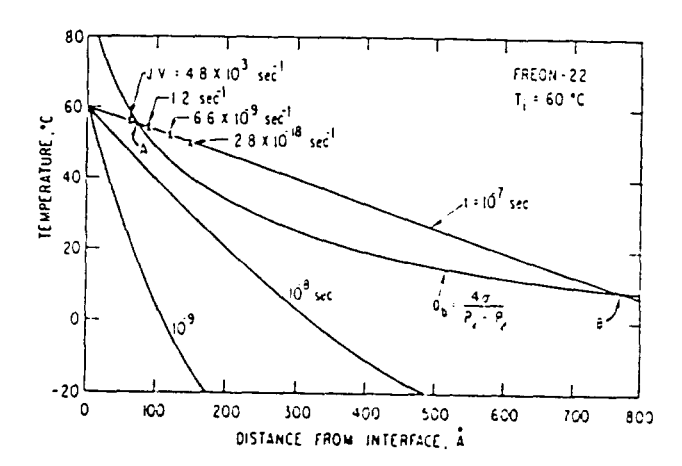
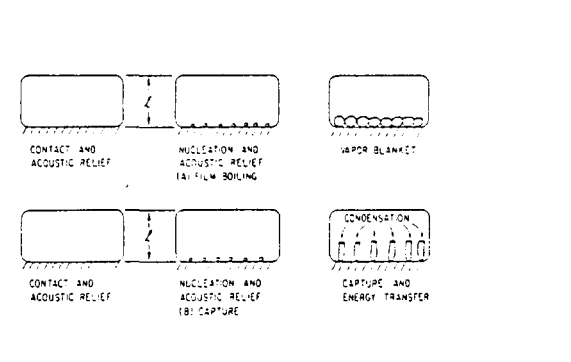


Fig. 32. Thermal boundary layer development and mechanical stability criterion (Henry, 1975)

liquid (c), which is given as

$$\Delta P = 1/2 N \rho_c D^2 c^2$$
. (40)

By assuming the overpressure the number of nucleation sites per contact area which suppresses further sites can be estimated. If the number of nucleation sites that exist simultaneously results in interference at the maximum stable bubble diameter the interface between two liquids will be vapor blanketed and the energy transfer will be limited based on film boiling. If physical interference does not occur, the high pressure vapor will rapidly grow into a condensing zone and a portion of the liquid coolant will be "captured" as a droplet on the surface. With this information the stability of a specified drop size, in terms of wetting and capture by the hot fuel liquid or sustained film boiling, is evaluated as a function of interface temperature as shown in Fig. 33. This stability limit characterizes the sizes of cold liquid droplets which are capable of initiating explosive vapor formation.



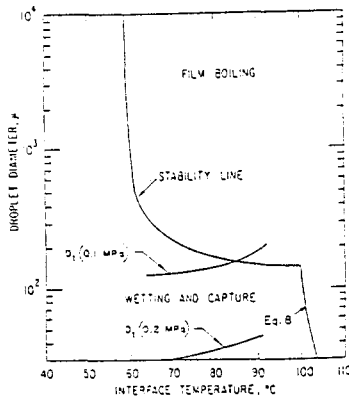


Fig. 33. Droplet film boiling and capture behavior (Henry 1975)

As the vapor cavity forms, the vapor pressure is far greater than the ambient pressure and the initial growth of the vapor bubble is inertially dominated. When a high pressure vapor source inside a liquid droplet approaches the opposite surface, the droplet will burst open producing a fine liquid spray and releasing the stored high pressure vapor which is an incipient shock wave to start the interaction. It is this very fine liquid spray, which is much smaller than the parent droplet and therefore certainly less than the capture size, which can provide fine mixture and large contact area necessary for extensive fragmentation and sustained propagation throughout the mixture. As the system pressure rises during the interaction, the drop stability criteria change. This change results in a larger droplet which can be captured with lower energy transfer. The growth of the vapor bubble is then thermally dominated in its lifetime and cannot induce overexpansion into a condensing zone. This result of degradation would be that explosive interactions should be self-limiting in terms of maximum interaction pressures.

The assumptions involved in the model for liquid coolant "capture" are:

- a) Intimate contact between liquids with a well-wetted interface.
- b) The interface temperature is greater than spontaneous nucleation temperature and less than thermodynamic critical temperature.
- c) The growth of the vapor bubble is inertially dominated and the pressure profile required for such growth is developed in one acoustic transmission time from the contact interface to free surface on the opposite side, and back to the interface.
- d) The overpressure in the cold liquid suppresses further nucleation sites. It is claimed that the analysis is rather insensitive to this assumption, i.e. a value of 2 bar or 15 bar could have been chosen without dramatically altering the results.

This model suggests that spontaneous nucleation and the resultant vapor growth is the mechanism for describing: (1) film boiling in a liquid/liquid system after intimate contact, (2) the limit of stability at a given temperature, (3) the spontaneous trigger for an explosive interaction, and (4) the propagation of the initiating event in this system. However, this model is limited by the following concepts:

- a) Fine coolant fragmentation (d << 1 mm) must occur before the explosion in the model. This is in contrast with experimental visual evidence which showed only coarse mixing (d >> 1 mm) ahead of the interaction front (Board and Hall, 1976) of either fuel or coolant.
- b) When the liquid-liquid interface temperature is greater than the critical temperature of the cold liquid, the model cannot explain spontaneous explosions. Nevertheless, it is not clear if the interface temperature would be actually greater than the critical temperature since the thermophysical properties change drastically near the critical point.
- c) The hypothesis that the spontaneous nucleation bubble cannot grow beyond the maximum stable size during the heating of the captured coolant droplet limits the validity of the model to a certain range of initial conditions. The bubble should grow without limit since there is no restriction against the growth of the bubble except the inertial force of the surrounding liquid and phase change at vapor/liquid interface.
- d) The growth of the vapor bubble is suppressed due to the acoustic relief in the model. Nevertheless a simple acoustic constraint can initiate the growth of the bubble before acoustic relief.
- e) Incoherent fragmentation is unlikely to produce a uniformly fragmented mixture at the capture size. The model assumes that the drops explode as soon as they reach the capture size.
- f) The model cannot explain the initial intimate contact mechanism that begins the whole process.
- g) The breakup of the coolant drop into fine liquid spray due to high pressure of the vapor bubble is rather ambiguous without any quantitative descriptions.
- h) Above all the model can only be applied to the free contact mode, especially where the coolant drop is captured in hot molten fuel.

The model provides a good representation of the explosive character for well-wetted liquid-liquid systems including the onset of explosive events. It proposes some necessary conditions for the occurrence of the explosion, which might not be sufficient, for the integral explosion process. Therefore the model could be understood as describing a triggering process of an FCI, but not as a fragmentation or large scale explosion propagation mechanism.

3.3.2 <u>Buchanan's Model</u> Buchanan (1973) proposed a complete model which describes the whole process of a fuel-coolant interaction. He shows a mechanism for the increase of contact area between fuel and coolant, which is essential to explain the observed rapid heat transfer. By using a feedback mechanism he describes the cyclic behavior of bubble growth and collapse during fuel-coolant interactions. Under certain conditions the subsequent cycles may be weaker than the preceding ones, and the initial perturbation decays and does not lead to an explosion. However, under other conditions, subsequent cycles are more energetic than the preceding ones, and an explosion occurs as the interaction grows.

The interaction is divided into five stages, the last four of which occur cyclically.

Stage 1

As a result of some unspecified triggering the liquids come into intimate contact and a vapor bubble is formed on the fuel surface. This stage is regarded as a means of supplying the initial perturbation which causes the first bubble formation adjacent to the fuel surface.

Stage 2

Given initial conditions for i-th cycle which are pressure and radius of a spherical bubble, it is assumed that the bubble expands adiabatically until the maximum radius is reached. At the maximum radius all the vapor is assumed to suddenly condense due to the surrounding subcooled liquid. A cavity now exists and collapses without heat transfer under the ambient pressure. Due to the axisymmetric collapse of the cavity, a jet of liquid forms directed toward the fuel surface. The dimension of the jet at the moment of impact is proportional to the initial cavity radius. Based upon Plesset and Chapman's (1971) calculation the velocity (V_0), the length (L_0), and the diameter (d_0) of the coolant jet impinging on the fuel surface are given as

$$V_{o} = V_{c} \left(\Delta P/\rho_{c}\right)^{1/2} \tag{41}$$

$$L_{o} = L_{c} R_{m} \tag{42}$$

$$d_{o} = d_{c} R_{m} \tag{43}$$

where: R_m: maximum bubble radius

ΔP: pressure difference between the cavity and the surroundings.

The constant V_C , L_C , and d_C are determined by the degree of departure from spherical symmetry and estimated for a bubble collapsing adjacent to the solid wall.

Stage 3

As the jet penetrates it disintegrates and mixes with the surrounding liquid. Christiansen (1973) showed that the length of the jet increases exponentially with a time constant proportional to ${\rm d_0/V_0}$, which represents the mixing of these liquids

$$L = L_0 \exp(t/\tau) \tag{44}$$

where:

$$\tau = fd_{O}/V_{O} \tag{45}$$

Considering its dependence on the density ratio of liquids in the evaluation of f, he assumed that the surface area of contact between the fuel and the coolant jet is given by

$$A = A_0 \exp(t/\tau) \tag{46}$$

$$\tau = 11/4 \left(\rho_f / \rho_c \right)^{1/2} d_o / V_o \tag{47}$$

Stage 4

As the jet penetrates the fuel, heat transfer occurs between the fuel and the jet. Assuming that the temperature of the jet is constant and no vapor film forms between the fuel and the coolant jet, the temperature of the jet is calculated by a first-order approximation with one-dimensional heat transfer across each element of fuel-coolant-fuel as shown in Fig. 34.

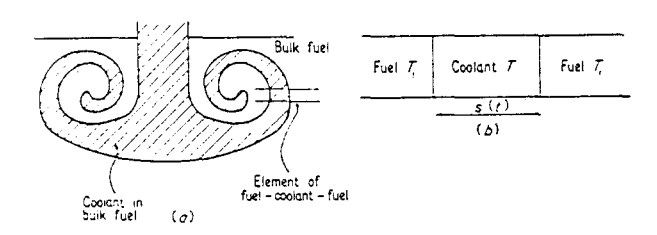


Fig. 34. (a) Schematic cross section of coolant sometime after jet penetration (b) Element of fuel-coolant-fuel in which heat transfer occurs one dimensionally

Stage 5

When the coolant jet has been heated to its saturation temperature it vaporizes provided nucleation sites are available (heterogeneous nucleation). If no nucleation sites are available

the jet must be heated to the homogeneous nucleation temperature before vaporization occurs. When the jet starts to vaporize by homogeneous nucleation, the rate of vaporization is so rapid that the latent heat cannot be supplied by normal heat transfer from the surrounding fuel. Instead the heat is supplied by the jet itself. It is further assumed that the vaporization process stops when $T_{\rm jet} = T_{\rm sat}$ for homogeneous nucleation. Hence, only a certain fraction of the coolant jet penetrated undergoes phase change, for example, 33% for water at one atmosphere. However, in heterogeneous nucleation, the vaporization is slow and the jet is assumed to be vaporized completely since there may be sufficient time for the latent heat to be supplied by the surrounding fuel. By assuming an instantaneous phase change, the pressure and radius of vaporized jet upon heating, which are also the initial pressure and radius of the bubble of the next cycle, can be found. The whole process then starts from stage 2 again.

The model is able to predict the ratio of peak pressures at a distance r due to subsequent cycles. At an external pressure of 1 bar, it is given as

$$\frac{P_{i}(r) - P_{0}}{P_{i-1}(r) - P_{0}} = \begin{cases} 6.673 \text{ (heterogeneous nucleation)} \\ 2.899 \text{ (homogeneous nucleation)} \end{cases}$$
 (48)

Figure 35 shows a qualitative pressure history at the point r. At some critical value of Po

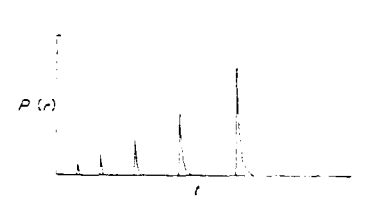


Fig. 35. Pressure at the point r as a function of time.

this ratio is unity. For larger values of P_0 than the threshold pressure (P_{th}) an initial perturbation is damped out. If the pressure resulting from the initial few cycles is not relieved, the sustained pressure will inhibit further cycles. Thus, the FCI is self-limiting if the resulting pressure is maintained.

Due to the complicated process of the FCI, the model has a number of assumptions. The assumptions and corresponding limitations of the model are:

- a) As a means of supplying an initial perturbation, an initial bubble is assumed to exist. As Vaughan et al. (1976) described, the model cannot describe the triggering phase of interactions and gives no justification for the bubble presence.
- b) Adiabatic expansion and collapse of the vapor bubble cannot provide reasonable results for the vapor bubble dynamics. The effects of the vapor in the bubble are likely to reduce the amount of jetting and this seems to affect the interaction dramatically.
- c) The formation of a coolant jet as a result of cavity collapse needs modification when it comes to a bubble collapsing adjacent to the high temperature fuel surface with phase change of the coolant. Besides, the collapse of the bubble is hardly tangential to the fuel surface.
- d) The constants for the geometry of a coolant jet have been evaluated for the bubble collapsing adjacent to a solid wall. When the target is molten modification should be made to account for the mobility of both the jet and the target.
- e) The contact area between liquids is assumed to increase exponentially. In real situations the contact area increase would seem to be limited by the solidification of the fuel, the vaporization of the coolant jet and disintegration of the coolant jet.
- f) The assumption of a uniform temperature of the coolant jet is not reasonable for short times. The accuracy may improve as the surface area increases due to rapid disintegration and fine mixing.
- g) The existence of a vapor film around coolant jet is totally ruled out to comply with the concept of direct liquid-liquid contact. It is explained by the fact that there is insufficient time for the heat transfer to be reduced by vapor blanketing before the jet as a whole (or some fraction of it) vaporizes. This may be valid considering the time scales involved.

- h) Probably the most important point is that the vaporization process is assumed to be instantaneous. There is no consideration of pressure relief to the surroundings upon bubble nucleation and expansion as a function of time. Since the vaporization by homogeneous nucleation is limited to a certain portion of the coolant jet, while it can vaporize completely by heterogeneous nucleation, pressure buildup due to homogeneous nucleation is lower than that by heterogeneous nucleation. This does not seem reasonable. If the pressure relief character in the mixture and the dependence of nucleation on time and available nucleation sites are fully considered, vaporization by homogeneous nucleation seems to lead to a more violent bubble growth and pressure buildup than that by heterogeneous nucleation.
- i) The whole process is regarded to repeat upon the growth and collapse of a vapor bubble on or adjacent to the fuel surface. A bubble can only be formed in a transition or nucleate boiling regime, which restricts the applicability of the model possibly to these boiling regimes. It may also be possible to induce such bubble growth and collapse locally by disturbing the stable vapor film by an external pressure pulse. However, the life of these bubbles does not seem to last long enough to support the cyclic behavior.

The results of the calculation indicate that the model is certainly a possible explanation of FCI, although some key assumptions limit its applicability (i.e., the final two points).

3.3.3 Kim's Model Kim (1985) proposed a model based on analysis of the small-scale single droplet FCI experiments performed by Nelson and Duda (1981, 1982). The modeling is composed of four stages, where the first stage provides the initial conditions for the interaction and the last three of which occur cyclically. Basically the dynamics of film boiling around a molten sphere govern the whole process of the FCI, to which an individual submodel for each cycle is added. Therefore, a system of differential equations are solved simultaneously to follow the behavior of bubble dynamics and fuel fragmentation.

Stage 1: Vapor Film Growth and Oscillation

This stage describes the transient film boiling around a molten fuel droplet in the coolant. A system of differential equations is developed expressing mass and energy conservation in the fuel, coolant liquid and vapor, as well as a spherical momentum equation, and solved simultaneously (see Kim and Corradini, 1984) as a function of time. The calculation is performed until the vapor film enters a quasi-steady state. Under certain initial conditions a steady state is not reached, but vapor film oscillations directly cause film collapse (Stage 2). Under the conditions of Nelson's test for an iron-oxide molten droplet, the film growth stabilizes, at which time an external pressure pulse is assumed to be applied to the fuel/coolant system. This external pulse mimics the actual test conditions for Nelson's experiment of an exploding bridgewire.

Stage 2: Film Collapse and Coolant Liquid Jet Formation

As the vapor film collapses due to triggering or overexpansion of the vapor film, the vapor-coolant interface becomes unstable. The instability of an interface between immiscible mediums with acceleration (i.e., Rayleigh-Taylor instability) exists even in a spherically symmetric system. Initially a small perturbation of the interface grows rapidly to form jets of coolant directed toward the fuel surface. The concept of coolant jet formation is then different from that of Buchanan's (1973) because its origin is directly linked to film oscillations and/or collapse. By using spherical harmonics the geometry of the perturbed interface is described. The motion of the unperturbed interface is governed by the Rayleigh equation. Equations of motion relative to the interfacial disturbance used are those derived by Plesset (1954), who considered the growth of a surface disturbance under the linearized approximation given by

$$|R_n| << R_0 \tag{49}$$

where: $R_n\colon$ time-dependent coefficients of expansion for jet $R_0\colon$ unperturbed bubble radius.

Stage 3: Coolant Jet Penetration and Entrapment in Fuel

When the surface disturbance grows fast enough and has a large kinetic energy, it forms coolant jets which penetrate the fuel surface. For the penetration of jet into fuel, the criteria given by Buchanan (1973) is used

$$0.5 \rho_{j} U_{j}^{2} \rightarrow \sigma_{y,fuel}$$
 (50)

where σ_{y} fuel is the yielding stress of fuel, which would be the surface tension force for a liquid drop (σ/D) . The growth of an entrapped coolant liquid droplet due to the incoming coolant jet and the penetration into the fuel is calculated based on kinematic considerations. Once a coolant drop is formed the existence of a vapor film around the coolant droplet is considered. A vapor film could form as soon as the coolant jet enters the fuel (case B) or vapor production could be delayed until the coolant droplet is heated up to its homogeneous nucleation temperature (case A). The latter case is considered more reasonable given the fact that local pressurization and rapid penetration of the jet may preclude film growth.

Stage 4: Entrapped Coolant Expansion and Fuel Fragmentation

As the encapsulated coolant drops submerge deep in the fuel, vapor would be produced around them due to the high heat transfer from the fuel. The contact mode between fuel and coolant is now the opposite of that given in Stage 1. The governing equations for this contact mode are derived by modifying those original equations. At a certain depth, the vapor containing these coolant drops coalesces with neighboring vapor bubbles and separates the outer portion of the molten fuel surface from the parent fuel droplet. The molten surface of fuel expands as a result of the continuous vaporization of coolant droplets encapsulated within it. During this expansion the fuel surface is again subjected to the growth of Rayleigh-Taylor instability disturbances due to the acceleration of the fuel surface and the density difference between fuel and vapor. The growth of interfacial disturbances during expansion is calculated based on the linear phase and nonlinear phase given by the experimental results of Emmons et al. (1960),

$$dn/dt = C_{ss}[(1 - \epsilon)a\lambda]^{0.5}$$
(51)

where: n : amplitude of surface disturbance

cs: empiritude of surface disturbance α : empiritude of o.67 as: acceleration rate α : density ratio $(\rho_{\alpha}/\rho_{\alpha})$ wavelength of surface disturbance.

The molten fuel surface breaks up when the amplitude of the surface disturbance is greater than the thickness of the fuel surface. Fragmented fuel particles move outward in the vapor film with a certain velocity which is the expansion velocity of the surface at the moment of fuel breakup. As a result of the increased fuel surface area the vaporization rate increases rapidly. The vapor film around a parent fuel droplet then grows enormously. This is analogous to the observed steam bubble in Nelson's tests. In a certain period of time the fragmented fuel particles leave the vapor film. As the vapor film overexpands, it reaches its maximum diameter and begins to collapse.

The whole process then proceeds from stage 2 again until the coolant jets do not have sufficient strength to penetrate the fuel or the fuel solidifies.

Figure 36 shows the diameter of vapor film as a function of time compared to one experiment of Nelson (Test 11.75-1). Since the existence of a vapor film around the entrapped coolant droplets in the fuel is assumed, case B, this retards the heat transfer rate significantly, and the growth of vapor film is not energetic. In fact the penetration of a coolant jet into the fuel no longer happens after the second cycle of bubble growth and collapse. Meanwhile, the FCI process shows a rapid and violent growth of a vapor film when coolant droplets are considered to be heated as a liquid and vaporized by homogeneous nucleation. The quantitative growth rate of vapor film is somewhat smaller than that found in experimental data. There exists a threshold value of the trigger pressure (2 bar), below which no or only mild interaction occurs and this is in qualitative agreement with Nelson's data (4 bar). Once the trigger pressure is greater than the threshold value the qualitative difference of the vapor film growth at different trigger pressures is found to be insignificant. The model predicts that, at elevated ambient pressure, the trigger must be increased to initiate an FCI. It is also found that the time scale of each cycle of bubble growth and collapse becomes smaller as the ambient pressure gets larger. Both of these predictions are in good agreement with Nelson's results.

There are a couple of parameters assumed in the model: the wavenumber for R-T instabilities and the initial amplitude of the surface disturbance of the vapor-coolant interface. The wavenumber seems to affect the overall film behavior rather significantly, and in all the calculations the fastest growing wavenumber for initial film collapse was chosen. It is likely that the growth of the surface disturbance is governed by this most unstable wavenumber. At very small amplitudes of the initial surface disturbance, the coolant jet hardly touches the fuel surface during the first collapse of the film. Once the amplitude is larger than a certain value (~ 1% of its wavelength) the overall behavior of vapor film is quite insensitive to the initial value. This was the value used in the calculations.

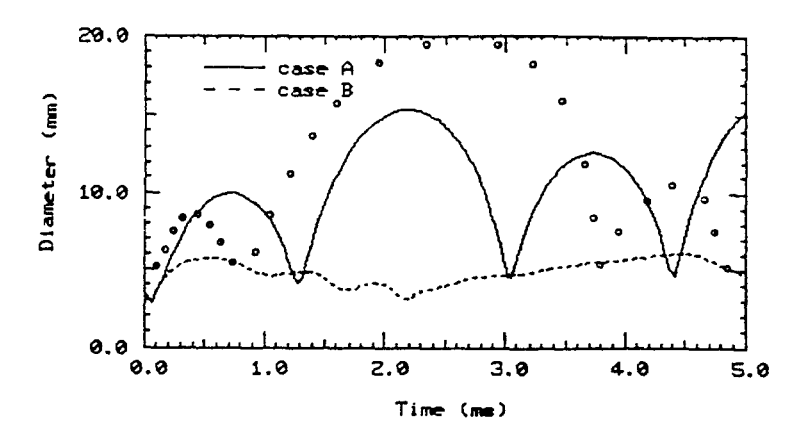


Fig. 36a Diameter of bubble as a function of time (Kim, 1985)

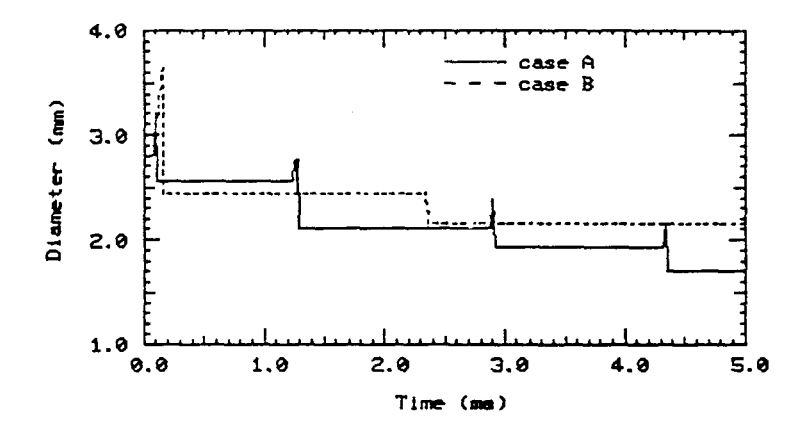


Fig. 36b Diameter of the parent full droplet

The assumptions and limitations of the model are:

- a) The fuel-coolant system analyzed was spherically symmetric. It implies that the variation of the film thickness is small compared to the droplet. This symmetry is valid only if the whole drop is immersed in a pressure pulse for a sufficiently long time or any pulse passage time is small compared to the time of film collapse. A spatially uniform film pressure is only valid when the time elapsing as a pressure disturbance is transmitted across the film is much less than the time involved in appreciable change in the average film pressure.
- b) The retention of all the vapor generated in the film was used and is only reasonable in certain ranges of coolant subcooling, diameter of fuel droplet, and heat fluxes from the fuel.

- c) The use of the linearized approximations for the growth of vapor/coolant interfacial disturbance is valid only if the amplitude of the disturbance satisfies Eq. (3.32). It was demonstrated that at the fastest growing wavelength, the difference of instability growth between linear and nonlinear approximations becomes insignificant.
- d) The coolant jet and surrounding fuel are assumed to be incompressible and irrotational. When a viscous fluid flows past a solid drop, the flow is asymptotically equal to the potential flow except for a thin boundary layer. For liquid drops with fully developed internal circulation the effects of separation and wake might be further suppressed.
- e) The shape of the coolant drop encapsulated in the fuel is assumed to be spherical and the breakup of a coolant drop during penetration is neglected. As long as the Weber number is less than the critical value the breakup does not occur. The effects of deformation of a coolant drop during penetration did not affect the penetration velocity and penetration depth very much.
- f) A spherical molten fuel surface is assumed to form as a result of coolant jet penetration and vaporization. This is a very idealized and simplifying assumption to study the overall behavior of vapor film, not a local eruption of fuel-coolant interaction. However, experimental observations (Nelson and Duda, 1981; Ando, 1980, 1982) indicate the ejection of fuel particles in a spherically symmetric manner, which suggests the possibility of a symmetric fuel surface formation above the entrapped coolant at least for a very short time.
- g) Since the model considers the interaction occurring at film boiling regimes, the model cannot predict the FCI behavior as soon as the temperature of the fuel surface falls below the minimum film boiling temperature. In its present form the model is only applicable to the free contact mode of fuel entering the coolant.

As one can see from a comparison of these three detailed models, there is an historical order to them in which the more recent models include some aspects of past models. Kim's model, being the most recently developed, contains key aspects of Fauske's and Buchanan's models. Basically the jet penetration model of Kim has some commonality with Buchanan's model. However, what is unique is that (1) film boiling is considered to be the initial condition (a necessary condition for initial premixing - Fauske 1973), (2) dynamic film oscillations and/or collapse is the method of forming the jet, and (3) models for eventual jet entrapment below the fuel surface based on transient jet kinematics. The model considers the concept of homogeneous nucleation of the coolant (Fauske, 1973; Henry and Fauske, 1975) as the means of supplying the energetic driving force for the local explosive vaporization and steam bubble expansion. Based on the heat transfer characteristics from the surrounding fuel to the entrapped coolant drops, it is found the efficiency of the explosive vaporization increases as the entrapped coolant drops become smaller and more homogeneously mixed within the fuel below its surface. This is a unique and different approach for the importance of the coolant droplet size compared to the drop capture model. However, it may be more reasonable because Kim's model indicates that film local oscillations and collapse provide the impetus for local "microscale" mixing between the fuel and coolant liquids. If one takes an overall view of the process the mixing phase of the vapor explosion allows the fuel and coolant to intermix and allows for an increase of the exposed surface area without significant vaporization because the liquids are in film boiling. In addition if one follows Kim's ideas it is the local oscillations of the film and its eventual collapse which allow the fuel and coolant to mix to a finer length scale at the exposed surface area due to jet formation, coolant entrapment and vaporization and subsequent fuel fragmentation. Homogeneity in mixing and reduction in the length scales for heat transfer are the keys to the process both in the macroscopic scale and the "microscale."

There are certain aspects that could be improved in the model, such as the effect of viscosity on the Rayleigh-Taylor instability growth and a more detailed description of the breakup of a coolant jet upon entrapment in fuel. The model does not account for the effect of significant increases in the viscosity on the growth rate of the instability disturbance. There are other effects that one could consider that would resolve the competing effects of other proposed fragmentation mechanisms (internal pressurization and solidification) to that of film collapse and jet formation and entrapment. For example consideration of the fuel solidification process during the timescale of the film collapse, and jet penetration was neglected here because it is not important for these high temperature fuel simulants (Fe $_{\rm Q}{}_{\rm V}$). However, this may be significant where fuel is near its solidification temperature as the jet enters the fuel and quenches local regions of the fuel surface.

Finally, one should note that all of these fragmentation models, in particular the complete models of Fauske, Buchanan and Kim, only address the initiation of the vapor explosion. These models focus on the explosion in one local region of the fuel-coolant mixture, and not on the spatial propagation of the process to other regions of the mixture. In this sense they focus on the necessary conditions for triggering and initial escalation of the vapor explosion into a large scale process but not on the characteristics of the large scale propagation process. Therefore, one should be careful in assuming that these fragmentation models are applicable to the whole process of a large scale vapor explosion. As the explosion gains strength one would

expect that purely hydrodynamic mechanisms for fuel fragmentation would become dominant, because the relative velocity between fuel and coolant is increasing and fragmentation by relative velocity induced R-T instabilities, K-H instabilities and boundary layer stripping would increase in importance. The key point that one should remember is that for the vapor explosion to become a large scale event one must satisfy these necessary conditions for triggering and explosion escalation. In fact if one wants to suppress the explosion or mitigate its effects one endeavors to better understand this triggering and escalation phase in order to preclude the growth of the interaction into a large scale explosion.

4. LARGE SCALE EXPLOSION PROPAGATION AND EXPANSION

4.1 Vapor Explosion Theory

There have been two major theoretical hypotheses to explain vapor explosion behavior. One advanced by Fauske is a set of necessary conditions for a large scale vapor explosion. This has been termed the spontaneous nucleation theory. The other formulated by Board and Hall is known as the thermal detonation theory, and focuses on the explosion propagation based originally upon purely hydrodynamic fragmentation behind the explosion shock front.

4.1.1 <u>Spontaneous Nucleation Theory</u> Spontaneous nucleation is a nucleation mechanism by which critical size vapor or cavities are formed as a result of molecular density fluctuations in a bulk liquid or at any preexisting liquid-vapor or liquid-gas interfaces. Based on the experimental findings of Henry et al. (1973, 1974), Fauske (1974) originally proposed a vapor explosion hypothesis as a set of criteria in which spontaneous nucleation was the plausible mechanism for explosive vapor formation given molten fuel and coolant in liquid-liquid contact. These criteria were based on the more fundamental investigations of Katz and Sliepcevich (1971), Nakanishi and Reid (1971), and Enger and Hartmann (1972).

To understand Fauske's criteria one must remember a few fundamental facts. First, the contact interface temperature of two semi-infinite masses at initially different temperatures with constant properties is found to be (Carslaw and Jaeger (1959))

$$T_{I} = \frac{T_{H}(k/a_{t})_{H} + T_{c}(k/a_{t})_{c}}{(k/a_{t})_{H} + (k/a_{t})_{c}}$$
(52)

where:

T = temperature

k = thermal conductivity

a₊ = thermal diffusivity
A = hot liquid fuel

c = cold liquid coolant

Second, according to the kinetic theory for gases and liquids, vapor bubbles can form in a bulk liquid due to molecular fluctuations. That is, a vapor can be nucleated in the bulk of the liquid when a vapor nucleus greater or equal to the critical size (r_{crit}) is formed

$$P_{g} - P_{c} = \frac{2\sigma}{\Gamma_{crit}}$$
 (53)

where P_g is the vapor pressure inside the vapor nucleus and P_c is the imposed liquid pressure corresponding to a saturation temperature T_{sat} . With a given internal bubble pressure P_g , the bubble is unstable, and collapses for $r < r_{crit}$ or grows for $r > r_{crit}$.

The reversible work for nucleation required to form this spherical vapor bubble nucleus in the bulk liquid is given as

$$W = 4\pi r_{crit}^{2} - \frac{4}{3} \pi r_{crit}^{3} [P_{c} - P_{g}].$$
 (54)

In a state of mechanical equilibrium this work is expressed as

$$W_{\text{eq}} = \frac{16 \pi \sigma^3}{3(P_{\text{q}} - P_{\text{c}})^2} . \tag{55}$$

Finally, the rate of bubble nucleation per unit volume and per unit time is given from kinetic theory as

$$J = wN \exp(-W_{eq}/K_BT)$$
 (56)

where N is a constant approximately equal to the number of molecules per unit volume (N = 10^{22} cm⁻³), w is the collision frequency of the liquid molecules and is a function of temperature with a value nearly constant (10^{10} s⁻¹). The ratio G_b = (W_{eg}/K_BT) is called the Gibb's number. It represents the ratio of the energy required for nucleation to the kinetic energy of the molecule. The predicted nucleation rate is extremely sensitive to temperature variations; i.e. within a couple of degrees, the bubble formation rate changes many orders of magnitude (Fig. 37). At a point above a specific nucleation rate, J_{hn} 10¹⁰, so many bubbles are formed

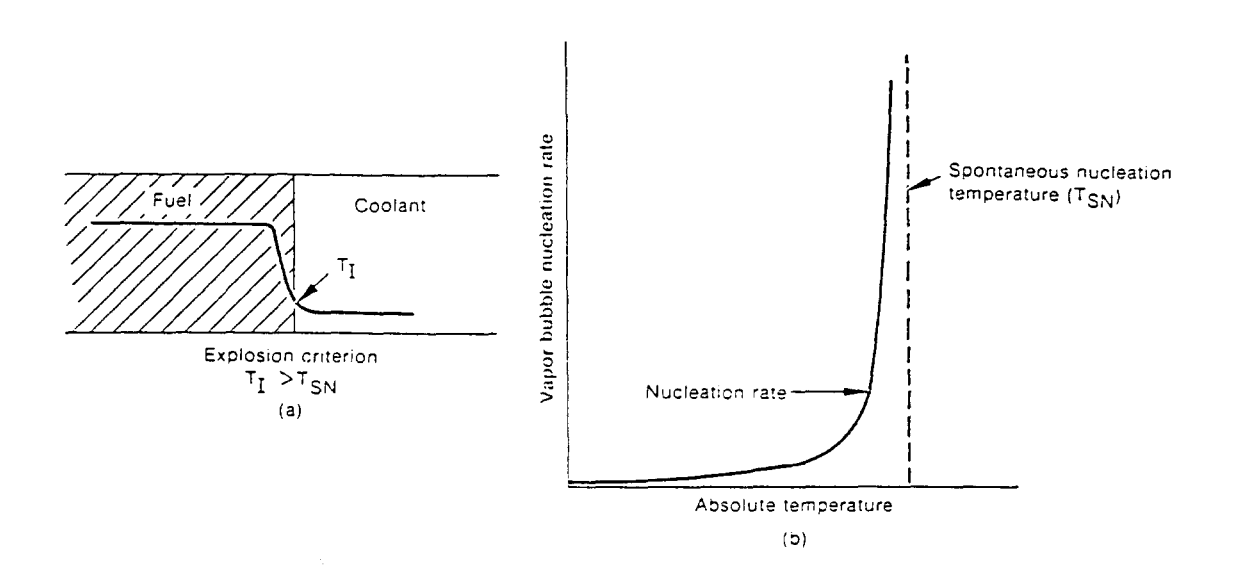


Fig. 37. Spontaneous nucleation model.

that the metastable liquid state reverses. The associated temperature $T_{hn} = T$ (J_{hn}) is called the homogeneous nucleation temperature of the fluid; e.g., T_{hn} , water $\cong 310\,^{\circ}\text{C}$. From Eq. 56 and available data one can show that many liquids will not nucleate homogeneously until they reach temperatures of about 90% of their thermodynamic critical temperature.

Now if this nucleation takes place at an interface (e.g., liquid-liquid), the required work to form the bubble can be decreased as the wettability of the surface decreases. The spontaneous nucleation temperature ($T_{\rm Sn}$) takes into account this wetting effect at the interface. Thus for a complete surface wetting fluid (contact angle = 0°), the spontaneous nucleation rate is the same as the homogeneous nucleation rate ($T_{\rm Sn} = T_{\rm hn}$), and for no surface wetting fluid (contact angle = 180°), the possible superheating equals zero ($T_{\rm Sn} = T_{\rm Sat}$) (see Table 3).

Based on these concepts, Fauske suggested that the following criteria must be satisfied in order to achieve a large scale vapor explosion:

(1) Existence of stable film boiling, so that a vapor film separates the two liquids and permits coarse premixing without excessive energy transfer; Henry and Fauske (1981) have added some ideas on mixing to this criterion recently and this has been previously discussed;

(2) Direct liquid-liquid contact due to collapse of the vapor film;

(3) Explosive boiling immediately upon contact, implying that the interfacial temperature must exceed the spontaneous nucleation temperature upon initial contact, causing rapid fragmentation and mixing of both the hot and cold fluid without time delay;

(4) Adequate inertial constraint to sustain a shock wave on a time scale required for a large scale explosion (this has remained a qualitative criterion).

Bankoff and Fauske (1974) as well as Anderson and Armstrong (1977) have postulated that at least with water and organic liquids the effect of wetting on the interfacial surface tension could strongly affect the possibility of spontaneous nucleation of the vapor. Henry and Fauske (1975) subsequently theorized that an upper limit exists for a self-triggered interaction, T < $T_{\rm crit}$, where $T_{\rm crit}$ is the critical temperature of the coolant.

Table 1. Heterogeneous nucleation at a liquid-liquid interface

Table 1. neterogened	ous nucleation at a liquid-	Tidata incertace
Superheating High Superheating	Medium Superheating	No Superheating
Temperature Tsn = Thn	Tsat 🕻 Tsn 🕻 Thn	Tsn = Tsat
Bubble Contact Mode Liquid A	Liquid A	Liquid A
Bubble B	Bubble B	Bubble B
Liquid C	Liquid C	Liquid C
Nucleation Work	T _{C/B}	TNB ← → → TNC
Wetting Angle • • • •	o°< 0 < 180°	θ = 180°

The spontaneous nucleation theory is difficult to assess because it is a set of necessary conditions that must be met for a large scale vapor explosion, not a complete model. They, therefore, must be compared to data with more detailed analyses applied. Nevertheless, the formulation of these criteria has significantly contributed to a better understanding of the vapor explosion.

There are some criticisms of these criteria which have not been resolved to date:

(1) As indicated by Cronenberg and Benz (1978) and Schumann (1982) the Fauske criteria provide no information on the amount of participating fuel and coolant masses which is one of the critical parameters to determine the large scale vapor explosion efficiency and work output and is, therefore, inconclusive about the expected energy conversion from fuel thermal energy to mechanical energy. There is also no complete mechanistic model applying the spontaneous nucleation theory to explain fuel fragmentation, the pressure history and subsequent conversion ratio behavior.

(2) In low temperature experiments by Enger and Hartmann (1972), Board et al. (1974a) and Anderson and Armstrong (1977) (e.g., LNG/water and Freon/water) vapor explosions were observed even though the criterion $T_{\rm I} > T_{\rm SN}$ was not always satisfied. Fauske (1974) has explained this discrepancy by pointing out that in these cases the spontaneous nucleation temperature is altered by dynamic changes in wetting characteristics, but this explanation

is not universally accepted. There are some indications that the high temperature systems by Board et al. (1974b) and Armstrong et al. (1976) (e.g., $U_2/sodium$) also explode at temperatures below T

- temperatures below T_{nn}.

 (3) Nelson and Buxton (1978) observed self-triggered spontaneous vapor explosions when the contact interface temperature of corium/water based on constant properties was well above the upper limit of temperature threshold, T_{crit}, for self-triggered interactions as proposed by Henry and Fauske (1975). That indicates that the upper temperature threshold is not applicable to at least light water reactor applications because the contact temperatures (if contact is at all possible) of molten corium and water would exceed the critical temperature of water. Most damaging industrial vapor explosions (e.g., aluminum/water, steel/water and smelt/water accidents) also occurred with an interface temperature well above T_{crit}. Also Buxton and Benedick (1979), Fry and Robinson (1979, 1980a, 1980b) and Mitchell et al. (1981) have reported measurements of supercritical explosion pressures, which cannot be accounted for by this spontaneous nucleation model. However, some investigators (i.e., Fauske, Theofanous, Ginsberg, Steam Explosion Review Group Report, 1985) have questioned these measurements because of the uncertainty in the measurement of liquid phase pressures.
- (4) Henry et al. (1976, 1979) performed high ambient pressure experiments with a Freon/oil system and a NaC1/H₂O system, and observed that increased ambient pressure does appear to suppress the spontaneous triggering of a vapor explosion. They explained that this pressure suppression is due to bubble growth characteristics during explosion propagation. But W.B. Hall (1977) presented calculations showing that bubble growth with acoustic loading can proceed without time delay for acoustic pressure relief. Nelson and Duda (1981, 1984) experimentally observed that the explosion could be externally triggered at pressures above those predicted by Henry et al. (1976, 1979) to be a cutoff point. Some investigators consider that the effect of high ambient pressures is to suppress the ability to trigger the explosion (Corradini, 1981; Kim, 1984, 1985), but can be reinitiated by a larger trigger pulse.
- (5) The effects of solidification phenomena for liquid fuel have not been accounted for in the original model. Later Bankoff and Fauske (1974) considered the spontaneous nucleation within solid fuel cracks due to thermal stresses in the solidified thin UO₂ shell. But Cronenberg and Coats (1976) and Ladish (1977) indicated that under perfect confact quenching conditions, liquid UO₂ will undergo similar homogeneous solid crust nucleation which may hamper further fragmentation.

One should note that Fauske's original criteria have been added to and modified by Henry, Bankoff and others. Therefore, criticisms concerning modifications to the basic criteria do not necessarily invalidate these criteria. The model initially was used to explain all vapor explosions as a product of spontaneous nucleation following extreme superheating; however, the spontaneous nucleation theory today may serve to partially explain the initial triggering and escalation mechanism for the vapor explosion. This alone may be quite important because the spontaneous nucleation model as conceived is a microscopic model which is based on the physical phenomena in the immediate neighborhood of the liquid-liquid interface that might trigger and escalate the local FCI into a large-scale explosion.

4.1.2 Thermal Detonation Model The initial idea of likening a vapor explosion to a chemical detonation came from Board et al. (1974a, 1975). In fact this idea was based on the experimental observations by Board and Hall (1974b) indicating that a vapor explosion could be governed mainly by fragmentation and intermixing processes accounted for behind a spatially propagating pressure shock wave. They have suggested a theoretical model for a propagating vapor explosion by applying the classical theory for a steady-state one-dimensional chemical detonation to the case of a plane explosion front propagating through a coarsely mixed region of fuel and coolant (Fig. 38). The general case of propagation of a plane detonation wave through a semi-infinite explosive medium has been discussed theoretically by a number of investigators beginning with Chapman (1889) and Jouguet (1907). In particular, Wood and Kirkwood (1960) investigated the advanced Chapman-Jouguet conditions for steady-state one-dimensional detonations and shocks.

Board suggested in his model that this steady-state propagation of a shock wave caused rapid fuel fragmentation behind the shock front due to relative velocity induced instabilities. This is a fundamentally different mechanism from Fauske's criteria for explosive vaporization. However, the two models are not necessarily mutually exclusive, and one may actually complement the other. In particular, as discussed previously, the spontaneous nucleation concept is quite useful as part of the explanation of triggering and explosion escalation, while hydrodynamic fuel fragmentation may become dominant once the explosion has escalated to a steady-state explosion front. Thus the former mechanism may be required to initiate the latter. Taken by itself, Board's model suggests that in a suitably large or constrained system a vapor explosion can "detonate" given a sufficient trigger strength.

Consider a long tube containing water and vapor film blanketed molten fuel droplets (Fig. 38); a coarse premixture. Next consider a shock wave propagating through this mixture. To an observer on the front the flow motion is steady and so in this system the basic equations for

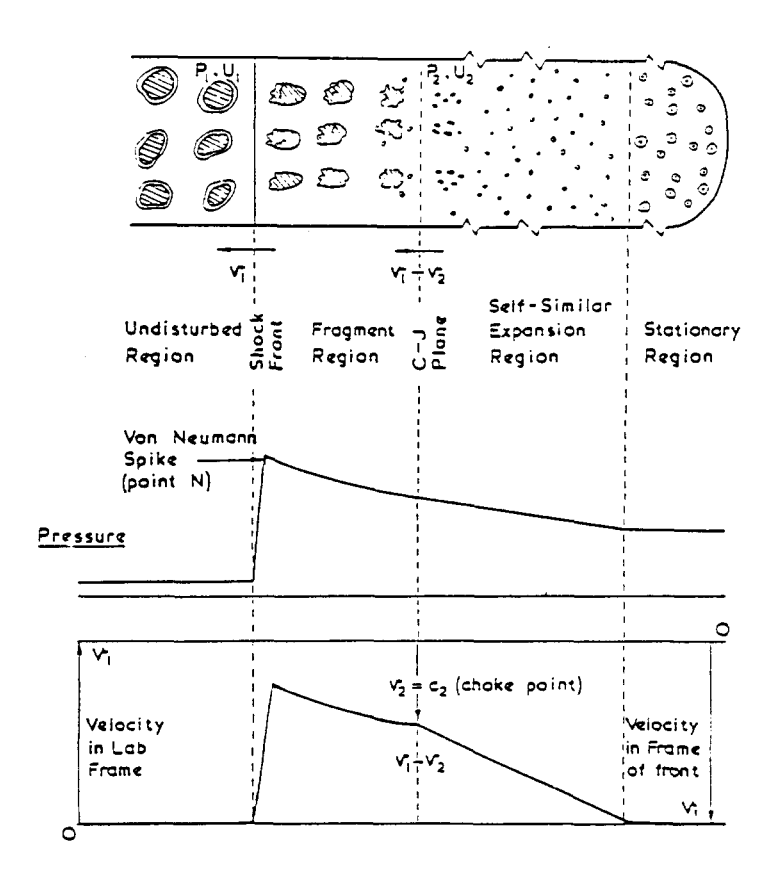


Fig. 38. Schematic illustration of a thermal detonation model.

homogeneous mixture of liquid coolant, vapor coolant, and fuel are determined by mass, momentum, and energy balances

$$\rho_1 u_1 = \rho_2 u_2 \tag{57}$$

$$\rho_1 u_1^2 + P_1 = \rho_2 u_2^2 + P_2 \tag{58}$$

$$h_1 + u_1^2/2 = h_2 + u_2^2/2$$
 (59)

where ρ is the density, u is the velocity and h is the enthalpy. Applying the momentum Eq. (58) and energy Eq. (59) to the material entering and leaving the plane shock front one can deduce that the possible states (P_2 , ρ_2 , u_2) of the material leaving the front are related to the pressure P_1 , density ρ_1 , and internal energy u_1 of the material entering the front by

$$\frac{1}{2} (P_1 + P_2)(1/\rho_1 + 1/\rho_2) = u_2 - u_1.$$
 (60)

This, together with the equation of state for the material leaving the front $P_2 = F(\rho_2, u_2)$, defines a unique relationship between the possible values of P_2 and ρ_2 -- this is called the Hugoniot curve or shock adiabatic curve.

Additionally from the theory of detonation it can be shown that for a specific set of initial conditions, there is only on equilibrium final state (point CJ in Fig. 39) for the

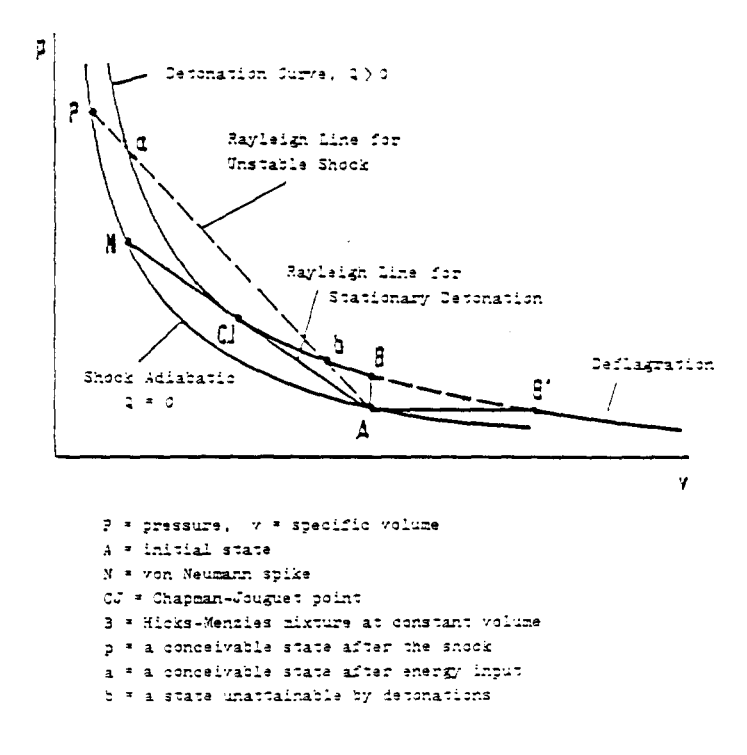


Fig. 39. Schematic illustration of shock-adiabatic and detonation curve.

material behind the front which ensures that the explosion is both stable and self-sustaining. In this state the velocity of the material leaving the front is just sonic (Mach No. = 1) with respect to the front -- this is called the Chapman-Jouguet condition corresponding to tangency of the Rayleigh line and the equilibrium Hugoniot curve.

The explosion propagates with a velocity which is greater than the speed of sound in the medium ahead of the front (Mach No. = $U_{shock}/C_o > 1$). The pressure and density both rise at the front to the point N on the shock adiabatic (Fig. 39) for the unreacted material (this is called "von Neumann spike" (1942)), while the velocity in the frame of the front falls from the shock velocity to a lower value. As fuel fragmentation and energy transfer occur, the fuel velocity increases and the mixture velocity reaches the speed of sound at the C-J plane.

Board considered that if a strong shock front progresses steadily through the material, then close to the front the relative velocities between the fluids may be sufficient to cause fine fragmentation of the hot material and hence rapid heat transfer. The front leaves behind a mixture in thermal equilibrium at high pressure, and subsequent expansion of this material will drive the front forward.

Board assumed certain physical mechanisms by which hydrodynamic fragmementation could be produced by (1) the complete collapse of vapor blanketing the fuel, and (2) fragmentation due to Kelvin-Helmholtz instabilities and boundary layer stripping which occur because of the differing

velocities between the fuel and coolant materials as the shock wave passes.

With such a thermal detonation it would be theoretically conceivable that there would be a higher degree of efficiency in converting thermal energy into mechanical work than that according to Hicks and Menzies (1965) because the coolant is compressed before mixing with the fuel (this neglects the work done on the system initially to collapse the vapor voids). Later Hall and Board (1977, 1979) generalized their earlier model to consider more explicitly the effects of sideways flow, interphase slip and expansion of the coolant phase. Further they developed a thermal detonation model in which vapor is generated within the reaction zone and showed how its efficiency could be low. Also they showed that thermal detonations (similar to chemical detonations) will only propagate if the sideways constraint is high compared to the length constraint of the reaction region.

The thermal detonation concept is an important contribution to vapor explosion modeling because it provides an overall conceptual picture on which further work can be based. However, some criticisms have been raised to the work of Board et al.

- (1) The stationary detonation model assumes a trigger to begin this event that is very large, requiring supercritical shock presures. Williams (1976) criticized this assumption by calculations for the $\rm U0_2/Na$ system showing that an initial triggering pressure of 80 to 700 bar was required with an initial vapor void fraction of 0.5 to 0.1.
- (2) Williams (1976) also indicated that the attainment of the von Neumann pressure spike is most likely prevented by the dispersion effect of a heterogeneous mixture of two components with different densities and sonic velocity. Because sharply defined pressure waves undergo multiple partial reflections at the interface between mixture constituents, an attenuated wave results.
- (3) Bankoff et al. (1976) indicated that the chemical detonation theory does not consider the effect of unequal weights between components in the mixture, which results in unequal phase velocities. Therefore, the reaction must also follow the slip line (i.e., the phase velocity ratio) as well as the pressure-specific volume diagram. In this case the pressure is generally not a maximum immediately behind the shock front. Accordingly a stationary detonation is only possible when the slip on the C-J plane has decreased to 0.
- (4) Bankoff et al. (1976) also indicated that the hydrodynamic fragmentation according to the interface stripping mechanism, may not take place fast enough to support thermal detonation because of the reduction of the relative velocity. Therefore, the thermal detonation concept cannot be accurately assessed without quantitative information for hydrodynamic fragmentation, and further thermal effects (e.g., spontaneous nucleation) should be considered for the extent of fragmentation especially for the nonisothermal situation.
 (5) Scott and Berthoud (1978), and Sharon and Bankoff (1981) doubted the geometric
- (5) Scott and Berthoud (1978), and Sharon and Bankoff (1981) doubted the geometric considerations in the detonation concept as to whether a reactor is even large enough to facilitate the development of a steady-state stationary detonation wave.
- (6) The initial film-boiling coarse mixture condition of Board-Hall model, where a vapor blanket is considered to initially surround the fuel particles, has been investigated by Gunnerson and Cronenberg (1980). Their results not only indicated that U02/sodium or U02/water systems could satisfy the initial coarse-mixture requirements but also illustrated that the minimum interfacial contact temperature necessary to sustain the film boiling process essentially coincides with the spontaneous nucleation temperature. Therefore, the vapor explosion could be also interpreted in terms of the spontaneous nucleation theory due to film boiling stability.
- (7) The Chapman-Jouguet detonation wave termination condition originates in classical single-phase single-reaction chemical detonation theory. Condiff (1982) indicated many difficulties in extending this theory to multi-phase thermal detonation; uniqueness of Rankine-Hugoniot (R-H) curve, straight line tangency point of R-H curve for sonic termination and sonic velocities depending upon flow regime, equilibration, nucleation or vaporization transients, etc. Condiff (1983) also pointed out that the thermal detonation theory is fundamentally based on a thin shock-limit approximation. This is because a shock wave has zero thickness on a hydrodynamic scale and in this limit the momentum transfer is zero. Unfortunately shock waves in two-phase flow may not be thin or well understood.

In spite of these criticisms and suggested modifications to the thermal detonation concept, it has received considerable support based on qualitative observations in many experiments (e.g., Briggs, 1976; Fry and Robinson, 1979, 1980; Goldammer, 1980; Mitchell, 1981, 1982, 1986; Schwalbe, 1982; see Appendix). All of these experiments apparently indicate that the explosion produces a shock wave which is analogous to a detonation explosion wave. Also note that thermal detonation is a macroscopic model which does not explain the microscopic mechanisms of triggering, fragmentation and heat transfer. Board suggested that relative velocity induced hydrodynamic fragmentation was a mechanism but did not rule out that other mechanisms may be operative. In fact in the following discussion of parametric explosion models it becomes

clearer that other mechanisms may be operative, although the macroscopic picture of the detonation model would be preserved.

4.2 Vapor Explosion Modeling

The fuel-coolant mixture can produce high pressure vapor when undergoing a vapor explosion, and do work against its surroundings. This explosion work may cause structural damage or generate missiles. One of the objectives for modeling the propagation and expansion of a vapor explosion is to provide information about its damage potential, debris size, and gas generation rates.

There are four basic methods by which a vapor explosion could be modeled during its propagation and expansion phases: (1) thermodynamic explosion models, 92) parametric explosion models, (3) mechanistic propagation models, and (4) explosion expansion models.

The "thermodynamic" model does not take into account any kinetic rate processes that may be involved. It only considers the overall mass and energy balances involved in the interaction. This type of model estimates the maximum work potential available from a vapor explosion given the masses of fuel and coolant participating. So this approach can give us information about the conservative upper bound to the work potential from an explosion. Such a thermodynamic model can be developed to estimate the maximum theoretical explosion work potential with two different end state conditions; constant ambient pressure or constant expansion volume.

For a more realistic assessment of the damage potential the explosion analysis must take into account the kinetic rate processes involved in the interaction. As a first approach "parametric" models have been developed to calculate the pressure history due to vapor explosions and the subsequent work output considering uncertainties of contact mode, fragmentation, mixing and heat transfer rates as empirical input parameters. Through sensitivity studies using these parametric models the relative importance of parameters involved in the vapor explosion can be qualitatively estimated and matched to available explosion data.

Based on these past efforts, mechanistic "propagation" models have been developed to consider the mechanistic behavior of an explosion and to explain large scale experimental data. The key feature of these models is that the kinetics of the explosion shock wave propagation, fuel fragmentation and heat transfer are modeled using postulated physical models for the constitutive relations in the conservation equations. Because these models can be quite complex they have been usually cast in a one-dimensional framework.

Finally, "explosion expansion" models have been developed. These have used relatively simple kinetics models for fuel fragmentation incorporated into general hydrodynamic codes for multiphase systems to predict the multi-dimensional expansion behavior of the explosion.

4.2.1 Thermodynamic Explosion Models A thermodynamic explosion model was originally developed by $\overline{\text{Hicks}}$ and $\overline{\text{Menzies}}$ (1965) to estimate the conservative upper limit of the vapor explosion work potential for postulated fast reactor meltdown accidents. This work potential was taken as equal to the change in internal energy of the fuel during an isentropic expansion from a compressed state to an expanded state. Based on the Hicks and Menzies method, several similar calculations have been performed for different applications.

Edwards (1967) calculated thermodynamic limits on the converison of heat to mechanical efficiency. Judd (1970) essentially used the same approach to obtain the thermodynamic efficiency of a molten fuel-sodium interaction. He used the more realistic equation of state to determine the sodium pressure at high temperature rather than the simplified form used previously. Pugh and Vaughan (1975) performed the same calculations as Hicks and Menzies. In addition, Vaughan et al. (1976) developed the computer code, ARES, for Hicks and Menzies's calculations. Peckover (1977) and Vaughan (1977) analytically did similar work on the optimum Hicks-Menzies calculations. Again Fogg (1977) developed a computer code for the numerical solution of the Hicks/Menzies equations for a fuel-coolant interaction. Coddington (1979) evaluated the mechanical energy yields that result from constant volume mixing of UO₂ and sodium using the most recent UO₂ and sodium equation of state data at that time. Judd (1980) also performed a thermodynamic calculation to find the upper limit to the work done by a molten fuel-coolant interaction. Corradini and Swenson (1981) considered the case in which the high pressure coolant expands to a specified volume for a LWR safety analysis and applied the thermodynamic model of Hicks and Menzies in order to increase the flexibility and extensibility of input data and graphical output compared to the previous models. It was assumed in this code that coolant vapor generated by fuel-coolant thermal interaction does work in expanding the

coolant subsystem to a specified pressure, volume or temperature, that is a pre-selected final state. Again for light water safety issues Corradini and Oh et al. (1983) concentrated on the specified final ambient pressure case, which could correspond to an ex-vessel explosion, with different calculations done for the specified volume case. Recently A.N. Hall (1985) constructed a thermodynamic model of molten fuel-coolant interactions. He applied Bernoulli's theorem to a flow of the mixture on its timescale of expansion to ambient pressure. Note that this application does not imply that the mixture expansion need be isentropic as in the Hicks-Menzies model. Therefore, the work efficiencies predicted by this model can be much smaller than those predicted by the Hicks-Menzies model. Finally, Seebold (1985) has employed a Hicks-Menzies computer model and performed a number of calculations for light water reactor (LWR) applications.

Since thermodynamic calculations do not take into account the specified path of the heat transfer or the fragmentation rate, the peak pressure and pressure history caused by the time delay between these various rate processes cannot be obtained. Also because some of the explosion damage in general will depend upon the severity of the pressure pulse, a transient analysis is essential in evaluating the detailed safety problem.

As described above one can consider a thermodynamic explosion model with two different final state conditions: (1) one is a model in which the high pressure coolant expands to a specified final ambient pressure, and (2) the other is a model in which the high pressure coolant expands to a specified expansion volume. We present the thermodynamic model as a basis of comparison for subsequent analysis with the example system defined to be the reactor pressure vessel in a LWR.

- 4.2.1.1. Specified Final Ambient Pressure Consider the vapor explosion to be an idealized process composed of two stages: (1) constant volume thermal equilibration of fuel and coolant, and (2) isentropic expansion of the products. In this process the following assumptions are made:
- a) All the heat transferred from the fuel during the process is transferred to the coolant (adiabatic boundary);
- Liquids are incompressible;
- Specific volume of liquid is negligible when compared to that of the vapor;
- d) Vapor behaves as a perfect gas;
- e) Specific heat and latent heat are constant.

These assumptions allow one to analytically estimate the thermodynamic work potential. Past work has shown that more detailed treatments do not alter the general behavior.

Consider the first process of the two-stage process where there is a fuel-coolant thermal interaction before expansion (constant volume process). Suppose that the mass of coolant, $m_{\rm C}$, at the absolute temperature, $I_{\rm C}$, mixes with the mass of fuel, $m_{\rm f}$, at the absolute temperature, $I_{\rm f}$, and thermal equilibrium is established between the two constituents. When one chooses the system boundary to be the mixture of fuel and coolant, one obtains the equilibrium temperature of the mixture

$$T_{e} = \frac{m_{c}C_{pc}T_{c} + m_{v}C_{pv}T_{v} + m_{f}C_{pf}T_{f}}{m_{c}C_{pc} + m_{v}C_{pv} + m_{f}C_{pf}}$$
(61)

where: C_{pc} = liquid coolant specific heat C_{pv} = vapor coolant specific heat C_{pf} = fuel specific heat.

From the thermodynamic state equation, one can obtain the coolant entropy change to this equilibrium state during the constant volume process. Next one can obtain the quality and the pressure of the equilibrium state.

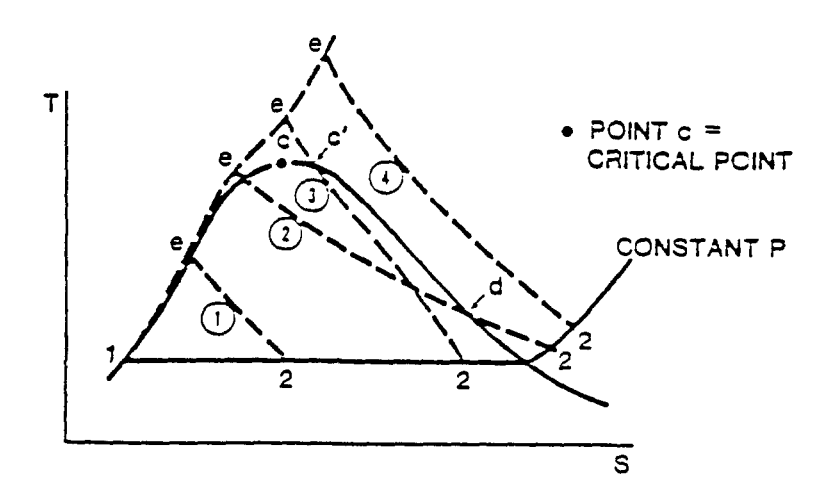
For the second stage of the process two kinds of isentropic expansion systems can be considered to estimate the maximum expansion work potential; one is the isentropic fuel-coolant mixture expansion and the other is the isentropic coolant expansion. The mixture expansion case is more conservative than the coolant expansion case because thermal equilibrium between the fuel to coolant is maintained during the expansion for the mixture case.

Suppose the fuel-coolant mixture expands in a reversible and adiabatic manner to obtain the maximum work potential. The total energy of the system and the environment is conserved during the whole process. From a thermodynamic analysis, one can define the work of the system as

$$\Delta W_{SYS} = -\Delta u = \Delta KE + \Delta PE + P_{O}(\Delta V_{SYS}). \qquad (62)$$

The actual work which can damage the surrounding structure at any time is the kinetic energy. However, one cannot calculate this portion in a thermodynamic analysis as a function of time. Therefore, the ΔW_{SyS} calculated should be viewed as an upper bound of the actual work potential; i.e. the maximum Kinetic energy would approach this value at some point in the expansion process.

There are a number of possible paths this expansion can take (Fig. 40). First, consider the case where the whole expansion process is within the saturation region. By differentiating and integrating the thermodynamic state principle for the mixture combined with the Clausius-Clapeyron equation one can get the equation for the final state quality, x_2 , given the final ambient pressure P_2 (and its saturation temperature Γ_2):



where

path 1: equilibrium state e saturation region final state 2 saturation region path 2: equilibrium state e saturation region fina1 state 2 superheated region path 3: equilibrium state e superheated region final state 2 saturation region path 4: equilibrium state e superheated region final state 2 superheated region

Fig. 40. Thermodynamic path of coolant in T-S diagram

$$(m_c c_{pc} + m_f c_{pf}) \ln(\frac{T_2}{T_e}) + m_c h_{fgc}(\frac{x_2}{T_2}) - m_c h_{fgc}(\frac{x_e}{T_e}) = 0$$
 (63)

where:

T₂ = temperature of final state
hfgc = coolant latent heat of vaporization
x_e = quality of equilibrium state
x₂ = quality of final state.

Next, consider only the portion of the expansion process in which the coolant state is a superheated state. One can get the final temperature based on the equation between the saturated vapor (x = 1) or the superheated state and the known final superheated state

$$T_2 = T(\frac{P_2}{P})^{1/n}$$
 (6)

where

$$n = \frac{m_c C_{pv} + m_f C_{pf}}{m_c R_c}$$
 (65)

By combining the above derivations one can express all the possible expansion paths during the process (Fig. 40). Notice that at approximately equal volumes of fuel and coolant the work potential reaches a maximum (Fig. 41).

In the thermodynamic explosion model one calculates the conversion ratio by using the system work at the end of the expansion

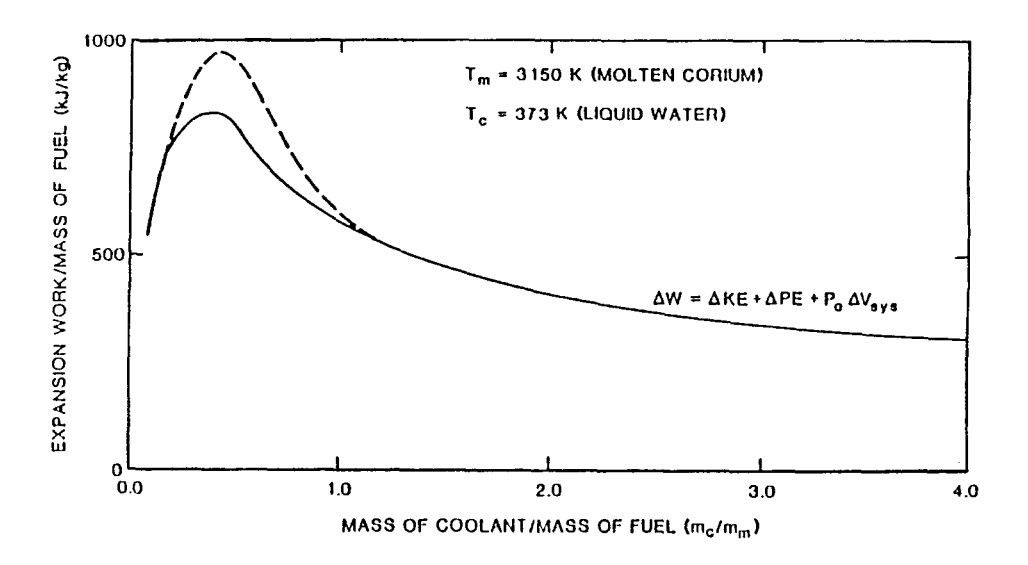


Fig. 41. Isentropic mixture expansion to atmospheric pressure.

$$C.R = \frac{\Delta W_{SyS}}{m_f C_{pf}(T_f - T_{ref})} = \frac{\Delta KE + \Delta PE + P_0 \Delta V_{SyS}}{m_f C_{pf}(T_f - T_{ref})}. \tag{66}$$

Because the portion of each term in ΔW_{sys} is not known one should realize this is the maximum work output (i.e., maximum theoretical kinetic energy). One can now use these estiamted upper bound values as a point of comparison as the more mechanistic models theoretically predict the actual explosion converison ratio.

4.2.1.2 Specified Final Expansion Volume Suppose that the vapor explosion occurs within a fixed final volume. For this condition there are two ways in which the vapor explosion can affect the surroundings. The first way is by the expansion work $(W_{\rm SyS})$ to the final volume. This is the same calculation as was presented in the previous section with the only difference being a known final volume instead of a pressure. The second way is by the final pressure in the fixed volume after the expansion. If this static pressure is large the structure may also be damaged. The former calculation has been done by Corradini and Swenson (1981), and the latter is briefly discussed below.

For this case the same assumptions are considered as discussed previously. The system has no heat transfer with the environment and in this case no work is done on the environment.

When the final state is in the saturation region, one gets from the first law

$$m_{f}^{C} c_{0} f(T_{f} - T_{2}) = m_{c}^{C} [c_{0} c(T_{2} - T_{c}) + x_{2} U_{fq2} - x_{1} U_{fq1}]$$
(67)

where: $U_{fgl} = coolant$ internal energy latent heat of the initial state $U_{fg2} = coolant$ internal energy latent heat of the final state.

When the final state is in the superheated region, one obtains

$$m_f C_{pf} (T_f - T_2) = m_c [C_{pv} T_2 - C_{pc} T_c - x_1 U_{fq1}]$$
 (68)

The temperature and the pressure of the final state are obtained from the above equations by a trial and error iterative method with the coolant equation of state.

Figure 42 shows the maximum quasi-static pressure generated from the expansion for a

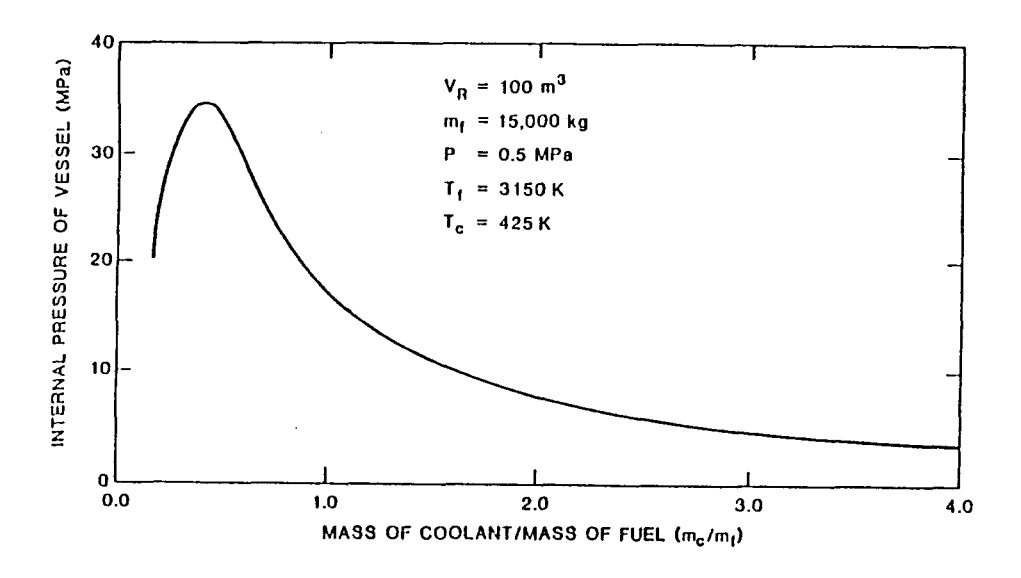


Fig. 42. Pressure generated for a constant final volume

constant final volume. Notice that as the mass of coolant increases to roughly equal volumes the maximum quasistatic pressure goes through a maximum and decreases substantially as $\rm m_c/m_f$ becomes large.

4.2.2 Parametric Explosion Models Many parametric models have been developed which describe the transient nature of fuel fragmentation and heat transport during a fuel-coolant interaction; as first initiated by Padilla (1970) (see Table 4.2). These models assume that fuel fragmentation has taken place resulting in very small particles all uniformly distributed in a finite volume of liquid coolant. This means that the first order effect on the vapor explosion, surface area generation, is parametrically assumed and modeling efforts are spent on second order effects such as the details of transient heat transfer. Most of these models can be characterized by a phase A; transient heat conduction in a predominantly liquid phase and a phase B; rapid vapor generation resulting in a two-phase expansion. Therefore, the pressure spike occurs in phase A due to rapid heat transfer and limited coolant expansion, and the pressure relief in phase B due to the volumetric expansion depending upon the acoustic constraint or the inertial constraint of the system.

It is important to point out that the results and the conclusions obtained in these various models have a meaning only when the values of the external input parameters can be justified either on the basis of sound physical considerations or on the available experimental data. In regard to vapor explosion experimental analyses, one of the original analysis tools was the equilibrium parametric model developed by Cho et al. (1971) for LMFBR applications.

In this review two parametric models were chosen: the Cho-Wright model and the Caldarola model. These two models are chosen because they are representative of the spectrum of parametric models developed to date (see Table 4.2) in which one must provide empirical input for the rate of fuel fragmentation and the characteristic size of the fragments.

4.2.2.1 <u>Cho-Wright Parametric Model</u> The Cho-Wright parametric model was especially developed for analysis of fuel-coolant interactions for postulated accidents in the liquid metal fast breeder reactor (LMFBR). The rate of energy exchange between the fuel and the coolant was considered to be

$$\frac{dQ}{dt} = hA(T_f - T) . (69)$$

The heat transfer coefficient, h, for each fuel particle dispersed in the sodium was given by

$$h = \frac{k_f}{\sqrt{\pi a_f t}} + \frac{k_r}{R} \tag{70}$$

which provided for the proper heat transfer rate in the asymptotes of short and long times. The heat transfer area, A, available per unit area of the heated coolant was determined by a user input characteristic fragmentation time and final fuel fragmentation diameter with the rate of fuel fragmentation taken as an exponential rate.

$$A = A_0[1 - \exp(-\frac{t}{t_f})]$$
 (71)

where

$$A_{o} = 6(m_{f}/m_{c})/(\rho_{f}D_{f})$$
 (72)

and t_f and D_f are supplied by the user based on empirical comparisons to data. In their early model (1971, 1972, 1973), the fuel and coolant in the explosion zone were considered to be lumped parameter masses, each at a common pressure but at different temperatures (i.e., thermodynamic equilibrium for the fuel and coolant separately). Three kinds of one-dimensional constraints were considered: (a) acoustic constraint of infinite extent for all time, (b) a finite inertial constraint in a single reactor subassembly for all time, and (c) an acoustic constraint up to the acoustic unloading time and a finite inertial constraint for expansion at longer times. The acoustic unloading time corresponds to the round-trip time of the initial pressure wave to the nearest free surface. In addition, a later model (1974) included the effect of coolant vapor blanketing (as well as any fuel fission gas), the effect of simple elastic deformation of the vessel wall, and the effect of a distribution of the fuel particle size. The major calculation results for a fast reactor subassembly geometry were the following:

ametric Models
ř
Features of
E E
Comparison of
ABLE 2
Ŧ

Model	# Reference	Year	Year Initial Separatry and Mixina				
			Survey and American	רו מקשתוו כתווסת	Heat Transfer	Hydrodynamics	Comments
30 C00 - 11	Fadi I I a	1970	Channel geometry Uniform dispersion of fuel particles in a heated region	No fragmentation Constant fuel particle size	1-0 heat conduction No heat transfer after vapor generation	Acoustic and inertial constraints	For sodium-cooled fast reactor Inertial work and acoustic work
ANL Model	Cho et al.	1471	Particle size distribution assumed, Single subassembly geometry	Fragmentation and mixing time simmulated by choice of heat transfer mechanism	Howayeneous equilibrium audei One-dimensional model Mode option; (a) linear gradient transient constraints; change over conduction farefaction wave returns (b) quasi-steady state	One-dimensional model Acoustic and inertial constraints, change over farefaction maye returns	for a 35 cm long molten zone in an FFTF subassembly (LMFRK) Frototype of many other models
Karlsruhe Model Cardarola	:l Cardarola	1972	Channel geometry with bottom reaction zone and top sodium Log-normal distribution of particle sizes	Instantaneous fragaentation	Phase A; no vapor, transient heat conduction Phase B; vapor generation by sodiue boiling	Scoustic and intertial constraints; change over when vapor is formed	For LMFBR applications No fragmentation acdel Three zones for the sodium;
BRENDY 1/11	Jacobs, Thurnay 1972	1972	Single channel geometry with fuel bottom and sodium top	No fragmentation, Conductivity Simulation for fragmentation Surface area increase	:-D heat conduction (Phase A) Effective conductivity introduced (Phase B)	BRENDY-I; 1-D Lagrangian BRENDY-II; acoustic or inertial constraints	For LMFBR application Compressible, frictional fluid
FUS-PEC 1/2	Martini	1972	Channel geometry Single particle size assumed	Continuous fragaentation with variable fuel aass interacting	Phase A; pure conduction into Acoustic constraint with liquid inertial constraint after Phase B; heat transfer into return of rarefaction was mixture of liquid and vapor	Acoustic constraint with inertial constraint after return of rerefaction wave	For fuel-sodium interaction FUS-PEC 2 considered HOZ solidification
T0M0F-1	Hal thecker	1972	Tank geometry Constant mixing ratio	Constant particle size	UO2 conduction Vapor file always present Unifore thereal state of Na	Gertial constraint Frictional flow	For fuel-sodium interaction
	Puig, Szeless	1972	Sub-assembly or whole-core geometry Constant mixing ratio	Constant particle size	UG2 conduction, optional cut off at saturation Uniform thermal state of Na	Incompressible spherical flow with optional compressible correction	Incompressible spherical flow For fuel-sodium interaction with optional compressible correction
TOFAL	Hoskin, Morgan Morgan	1972	Shock tube geometry constant mixing ratio	Separate model required	Meat input into coolant channel from separate calc, thermal equilibrium model	1-0 comprõessible flow Lagrangian code	Farameters: length of mixing tone, coolant in mixing tone heated, heat ingut time
Cadarache Model Antonakas		1973	Single sub-asseably geometry	Progressive fuel division into two equal size	Transient conduction that Ceases when vapor formed	Acoustic and inertial constraint; change over when vapor formed	For fuel-sedium interaction
CORFOU	Syrmalenius	1973	Single sub-assembly geometry	Fragmentation (large scale break up) and dispersion (small scale break up) on different time scales	Heat transfer from fuel to Mon-interacting liquid sliquid sodium, Monequilibrium taken as incompressibe mass and heat transfer betwee (inertial loading) wapor and ilquid	Non-interacting liquid is taken as incompressilbe (inertial loading)	For fuel-coolant interaction Thermal disequilibrium factor considered
SUBAR	igseta et al.	1973	Snate subassembly geometry Spatrally uniform mixing	instantaneous fragmentation Fixed fuel particle size	Transient heat conduction Two-phase thermal equilbrium model	Axial and radial mixture expansions and structure response (1-0 compressive)	LMFBR application Similar to Cho's model

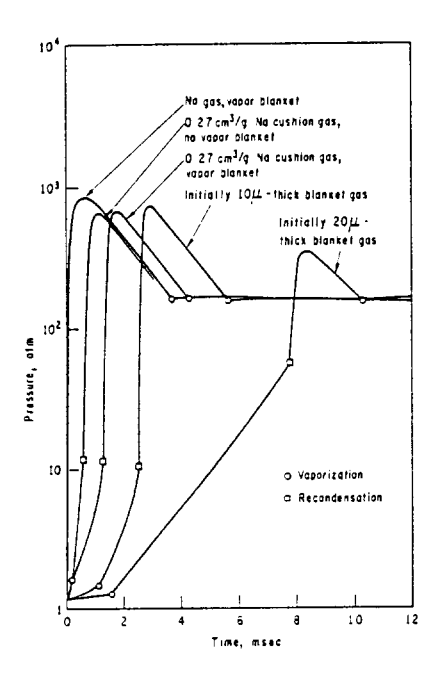
CESR Model	Board et al.	1973	Shock tube geometry Arbitrary mining ratio	Instantaneous fragmentatio: Specify surface area	Equilibrium modely uniform texp. distribution within vapur and hot liquid Nonequilibrium model; temp, distribution within vapor and liquid	inertial constraint with constant cross sectional area (unheated i quidi	Comparison to metal-warer shock tube exp ts Energy flux is treated as a power input
ANL Node)	Cho et al.	1974	1-b channel geometry with bottom mixing zone and top sodium slug Specified initial mixing	Finite rate of fragmentation (exponential function)	Linear teap, profile in the Three option vapor or gas blanket blancettal. Vapor generation depends upon of all and blanel surface generation rate.	s; a acoustic c) comination	FFF core standation Gas vapor blanketing and elastic deformation of vessel considered
Karsruhe Node!	Caldarola	1975	Channel geometry with bottom mixing zone and top slug Variable mixing time	Linear fragaentation with in each of several sections Fuel size is fixed	Trastent conduction within scherical foel particle Termal equilibrium model	Acoustic and incitial constraint changeover when vapor formed	LMFBR application Modified version of previous model
MURTI	Jacob	1975	Multi-region thermal interaction	Interaction start successively in each of several sections with time dely	i-û heat conduction Termal resistant layer at Ete fuel-coolant interface	Acoustic and the inertial constraint 1-B Lagrangian formulation	Propagation interattion can be talen into account
i i i i i i i i i i i i i i i i i i i	Fishlock	1975	Sub-assembly geometry	Seperate model required	Meet input into coolant from separate calc, or assumed	Acoustic constraint followed by inertial constraint	Calculate sodium expulsion rates in sub-assembly geomery (LMFBA)
TEXAS	Breton et al.	1976	Channel geometry	Continuous fragmentation with variable mass of fuel during fragmentation time	Phase A; transient conduction inertial constraint Fhase B; quasi-steady state Four options on contact area	inactial constraint	Application to the FEF exp'ts
ispra Mode!	Goldamer et al. 1976	. 1976	Channel geometry with bottom fuel and impacting liquid Intimate contact with fuel after fall of sodium column	Area of contact due to coolant impact and increases continuously during acoustic travel time	Phase A; heat conduction to solium during the intimate contact, Fhase B; heat conduction through vapor after return of rarefaction mave Vaporization and condensation	Inertial constraint, Ejection for analysis of UGC:sodium and re-entry of the coolant—and UGC:water experiments column calculate:	For analysis of U22'sodiua and U02;kater experiments
VS-4	Putten et al.	1976	Thermal interaction zone split into a number of axial regions with different particle radii	Fuel particles divided into groups which start to interact successively at different times	Meal transport inside fuel particles and through a vapor film layer, Thermodynamic equilibrium between liquid and vapor	Isentropic sound velocity function of pressure and temperature Friction effects considered	Anial dependence of thermal interaction
Tol yo Medel	Kondo et al.	1976	Multi-channel geometry Mixing starts independently in each channel		Statlar to ANL Model	Coupling of the incoapressibl To study an effect of the column with each channel non-coherent mixing	To study an effect of the non-coherent aixing
FCI-II/ ASPRIN-II	Sawada et al.	1976	Channel geneetry Specified mixing condition	Specified exponential fragmentation model	Fhase A; single phase transient conduction Phase B; quasi-steady state Q, Iwo phase heat transfer Heat josses to the surroundings	1-D compressible flow in Lagrangian formulation, Gussi-2-D Newtonian flow with vessel deformation as	FCI-II based on AML Model, ASFRIA-II; modilied version of the reactor containment response analysis code

Code for UO2/Water system (LWP application)	LMR application Comparison pressure loading to PAR failure limit	Code far FCI in a chennel geo- metry ie.g. shock tube exp'tsi ; UOZ/Na system	Code for FCI in a multi-channel geometry (e.g. LMFBA subassembly)	To find heat transfer coefficient range based on Ninfrith exp'ts data	To analyze Sandia F115 exp'ts (LWR application) Full Water/Steam equation of state
I-D compressible model inertial constraint	Fressure loads regulting from LWR application the fuel energy release Comparison pres FWR failure lim	Inertial constraint Compressible energy and accustic trevel time	Inertial constraint Acoustic characteristics	Two different loadings; (a) inertial loading (b) acoustic loading	
intrade contact between mother feel and coolant is issueed during fragmentation. Sapid phase changes in the fluid due to therail consideration neequilibriue consideration.	1-1, non-steady state heat transfer model Vapor film transparent to thermal radiation	Phase A; fuel-coolant contact Inertial constraint speecheated coolant layer by Compressible energy impact), Phase B; ejection an acoustic trevel time resorty of coolant (evaporation and heat conduction).	Stailsr to KAMIMA model	Transient heat conduction with schitrary heat transfer coeficient	Iransient heat conduction and Pianer expansion with inerti- radiation, Vapor evaporation constraint, Slug entrainment and condensation, Simple flow due to Taylor Instabilities ragins map
Finite fragentation and enxing time assummed	Instantaneous fragmentation Uniform fuel particle distribution with vapor fils Lumped fuel particle	Surface increase by impact kinetic energy	Uniform particle distribution with a speicified radius Mixing zone size determined by the impact velocity of coolant	Instantaneous fragmentation with log-normal distribution	Uniform particle distribution with exponential rate of frag- mentation into a specified radius
1976 Chamber geometry	Chamber geomatry Specified mixing condition	Cooling channel geometry; Surface increamolten fuel in its bottom and kinetic energy coolant in the rest of tube	Multi-channel geometry Mixing zone of 50 % UO2 and 50 % sodium	Chamber gepmetry with mixing zone at the bottom and slug zone on the top	Chamber geometry with mixing zone at the bottom and slug sone on the top
Teschendorf 1976 Kahba	Drescher et al. 1976 Chamber Specifi	Goldasser, Mehr 1977	Goldammer, Mehr 1980	Flatcher 1984	Oh, Corradini 1984
1358	01-3K31	KANING	Sani	Winfrith Model Flatcher	UN Mode!

- (1) The peak pressure decreases and the pressure rise time becomes longer as (a) the initial thickness of the vapor blanket increased and as (b) the fuel fragment size or fragmentation time became larger (Fig. 43);
- (2) The wall deformation appears to have a negligible effect on the pressure-time history;
- (3) The use of a mean particle diameter instead of a fragment size distribution would not introduce any gross errors.

One can indicate a few limitations of this parametric model. This model is an equilibrium model, therefore the vapor generation rate was not the result of excess energy transfer to the vapor-liquid coolant interface from the fuel, but rather was calculated from the thermodynamic equilibrium equation of state for the sodium coolant. This has the effect of suppressing vapor formation early in the calculation as the coolant heats up to saturation; thus the early time pressures may be overestimated with small amounts of vapor present as single phase pressurization of the liquid occurs, and underestimated with a large initial void fraction. Later in time the vapor pressure may be sustained at higher values for longer times because so much energy has now been transferred to the coolant. This may cause an overestimate of the conversion ratio. Also the heat transfer mechanism did not take into account radiation energy transfer and neglected the thermal inertia of the vapor blanket. This last assumption is valid for a sodium coolant but not in general. There was no correction for the continuous phase change of the coolant in the interaction zone (i.e., a flow regime map), which means that the heat transfer area of liquid coolant around the fuel may be overestimated during the latter stage of the expansion process when the continuous phase becomes coolant vapor. A secondary effect of neglecting the flow regime change is that coolant liquid outside the explosion zone would be entrained by surface instabilities (e.g., R-T instability) as the expansion proceeds. These phase change corrections and the quenching effect due to further coolant entrainment could reduce the vapor generation rate and lead to a decrease in the predicted overall conversion ratio.

The parametric model was used to match specific in-pile and out-of-pile LMFBR experiments; e.g., the TREAT M-series and H-series tests. The technique used was to find the proper values



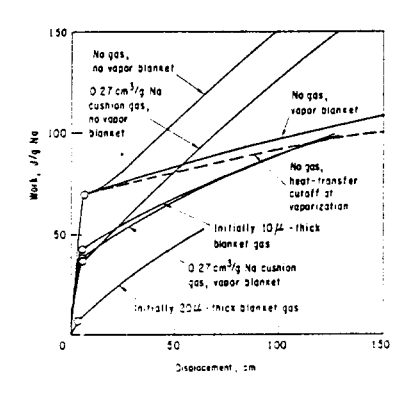


Fig. 43. Effects of gas-vapor blanketing

of the fuel fragmentation size and time to match measured test data. The fuel fragment size, fragmentation-mixing time, and the fuel-to-sodium mass ratio were found to be in the range of 117-234 $\mu m,~0-10$ ms, and 5.5-12.36, respectively, for these test conditions. These limitations of the model were recently modified by Oh et al. (1984, 1985) to allow a more general parametric treatment; e.g., a nonequilibrium coolant treatment and a flow regime map.

4.2.2.2 <u>Cardarola Parametric Model</u> An extensive parametric study was also carried out by Cardarola (1972, 1975) for <u>LMFBR</u> applications. One difference from Cho's model is that the sodium in the interaction zone was distinguished into three zones, namely the liquid, the vapor film, and the mixed vapor, which are all at the same pressure. The ratio of mixed vapor in the liquid and the vapor film around the fuel particles was obtained based on the force balance when the vapor flows away along the space between the fuel surface and the liquid coolant surface. The result shows that the small particles have a vapor layer thickness larger than the big particles. It is worth noting here that there is a competing effect between the amount of vapor generation due to energy transfer and the insulating effect of the vapor film. In this model sodium vapor was also assumed to be in thermal equilibrium with its liquid. This means that the mixed vapor is saturated vapor and has the same temperature as the liquid. In his early theoretical model (1972) no time dependent fragmentation model was considered, which means that a constant number and size of the fuel particles were assumed during the entire interaction. In the later model (1975) the mass of fuel and sodium participating in the interaction was considered to vary as a linear function of time. The main conclusions of this model are the following:

- (1) The total work done by the interaction strongly decreases with increasing fragmentation time and mixing time constant, which is similar to Cho's results. However, for values greater than 5 ms the reduction was not found to be very important;
- (2) Vapor blanketing during phase B is effective only if it is accompanied by a relatively slow process of fragmentation and mixing;
- (3) It is possible to considerably reduce the total work if one uses higher values of the vapor film time constant defined by this time constant determines the relative ratio of mixed and film vapor.

$$t_b = \frac{\rho_f c_f R^2}{3K_v} \tag{73}$$

where: $F_f = average particle radius$

Cf = fuel specific thermal capacity

K' = thermal conductivity of vapor film;

- (4) The total work increases with the initial height of the sodium piston acting as the inertial
- (5) Effects of fuel fragment size distribution and of gas constant are important only for very rapid fragmentation and mixing.

These results are not unlike those found by Cho in his analysis.

In this model the criterion for change from phase A to phase B was when the bulk coolant temperature is calculated to be greater than the saturation temperature; however, the criterion of Cho using the acoustic unloading time seems to be more appropriate. The assumption of having no vapor exist in phase A is not correct for the premixing condition of uniformly mixed fuel particles in the interaction zone. Also it must be noticed that the vapor around the fuel particles in phase B may be superheated in reality, so that its thermal conductivity is expected to be lower than the saturated vapor and the thermal inertia of the vapor increases. This effect will eventually decrease the total mechanical work output calculated. Most of the other limitations are similar to those mentioned previously for Cho's model.

One should note that the parametric model cannot predict the thermal temperature threshold for vapor explosions which was observed in many experiments (e.g., Henry et al. 1973, 1974). Also in order to physically describe the energy transfer mechanism involved in the interfacial interactions nonequilibrium modeling of the coolant should be considered, because vapor film superheating and the vapor generation rate at the interface could be important factors early in the explosion in determining the pressure history and overall explosion conversion ratio. Most of the parametric models use an equilibrium model, in which the coolant is treated as one homogeneous component. This means that the energy transfer from the fuel to the coolant at early

times is primarily used to raise the temperature of the whole coolant mass in the interaction zone to saturation rather than to superheat the vapor film around the fuel. As a result, the magnitude of the peak pressure and the delayed characteristic time for peak pressure when vapor is present would be expected in the equilibrium model compared to a nonequilibrium treatment. One can overcome this difficulty to better predict the experimental data by independently adjusting the important parameters of the model. This means that the input set for the calculation to match experimental data is not unique in parametric models. However, these parametric studies have provided useful contributions in identifying the key parameters which have significant effects on the pressure behavior and the conversion ratio of the vapor explosion such as fuel-to-coolant mass ratio, characteristic fragmentation time and size, and expansion inertial constraints.

4.2.3 Mechanistic Propagation Models A significant contribution to the overall description of the vapor explosion was provided by the steady-state detonation theory of Board et al (1974, 1975) and this thermal detonation concept is widely used as a possible construct for the vapor explosion. The process could be subdivided into three stages. In the first the two liquids are coarsely mixed with relatively low heat transfer between them. In the second a trigger provides an initial pressure pulse to induce a local interaction. Finally this pressure wave escalates and propagates through a coarse mixture causing vapor film collapse and establishing a flow field behind the shock front. Subsequently hydrodynamic or thermal mechanisms lead to fine fragmentation of the fuel droplets and results in rapid heat transfer which produces expansion of the more volatile coolant liquid. This expansion sustains the shock wave and produces a propagating vapor explosion. Since then there has been visual evidence from a number of experiments (e.g., Briggs (1976), Fry and Robinson (1979, 1980), Goldammer (1980), Mitchell (1981, 1982, 1986), Schwalbe (1982)) that the propagation of a vapor explosion has a relation to the shock front propagation. For the remainder of this discussion the explosion escalation and propagation given a mixture and a trigger will be considered.

The original steady-state detonation model developed by Board et al. (1974) was a thermal equilibrium model which implied essentially complete fragmentation of the fuel drops to fine debris and a kinetic equilibrium model which meant no velocity differential between the fuel debris and the coolant. Therefore, the conditions at the C-J plane are determined solely by the upstream conditions and the tangency condition, and are independent of the kinetics of the fragmentation process and the heat transfer process.

Actually the steady-state detonation model was based on the observations of propagation in metal-water thermal interactions. But few experiments have been able to give clear evidence of a high conversion ratio of the thermal energy into mechanical work as predicted by the model. Therefore, R.W. Hall and Board (1977, 1979) and Baines et al. (1980) developed a steady-state "vapor detonation" model, which allows for thermal nonequilibrium effects in the coolant due to the vapor generation within the reaction region. In this model, it was assumed that immediately behind the shock all the vapor is condensed in the shock and the liquid phase is compressed exceeding the saturation pressure of the coolant. Subsequently the liquid phase expansion begins and falls to saturation pressure where vapor generation starts. This vapor generation may limit further fuel-coolant heat transfer. As a result of this process the efficiency could be lower than thermodynamic maximum. One should note that even though these models employ the hydrodynamic fragmentation concept due to the velocity differentials they do not explicitly take into account the relative velocities between the fuel and coolant in the detonation zone when calculating the overall expansion characteristics. Rather fragmentation is assumed to occur with sufficient rapidity that local thermal equilibrium is likely achieved.

To consider these multiphase velocity nonequilibium conditions, various steady-state detonation models were developed using stability criteria to determine the steady propagation cases. Sharon and Bankoff (1978, 1978, 1981) developed a steady-state detonation model of one-dimensional shock wave propagation through a coarse mixture introducing the relaxation zone which allows the hydrodynamic fragmentation due to boundary-layer stripping and/or Taylor instability (Figs. 44-45). Scott and Berthoud (1978) independently formulated a similar multiphase hydrodynamic model to describe the behavior of a two-phase mixture to shock waves. Their calculations on propagating vapor explosions have largely concentrated on determining steady-state conditions to see if a self-sustaining propagation is possible during the explosion. In these models an effective two-phase flow simplification was employed to define the two-phase flow kinetics at any point of the propagation reaction zone (sometimes called relaxation zone) in terms of a first phase consisting of unfragmented fuel droplets with one phase velocity and thermal state, and a second fluid state which is a composite of finely fragmented fuel debris and coolant. This second fluid phase also has a single-phase velocity and thermal state. These models assume the time scales for thermal and velocity equilibration of the fragmented fuel and coolant to be much shorter than those for fragmentation or similar equilibration of unfragmented fuel droplets and coolant. Thus, in this case the equilibrium requirement can be met by zero

relative velocity at the C-J plane. It seems that this assumption of velocity equilibrium at the C-J plane is much more appropriate than that of complete hydrodynamic fragmentation used in the original model.

Schwalbe et al. (1981) also developed a similar steady-state thermal detonation model with the same velocity equilibrium assumptions at the C-J plane to interpret tin-water and aluminum-water experiments by Fry and Robinson (1979, 1980). In all of these models the C-J wave analysis is no longer uniquely determined without detailed knowledge of constitutive relations for kinetics of fuel fragmentation and fuel-coolant equilibration. Therefore, Condiff (1982) reformulated a two-phase flow model of one-dimensional steady-state detonation to separate the realistic C-J plane prediction of detonation strenghts which can be obtained from jump balance conservation conditions, thermodynamic relations and sonic termination, from that of fragmentation kinetic rate-dependent detonation zone lengths. No comparison was made with the experimental results by Condiff.

As a result of these steady-state modeling efforts and calculations the existence of self-sustaining steady-state detonation waves within a coarse fuel-coolant mixture, based on hydrody-namic fragmentation mechanisms, seems to be theoretically possible in appropriate constrained geometries. However, predicted steady-state conditions may be far away from the conditions produced in the experiments and accident situations; especially because high trigger

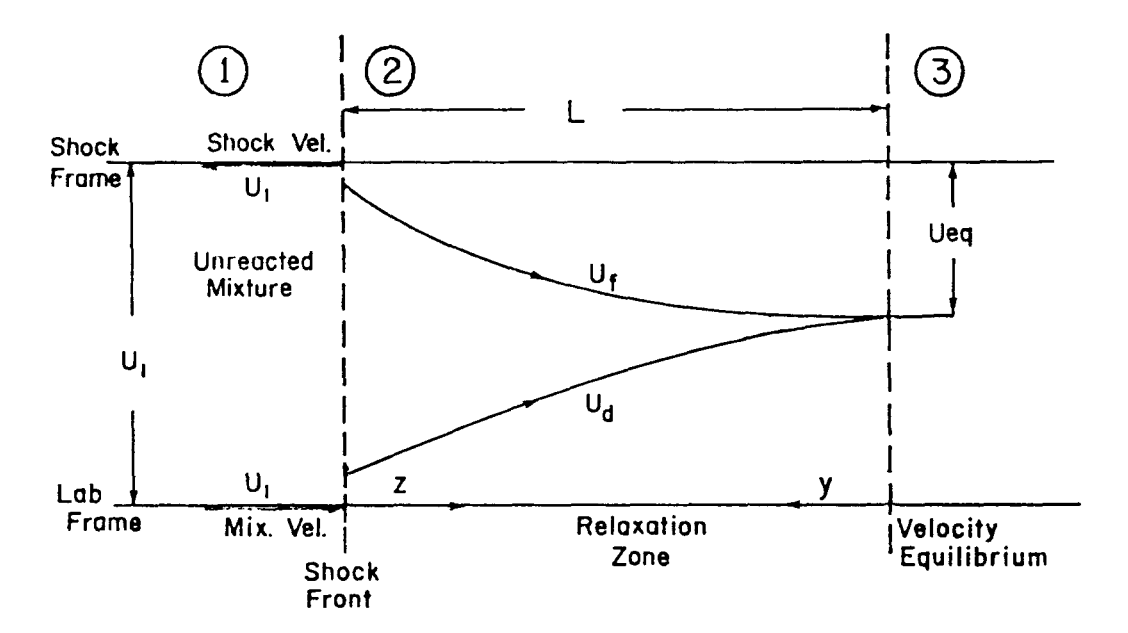


Fig. 44. Description of the different interaction zones.

pressures (10-100 MPa) and large reaction zone dimensions were required to develop these steady-state detonations (Fig. 45). Also, for a given set of initial conditions the steady-state models provide only a special case, namely the case of a self-sustained detonation wave. No consideration was given to the more realistic problem whether or not for these cases a propagating vapor explosion may escalate from an initial low pressure trigger within a reasonable fuel-coolant mixture length to a steady-state detonation. Therefore, for the theoretical analysis of the escalation of an arbitrary trigger pulse into an explosion in a given fuel-coolant mixture, a transient propagation model is needed.

Fishlock (1979) developed a transient thermal detonation model using a one-dimensional Lagrangian hydrodynamic approach to perform calculations on propagating vapor explosions in both the aluminum/water and $\rm UO_2/sodium$ system. Since this model assumes that both hot and cold liquids have the same velocity at a given position in the mixture, one must make an assumption as to the relative velocity at the shock front to employ the hydrodynamic fragmentation concept. Thus the differential velocity at the shock front was conservatively assumed to equal the

calculated single liquid flow velocity. This assumption tends to significantly overestimate the fuel fragmentation rate and therefore cause a much more rapid escalation than one would expect. In this way Fishlock was able to consider three possible processes for the fragmentation of the hot liquid such as shock velocity fragmentation, impact fragmentation, and mixing due to asymmetric vapor bubble collapse. These calculations suggested that the fragmentation processes considered here may indeed contribute significantly to the fragmentation in a propagating vapor explosion and that they may produce rapid escalation from a relatively small disturbance (Fig. 46). This conclusion would be affected by the relative velocity assumption used and therefore must be scrutinized carefully. The calculation also showed that when the same assumptions about the initial conditions and fragmentation processes are made for the aluminum/water and U02/sodium systems then similar results were obtained for the interaction.

Mosinger (1980) performed numerical shock tube calculations in order to investigate the shock wave induced fragmentation process of fuel drops in a fuel-coolant interaction. For that purpose the two-phase code DRIX-2D was used considering a water drop within a vapor environment. The code DRIX-2D was developed for transient two-dimensional problems in two-phase water flows. The relative velocity between the two phases is calculated by means of a drift-flux approximation. Harlow and Ruppel (1981) also performed the propagation calculations using the computer code SALE-2D developed by Amsden et al. (1980) to describe the propagation

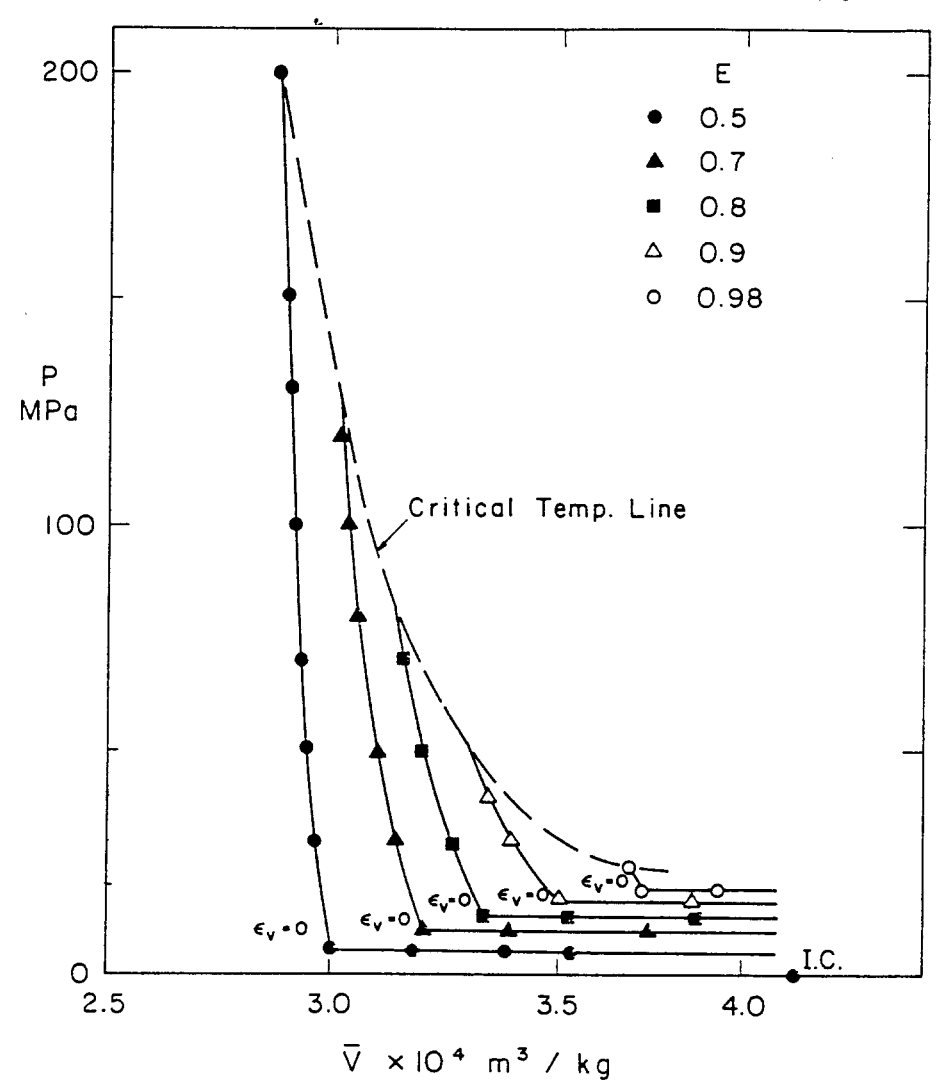


Fig. 45. Partial detonation hugoniots for Sn/H_20 m_{fuel}/m coolant = 6.5 (Board/Hall case)

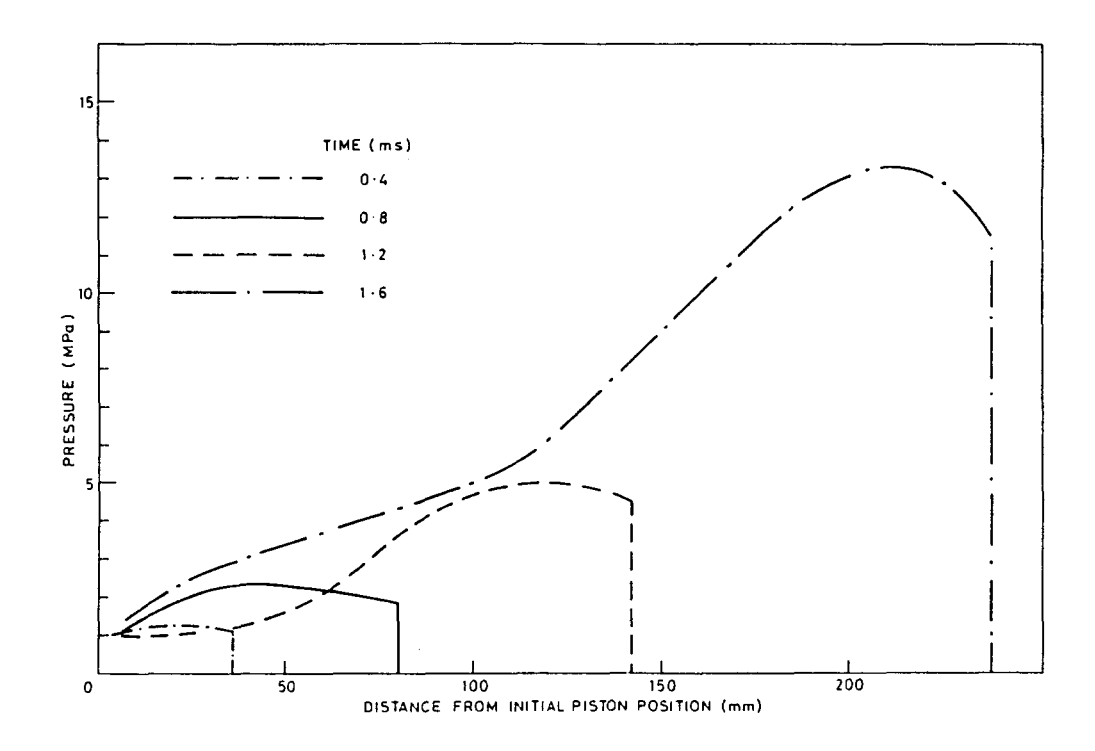


Fig. 46. Aluminum/water calculation-escalation of pressure with time

characteristics in horizontal stratification geometry. The computer code SALE-2D was modified to calculate the dynamics of two different fluids. In this preliminary calculation they considered one liquid which is separated into two regions by a vapor film. However, these two-dimensional hydrodynamic codes were just fluid dynamics calculations for two-phase flow analysis without any detailed mechanistic models to describe the fuel fragmentation and the heat transfer mechanisms. They were only useful in determining the pressure wave characteristics independent of the feedback from fuel fragmentation.

Corradini (1982) used a transient multiphase one-dimensional code, WONDY, developed by Lawrence and Mason (1975) to describe the propagation phenomenon. This Lagrangian hydrodynamic model dealt with three materials--fuel droplets, vapor, and liquid coolant but has one bulk velocity of fuel-coolant mixture. This wave code was designed to solve conventional continuum relations, but was modified by Corradini (1982) to incorporate this multiphase system and a thermal fuel fragmentation model for a large-scale explosion. The thermal fragmentation mechanism used in this calculation considered that high vapor pressure due to rapid vapor generation after local film collapse causes Taylor instabilities which produce coolant jets that fragment the fuel. This analysis indicated that a vapor explosion propagation can grow from a small trigger disturbance; however, it did not reach steady-state detonation conditions in all the calculations performed even after a few meters of propagation distance. In fact as the initial void fraction increased the propagation speed and pressure decreased (Fig. 47) markedly

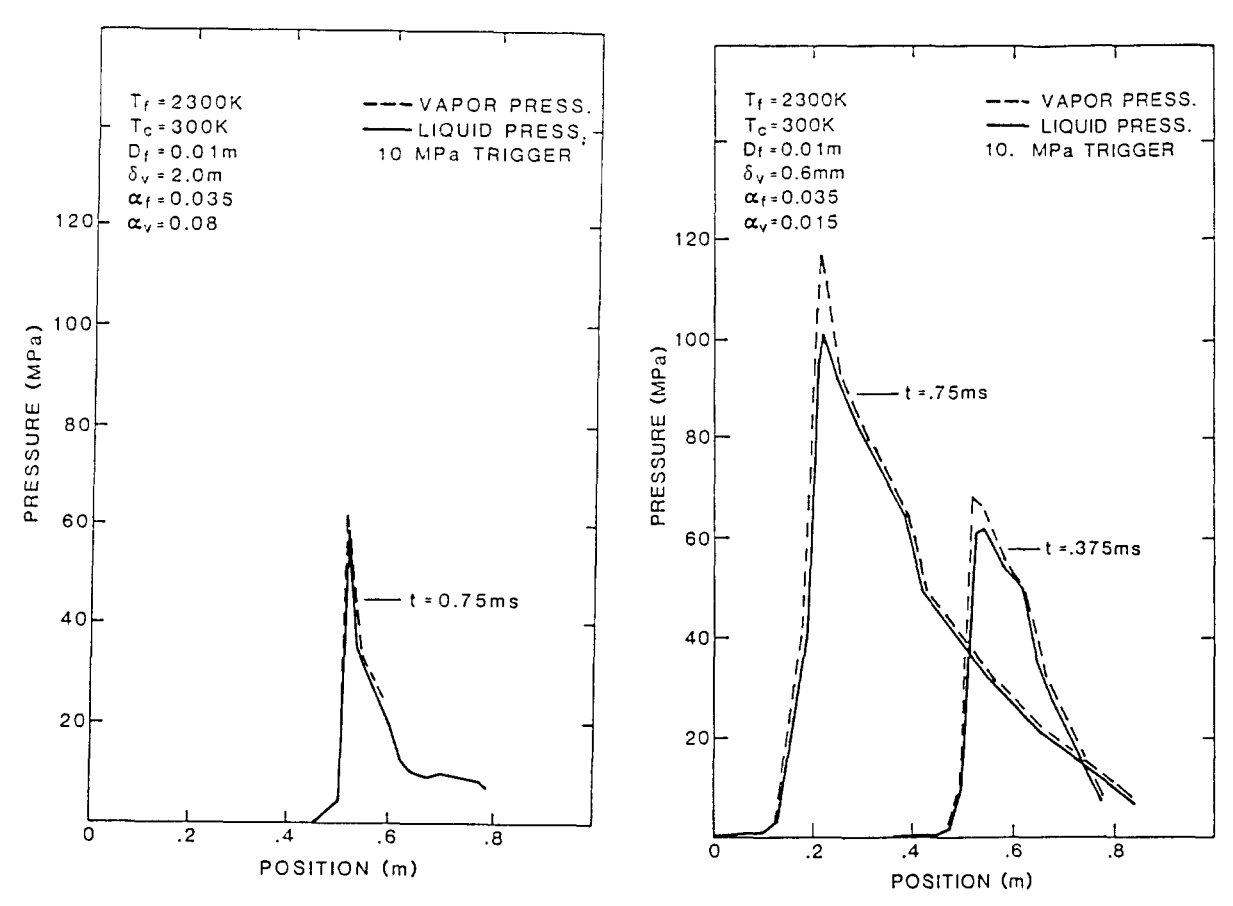


Fig. 47. One-dimensional, thermal fragmentation model propagation of an explosion through a corium-water mixture as a function of the vapor void fraction. (Corradini 1982)

causing the escalation phase to become longer (1% < α < 10%, 500 m/s < V_{prop} < 1000 m/s). Also a purely hydrodynamic fuel fragmentation mechanism was calculated to be incapable of causing escalation from a small trigger pulse (P_{trig} < 1 MPa), because the induced relative velocity is too low to cause rapid enough fuel fragmentation. Large initial trigger pressures would be required similar to those predicted by Williams (1976). This is in contrast to the results of Fishlock. The major limitation of this work was that the hydrodynamic model only considered fuel in a continuous liquid coolant phase and thus was limited to small initial coolant vapor fractions ($\alpha_{\rm V}$ < 25%) and could not calculate accurate results when the explosion entered its expansion phase; i.e., high void fractions.

Carachalios et al. (1983, 1985) developed a transient one-dimensional multiphase model to describe the triggering and escalation behavior of a thermal detonation. This model is an Eulerian hydrodynamic code to describe the transient flow field behind the shock front. A shock fitting method provides the values of the flow field just behind the shock front as well as the propagation velocity. In this model it is assumed that the shock wave propagating in the coarse mixture causes vapor collapse and establishes a flow field with three phases and two velocities behind the front. One should note here that the hydrodynamic fragmentation due to differential velocity and the energy transfer based on this could be considered consistently in this model. As in other past transient models which allow for only one velocity within the flow field one has to assume this fragmentation mechanism explicitly as an input. The escalating behavior of the detonation waves was examined by parameterizing the ignition energy, and escalation length and time needed to reach a steady state behavior. By choosing suitable values for the model free parameters a comparison with the results from the standard experiment T-107 of Fry and Robinson (1979) was carried out. The propagation behavior of the wave as well as the pressure development at the single pressure transducers was nicely simulated by assuming a homogeneous

mixture. The transient model showed further restrictions of the heat release caused by the duration of the escalation process and the finite heat transfer from the fragments in contast to the instantaneous release assumed in the steady state models (e.g., Sharon and Bankoff (1978), Schwalbe et al. (1980)). The major limitation of this transient model is that one must parametrically assume the initial trigger ignition energy to be large enough to induce an explosion. In the analysis of the experiments of Fry and Robinson (1979)) the trigger necessary to induce a propagating explosion was significantly greater (1-2 orders of magnitude) than the external trigger pressure actually used in the tests. If the ignition trigger energy falls below a certain value no propagation occurs. Thus, although the model is transient, it requires a large ignition trigger energy to induce a propagation explosion, much larger than one used in experiments or would expect under accident conditions. Therefore, it seems to lack the proper physics to model escalation of the explosion from a small trigger source, which is observed experimentally. This may be due to the fact that it only considers hydrodynamic fragmentation and not thermal effects as discussed previously (Fauske, 1973; Buchanan, 1973; Kim, 1984, 1985).

Oh and Corradini (1985) developed a nonequilibrium vapor explosion model using the shock wave propagation concept to analyze the FITS experiments at Sandia. In fact this model is a transient one-dimensional explosion model for a planar expansion or hemispherical expansion case with a mechanistic fragmentation model. Most fragmentation models used in the previous propagation calculations did not have a direct correlation to the dynamic pressure escalation in the explosion zone and its propagation behavior through the mixture. In this calculation a dynamic fuel fragmentation model has been developed based on the fine fragmentation concept due to coolant jet entrapment, expansion, overexpansion, collapse and cyclic repeating of this process (Kim, 1985). The process continues until the system depressurizes and the local rapid fragmentation ceases as the explosion zone disassembles. The final expression for the fuel fragmentation rate was expressed as

$$\dot{m}_{fr} = \frac{\rho_f N_{mix} \pi D_f^2 U_{frago}}{3} \exp\left[-\frac{2U_{frago}t}{D_f}\right]$$
 (74)

where

$$U_{frago} = \left(\frac{P - P_o}{\rho_c (1 + (\rho_f/\rho_c)^{1/2})}\right)^{1/2} . \tag{75}$$

where most terms have been previously defined; N_{mix} is the number of fuel drops in the fuel-coolant mixture with diameter, $D_{\rm f}$. Inherent in this calculation was a knowledge of the fragmentation time which was determined by the time for the explosion propagation wave to traverse the mixture zone and slug to the nearest free surface. The shock wave propagation velocity was calculated by assuming a one-dimensional plane explosion front which is steadily progressing through the uniformly mixed materials initially at rest, and leaving behind it a local mixture moving at equal velocities. This model has a limitation for the fuel fragmentation mechanism due to coolant jet penetration under the situation when the initial liquid coolant volume becomes so small that it is not the continuous phase in the mixture. Under these conditions the model cannot be reliably used. This limitation extends to most of the past models that assume the fuel is mixed in a continuum of liquid coolant. In this case because coolant jet entrapment after film collapse is proposed the limitation is not just on flow regime transitions but also on the mechanism for fragmentation. The model prediction for FITS test (e.g., MD-19) shows an underestimation of the peak pressure for an initial void fraction of 50% which is large compared to the experimental observation. However, one can match MD-19 pressure data by reducing the initial void fraction to 10% (Fig. 48). Based on analysis of the Sandia experiments, Oh found that the initial conditions of the mixture (fuel mass, coolant mass and vapor void fraction) were the prime determinants in accurately predicting the explosion pressure history and conversion ratio. Full-scale calculations for a light water reactor in-vessel situation indicates that the mass ratio of coolant to fuel involved in the explosion could be considerably smaller as compared to the FITS-scale experiment. This result, combined with the larger inertial constraint, results in higher predicted pressures inside the explo

4.2.4 Explosion Expansion Models In vapor explosion experiments the explosion can exhibit multidimensional characteristics. These characteristics could cause a nonuniform pressure loading of the surrounding structure and may mitigate the explosive work potential from what would be estimated by a one-dimensional analysis. A similar situation may exist in full-scale accident situations; e.g., in a postulated reactor accident or in an industrial accident.

Coddington and Staniforth (1980) performed calculations on a propagating vapor explosion using the SIMMER code to analyze the Winfrith Thermir experiments (Bird, 1979; Fry, 1979). The 2-D effect in the test was that the far end of the test vessel began to pressurize while the explosion shock wave was still propagating through the mixture region, because the area outside of the mixture region was considered to be single phase water. The SIMMER code is a two-dimensional multiphase hydrodynamic code developed by Smith (1979) and sometimes used by its developers for vapor explosion analysis This code can provide a prediction of the vapor explosion, although some changes to the code were required to describe: (1) a quasi-steady film boiling period, (2) a trigger to initiate the explosion, and (3) an escalation and propagation of the explosion. The advantage of this code is that it models directly the multifluid and the two-phase (vapor, liquid) aspects of the problem and therefore allows one to examine the collapse of the initial vapor film and production of coolant vapor as a result of the fuel heat transfer. However, this computer model cannot calculate a hot/cold liquid differential velocity directly because the model has only one liquid velocity field. SIMMER also does not allow for radiation heat transfer. Thus this model did not use a mechanistic model for fuel fragmentation and heat transfer. Rather the original fuel-coolant liquid transfer model was altered to simulate an explosive heat transfer rate by considering liquid-liquid droplet collisions. Such a technique was used to model a vapor explosion expansion in the Zion LWR probabilistic safety analysis (1980). The results of this analysis indicated that the kinetic energy of the slug from the explosion could be large but would impact the RPV head in a two-dimensional fashion reducing the pressure loading and the likelihood of generating a missile that could damage containment. More recently Bohl (1982, 1986) has been developing modifications to the SIMMER model to allow for a more realistic treatment of vapor explosions.

Corradini (1981) developed a simple empirical explosion model and incorporated it into a two-dimensional hydrodynamics code, CSQ, developed by Thompson (1979). In this model the vapor explosion was modeled as a chemical explosion within the coolant after the fuel coolant heat transfer had occurred. The empirical explosion model considered the water and the steam intermixed with the fuel to be analogous to a chemical explosive and considered the thermal energy of the fuel melt released to the coolant to be analogous to the chemical heat of reaction during an explosion. This model was based on the concept that in the explosion zone the fuel and coolant interact rapidly enough to attain local thermal equilibrium before substantial coolant expansion occurs. Simple hand calculations were performed to set up the representative initial conditions This CSQ model is not mechanistic, because it requires three for experimental analysis. empirical input variables that are not mechanistically modeled beyond the initial mixing conditions: (1) the explosion propagation velocity, (2) the fuel-coolant equilibrium time, and (3) energy transferred to the coolant per unit mass of coolant in the explosion zone. This type of analysis gives some multidimensional insight into the experiments in terms of presure histories, conversion ratio, the expansion velocity and the mass of coolant participating for a given mass of fuel needed to match the experimental data. However, because of the empirical input needed, it is useful mainly as a post-test analysis tool or for parametric expansion calculations. It was found that for intermediate scale explosion experiments by Mitchell et al. (1981) the explosion can propagate spatially with quite large velocity (200 to 600 m/s) before any significant expansion occurs, and that not all of the coolant may participate in the initial explosive interaction. However, after the fuel has been quenched, it is possible that additional coolant does participate during the expansion phase due to surrounding coolant entrainment and convective mixing. As a result, the explosion work potential would be reduced.

Hadid et al. (1985) recently used a general multiphase multidimensional hydrodynamics code, PHOENICS, to calculate the fuel-coolant mixing in the lower plenum of a PWR in a severe accident. The PHOENICS code, developed by Spalding (198), can solve the one-, two-, or three-dimensional transient conservation equations in either Cartesian or cylindrical polar coordinates. Interfacial transport expressions for mass, momentum, and energy, or any other conserved quantity, can be supplied by using a fully implicit, and hence iterative, formulation. Hadid et al. calculated transient velocity and fuel/coolant concentration fields throughout the pool, but did not use any mechanistic model for fuel breakup during mixing. Rather the initial fuel diameter was assumed. Therefore his calculation is similar to a three-dimensional parametric model where at the beginning of the calculation the fuel is uniformly prefragmented to a specified size and is allowed to contact the coolant. After the mixture concentrations are calculated a Hicks-Menzies thermodynamic analysis is performed to calculate the explosion conversion ratio, where each Eulerian cell of the PHOENICS calculation is used as the initial condition for the thermodynamic analysis. The results of such an analysis are bounding in that the isentropic work from the explosion is predicted given the initial mixing conditions.

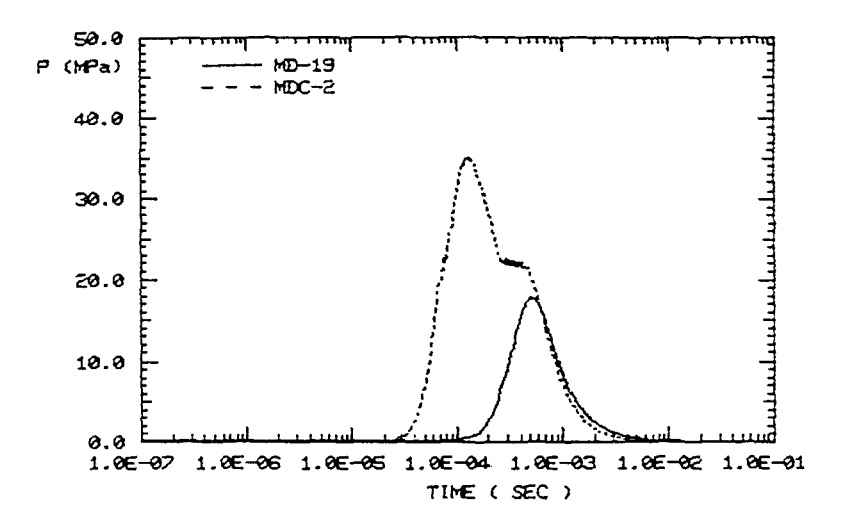


Fig. a Pressure vs. Time

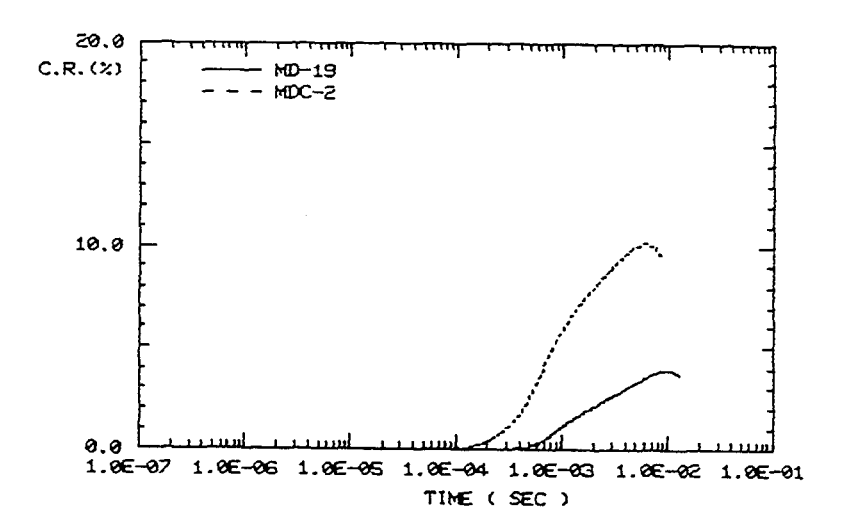


Fig b Explosion Conversion Ratio (Ek/Efi) vs. Time

Fig. 48. Analysis of EXO-FITS test MD-19 and MDC-2 using a thermal fragmentation mode for propagation and expansion. (Oh 1985)

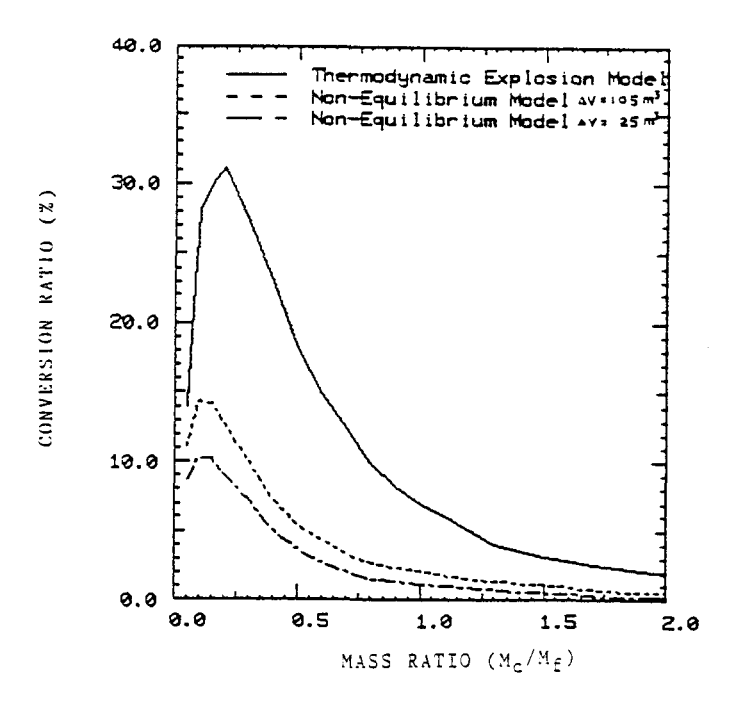


Fig. 49. Conversion ratio comparison of thermodynamic and nonequilibrium model as a function of cooland/fuel mass ratio for full-scale

dimensional parametric model where at the beginning of the calculation the fuel is uniformly prefragmented to a specified size and is allowed to contact the coolant. After the mixture concentrations are calculated a Hicks-Menzies thermodynamic analysis is performed to calculate the explosion converison ratio, where each Eulerian cell of the PHOENICS calculation is used as the initial condition for the thermodynamic analysis. The results of such an analysis are bounding in that the isentropic work from the explosion is predicted given the initial mixing conditions.

As stated above some investigators have used the multi-dimensional multi-phase hydrodynamic code such as SIMMER, CSQ, and PHOENICS to investigate the vapor explosion problem. These can provide multidimensional insights to the explosion with given empirical input: SIMMER--fuel-fragment size and liquid/liquid heat transfer, CSQ--energy transfer rate, and PHONEICS--fuel fragmentation size. However, all these tools use a simple approach for modeling the explosion physics with sophisticated hydrodynamic formulations for the general multiphase expansion. One should characterize such analyses as parametric with assumed initial conditions based on other analyses. These tools should only be used in concert with mechanistic models or constitutive relations for a specific problem. The reason for this is that scaling the phenomena is quite important and one must use the mechanistic models to address the question of scaling. Then these parametric tools could be used to look at multidimensional effects. In order to accomplish this one might have to alter portions of the model, because one could not just combine separate mechanistic models due to their dependencies and complexities. Therefore these parametric analysis must be used in concert with mechanistic models and scaling laws to determine their proper role in explosion analysis.

5. VAPOR EXPLOSIONS CONSIDERATIONS IN LIGHT WATER REACTOR SAFETY

In a present day nuclear fission reactor if complete and prolonged failure of normal and emergency coolant flow occurs, fission product decay heat could cause melting of the reactor fuel. If a sufficiently large mass of molten fuel mixes with the coolant and a vapor explosion results, the subsequent vapor expansion might cause a breach in the containment of the radio-

active fission products. These radioactive fission products could then be released to the environment threatening the safety of the general public. Although this type of nuclear accident is postulated, the health consequences are large enough that it is considered in reactor safety studies.

A comprehensive risk assessment effort in the Reactor Safety Study, WASH-1400 (1975), was the first study to estimate the likelihood of containment failure by a number of physical processes, one of which being a vapor explosion. The study focused on two specific reactor designs, the Surry pressurized water reactor and the Peach Bottom boiling water reactor. For the vapor explosion process it was determined that the containment could be threatened by three possible damage mechanisms: (1) dynamic liquid phase pressures on structure, (2) static overpressurization of the containment by steam production, and (3) a solid missile generated from the impact of a liquid slug accelerated by the vapor explosion. Based on analyses it was determined that for these designs the major concern from the vapor explosion was a direct failure of the containment caused by missile generation (designated "alpha-mode" failure). This might occur when a vapor explosion occurs in the lower plenum of the reactor vessel and the surrounding water and/or fuel are accelerated as a slug to impact the reactor vessel head generating a solid missile. Based on the analysis of available experimental data at that time and on parametric analyses, WASH-1400 estimated the conditional probability of alpha-mode failure (given a complete core melt) to be 10⁻²/reactor-yr with an upper bound value of 10⁻²/reactor-yr. Since the accident at Three Mile Island, a number of investigations (e.g., Theofanous et al., 1982, 1986; Fauske et al., 1981; Corradini et al., 1979, 1981a, b: Swenson et al., 1981; Berman et al., 1984; Bohl, 1986) have reexamined this phenomenon and estimated the probability of its occurrence given a core meltdown accident.

In the estimate of the alpha-mode failure probability the authors of WASH-1400 subdivided the vapor explosion phenomenon into three general categories:

- Initial conditions; this involves the geometrical configuration of the reactor vessel at the time of fuel-coolant contact and the amount of fuel and coolant available for the interaction.
- Mixing and conversion ratio; this involves the basic physics of the vapor explosion (as reviewed here), such as fuel-coolant mixing, triggering, propagation and the resultant conversion ratio of fuel thermal energy to the slug kinetic energy.
- 3) Slug-missile dynamics; this involves the expansion characteristics of the slug within the specific reactor geometry, and the coupling to solid missile generation and containment penetration.

In the first area the analyses indicated that a substantial fraction of the core would be molten (50% or more) at a time when the reactor vessel lower plenum was still full of water. Therefore a probability of one was assumed for the possibility of fuel-coolant contact. In the second area, parametric analyses indicated that about 20% of the core was needed to participate in a vapor explosion to result in a large enough efficiency to threaten containment integrity. In addition it was felt that it was difficult for a liquid slug to effectively transfer its impulse and energy to the reactor vessel head and generate a large solid missile; this was considered particularly true for a BWR with its massive upper internal structures. Based on analyses, probabilities of 0.1 were assigned to both categories.

In a recent review of the probability of alpha-mode failure (see Steam Explosion Review Group, Ginsberg et al., 1985), the same three categories were used to subjectively estimate the alpha-mode containment failure probability. The groups of experts performed independent analyses and examined available experimental data to arrive at their opinions (Table 3). The spectrum of opinions indicated that the probability of alpha-mode failure is considered to be much less likely than what was estimated in WASH-1400 both for the best estimate value and the upper bound value. For some individuals, the estimates for failure probabilities were lowered in the case of (1) high pressure melt-down scenarios because a trigger would not be available, or (2) BWR geometries because of the massive internal structures that would mitigate slug expansion. Based on analyses of Cybulskis (Ginsberg, et al., 1985) it was also concluded that if these estimates are correct (i.e., less than or equal to 10^{-2}), the vapor explosion is not a significant contributor to the risk from a core melt accident. A number of physical processes that were considered in the analysis are summarized in Appendix C. The reader is encouraged to examine this recent report as well as previously cited supporting documents to gain detailed insight into the likelihood of alpha-mode failure in light water reactors.

Table 3. PWR Low-Pressure Sequence Subjective Conditional Probability Summary

				L	PAILURE PROBABILITY	BABILITY
INVESTIGATOR	INITIAL	MIXING & CONVERSION	SLUG		BEST ESTIMATE	UPPER LINIT
Bankof f		шинин		<u> </u>	< 10-4	
Bohl/Butler	.1 - 1.0	01 10.	10-4 - 1	<u> </u>	3x10-4	10-1
Briggs	8.0	0.05	0.3	l	<10-2	
Catton	3×10 ⁻³	3×10 ⁻²	9.0		5×10-5	
Cho		ининин		3	WASH-1400 very conserva- tive. Fallure extremely unlikely.	00 very conserva- Fallure extremely unlikely.
Corradini	1.0	$10^{-4} - 10^{-2}$	1.0	<u> </u>	10-4 - 10-2	. 10 ⁻²
Cybulskis	6.0	9×10 ⁻³	10-2	<u> </u>	10-4	10-2
Fauske			шиши	i >	Vanishingly small (=0)	mall (≈0)
Cinsberg	.75	5×10 ⁻³			4×10 ⁻³	4×10-2
Mayinger	шишиш		шинин		No endanger PWR cor	No endangerment of FRG/ PWR containment
Squarer	$10^{-2} - 10^{-1}$	10-1	10-2	<u> </u>	10-5-	-10-5 - 10-4
Theofanous			шиши	<u> </u>	<10_,	۹_01>
WASII-1400	0.1.0	$10^{-1}(+.5,-1)$ $10^{-1}(+.5,-1)$	10-1(+.5, -1)		10-2	10_1

"Hash marks" indicate atrong emphasis in investigator arguments. Solid lines indicate that investigator considered phenomena in this state of sequence. Note:

APPENDIX A. BRIEF REVIEW OF SMALL-SCALE FUEL-COOLANT INTERACTION EXPERIMENTS

A large number of small-scale experiments have been performed to study the fragmentation mechanism of fuel-coolant interactions. We classify an experiment to be "small-scale" when the amount of fuel (or coolant) is very small on an absolute basis or relative to the mass of the other liquid. An example of this would be that of a single drop of fuel in a large pool of coolant. Historically small-scale experiments have been classified according to the mode of fuel/coolant contact: free and forced contact mode. Table A.1 gives a summary of a small-scale fuel-coolant interaction experiments.

In the free contact mode, the molten fuel falls into the cold liquid in the shape of a single drop. The droplet is sufficiently small that the interfacial tension induces a roughly spherical shape. After a certain fall distance the droplet strikes the cold liquid, moving into the vessel. It penetrates the coolant surface and falls even further until it reaches the bottom of the vessel. In some experiments an interaction occurs as soon as it contacts the coolant surface; in others during its fall through the cool liquid or when it falls on the bottom of the vessel. The interaction can be initiated spontaneously or by an external pressure pulse. Among other things, the following information can be derived from the experiments:

- a) All the experiments show a "dwell time" between initial contact and interaction. increases with both fuel temperature and coolant temperature. Together with optical observation it suggests that stable film boiling inhibits the interaction until the fuel cools down to some threshold temperature at which time the film becomes unstable and collapses.
- b) If the major portion of fuel solidifies before the vapor film breaks down no FCI occurs. The interaction of molten copper is one exception (Zyszkowski 1976) to this observation primarily due to stresses on the solid crust, which cause cracking and liquid fuel ejection.
- c) For experiments with tin and water the limiting temperature of tin was found to be 300°C, below which no FCI occurs. This limiting temperature is independent of water temperature and is above the melt temperature of tin $(232^{\circ}C)$. It does correspond to the instantaneous interface temperature at which a solid crust rapidly forms on the tin surface.
- d) In experiments with UO2/sodium stable film boiling is observed at least for a short time, particularly when the sodium is near its saturation temperature. The enery yield in this configuration is low.
- e) For small masses of fuel single interactions were observed. As the mass of fuel increases the possibility of multiple cyclic interactions increases.
- f) The existence of a noncondensable gas impedes the direct contact between fuel and coolant by means of a gas cushion, and thus prevents a spontaneous fuel-coolant interaction.

Another method of forcing two liquids into contact is "shock tube" experiments, where a coolant column impacts onto a molten fuel surface. The impact of cold liquid precipitates a high pressure even without a fuel-coolant interaction. At a sufficiently high impact velocity, this process impedes the development of an isolating vapor film so that coolant and fuel are forced into contact. Typically, there is more contact between fuel and coolant as the coolant column oscillates (bounces). The greatest interaction occurs on initial or second impact depending upon the fuel-coolant pair; the reason for this difference is unknown. Even though there are a number of experiments, serious analysis has been seldom carried out. A systematic study of the effects of the major variables has never been completed.

In injection experiments a small amount of one of the liquids, usually the coolant, is injected into the other by means of a needle. This achieves a condition in which one liquid is totally enveloped by another. In this way a film of inert gas or possibly even a vapor film, which tends to separate coolant from fuel, can be avoided. From numerous experiments the following observations are made:

- a) Energetic fuel-coolant interactions were observed when small quantities of sodium are
- injected into ${\tt UO}_2$, as well as water into molten salt; implying coolant heatup to some limit. b) Most of the experiments exhibit a dwell time. Violent boiling of sodium was observed during this waiting period. This might suggest that vapor generation inhibits the interaction initially, allowing the possiblity of coarse intermixing, thus setting up the conditions for a coherent vapor explosion.
- c) For some experiments (Anderson and Bova, 1976) the analysis showed that the measured mechanical work is greater than the thermal energy which is transferred from fuel to coolant during the dwell time.
- d) The dwell time in the tin/water interaction was found to increase systematically with fuel temperature, as in the dropping experiments. This may suggest that the trigger of fuelcoolant interactions in any contact mode may be similar in nature.
- e) Experiments injection sodium into stainless steel resulted in a weaker interaction than those injecting sodium in UO_2 . This is perhaps the consequence of the lower fuel temperature of stainless steel than that of UO_2 . However, the detailed nature of these differences is still undetermined.

Contact Mode Affuel is dropped or Injected into coolant BiCoolant is injected into buil fuel

college ladys untike later survivor ton asset tone or frames and

	system hat/cold	fuel RASS Of volume	fuel (G)	coolant aass or volume	coolant temp. (C)	get	entering velocity (m/s)	Neber	ande Ande	(#Pa)	tine (ms)	rearis	reference
25.75 25.00 16.53 lifes 25.47 26.00	1+Cu/Water	0.91-1.03 9		10-15 cc	16-18	Ę			æ				Zestowski (1977)
1.57 1.50	*Li/Water	25.4-150 g		6.53 litre		315	2.3-4.7		⋖		ž	of self-sustains or violest.	Hoane (1955)
10-15 178-70 1	203/Na	1-2 cc	2040		450-713	Æ			-	0.7	J	as Copyercion ratio	The second of the second of
10-35 70-75 1 cc 22	annum/Na		909-1950		220	717	3,45		- 42		5		Court Balon (1015)
1.556 cc 1.551 1.551 1.551 1.551 1.552 1	atomo/Kafer	100-125 0	790-970	-	5		•	1000	:		á	and the second of the second o	10011 13001 1 1000
15.56 cc 15.51 17.5 17	a Mater	20 12 0			; -	2	;	200			Ě.	a statement administration.	Rener et al. (1976b)
1.539 16.53 11cc 12 at		77 07 7			- 9	=			Œ.		~	ormation and rupture of the aluminum bubble	Brauer (1968)
150 g	#Inua/Kater	1.5-36 CC			2	717			æ		=	ncrease in the extent of frag. of Al when 1 % of Bi added.	Flory et al. (1969)
0.75 0.00 0.40 arr 0.45 arr 0.	elnus/Water	150 9		6.53 litre		alf	2.3-4.7		<e< td=""><td></td><td>ũ</td><td>ormation of oxide file.</td><td>Higgins (1955)</td></e<>		ũ	ormation of oxide file.	Higgins (1955)
10-150 0.1	atous/Hater	20 9				714			.		Œ	loudable ard selting apparatus	Nelson, Buxton (1977)
14-15 g 720-200 13-71 air 2.7-3.1 b 10 p p 14 50 metric betto cevely formed. 14-15 g 200-200 13-71 air 2.7-3.1 b 10 p p 14 50 metric betto cevely formed. 15-20-20 23 metric	einus/Hater	0.3 cc	800-1500		0,60	al.r	3. 45		•		×	o fragmentation	Swift, Baker (1965)
10.4 200-70 25 cm 21 21 22 22 23 24 25 25 25 25 25 25 25	ainua/Water	10-15 9	720-820		15-31	715	2.7-3.1		-ax		ž	o fragmentation. Bottom cavity formed.	Witte et al. (1971)
Chief-Chief 20 20 20 20 20 20 20 2	ninum/Kater		300-950			-			8	¥: 01	t	hork-Tube experiments.	Mr. obt Maharatone (1914)
	Dinus/Mater	0.4 0	820		18-21	315			•	:	ت ا	month of the state	2003-0-0-0-0-0-0-0-0-0-0-0-0-0-0-0-0-0-0
\$0.40 \$4.04 \$1.00 \$2.0 \$1.1 \$1.2	rcolo-158/Nater	d(jet)=0.16cm	150-300		74	2			4		*	part can estacted total transfer and transfer	Driving With 1072
1.5-9 cc 1.00 1.0	auth// N7	00-02	670-830		-210		,		. <		1 0	ere mas injected join the other mater.	(7/cl) alluskatoria
0.09-0.79 300-300	meth/Water	5 ° °		75 av11aa	2,5	Ę 4	; ;	97		2	ñ	oliditled as thin plates.	Witte et al. (1971)
1.5-50 cc 1.5-	nicht / Habar	F 27 90 0		ממוומו כז	3 5	¥	9 5	2		57			Bjorkquist (1975)
0.3 0.4 0.5	TOTAL MALES	0.07-0.47	200-000		2	7.14	<u>ج</u>	0./-15.0	a .				Cho et al. (1974)
1.2-0 12 13 14 14 15 15 14 15 15 15	12.79.70.71	5 -0-0-0	000-00		R :	1	÷:	b./-13.0	æ ·		J	xtent of fragmentation decreases with water temperature.	Cha, Gunther (1973)
0.3 cc 870 0.3 arr 2.44-68 20-350 A Ne frageentation at 60C water 20-69 0.3 arr 2.7-3.1 A Bountz-tube experiment at 60C water 20-69 0.3 arr 2.7-3.1 A Bountz-tube experiment at 60C water 20-69 0.3 arr 2.7-3.1 A Bountz-tube experiment at 60C water 20-69 0.3 arr 2.7-3.1 A Bountz-tube experiment at 60C water 20-69 0.3 arr 2.7-3.1 A Bountz-tube experiment at 60C water 2.0-49 0.3 arr 2.7-3.1 A Bountz-tube experiment at 60C water 2.0-49 0.3 arr 2.7-3.1 A Bountz-tube experiment at 60C water 2.0-49 0.3 arr 2.7-3.1 A Bountz-tube experiment at 60C water 2.0-49 0.3 arr 2.7-3.1 A Bountz-tube experiment at 60C water 2.0-49 0.3 arr 2.7-3.1 A Bountz-tube experiment at 60C water 2.0-49 0.3 arr 2.7-3.1 A Bountz-tube experiment at 60C water 2.0-49 0.3 arr 2.7-3 arr	natu/nater	1.3-30 CC	•		<u> </u>	ä			-				Flory et al. (1969)
0.3 cc 20-04 20-05 20-	Nuth/Kater		3		23	J16	2.44-4.88	20-320	Œ				Ivins (1967)
0.81-6.1 g 100-1800	buth/Water	0.3 נר	872		0,60	Į.	3.45		<≖		ž	e fragmentation at 600 mater	Swift, Baker (1965)
0.83-6.19 456-740 40 cc 26.0-48.9 air 0.6 30-53 A Buartz-tube experisent 1.5-2.0 cc 30-40 cc 30-40 cc 30-40 cc 30-40 cc 310 cc 31 c	nth/Nater	20-60 9	098-009		2	JI P	2.7-3.1		æ				Witte et al. (1971)
1.5-1.4 g 1200-1200 510 cc 200-400 21 c 200-400 21 c 200-400 21 c 200-400 21 c	uth/Kater	0.83-6.1 9	429-740		6.6-48.9	A1.	9.0	30-63	æ		đ	uartz-tube experiment	Witte et al. (1973)
1.2-1.4 1200-1700 310 cc 317 318	o Bend/Water	1. 5 -50 cc			2	air			•				Flory et al. (1969)
1.2-1.4 g 1200-1700 510 cc 317	ser / Ka	0.69			200-400	41.5			∢		•	etal "jets" solidified.	Zvszkowski (1975a)
1.8-2.1 g 1300-1800 630 cc 15 air	er/Water	1.2-1.4 9 1	200-1700			315					Z	umerous local eruption at beginning of frag.	Ando (1960)
1.5-50 as 1.5-	er/Hater	1.8-2.1 9 1	300-1890			315			9	5-0,950.		Threshold trioner to cause prompt frag.	Ando, Caldarola (1982)
0.5 g 1080-1800 10-50 cc 15-80 arr, Ar. NZ 0.14-0.53 A 1.5 9.3-1.0 forestion of estal jet from the sain asses 1.5 g 1100-1600 20-50 cc 15-80 arr, Ar. NZ 0.14-0.53 A 1.5 9.3-1.0 forestion of estal jet from the sain asses 1.5 g 1100-1600 20-50 cc 20-50 air 1.0-4.0 5.1-92 A 1.5 9.3-1.0 forestion of estal jet from the sain asses 1.5 g 1.00-192 de. 0.1-10 de. air 1.0-4.0 5.1-92 A 1.5 9.3-1.0 forestion of estal jet from the sain asses 1.5 9.3-1.0 forestion of estal jet from a sain asses 1.5 9.3-1.0 forestion of estal jet from a sain asses 1.5 9.3-1.0 forestion a set long stability criterion. air 1.0-4.0 5.1-92 A 1.5 9.3-1.0 forestion a set long stability criterion. A 1.5 9.3-1.0 forestion a set long stability criterion. A 1.5 9.3-1.0 forestion a set long stability criterion. A 1.5 9.3-1.0 forestion a set long stability criterion. A 1.5 9.3-1.0 forestion a set long stability criterion. A 1.5 9.3-1.0 forestion a set long stability criterion. A 1.5 9.3-1.0 forestion a set long stability criterion. A 1.5 9.3-1.0 forestion a set long stability criterion. A 1.5 9.3-1.0 forestion a set long stability criterion. A 1.5 9.3-1.0 forestion a set long stability criterion. A 1.5 9.3-1.0 forestion a set long stability criterion. A 1.5 9.3 9.3 9.3 9.3 9.3 9.3 9.3 9.3 9.3 9.3	er/Hater	1.5-50 44			==	JIF			⋖				Flore of all (1969)
0.5-1.5 g 1100-1600 20-30 CC 13-60 air Ar 1	per/Kater	0.5 0	080-1800		15-80	Br. Ar. NZ	0.14-0.53		. 4		2	theres! over occurs or as as assessed	Treatment and the
101 102 1500 cc 27 317 103 1500 cc 27 317 103 1500 cc 27 317 103 1500 cc 20 1500 cc 27 317 103 1	er/Water	0.5-1.5 a 1	100-1600		5-80	1			. 4			of the field of the first field at the field at the first field at the field at the first	(ACAC) INSERT
101 20 100-192 1-00 tt 21 100 tt 21 21 21 21 21 21 21	na-f/Habar				:							מושקוניתי מו שבופן לבן נוספ נשב שפוח הפנים	1752 EDMSK1 (1977)
101 102 cc 50-800 30 31 10-192 dc 10-192	in Little	5 6			3	į :					= (loodable ard melting apparatus	Nelson, Buxton (1977)
10-17 10-1	on 12/Minoral Act	*	CB1 - CV1	91-10					ь.		Ξ.	loodable arc melting apparatus	Nelson, Burton (1977)
0.3 CC 20-600 50 air 1.04.0 3.572 A Bynamic impact break-up at the lower temperature 0.3 CC 20-600 0 air 3.45 A Mode frequentation of 15-20 CC 20 air 3.45 A Mode frequentation and analysis of 20.3 CC 20 air 3.45 A Mode frequentation of 20.3 Good air 3.45 A Mode frequentation of 20.3 Good air 3.45 A Spontaneous explosions at lower drup-fall-height. Significant solution of a set of 20.45 A Spontaneous explosions at lower temp. Significant solution of a set of 20.45 A Mode frequentation of a set of 20.45 A Mode frequentation. Significant solution of a set of 20.45 A Mode frequentation. Significant solution of a set of 20.45 A Mode frequentation. Significant solution of a set of 20.45 A Mode frequentation. Significant solution of a set of 20.45 A Mode frequentation. Significant solution of 20.45 A Mode frequentation. Significant solution of 20.45 A Mode frequentation. Significant solution of 20.45 A Mode frequentation. Significant frequentation. Significant frequentation. Significant frequentation. Significant frequentation. Significant frequentation. Significant frequent frequen	11/11/11/11/11 Old	•	741-701	ar 01-10'-	;	415		;	Œ		. =	est of the drap stability criterion.	Henry, Fauste (1979)
0.3 cr 2600 0 air 3.45 A Nö frageentation 0.3-0.6 g 1010-1050 15-20 cr 20 air 3.45 A Nötrageentation 0.3-0.6 g 1010-1050 15-20 cr 20 air 3.45 A Nötrageentation 1. Nater 50 eg 2233 3400 cc 20 air 0.45-0.61 A Spontaneous explosions at lower drop-fall-height. 1. Nater 50 eg 2233 3400 cc 3.0 air 0.45-0.61 A Spontaneous explosions at lower drop-fall-height. 1. Notative digital-0.150	1 us/ Water	0.02 66	20-00		3,	ž	1.0-4.0	5. 3-92	⋖		€	ynamic impact break-up at the lawer temperature	[vins (1967)
Nater	1/Mater	9. 3 cc	2000		0	ai C	3.45		⋖		ž	o fragmentation	Swift, Baker (1965)
Wister 50 eq 2233 3400 cc 30 air 0.45-0.61	/Nater	0.3-0.bg 1	010-1020		8	Ę			Œ		ž	etal jet formed.	Zyszkowski (1975a)
Maker 10 ag 2233 3400 cc 30 air 0.45-0.61 A Spontaneous explosions at lower drop-fall-height.	Oxide/Nater					317			Œ		Ş	iscosity effects	H. Fia (1985)
1/4 1/4	Oxide/Hater	50 00	2233		25	316	0.45-0.61		⋖		Š	pontaneous explosions at lower drop-fall-height.	Nelson.Duda (1981)
	Oxide/Water	. 6 OS	870-2770		- 8-0	317	0,4-6.95		Œ		=	artistion of melt composition, viscosity, and ambient pressure	Nel 500, Buda (1982)
30 g 800 -210 air 3.2 A Solidited as thin plates. We fragmentation 40 cc 1sat air 0.6 A We fragmentation. 450-500 g 150-500 1.0 cc 22 no 2.4 1000 B NO violent fragmentation. 0.13-0.49 g 350-700 22 air 0.49 6.6-10.7 A O.67 g 300-750 0-40 air 0.45 3 A Low entrance velocity and spherical drop intensity FC1 few, 100 g 350-500 B-60 air 0.44-5.4 B-1200 A Low entrance velocity and spherical drop intensity FC1	d-Tin Alloy/Water	d(jet)=0.16cm	200-920		74	2			4		•	Foocers" expansion of set at the lower tean of melt	Bradley Witte (1972)
40cc 1sat air 0.6 A No fragmentation. 450-500 g 350-500 l.0 cc 22 no 2.4 1000 B NO vicient fragmentation. 0.13-0.49 g 350-700 22 no 0.49 6.0-10.7 A NO vicient fragmentation. 0.67 g 300-750 0-40 air 0.45 g A Low entrance velocity and spherical drop intensity FC1 few,100 g 350-550 B-60 air 0.44-5.4 B-1200 A Low entrance velocity and spherical drop intensity FC1	Q/LN2	30 9	800		-210	, II	3.2		er.		ű	olidified as this slates. We framestation	Mitto at al (1971)
450-500 g 350-500 1.0 cc 22 no 2.4 1000 B NO violent fragentation. 0.15-0.49 g 350-700 22 air 0.49 6.6-10.7 A 0.67 g 300-750 0-40 air 0.45 3 A Low entrance velocity and spherical drop intensity FCI FW 100 g 350-500 B-60 air 0.44-5.4 B-1200 A Low entrance velocity and spherical drop intensity FCI	A/LN2				15.2	316	9.0		-70		2	a francotation	Market at 12 12 12 13 13 13 13 13 13 13 13 13 13 13 13 13
0.15-0.49 g 530-700 22 air 0.99 6.6-10.7 A 0.67 g 300-750 0-40 air 0.45 3 A Low entrance velocity and spherical drop intensity FCI (ew.100 g 350-550 B-60 air 0.44-5.4 B-1200 A Low entrance velocity and spherical drop intensity FCI	d/Water	650-500	150-500			8		1600					Mile et 41, 117/3/
0.87 g 300-700 0-40 air 0.45 H 8-1200 A Low entrance velocity and spherical drop intensity FCI (***)100 g 350-50	d/Kator	0 17-0 49 0	150-700		: 2	? ;	80 0	2 01 7			è	A storent if agentation.	Mener et al. (1976b)
few, 100 g 350-650 B-60 air 0.44-5.4 B-1200 A Low entrance velocity and spherical drop intensity FCI	d/Nater	0.47	100-750		0-40				. <				Cha et al. (1974)
Figure 3.30.500 B-00 air 0.44.3.4 B-12.00 is low entrance velocity and spherical drop intensify FCI	d/Mater	6 1000	760		2 9	-		7 6	= -				Flory et al. (1969)
	77.00	5 001, mar	000-000		P-90	JIE	6.44-5.4	0071-8	Œ		_	ow entrance velocity and soberical drop intensify £01	Grobbirt of all (1974)

1		003		4 24 6			;					
Lead/Hater Lift+Kfl/Hater	1.44-8.45 9	ARC-174	2 1:1:1	40 CC 26.7-35.0	417	o	55-55	. a		Guartz-tube Short-tube	inartz-tube experiment Chori-tube experiments feash processes did not exceed sensor processes	Witte et al. (1975) Willage of al. (1975)
Magnesius/Water	160 g		16.53 litre		alr	2.3-4.7		•		Sharp-blast.		
Ragnest un/Nater	7	70		20	Æ			•	6:0		Saail particles undergo more reaction than the larger ones.	Linestainen (1963)
Ner cury/Nater	1.5-50 84			15	air			•		Formation	Formation of hollow thin-walled bubbles and subsequent burst.	Flory et al. (1964)
Nercury/Nater	50-65 9	23		71	2 is	 		æ		Bottom cav	Bottom cavity formed	Mitte et al. (1971)
Mild Steel/Na	0.3 cc	1500-24		52	air	3, 45		4				Swift, Baker (1965)
Malten Salt/Water	6 08 6		٠, در	20					100-200	_	Iwo step interaction; Bulk mixing and breakup	Andersan, Bova (1976)
Molten Salt/Water	. 99 1	920	Б	į	2	3 cc/s	2	<u>.</u>		Injection	njection of water under the surface of molten sait.	Arastrang (1970d)
Rol ybdenus/Na	0.3 cc		,	520	Į.	3.45		4 (No fragmentation	itation	Swift, Baker (1965)
Ra/Mater	5 661	964	2 5	C	-12			25 , •		Water inje	Water injection into the molten sodiumin quartz-tube.	[vins (1969a)
Matt/Water	e .	600	0.09 CC					σ.				Anderson, Armstrong (1972)
Mari Frances	6	00.6	2	Š		;				year to tube tests	Je tests.	149A1) SutA
Nickel/MA	V.S CC 1409-71	₿		90		₽ .		ac «				Swift, Baker (1965)
Michigan de Cer	9,40	0076	16.33 HTCP	95.0	1	7.5-7.7						Higgins (1955)
Potage in adida/lister	100		-	3 4	į			.				Swift, Barer (1752)
Boco'o sotal/two	6 001	3 9	3	g <	;	37 2				2000	300	iving (1769a)
Don't see a see a	1 1	200		> <	;	;				no 11 agreement on	ונפנוטו	Swift, Barer (1765)
CC(Top 104) No	0.3 (6.1425-24	000		يو د	į ;			z <		And his old	to the state of th	Swift, Baker (1765)
THE PARTY OF THE PARTY OF	11 619	2		3 6	-					יות ביוברו	מו מומק ומופרסטרה מנו נדו	Cotil Pared (14co)
Serigge Suggests	2.5	77		079-007	1	9 4		.		nove throu	nore infough dispersion at higher sodium temperature.	Swift, Baker (1905)
55(1) pe 5041/11q. L1	3 C.	0067-0761	į	CIZ :	, ,	·.		ar.		Fragmentst	reagnentation less extensive than in sodium	Swift, Baker (1965)
SSLINDE SZIIVNA	900	1800-7300	300 6	200-600	=			•	 •	Fressure e	fressure event before complete submergence	Arastrong et al. (1971)
SS(Type 321)/Water	225 9	-	16.53 litre		A1	2.3-4.7		⋖		Some oxide formed	formed	Higgins (1955)
SS/Na	75-80 9	75-80 g 1500-1800	1.6 cc	200-420		20-30		æ		E plosions	Esplosions occurred (5 as after the completion of injection.	Abbey et al. (1975)
SS/Nater	20 9				315			_		Floodable	loodable arc melting apparatus	Nelson, buxton (1977)
SS/Nater	0.69		35 CC	7.1	달			4				Zyszkowski (1975a)
55/lig. Potassium	0.3 cc	0.3 cc 1425-2490		250	21.6	3.45		Œ		Slightly e	Slightly extensive fragmentation compared to those in sodium	Swift, Baker (1965)
Salt/Water								.		Shock-tube	Shock-tube experiments.	Segev et al. (1979)
Silver Chloride/Water	6 1>			06-0	7.5	1.0		•				Cho, Gunther (1973)
Silver Chrolide/Water	0.03-0.28	550-600		4-88	at.		12.9-27.1	æ				Cho et al. (1974)
Silver/Na	0.3 cc	1900		220	air			₫				Switt, Bater (1965)
Silver/Water	0.3 cc	1400		•	717	3.45		•		No Fragmentation	tation	Swift, Baker (1965)
Silver/Water	0.6-1.3 g 1080-1350	1080-1350	20-25 cc	17-20	air, Ar			Œ		One partic	One particle. Large shrintage,	2vsztoust (1975a)
Smelt/Green lig.	160 g			85	air			•		Violence 1	Wiolence increases with increasing particle size.	Nelson, Fennedy (1956)
Smelt/Green lig.	170 9	870-930	1.5 litre	78-82	114			Œ		The concen	the concentrations of sait and caustic soda were varied.	Sallack (1955)
Smelt/Water	100 1			15	air			⋖		Effects of	Effects of sulphidity and inhibitors on smelt were studied.	Welson, Kennedy (1955)
Sae!t/Water	170 9	870-930	1.5 litre	10-100	àir			٠.E		Violence d	Violence decreases with water temperature.	Sallack (1955)
Sn+Pb/Hater	3 0 4			23	air			4				Actracken (1973)
Steel/Sodium	2.2	1600	5 6	500		2.4	1000	æ	-0			Asher et al. (1976a)
Tantalus/Na	0.3 cc	٣.		33	a i	3,45		•		No fragmentation	fatton	Swift, Baker (1965)
fin/Nater	e S		60 litre	8-52	716			4	6.2	Multiple 1	Multiple interactions.	Arabers et al. (1975)
fin/Water	25 9			9-45								Arakeri et al. (1975)
Tin/Water		250-900		£-70	Į.	0.99-7.73	7.5-540	√ E		Increase in	increase in the extent of fragmentation with drop entrance velocity.	Arastrang (1970b)
Tin/Nater	2.3-4.3 9	200-100			718			<≠		Change of	Change of TIZ with the mass of the melt.	Asher et al. (197cb)
lin/Water	100,300 g	250-400 (250-900 0.5,1.0 cc	23	9	7:	1660	20.		fittierent	different TIZ for the injection mode compared to the Dullforce's.	Asher et al. (1975b)
Tin/Hater	0.8,6.69	300-1100	300-1100 25 gallon	22	Æ	1.16	16, 12	1.7	62.0,1.1			Bjorkquist (1975)
Tin/Nater	d=0.31cm	300-700		20-40	411	÷:		1.6 e	3.15-0.0 up tp 50		Higher pressure oscillation at lower mater temperature.	Bjornard et al. 119741
Tin/Water	fen gras	400-B00		20-80	J Te	0.62-0.98		θ.	0.7-0.5	Escalation	Escalation of perturbation by successive growth and collapse cycles.	Board et al. 11974)
In/Water	6	8	;					er.		Sudden Inc.	budden increase in ambient pressure induces explosions.	Board, Hall (1974a)
Tin/Nater	200 g	926-750	900 CE	80	į			e.	0.15	Evidence of	Exidence of spatial propagation.	Board, Hall (1974b)

2 0-2-540 A 2-2-550 A 2-2-	The state of the s
0.140.5 g 230-90 (45-2)17cc 10-90 atr 0.10 0.55-550 h 1 1 2 300-100 3940 cc 10-90 atr 0.10 0.15 0.5 4 4 c 20-0 10 4 c 20-0	increased extent of fragmentation at high entering velocity of drop.
12 3 400-700 415-211170 11 2 410-70 11 11 2 410-70 11 11 2 410-70 11 11 2 410-70 11 11 2 410-70 11 11 2 410-70 2 410-70 2	Extent of fragmentation decreases with increasing water temperature
1.5-7.6 a. 2.09-1000 3800 (cc. 10-95 s. He 6.75 h 4 (cc. 25)-6 (dc. 25) a. ir 2.444-4.88 20-25 h 4 (cc. 25)-5 (dc. 25) a. ir 2.444-4.88 20-25 h 4 (cc. 25)-25 (dc. 25) a. ir 2.444-8.8 20-25 h 4 (cc. 25)-25 (dc. 25) a. ir 2.444-8.8 20-25 h 4 (cc. 25)-25 (dc. 25) a. ir 2.444-8.8 20-25 h 4 (cc. 25)-25 (dc. 25) a. ir 2.45	
11.5-50 as 200-980	identification of III for spontaneous explosions.
1100 g 500 1 CC 25 atr 2.444.88 20-225 R 4 CC 250-756 1 C 25 atr 3.45 R 5 R 5 R 5 R 5 R 5 R 5 R 5 R 5 R 5 R	Formation of ripples on the surface of the drop
100 g 200 1 CC 25 317 8 8 9 9 9 9 9 9 9 9	
0.3 cc 200-750 12 21 17 18 18 18 18 18 18 1	Violent explosion followed by bulge of the self surface after injection, lying (1948s)
0.3 cc 800	
29-23 cs. 819-819 0.4-5.65 g 135-819 0.8 g 173-826 to cc. 23.9-51.6 air 3.5 f 0.1.4 5.65 g 135-826 0.1.4 g 192 15-25 cc. 18-23 air 3.6 f 0.1.3 g 180-80 0.2 cs. 829 300 27.5 cc. 18-23 air 3.6 f 0.2 cs. 829 300 27.5 cc. 18-23 air 3.6 f 0.2 cs. 829 300 27.5 cc. 18-23 air 3.6 f 0.3 cs. 8290 300 cc. 300 cc. 400 air 3.6 f 0.2 cs. 8290 300 cc. 300 cc. 400 air 3.6 f 0.2 cs. 8290 300 cs. 15.0 cc. 400 air 3.6 f 0.3 cs. 8290 300 cs. 15.0 cc. 400 air 3.6 f 0.4 cs. 8290 300 cs. 15.0 cc. 400 air 3.5 f 0.5 d 29-50 g 300 cs. 15.0 cc. 400 air 3.5 f 0.5 d 29-50 g 300 cs. 15.0 cc. 400 air 3.5 f 0.5 d 29-50 g 300 cs. 15.0 cc. 400 air 3.5 f 0.5 d 29-50 g 300 cs. 15.0 cc. 400 air 3.5 f 0.5 d 29-50 g 300 cs. 15.0 cc. 400 air 3.5 f 0.5 d 29-50 g 300 cs. 15.0 cc. 200-100 0.5 d 29-50 g 300 cs. 15.0 cc. 200-100 0.5 d 29-50 g 300 cs. 15.0 cc. 200-100 0.5 cc. 1200-2450 250 air 3.45 f 0.5 cc. 1200-2450 250 250 250 air 3.45 f 0.5 cc. 1200-2450 250 250 250 air 3.45 f 0.5 cc. 1200-2450 250 250 250 250 250 250 250 250 250 2	
0.4.5.2.9 335-830 0.0.5.3.9.4.51.0 0.0.6 31-46 A 0.0.8 0	No fragrentation at 600 water.
0.475.65 g 335-878 d o c c 23.4751.6 a arr 0.6 g 37-40 A 0 c c 23.4751.6 a arr 0.6 g 37-40 A 0 c c 23.4751.6 a arr 0.6 g 37-40 A 0 c c 23.4751.6 a arr 0.6 g 37-40 A 0 c c 23.4751.6 a arr 0.6 g 37-40 A 0 c c 23.4751.6 a arr 0.6 g 37-40 A 0 c c 23.4751.6 a arr 0.6 g 37-40 A 0 c c 20.400 A 0 arr 0.742 g 2000 310 c c 200 a arr 0.742 g 2000 310 c c 200 a arr 0.742 g 2000 310 c c 200 a arr 0.742 g 2000 0.15-0.3 g 400 a arr 0.5-9.5 B 4.45 B 4.45 B 30-50 g 2000 0.15-0.3 g 400 a arr 0.5-9.5 B 4.45 B 4.45 B 30-50 g 2000 0.15-0.3 g 400 a arr 0.5-9.5 B 4.45 B 4.45 B 30-50 g 2000 0.15-0.3 g 20-50 0 a arr 0.5-9.5 B 4.45 B 4.	
0.8 q 1/2 15-25 cc 18-25 atr 1.45 h 1.0 q 300 cc 300 atr 2.45 h 1.0 q 300 cc 300-100 atr 3.0-9.5 h 1.0 -2.29	Suartz-tube experiment.
0.3 cc 2050 356 air 3.45 h 1.3 g 3500 5.7-6.3 g 400 air 3.6-9.5 h 1.4 g 2300 5.7-6.3 g 400 air 3.6-9.5 h 1.4 g 2300 5.7-6.3 g 400 air 3.6-9.5 h 1.4 g 2300 2.3, c 200 air 3.6-9.5 h 1.4 g 2300 2.3, c 200 air 3.6-9.5 h 1.4 g 2900 310 cc 200 air 3.5-9.5 h 1.5 g 2900 310 cc 200 air 3.5-9.5 h 1.5 g 2900 310 cc 400 air 3.5-9.5 h 1.5 g 2900 310 cc 400 air 3.5-9.5 h 1.5 g 2900 0.15-0.3 g 400 air 3.5-9.5 h 1.5 g 2900 1.5 g 200 2.3, c 400 air 3.5-9.5 h 1.5 g 2900 1.5 g 200-500 air 3.5-9.5 h 1.5 g 2900 1.5 g 200-500 air 3.5-9.5 h 1.5 g 2900 1.5 g 200-500 air 3.5-9.5 h 1.5 g 2900 1.5 g 200-500 air 3.5-9.5 h 1.5 g 2900 1.5 g 200-500 air 3.5-9.5 h 1.5 g 2900 1.5 g 200-500 air 3.5-9.5 h 1.5 g 2900 1.5 g 200-500 air 3.5-9.5 h 1.5 g 2900 1.5 g 200-500 air 3.5-9.5 h 1.5 g 2900 1.5 g 200-500 air 3.5-9.5 h 1.5 g 2000 1.5 g 200-500 air 3.5-9.5 h 1.5 g 2000 1.5 g 200-500 air 3.5-9.5 h 1.5 g 2000 1.5 g 200-500 air 3.5-9.5 h 1.5 g 2000 1.5 g 2000 1.5 g 200-500 air 3.5-9.5 h 1.5 g 2000 1.5 g 2000 1.5 g 200-500 air 3.5 h 1.5 g 2000 1.5 g 2000 1.5 g 2000 1.5 g 2000 air 3.5 h 1.5 g 2000 1.5 g 2000 1.5 g 2000 1.5 g 2000 air 3.5 h 1.5 g 2000 1.5 g 200	Rouge at the surface.
7.0 g 3500 17.0 air h 1.0 g 1.	
7.0 g	A pellet of UUZ surrounded by a stainless steel.
10.2-12.9 2.00-400 3.0-9.5 4.15 4.	
79-529 3200 5.7-6.3 q 400 air 5.0-9.5 A ₁ E B. 9	Amblard et al. (1974)
8.8 g 2940 230 cc 200 air h 2.38 10.2.1.72 g 2900 300 cc 200 air c 2-60 h 4.45 23.4 g 2900 300 cc 600 air c 2-60 h 4.45 30.5 g 2900 2.3.5.0 cc 600 air c 3-5.2 h 6.45 22.9 g 3000 2.3.5.0 cc 600 air c 3-5.2 h 6.45 30.9 g 3000 2.3.5.0 cc 600 air c 3-5.4.5 30.9 g 200-600 air c 3-5.2 h 6.45 30.9 g 200-600 air c 3-5.4 30.9 g	finderson, Arestrone 11972)
1,1,2,9 2900 310 cc 200 air 2-60 A 4.45 10,2-12,9 2900 300 cc 400 air 5.2 29 3000 2,3,5,0 cc 400 air 5,2 29 3000 2,3,5,0 cc 400 air 3,5-9,5 29 3000 2,900 39 30 400 air 3,5-9,5 29 3000 3000 5 400 air 3,5-9,5 30 3000 3000 5 400 air 3,5-9,5 30 3000 3000 30 400 air 3,5-9,5 30 3000 3000 30 400 air 3,5-9,5 30 3000 3000 30 400 air 3,45 30 3000 3100 3100 3100 310 30 3000 3100 3100 310 310 30 3000 3100 310 310 30 3000 3100 310 310 30 3000 3100 310 310 30 3000 3100 310 310 30 30 3100 310 310 30 30 3100 310 310 30 30 310 310 30 30 310 310 30 30 30 310 310 30 30 30 30 310 30 30 30 30 30 30 30	Ovelic process of 802 eruntion.
10.2-12.9 g 2900 300 cc 400 air 2-60 A 4.45 21-50 g 3000 2.55.0 cc 400 air 3.5-9.5 22-50 g 3000 2.55.0 cc 400 air 3.5-9.5 23-50 g 3000 2.55.0 cc 400 air 3.5-9.5 400 g 2900 300 g 200-600 4-0 g 3100-3400 39 g 200-600 4-0 g 3100-3400 39 g 300 g 200-600 4-0 g 3100-3400 30 g 30 g 200-600 4-0 g 3100-3400 30 g 30 g 30 g 30 g 4-0 g 3100-3400 30 g 30 g 30 g 30 g 4-0 g 3100-3400 31 g 3.45 A 4-0 g 30 g 30 g 30 g 30 g 30 g 4-10 g 3100-3400 3 g 30 g 4-2 g 31 g 3 g 3 g 4-2 g 31 g 3 g 3 g 3 g 4-2 g 3 g 3 g 3 g 3 g 4-2 g 3 g 3 g 3 g 3 g 4-2 g 3 g 3 g 3 g 3 g 4-2 g 3 g 3 g 3 g 3 g 4-2 g 3 g 3 g 3 g 3 g 4-2 g 3 g 3 g 3 g 3 g 4-2 g 3 g 3 g 3 g 3 g 4-2 g 3 g 3 g 3 g 4-3 g 3 g 3 g 3 g 5-3 g 3 g	the east noured consisted of 2 drop, one larger than the other.
23.6 g 2900 3.00 cc 600 air 5.2 g 8 6.0 air 5.5 g 6.0 air 5.5 g 8 6.0 air 5.5 g 6.0 air 5.5 g 7000 2.35.0 cc 600 air 5.5 g 8 6.0 air 5.5 g 7000 1.5 G 7000	UB2 fell as a number of discrete drops.
29-59 3000 2.3,5.0 cc 400 arr 3.5-9.5 B 4.0 arr	
29-59 9 3000 0.15-0.3 9 400 air 3.5-9.5 B 15 5 9 10 0 0.45 B 10 0 0 0.05 0 0.05 0.0 air 3.5-9.5 B 10 0 0.45 B 10 0 0 0.05 0 0.05 0 0.05 0.0 air 3.5-9.5 B 10 0 0.05 0 0.05 0.0 air 3.5-9.5 B 10 0 0.05 0.0 air 3.5-9.5 B 10 0.05 0.05 0.05 0.05 0.05 0.05 0.05 0	TILDET COLLEGE
100 g 2900 300 g 200-400 air 310 g 30-400 air 30-30 g 30-30 g 30-400 air 30-30 g	forestion of endine dean into the forest
100 g 2900 5 g 400 no 10 g 400 n	53 injection of souther or up into out post
99-59	o cycles out ilegents seculi and fugurated
8-36 9 100-340 100 100 100 100 100 100 100 100 100 1	thirties capetiments. Napid vapor generation between explosions.
10-10 g 3100-3400 10 g 0.7-10.0 g 20 30-170 cc 200-300 air 27-50 g 3000-3100 0.15-0.3 g 0.3 cc 1800-2200 250 air 3.45 0.3 cc 1800-2200 250 air 3.45 0.3 cc 1800-2200 250 air 3.45 0.3 cc 400-210 0 air 1.5-50 aa 4 air 1.5-50 aa 4 air 1.5-50 aa 1.5-50 aa	7.2USK@ (14/3)
0.7-10.0 g 30.00-3100 c.15-0.3 g 40 - 1 3.5-9.5 g 8 - 1 3.5-9.	
0.7-10.0 g 3020 30-170 cc 200-300 air A 400 - 3.5-9.5 g 400-3100 0.13-0.3 g 400 - 3.5-9.5 g 400-3100 0.13-0.3 g 400-2200	Tyrucetimist measury of melting of melting of meltinger (1973)
79-59 3000-3100 0.15-0.3 g 400 - 3.5-9.5 g 8 0.3 cc 800-2100 0.15-0.3 g 400 - 3.5-9.5 g 8 0.3 cc 800-2100 0.15-0.3 g 400 - 3.5-9.5 g 8 0.3 cc 800-2100 0.15-0.3 g 250 air 3.45 g 6 0.3 cc 800 1-50 cc air 3.45 g 6 0.3 cc 800 1-50 cc air 3.45 g 6 0.3 cc 800 1-50 cc air 3.45 g 6 0.3 cc 800 1-50 cc air 3.45 g 6 0.3 cc 800 1-50 cc air 3.45 g 6 0.3 cc 800 1-50 cc air 3.45 g 6 0.3 cc 800 1-50 cc air 3.45 g 6 0.3 cc 800 1-50 cc air 3.45 g 6 0.3 cc 800 1-50 cc air 3.45 g 6 0.3 cc 800 0 1-50 cc air 3.45 g 6 0.3 cc 800 0 1-50 cc air 3.45 g 6 0.3 cc 800 0 1-50 cc 800 0	DOTATION TO THE PROPERTY OF TH
0.3 cc 1200-2450 250 air 3.45 A B B B B B B B B B B B B B B B B B B	Partially solidified droplet still undergoes an extensive fragmentation.Mizuta (1974)
0.3 cc 1200-2200 250 air 3.13 fg 6 5-50 0.3 cc 1200-2200 250 air 3.15 fg 6 5-50 0.3 cc 1200-2200 250 air 3.15 fg 6 5-50 0.3 cc 1200-2200 250 air 3.15 fg 6 5-50 0.3 cc 1200-2200 250 air 3.15 fg 6 5-50 0.3 cc 20 air 3.15 fg 6 5-50 0.3 cc 40-20 0	
0.3 cc 1800-2020 0.3 cc 400-200 0.3 cc 400-300 0.3	
0.12 c. 100-2200 2.50 a.17 5.15 A 5 5 6 6 6 6 6 6 6 6 6 6 6 6 6 6 6 6	Formation of a fragile filamentary network
5-80 1-30 cc air A 5-80 1-30 cc air A 6 5-80 1-30 cc air 3.45 A 6 6 6 6 6 6 6 6 6 6 6 6 6 6 6 6 6 6	
3-90 1-30 cc air A 5-90 1-30 cc air A 120-510 d-5aa about In 4 air 3.45 1.5-50 aa	and formation. Foamed up and popped with audible noise.
3-80 1-30 cc air A 120-510 4 air 3.45 0.3 cc 600 0 air 3.45 1.5-50 aa 15 0.12-0.23 500-800 4-23 air 0.99 1.5-50 aa 16 0.3 cc 825 0.47-0.89 380-660 20-25 cc 20 air 3.5 220 3 cc 1730-2100 20-25 cc 20 air 3.5 0.3 cc 1730-2100 20-25 cc 20 air 3.5	
120-510 1-30 cc air h	Few ice formation and no popping Makanishi,Reid (1971)
1.5-50 as about fa 4 air 3.45 A	Popping. Natanishi, Reid (1971)
0.344 about 14 air 3.45 A 15 A	
0.3 cc 600 0 atr 3.45 p p 1.5-50 at 100-500 12-0.23 atr 5.45 p p 1.2-50 as 600 0 atr 5.45 p p 1.5-50 as 600 0 atr 5.45 p p 1.5-50 as 600 0 atr 5.45 p p 1.5-50 as 600 0 atr 5.44 p p 1.5-50 atr 5.0 atr 5.	No fraymentation, but cold liquid entrapped in the drop Brauer (1968)
1.5-50 **	Smift, Baker (1965)
4 cc 400-700 12 air h	Flory et al. 11959
0.12-0.23 g 500-800 d -23 air 3.45 A 1.5-50 as 600 0 air 3.45 A 1.5-50 as 600 0 air 3.45 A 1.5-50 as 600 3.0 air 2.44-4.88 A 0.3 cc 823 0,60 air 3.45 A 1.5-50 as 600 2.0 air 3.45 A 1.5-50 air 3.4	McCracken (1973)
0.12-0.23 g 500-800	Shock-tube experiments Segev et al. (1979)
0.12-0.23 g 500-800	
1.5-50 ms	Cho et al. (1974)
0.3 cc 825 0,00 atr 3.45 A 0.47-0.89 A 0.47-0.89 30-830 0,00 atr 3.45 A 0.47-0.89 309-660 20-25 cc 20 atr 3.2 A 0.47-0.89 309-660 20-25 cc 20 atr 2.3-4.7 A 0.3 cc 1760-2100 25 11 tre 2.3-4.7 A 0.3 cc 1760-2100 25 0 atr 2.3-4.7 A 0.3 cc 1760-2100	Flory et el. (1959)
0.3 cc 825 0,60 atr 3.45 A 20 500-830 20 atr 3.2 A 0.47-0.8 g 380-60 20-25 cc 20 atr 0.3 cc 1360-2100 25 atr 2.3-4,7 A 0.3 cc 1360-2100 250 atr 3.45	(1961) 10101
20 9 500-930 20 atr 3.2 a 0.47-0.8 9 380-660 20-25 cc 20 atr 16.53 litre air 2.3-4,7 a 0.3 cc 1780-2101 250 atr 3.4 s	No fragentation Smitt. Bater (1965)
0.47-0.8 g 389-660 20-25 cc 20 arr A 2 2 2 g 16.53 litre arr 2.5-4.7 A 0.3 cc 1780-2100 250 arr 7 as	Bottom cavity formed
227 g 16.53 litre air 2.3-4.7 h 6.3 cc 1266-2100 250 ar 3 45 h	urface.
0.3 cc 1760-2100	
17 007	Swalt, balen (1955)
	Hannet (1958)

APPENDIX B. BRIEF REVIEW OF LARGE SCALE VAPOR EXPLOSION EXPERIMENTS

It is difficult to present all of the previously conducted large scale vapor explosion experiments. This is primarily because there were many experiments which were scoping in nature and not completely documented. Consequently, the focus here is on the major large scale experiments which have investigated the vapor explosion phenomena (Table 8.1).

Vapor explosion experiments can be divided into two categories in regard to reactor safety applications, In-Pile and Out-of-Pile experiments. An "In-Pile" experiment is conducted inside a nuclear reactor core, where the fresh and irradiated fuels are used and other phenomena in addition to fuel-coolant interactions may be investigated. Conversely, an "Out-of-Pile" experiment is conducted in a experimental chamber outside the reactor. We focus on this latter category since the fundamental elements of the explosion can be studied. These experiments allow for better measurement of initial conditions and the resultant test data.

In this brief experimental review, the "conversion ratio" is defined as the ratio of the work (e.g. kinetic energy) measured to the fuel internal energy. This definition is different from that of explosion "efficiency" which is defined as the ratio of work measured to the thermodynamic maximum work output assuming an isentropic expansion process (see Section 4 on the thermodynamic explosion model)

B.1. Ispra Experiments

A large series of experiments was performed at Ispra. Early experiments were performed using 0.5 kg of molten tin distributed along a narrow trough, initially in an open tank, and later in a narrow vessel. A coherent propagation was observed when the tin and water became intermixed due to a minor local interaction. Fasoli et al. (1973) performed steel/sodium, water and 100/sodium experiments with a cover gas and observed minor pressurizations.

Holtbecker et al. (1973) reported large-scale dropping experiments with molten UO₂ and steel. These tests resulted in extremely fine fragmentation of the fuel and steel and illustrated the absence of violent coherent interactions between the hot materials and liquid sodium. Also Holtbecker et al. (1974) poured about 10 kg molten steel between 1500-1800°C into a large water tank. In this experiment no pressure pulses and no fine fragmentation were produced. On the other hand, a single test with 5 kg steel in a smaller tank produced a very violent interaction, confirming widespread foundary experience of the hazards of this combination.

Clerical et al. (1976) conducted large scale tank experiments with $\rm UO_2/Na$, dropping 4 kg $\rm UO_2$ into a 0.2 m³ tank. No violent actions were observed. Results showed a number of minor pressure pulses, though of much lower amplitude (1 bar). In 1976, Ispra developed a $\rm UO_2/NO$ shock tube, but no high pressures were observed in this system unlike most other shock tube experiments.

Benz et al. (1979) reported the results of several years of work on vapor explosions using the Ispra tank facility at the Euratom Laboratory. Molten steel, molten $\rm UO_2$ or granulate $\rm UO_2$ were freely dropped into a vessel containing water. Two vessels with volumes 350 and 6.5 liters respectively were used. The pressure in the tanks was measured at various positions. Strain gauges were also applied to the vessel so that the stresses in the walls could be determined. Experiments in the larger vessel could be watched through a window and filmed using a high speed camera. The particle size distribution was studied after the experiments. They performed about fifty successful tests in the different range of parameters, but no vapor explosions were observed in any of the experiments. However, relatively fast pressurization transients (< 1 s) were observed; up to 2 bars in the large vessel and up to 25 bars in the small vessel.

B.2. Winfrith Experiments

Briggs (1976) performed aluminum/water experiments with much more sophisticated instrumentation compared to previous experiments using the same materials by Long (1957) and Hess and Brondyke (1969). Briggs' films showed that the interaction usually started at the chamber base after a course fuel dispersion was established in the lower half of the tank with a relatively long dwell time (1 s). The interaction front propagated rapidly through the coarse dispersion with a velocity of about 200 m/s. The region behind the propagation front was no longer visible and could not be clearly defined whether it was due to fine fragmentation or due to the aluminum/vapor/liquid interface. In some cases pressure up to 400 bars was recorded, but it was not clear if those pressure rises resembled a shock front. The efficiency of the explosion was calculated to be in the range of 10% of the thermodynamic maximum based on pressure history impulse estimates. He also performed tin/water experiments pouring a large amount (20 kg) of molten tin into a water tank in the same facility. For tin at 500°C and cold water, continuous but

incoherent interactions were observed. For tin at 800°C and wter, 60°C, initial coarse mixing was observed and a similar propagation interaction occurred.

In the THERMIR experiments by Fry and Robinson (1979, 1980a, 1980b) the interactions between aluminum or tin and water were again investigated to gain information on the propagation phase. Molten fuel up to 16 kg at 800°C was dropped into a water tank at ambient pressure and temperature between 6°C and 85°C . Two kinds of vessels were used: a transparent plexiglas vessel and a strong steel vessel. In both cases spontaneously triggered vapor explosions were observed with the aluminum as well as tin. Clearly these experiments indicated detonation characteristics with the propagation velocity between 250-550 m/s as predicted by Board et al. (1975). Some experimental data also support these interpretations; flow velocity after passage of the shock wave and drop fragmentation due to relative velocities. They also reported on five tin/water experiments at 300°C and 95-98°C, respectively. Violent spontaneous vapor explosions were observed even though the calculated interface temperature (240°C) was below the spontaneous nucleation temperature of water (300°C).

Bird and Millington (1979) performed $\rm UO_2/water$ experiments, in which 0.5 kg of thermically generated $\rm UO_2$ at 3100-3400°C was introduced into a closed vessel containing 52 liters of water at 5-15°C and inert gas above it. The experiments were filmed using a high speed camera and the pressures were measured at various positions on the vessel wall and in the gas volume above the water. The main difference between this experiment and that of Buxton and Benedick (1979) is that in this case, the fuel is released under the water surface, whereas Buxton et al. let the fuel pour into the water and mix, which may happen in a reactor accident. Thirty-seven tests were reported, but explosions occurred only in eight tests. The highest conversion ratio was 1.8%, but on the average it was less than 1%.

Bird (1984) more recently reported a new series of experiments to investigate the mass scaling effects of the fuel-coolant interaction, based on replication with 24 kg melts of earlier work carried at the 0.5 kg scale. Thermite-generated uranium dioxide/molybdenum fuels in quantities of 24 kg were released under the surface of a pool of water within a pressure vessel. Spontaneous and triggered vapor explosions were observed with similar characteristics at the different scale. The conversion ratio of thermal energy to mechanical energy was low and was unchanged over a range of participating fuel mass from 0.03 to 18.0 kg. The conversion ratio increased with decreasing water subcooling, with a maximum of 4.3% at saturation. In this geometry and at the larger scale, the fraction of participating fuel increased with increasing system pressure -- from about 13% at 1 bar to 75% at 10 bars. This was based on an arbitrary criterion of fuel participation of debris diameters less than 250 μm from conduction heat transfer considerations. Overall particle distributions of debris were in the range of 0.1-10 mm. Debris distributions were relatively unaffected by the water subcooling, but became markedly finer with increased system pressure. No measurements were made of propagation velocities.

B.3. Argonne Experiments

Large scale dropping experiments were conducted at Argonne National Laboratory, using water or mineral oil as the fuel and Freon-22 (boiling point -40° C) as the volatile coolant to study the behavior of vapor explosions. The first ANL experiment by Henry et al. (1974) showed that there was a relatively narrow range of fuel temperature in which vigorous explosions occurred. The lowest limit (threshold) was identified as that which produced an instantaneous contact temperature equal to the homogeneous nucleation temperature of the Freon (54°C).

Henry et al. (1976a) varied both the initial hot and the cold temperatures for the R-22 and mineral oil pair and verified this temperature threshold for coherent energetic FCI's. They also showed that the threshold was associated with the intermixing (dwell) time. This was subsequently quantified by Armstrong and Anderson (1976), who showed that the pressure increased linearly with dwell times. Also, Freon/mineral oil experiments showed that the fuel temperature threshold was sensitive to Freon subcooling, but this result is opposite to Freon/water experiment by Board et al. (1974) showing Freon subcooling did not affect the explosion.

Figure 8.1 shows Armstrong's experimental apparatus for R-22/water tests, which is characteristic of the test geometries where the size of the system is the same order of magnitude as the size of the fluid masses. Figure 8.2 shows the resulting interaction pressures from many experiments. As the plot illustrates when the interface temperature between the fuel and coolant exceeds the homogeneous nucleation temperature, the peak reaction pressure rises remarkably indicating a temperature threshold for energetic FCI's. Henry and Fauske used these observations and past data in support of their spontaneous nucleation theory.

Segev and Henry (1978) and Segev et al. (1979) also performed a series of experiments in shock tube geometries where the simulant materials, the initial temperatures and initial driving pressure were varied. Henry reached two main conclusions from the results:

- (1) There is a temperature threshold to these interactions which corresponds to the spontaneous nucleation temperature, above which the direct interaction pressures increase substantially, indicating energentic FCI's;
- (2) These energetic interactions can be suppressed by increasing the ambient pressure in the shock tube. This behavior is similar to the results by Henry et al. (1974) and Henry and Fauske (1976) in dropping experiments.

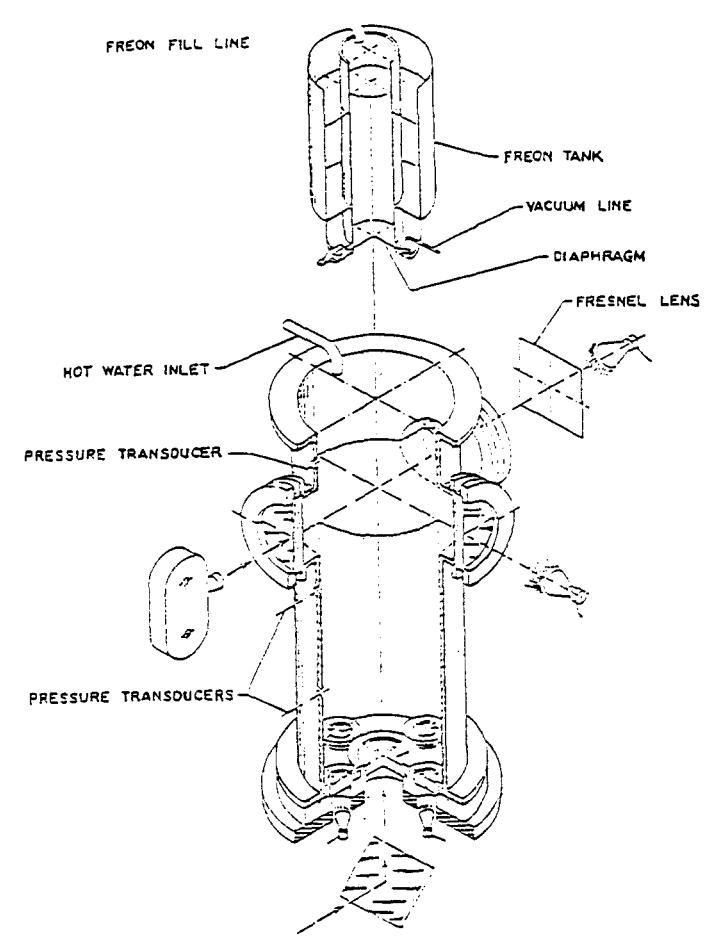


Fig. B.1. Armstrong's experimental apparatus

B.4. Board's Experiments

Board et al. (1974) conducted FCI simulant experiments using water and Freon to investigate the role of spontaneous nucleation in the vapor explosion. Board disputed the results of Henry's experiments (1974) and maintained that the mechanism for the trigger and propagation of the explosion is not necessarily the same as that for coarse intermixing of the pair. His point was that there may be a mechanism that could permit this coarse intermixing below this spontaneous nucleation threshold and that the FCI could occur below this limit.

Board et al. (1976) also performed experiments involving up to 2 kg of molten tin distributed along a 1 meter long water filled shock tube and observed the characteristics of propagation behavior. The interaction showed the form of a single shock wave (50 bar with 100 μs rise time and 100 ms pulse width) which traveled up the tube with a velocity of 100-200 m/s. The

magnitude and nature of the interaction was unaffected by the use of a detonator instead of spontaneous triggering. Some experiments with molten tin and water showed that such propagation can occur through self-driven vapor blanket collapse and the explosive release of energy is associated with rapid fragmentation and mixing rather than superheating of the surrounding water. Board suggested that all large scale thermal explosions propagate supersonically through the medium ahead of them. This conclusion was supported by the propagation velocities observed experimentally (100 m/s); these are of the order of sound velocities in two-phase media; the observations in the Freon/water and tin/water system conformed to the presence of this proposed supersonic front.

B.5. Sandia Experiments

Large scale vapor explosion experiments have been carried out at Sandia National Laboratories in two different series (Open Geogmetry and FITS) to identify experimentally the magnitude and time characteristics of pressure pulses and other initial conditions necessary to

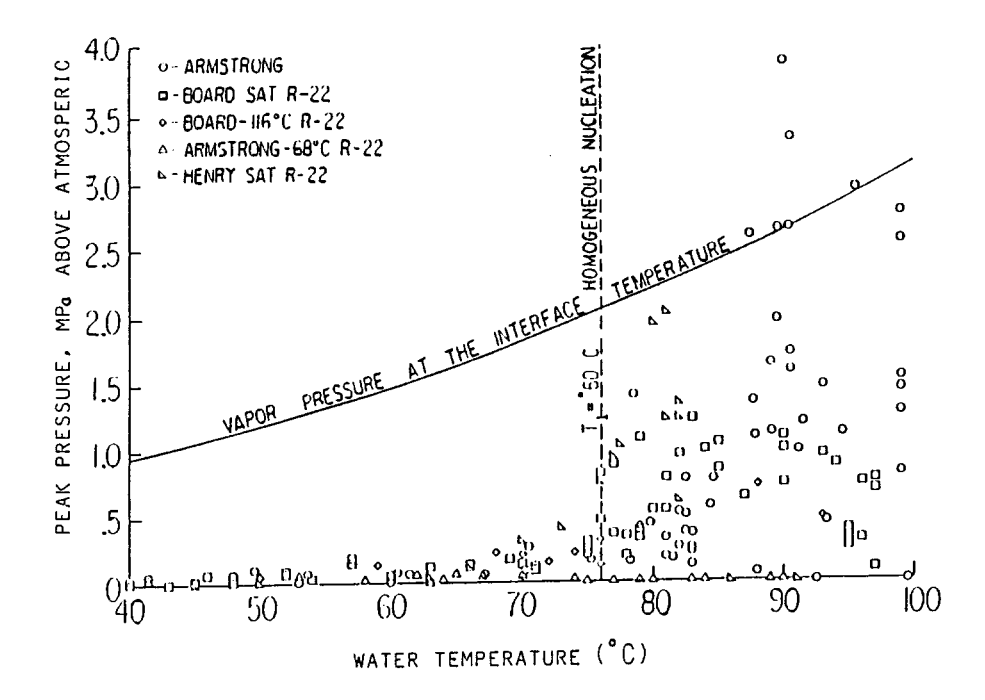


Fig. B.2. Compendium of R-22/water data on peak interaction pressure

trigger and to propagate explosive interactions between water and molten materials in an LWR. LWR molten core material simulants were used as the fuel to more accurately determine its affect on the vapor explosion (Table B.2). In both of these experimental series, artificial triggers were sometimes used to initiate the interaction in certain tests.

A. Open Geometry Experiments. Buxton and Benedick (1979) conducted a series of experiments to determine the conversion ratio of the fuel thermal energy into mechanical work at a large scale (5-20 kg fuel mass). The tests were designed to be open geometry experiments because they were intended to be scoping in nature, performed in an open vessel with minimal instrumentation. Over 60 experiments were conducted using thermitically generated iron/alumina as a fuel simulant, Fe-Al₂O₃, and corium-A+R. Fe-Al₂O₃ was used in the majority of tests (50), because it is a reasonable simulant for the corium melts; in addition to being nonhazardous, it was very inexpensive and easy to produce. The thermitically generated fuel mass delivered into the water, on the average, between 10 to 20 kg, much larger than that used in previous experiments. The experiments were conducted in an open vessel (Fig. B.3). The mechanical work generated by the explosion was determined by measuring the impulse delivered downward to crushable honeycomb blocks and by estimating the potential energy of the upward ejected debris (water and fuel). Most of the tests resulted in spontaneous explosions with conversion ratios in the

Table B.2

Property	FITS Icon/Alumina	FITS Tron/Oxlde	FITS Corium A+R	Actual Corium	Corlum in Fauske Paper
Fuel	Fe-Nl ₂ O ₃	Fe ₃ 0 ₄	UO2-ZrO2-SS	U 0-Zr. SS	1102,2102
Composition	55w/o, 45w/o		53w/o,17w/o,30w/o	tinknown*	Not Given
Melt temp (K)	1000, 2300	1000	2750-2800, 1800	1800-3100, 1800	2800
Denaity** (kg/m³)	3000	1500	7000	Dependa on comp.	Not Given
Specific heat** (J/kg-K)	1060	000	507	Depends on comp.	Not Given
Thermal cond. ** (W/m-K)	22	4	6.5	Depends on comp.	Not Given
Emissivity**	0.5-0.7	0.7	0.5-0.7	Depends on comp.	1
Heat of reaction (MJ/kg H ₂)	16		20	20 for SS 150 for Zr	Neglected
Fueltemp (K)	2700-3200	-2000	2700-3200	1800 - 3600	2800-3200
Coolant	Water		Water	Water	Hater
Initial temp [†] (K)	280-367		280-300	290-620	373

Actual corium may be a complex mix of the quaternary U-O-2r-SS system, depending on the extent of zirconium oxidation before melting and stainless-steel structure melted.

lower end of the observed range (0.2 to 1.5%). As the mass of water increased, the conversion ratio increased. No energetic explosions with corium-A+R were observed; a maximum conversion ratio was less than 0.05% (Buxton et al. (1980)). Subsequent FITS tests with corium did result in more energetic explosions. The pressure measurements, which were obtained during the explosions, indicated peak pressures between 20-70 bars (Fig. B.4). The debris believed to have directly participated in the explosion were found to have high surface area (an order of magnitude larger than for equivalent diameter spheres). It should be noted that, because these experiments were done in an open geometry, very little of the debris was normally recovered from an experiment.

B. FITS Experiments. The second large scale experiments series has begun and is designed FITS (Fully Instrumented Test Series). The purpose of these tests is to determine the explosion conversion ratio as a function of ambient pressure, fuel composition, and other initial conditions in an enclosed interaction chamber (Fig. B.5). The experiments were instrumented to provide measurements of short and long-term pressure data both in the liquid and gas phase, work, fuel debris characterization, and visual observation of the explosion.

Mitchell et al, (1981, 1982, 1986; also see Berman et al. SNL Quarterlies) performed almost fifty FITS experiments with the fuel masses between 2 kg and 20 kg. The major fuel simulant used was thermitically generated Fe-Al $_2$ O $_3$ and remaining tests used a thermite corium (Table B.2). The key observations are as follows:

- The large scale interaction visually resembles a detonation-like structure seen in chemical explosions.
- (2) The peak pressures are large (sometimes measured to be supercritical), but decreases quite quickly to sustained pressure similar to Buxton's reported values.
- (3) A violent explosion can be triggered at a high-ambient pressure (1.0 MPa) by increasing the external trigger size.
- (4) Corium simulant melts do explode with similar efficiencies to iron-alumina.

^{**} Homogeneous average quantities.

The explosion conversion ratio with Fe-Al₂O₃ was consistently between 1 to 3%. A high narrow pressure spike (e.g., MD-19 test; 20 MPa for 1 ms) (Fig. B.6) were always observed at the leading edge of the explosion wave as it quickly propagates through the mixture and lower sustained pressure follow behind this peak. The propagation velocity varied between 200 and 600

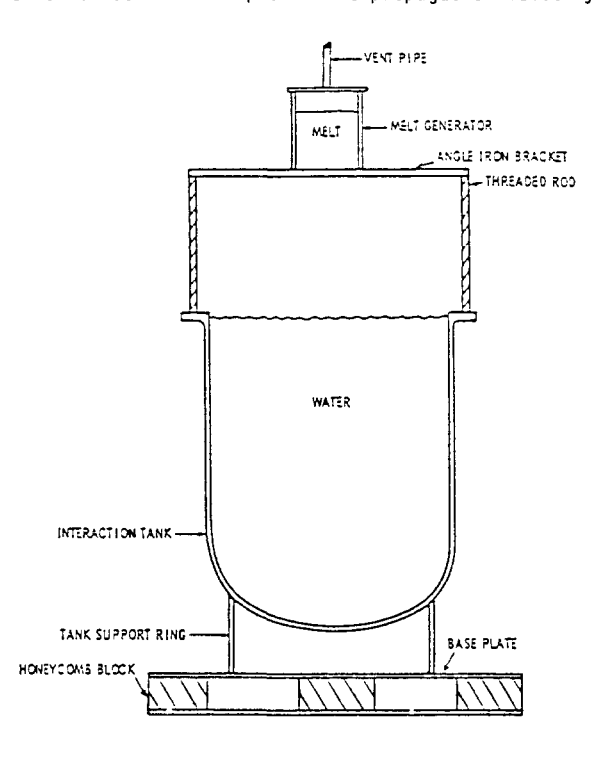


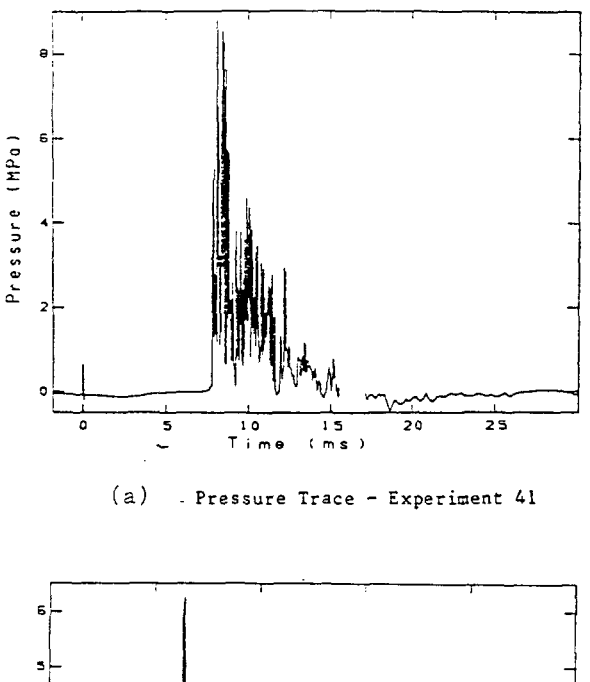
Fig. B.3. Interaction vessel of open geometry experiments

m/s. The trigger, when used, was a detonator, like that used in the open geometry tests (0.6 g of PETN explosive). The fuel coarsely intermixed with the coolant prior to the interaction (time 0.2 s). A spontaneous explosion usually began near the experiment chamber base. The weight-averaged mean particle size after the explosion was $100-1000~\mu m$, and without an explosion 1 to 10 mm (Fig. B.7). A recent experiment, RC-2, performed in a rigid wall cylindrical chamber (all past tests were performed in a lucite chamber -- i.e. weak wall) resulted in a much more efficient explosion. Estimates of the conversion ratio are varied because of uncertainties as to the pressure history and the amount of mass ejected during the explosion. These estimates were also made based on structural damage. The reported range of conversion ratio was between 5-17% (Berman et al., Quarterly, 1984).

B.1.1 <u>Smelt-Water Experiments</u>

The paper industry involves one process of the dissolution of molten smelt (mostly sodium carbonate) in water. Thus the occurrence of smelt-water explosions have been associated with the kraft chemical recovery operations from the inception of the kraft process. Every year, about 1% of the pulp recovery boilers in North American are destroyed when water is accidently introduced into the furnaces above a pool of molten smelt causing a vapor explosion. Over the last thirty years more than forty large scale explosion accidents have occurred. This brief review is originally based on a special report on smelt-water explosions by Shick and Grace (1982).

The first published study of the smelt-water system was an investigation of dissolving tank explosions by Sallack (1955). He carried out laboratory experiments by pouring smelt from a crucible into a pan of water or green liquor. Pure Na_2CO_3 smelts were not explosive, but the addition of 5% NaCl or 10% NaOH made smelts explosive. Green liquor reacted more violently than water, and increased green liquor temperature reduced explosion violence.



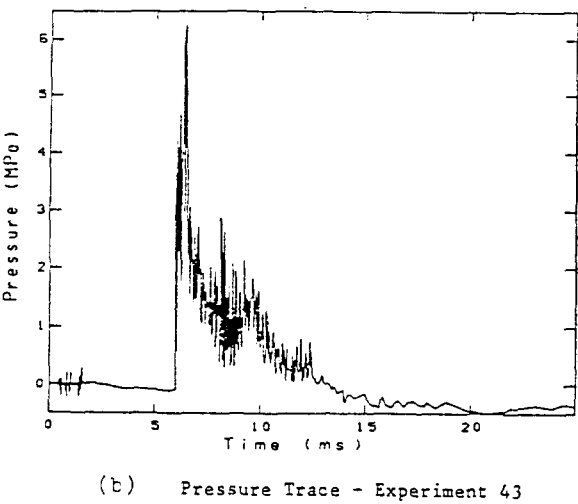


Fig. B.4. Pressure transients of open geometry experiments

Nelson and Kennedy (1956) reported on similar experiments with over 50 synthetic smelts as well as 5 commercial soda and 38 kraft smelt samples. They concluded that the action was primarily a physical phenomenon and dissolving tank explosions were caused by unfragmented coherent streams of smelt during rushes, which could be prevented if the streams were adequately dispersed by green liquor or steam shatter jets. Nelson and Kennedy mentioned work on an aromatic device to regulate the pressure of the shatter steam by the rate of flow through the smelt spout. A patent issued later to Gettle (1962) and assigned to Combustion Engineering, Inc., described a method of control based on sensing the temperature rise of the smelt spout cooling water. The widespread adoption of smelt shatter jets to break up the smelt stream and the recognition that undissolved smelt should not be allowed to accumulate in the bottom of the dissolving tank resulted in a significant decline in the frequency and severity of dissolving tank explosions.

The more serious problem has been explosions within the recovery boiler itself. After the work of Nelson and Kennedy (1956) on dissolving tank explosions, attention focused on furnace explosions. Rogers et al. (1961) reported the results of a series of experiments in which one

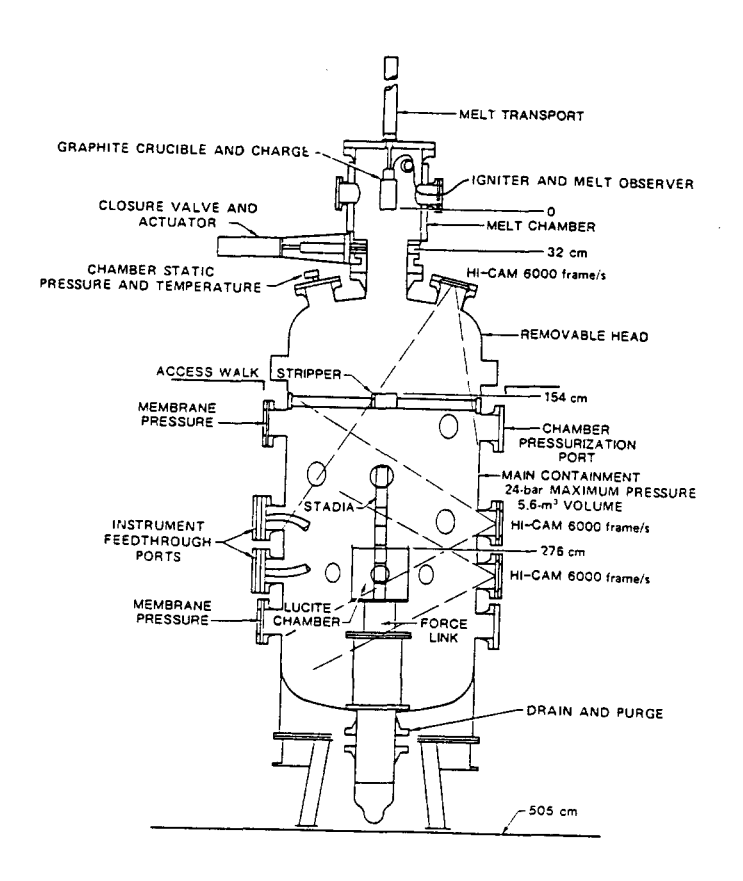


Fig. B.5. FITS experimental apparatus

gallon of water or green liquor was injected under the surface of 20 pounds of synthetic smelts prepared from sodium carbonate, sodium sulfate, sodium sulfide, and a mixture of these. They found that the pressure pulse obtained with sodium carbonate and water was only about one-third that obtained with sodium sulfide and water. They found hydrogen was released and sodium sulfate was formed during these violent interactions. Thus they considered smelt-water explosions as being combustible gas explosions, with a smelt-water reaction responsible for generating the combustible gas. However, it is doubtful that this endothermic, hydrogen-forming reaction contributed significantly to the violence of the explosive interaction for smelt and water.

In 1963, a group of 58 pulp manufacturers joined with Fourdrinier Kraft Board Institute, Inc. to form the Smelt-Water Research Group to sponsor research on smelt-water explosions. Seven reports by The Institute of Paper Chemistry (1964-1966), including the summary report,

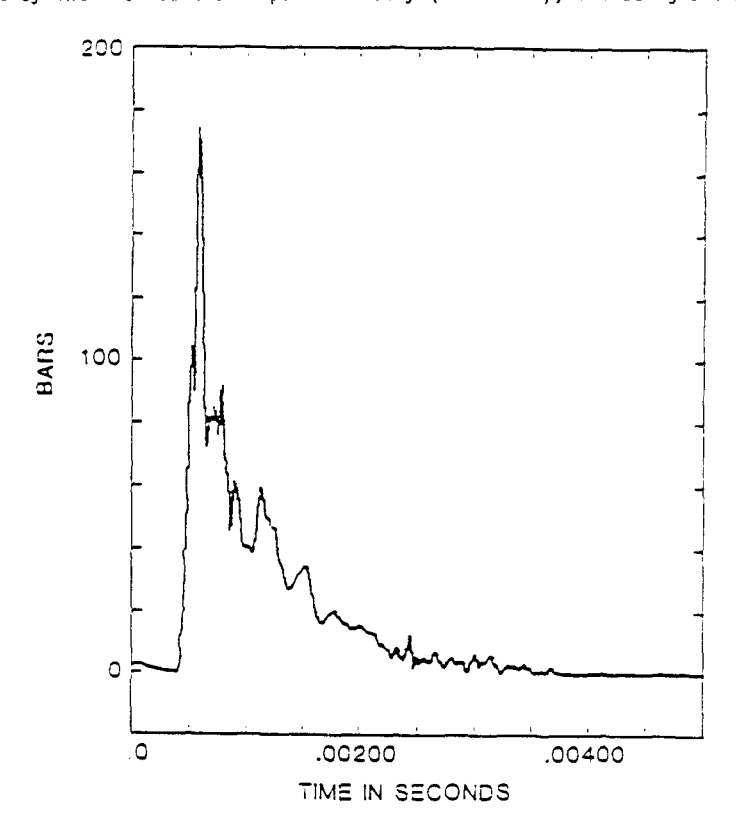


Fig. B.6. Typical water chamber base pressure in FITS experiment

were issued. Probably the main contribution of this work was the conclusive demonstration that smelt-water explosions were noncombustible. The key experiment involved obtaining explosions when water was injected into molten smelt under an inert atmosphere in a closed container. An empirical study of the effects of agents added to the smelt was carried out by the Smelt-Water Research Group (1966). Over 118 tests were run. Most agents were not effective in reducing the violence of explosions. A few agents reduced the violence and sometimes eliminated explosions. Even though no pattern or mechanism was identified, H.W. Nelson and Norton (1969) and H.W. Nelson (1971) obtained patents for use of solutions of ammonium sulfate or polymeric glycols, and solid sodium or ammonium bicarbonate or ammonium carbonate to quench char beds in recovery furnaces.

Battelle Memorial Institute completed a smelt-water study in 1972 and the summary report was issued in January, 1973. This final report by Krause et al. (1973) contains a wealth of information on explosivity vs. the chemical composition of smelts, on the physical properties of smelt and smelt components, and on explosion mechanisms. The Battelle explosivity tests were performed by injecting 30 to 1000 milligrams of water into a graphite crucible containing about 70 grams of molten smelt or by introducing 80-300 milligrams of water as a drop on the end of a ceramic tube, which was dropped into the crucible of smelt. It is probable that these experimental techniques had some influence both on the experimental results and on the conception of an explosion mechanism.

H.W. Nelson (1973) pointed out the very great similarities of the smelt-water explosion system to the purely physical explosions reported between many molten metals and water as well as liquified natural gas and water. These were recognized at that time as examples of liquid-liquid (superheated liquid or vapor explosions). This "superheat theory" did incorporate some of the spontaneous nucleation concepts into the explanation of smelt-water explosions, but it is

not complete since it does not address coherence. Shick (1976) had begun to question the simple application of the superheated liquid trigger mechanism to smelt-water explosions under no impact conditions. Based on the experimental work by Apfel (1971) and the predictions by Yayanos (1970) showing the potential for increase in the superheat-limit temperature of a salt solution, Shick (1980) proposed the concentration gradient trigger mechanism that whenever there is contact between smelt and an aqueous liquid, the properties of both are changed at the interface in accordance with the solubility of each in the other. In this way, nucleation can be delayed even with a very high interface temperature, permitting a very significant degree of superheat to develop in the bulk of the aqueous phase.

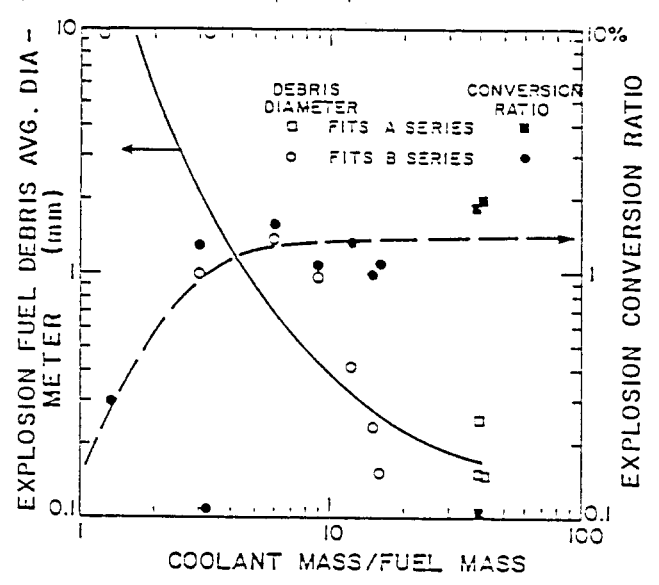


Fig. B.7. Explosion conversion ratio and debris diameter as a function of coolant-to-fuel-mass ratio

A major study of smelt-water was recently carried out under sponsorship of the Swedish Recovery Boiler Committee. Bergman and Laufke (1979) performed the experiments to permit comparison of smelt-water blast effects with those of conventional explosives and to determine the potential for minimizing furnace damage and danger to personnel by provision of suitable pressure relief areas in the furnace construction. The experiments involved the addition of 10-100 g of water into 10-30 kg of molten smelt with three different adding techniques. It is important to note that explosions were obtained with pure Na_2CO_3 , since the earlier studies at Combustion Engineering and Battelle never gave explosions with Na_2CO_3 and water. Ludwig (1980) conducted a damaging dissolving tank explosion experiment with a nonsulfur system. With regard to the relative explosiveness of water injected into sodium carbonate in these experiments, the authors hypothesized that this would be a function of the quantity of water injected, rising from zero with about 50 milligrams, as reported by Krause et al (1973) in the Battelle studies, to 50% at 50 grams in these tests and projected to reach 100% at about 50 kg. The authors neglected the difference in injection technique between the two studies and also the work of Rogers et al. (1961) in which the impulse for sodium carbonate when one gallon (3.8 kg) of water was injected under 20 pounds of smelt was also only about one-third to one-half the pressure pulse obtained with a kraft-type smelt. The authors note that the maximum blast effect they obtained under ideal conditions corresponded to about 0.2 pounds of TNT per pound of water, vs. a theoretical value in the literature of about 0.5 pounds per pound of water. In actual furnace practice, much lower yields would normally be expected, because the conditions would not be

Small-scale studies of smelt-water interactions are currently in progress at the Institute of Paper Chemistry using a dropped tube containing a suspended drop similar to that used in the Battelle study.

B.2. LNG Experiments

In recent years, cryogen-water explosions where water is the hot liquid (fuel) and the boiling cryogen (coolant) produces the high pressure vapor have become a safety concern in the

transport of liquified natural gas (LNG) and other industrial processes using cryogenics. The concern here is not only the work potential from the vapor explosion but also the possible ignition and combustion of the vaporized natural gas dispersed in the air.

Nakanishi and Reid (1971) surveyed the published and much of the unpublished literature dealing with the spilling of LNG in water. In 1956, Couch International Methane Service Ltd. conducted a series of spill experiments with LNG. In tests made in Louisiana, 75 bbl/hr were spilled into a canal for several days with peak flows of 325 bbl/hr for several hours. The LNG spread on the surface evaporated and burned, yet ice formed underneath. In 1965, Conch also conducted tests with a 5 gal aquarium containing water. LNG was spilled both on top of and under the water surface. An icy-foam resulted, but no explosion occurred. Similarly, no problems were encountered in another test wherein some 4900 gal of LNG were spilled in 7 min from a vessel moving at 9-10 knots. A dump of 8000 gal of LNG into the sea at Marsa el Brega (Libya) by Esso was also uneventful. An interesting small scale test was carried out by Conoco. In this case, LNG was poured into a 5 gal can containing water and allowed to evaporate. More LNG was then added and a gallon of water poured on top. An explosion resulted every time except when pure liquified methane was substituted for LNG. In an uncontrolled test, Wisconsin Gas Co., while draining LNG from a storage tank, noted explosions as the LNG flowed into a nearby pond. There was about a 2 min delay after initial contact, and ice chunks were thrown 100-150 ft away. In 1971, a similar occurrence was noted by the Memphis Light, Gas and Water Division. The Tokyo Gas Co. (Japan) also carried out tests that involved the spillage of LNG on water. The quantities used were 1.2-2.4 liters. No explosions were ever reported. Shell Pipe Line Corp. was actively engaged in research on LNG-water interactions. Earlier Shell work dealt with LNG spills on both hot and cold water. In cold water ($<30^{\circ}$ C), ice crusts were noted. In 1971 some unusual results were noted by Esso Research and Engineering. As most others had found, pouring LNG on top of water never led to an explosion. However, if LNG was poured on water, and, before evaporation was complete, water was poured in the vessel, an explosion resulted. Most quantitative experiments until that time were done by Burgess et al. (1970) under contract to the Coast Guard, and the U.S. Bureau of Mines. They conducted a number of tests to study the heat transfer between LNG and water and between liquid nitrogen (LN2) and water. In most tests, either LNG and LN2 was poured upon the surface of water contained in a small aquarium tank. Two significant observations were: first, the interface between LN2 and water was extremely turbulent, whereas the LNG and water, the interface was quite calm, and second, though ice forms in both cases, it took considerably longer for this crust to appear for the LN2 spills.

The superheat model (later called spontaneous nucleation) has been generally accepted to explain explosive boiling between LNG and water. The experimental results by Burgess et al. (1972) and Enger and Hartmen (1972) agreed to this supposition saying that no explosive boiling incident is predicted if the water temperature is below the homogeneous nucleation temperature of the LNG. Thus, this theory can predict when explosive boiling is possible, but it does not tell us anything about the damage potential due to the event.

Even though no industrial accidents have taken place between LNG and water, many laboratory studies have been carried out to delineate the hazardous ranges of LNG composition and water temperature, especially by Porteous and Blander (1975) and Porteous et al. (1976). Laboratory scale tests have shown, however, that with the usual concentrations of methane, ethane, and propane in commercial LNG, an explosive boiling event following a spill is very unlikely.

Since 1978, large-scale LNG spills on water have been conducted by a joint team from the Lawrence Livermore National Laboratory (LLNL) and the Naval Weapons Center (NWC) sponsored by the U.S. Department of Energy (DDE). There were three test series: Avocet in 1978, primarily for instrument evaluation; Burro in 1980, primarily for cloud dispersion studies; and Coyote in 1981, primarily for cloud fire and rapid-phase-transition (RPT) studies. The 1978 Avocet LNG spills involved volumes of about 4.5 m³ and spill rates of approximately 3.5 m³/min. Several small RPT explosions were observed during the tests, all occurring immediately at the beginning of the spill. The Burro and Coyote test series were conducted at the NWC China Lake facilities having a 40 m³ LNG spill capacity with a maximum spill rate of 20 m³/min. The spill plate is located below the pipe exit in order to keep the LNG from impinging upon and eroding the pond bottom. Koopman et al. (1981, 1982) reported the results of Burro 9 tests. In addition, McRae (1983) and McRae et al. (1984) published the Coyote and the Burro test series data and analysis. In these reports eight out of a total 26 spills produced RPT explosions in which the RPT explosions increased the area and height of the flammable zone significantly. Two distinct types of RPTs occurred during these experiments: early RPTs -- close to the spill point, primarily underwater and delayed RPTs -- near the edge of the LNG pool, and at the surface of the LNG on water at China Lake. The probability and magnitude of early RPTs increased as the depth of penetration of the LNG into the water increased and at higher spill rates. However, there was no indication of possible detonation of the cloud.

system p hot/cold s	fuel mass or volume	fuel (C)	coolant mass or volume	coolant temp e (C)	t cover 945	entering velocity (n/s)	Keber nusber	exp.1 peak mode P.(MPa)	dwell time (as)	ratio (%)	rearks	reference	year
Al/Nater	20 kg	906-029	.3-4d Cu.	3-4d cu.ft 28-195	5 417	4.5-8.3		4			whilest and not to exter and remain when the bear in the bear in the bear and the b		
#}/Water	1/4 0001	700-950		Subran	_			. 01	, ,		control explosion out to water formulated to the control of decising or painting the bottom	Long	
Al/Nater	20 20	200ve 982	•	15	<u>.</u>	1.0-7.7		. «	;		since the tar arms in the new arms of the despectation for the size of the standard to the size of the	Wright et al.	
dater/LN6 s	8 liter	!	Saalloo	;	1	Lies		c or			CHEMIAL CALLING, to prevent explosion max. Water depth & organic coating	Hess, Brondyke	1463
Al/Mater 1		007			•	11116		a <			unity this experiment has reported explosions when LNG mas poured on top on top of mater	Burgess et al. 1970	. 1976
Mater/Freon-22		3		44-87	100	1 mbdr (t o			very high pressure puises usually occured on 2nd impact, highly fragmented aluminum debris	Darby et al.	1972
Lead. Salt/Mater				2	į			n <			valor explosions, ice forms for loner temps, superheat explanation test of LNG explosions	Enger, Hartman 1972	197
Al/Sodium .		2670			i	impact		t a			shock tube expits, no appreciable pressure above the impact pressure, suression by the incondensible yas	Hillary et al. 1972	. 197
Al+Mo/Sodium :		3000		250				B shout t	107		Since the exp t, many repeated pressure pulses, none large	Holtbecker et a1972	197
later/Freon		8		9	317				k U		The is settled under a coolant, per each gas content by contamination extremely fine debris in sodium	Pottinger et a11972	1197
Mater/Freon		37-98.5		9	-						Lour and the C. (Matter) to 1 lack of interaction when lwater) 92 CSupport Fauske's hypothesis	Henry et al.	1973
Kater/Freon	700 .1	50-02		-42116				S 1-8-5			Market into the Louisetty to Significant Valorization	Henry et al.	1973
Tin/Water	50 4	800		•	1						Expression users with most interest of reson subcooling	Board et al.	197
lin/Water	200	650-750		2				200			Transfer of the state of the st	Board, Hall	18
Tin/Water	200	90.	900 CU.CS	8	į			, =	,		Franchistory (1 tradatory) of the state of the state of the spatial propagation	Board, Hall	1974
dater/Freon	•	u			į				10-20		feducial interesting and properties of the control	Board, Hall	167
Mineral oil/Freon-22		145-190		Ŧ	a).			B 1.0B			Moreolacine when oil form villed works oil from the casing system constraint ortiveds the explosion event.	Henr y	<u>.</u>
Mater/Freon-22	100-300	12-21		7	Ĭ						no expression miner out temp / 100. Explosion Th for Groon=23 = \$4.60 No explosion than It is not	Heary et al.	À
Nineral oil/Freon-22	100-300 ml	100-190		Ŧ	ī			В 2.1			Englocing when oil team) 170f	Henry et al.	
Mineral oil/Freon-12	100-300 at	120-170		es-	Ĭ			B 1.23			Explosion when nil team > 100	Henry et al.	-
Mater/Liquid NH3 #	0.4-5 gallon	_	large		Ę			⋖			under mater release, no explosion in to 057 of MHX chasically reacted	Henry et al.	
J02/Sodius	3.2 kg		300 9	410	Ĭ	Inj.P=5ats		8 0.98			Rand vanishing his only 200 and 1002 more framework from the Confers of the confe	Maj et al. 1974	//
Salt/Water											toporo votado i	Andreas of all	
Salt/Water	2 kg				Ħ	8-7 m/s		B 0.2-1.9			Mater column tenant on a entire calt coal bear it one	Mnder 500 Pt 31.1973	
U02/Sodius	2 kg		1 01	200	al.			•			Extremely time denomination but no windows characterists	HNOET SOR ET 41.1973	
Steel/Sadium	3 49		101	200	Ĭ						Extremely dine franchants in our minimum franchants.	Holibecker et 11975	//
In/Water	9 kg	4 20			į						Franchiston arrangement by court have	Holtbecker et a19/5	
Cu/Water	2.25-4.5 kg		112.05		ij			-			Full hans, come database to container	, .	5
Mg+Pb/Water	4 kg	08 1			į			•			Frankling with a land han - water container discount	- sq.	5
kass/Water	9 kg	B 20			Ţ			a			Frauentition accompanied by han, where task is terrary	74ye	2,63
My/Mater	2.25 kg	650			į			•			No interaction	1 4 de	2 4
Ju/Hater	0.9-4.5 kg		iarge		Ä			a s			No interaction	200	6/41
' fustor	6												

1985 1985	19 747-809 1747-809 203,747 20	1.2a 3-24 12-13 12-13 200 200 380 380 20-230 20-230 20-230 5-15 5-15 5-15 5-15 5-15 5-16 6-95 6-95 6-95 6-95 6-95 6-95 6-95 6-9	4.6-9.9 a/s 4.5 a/s 4.5 a/s 30 a/s 30 a/s 30 a/s 30 a/s	(0.2 2.2 (0.2	Severe, anderate, mild interaction, Propagation velocity = 200 m/s MKRMIR experiments No interaction Misself Resperiments No interaction Misself Resperiments No interaction Misself Resperiments Misself Respectively Misself Respection, No pluses (max peak 600M curcible broken Mapper explosion of lesser magnitude than the previous ones Motrogetring, Pressure rise time - Zage, Condensation time - 10 sec. Ispra tank facility Moteplosive interaction of less code and mider (file boiling Ispra tank facility Moteplosive interaction of less code and mider (file boiling Ispra tank facility Moteplosive interaction of Lipself Respondent of Misself Respondent Misself Misself Respondent Misself Respondent Misself Misself Respondent Misself Mi	Briggs Briggs Briggs Asher Bird,Mill Bird,Mi
1501-180 1.5 ct. 20 1.7 c	597,407 597,407 597,407 1500 1500 1500 1500 1500 1500 1500 15	7-10 12-13 12-13 12-03 13-03 1	4.5 a/s 4.5 a/s 3.0 a/s	(0.2 (0.2.2.5 (0.2.2.5 1.0-2.0 1.0-2.0	No interaction No interaction INEMNIK experiments No interaction INEMNIK experiments INEMNIK experiments Supplicant pressure pulse folled by lesser one, Drucible fracture Explosion occurred (3ss after the completion of the injection, law pluses (asx pressure)100NI Series of pulses, make passes, has peak abody crucible and "splat-cooled" Series of pressure rate pulses, has peak abody crucible broken Vapor explosion of lesser agantude than the previous ones. No triggering, Pressure rate time - 2ser, Condensation time - 10 sec. Ispra tank facility No explosive interaction, ivel is cooled down under file boiling. Ispra tank facility No explosive interaction, ivel is cooled down under file boiling. Ispra tank facility No explosive interaction but rapid exagoration 2.6 Litres cover gas voluee (0.4MPa), Locally high fuel to coolant ratio explosion, fine fragentation 2.6 Litres cover gas voluee (0.1MPa), Reduced expansion and fragentation 3.6 Litres cover gas voluee (0.1MPa), Reduced expansion and fragentation 3.6 Litres cover gas voluee (0.1MPa), Reduced expansion and fragentation 3.6 Litres cover gas voluee (0.1MPa), Reduced expansion and fragentation 3.6 Litres cover gas voluee (0.1MPa), Reduced expansion and fragentation 3.6 Litres cover gas voluee (0.1MPa), Reduced expansion and fragentation 3.6 Litres cover gas voluee (0.1MPa), Reduced expansion and fragentation 3.6 Litres cover gas voluee (0.1MPa), Reduced expansion and fragentation 3.6 Litres cover gas voluee (0.1MPa), Reduced expansion and fragentation 3.6 Litres cover gas voluee (0.1MPa), Reduced expansion 3.7 Litres cover gas voluee (0.1MPa), Reduced expansion 3.8 Litres cover gas voluee (0.1MPa), Reduced expansion 3.9 Litres cover gas voluee (0.1MPa), Reduced expansion 3.0 Litres cover gas voluee (0.1MPa) Red	
1209 1.0 ct. 20 1.0 ct. 30 1.0 ct. 3	150-1800 1750-1800	12-13 200-450 400-450 400-450 380 380 20-230 20-230 5-15 5-15 5-15 5-15 5-15 5-16 5-16 5-16	4.5 a/s 4.5 a/s 20 a/s 20 a/s 30 a/s 20 a/s 30 a/s	(0.2 (0.22.2. (0.22.2.2.1.1.2-4.2.0 1.0-2.0	No interaction Significant pressure pulse folled by lesser one, Durible Fracture Explosion occurred (3ss after the completion of the injection, lwo pluses (ass pressure)100N) Series of pulses detected, All steel ejected from criticals and 'splat-cooled' Series of pressure pulses, Max peak 500N crucible broken Series of pressure pulses, Max peak 500N crucible broken Series of pressure pulses, Max peak 500N crucible broken Series of pressure pulses, Max peak 500N crucible broken Series of pressure pulses, Max peak 500N crucible broken Natingering, Pressure rise time - 2 sec. Condensation time - 10 sec. Ispra tank facility No explosive interaction, but rapid evaporation No explosive interaction No explosive No explosive No explosive No explosive No explosive No explos	
1300 15 ct 200 317 30 345 5 5 5 5 5 5 5 5 5	1500 1500 1500 1500 1500 1530 1530 1530	240 400-450 380 380 200 20-230 20-230 5-15 5-15 5-15 5-15 5-15 5-16 6-8 20(0,1HPa) es 50(0,5HPa)	30 a/s 30 a/s 30 a/s 30 a/s 30 a/s 1apsct	(0.2 (0.2-2); (0.2-2); (0.2-2); 1.0-4.2 1.0-2.0	Significant pressure pulse folled by lesser one, Crucible fracture Explisand occurred Cass after the condition of the injection, he pluees (was pressure)100M) Series of pulses detected, All steel ejected from crucible and "splat-cooled" Series of pulses detected, All steel ejected from crucible and "splat-cooled" Series of pulses detected, All steel ejected from crucible and series of pressure pulses, Ma peak 600M crucible broken. Series of pressure pulses, Ma peak 600M crucible broken. Note polosion of lesser magnitude than the previous ones. Note polosion of lesser magnitude than the previous ones. Note polosion of lesser magnitude than the previous ones. Note polosion of lesser magnitude than the previous of less required to the properties of the previous of the fragmentation. Note polosion in the action of the fragmentation. Note polosion of lesser over gas volume (0.1MPa), Reduced expansion and fragmentation. Note polosion of lesser properties of the presentiation of the properties of the pro	
1707-1800 15 ct. 300 31 ct. 20 st. 30 31 ct. 30	1750-18800 1500 1500 1500 1650 1650 1650 1650-1800 1505-1800 1505-1800 1606-7300 1606-	400-450 380 380 380 200 200 20-230 20-230 5-15 5-15 5-15 5-15 5-15 6-8 86-0-18Pai	20 6/5 20 6/5 30 6/5 30 6/5 10 6/5 10 6/5	(0.2 (0.2-2: (0.2-2: 1.2-4:2 1.0-2:0 5-8	Explosion occurred (3ss after the completion of the injection, lwo pluses (ass pressure.)100H) Series of pulses, the speak offorcurible and 'splat-cooled' Series of pressure pulses, has pask soft curtible and 'splat-cooled' Series of pressure pulses, has pask soft curtible the mental of the series and in the series series of pressure pulses, has pask soft offers one was the series and the series of the se	
150 1-6 c. 20 31 31 31 31 31 31 31 3	1500 1530 1530 1530 1530 1530 1530 1500-1800 15.55 kg 3100-3400 15.55 kg 3100-3400 16.55 kg 3100-3400 16.55 kg 3100-3400 17.55 kg 3100-3400 18.50 kg 850 19.50 kg	380 380 380 200 20-230 20-230 20-15 5-15 5-15 5-15 5-15 5-16 5-16 5-16 5	30 4/5 20 4/5 30 4/5 14pact		Series of pulses detected, All steel ejected from crucible and 'splat-cooled' Series of pressure pulses, Max peak 600M crucible broten Vapor explosion of lesser amantude than the previous ones. No triggering, Pressure rise than - 2 ser, Condensation time - 10 ser. Ispra tank facility No explosive interaction, fuel is cooled down under file boiling. Ispra tank facility No explosive interaction but rapid exponation. 3.6 Lifers cover gas volume (0.4MPa), Locally Ming fuel to coolant ratio explosion, fine fragmentation 1.2 or 3.6 Lires cover gas volume (0.4MPa), Elong pressurzation 1.3 lifers cover gas volume (0.4MPa), Meduced expansion and fragmentation 2.6 Lifers cover gas volume (0.4MPa), Meduced expansion and fragmentation 2.6 Lifers cover gas volume (0.4MPa), Meduced expansion and fragmentation 2.6 Lifers cover gas volume (0.4MPa), Meduced expansion and fragmentation 2.6 Lifers cover gas volume (0.4MPa), Meduced expansion and fragmentation 2.6 Lifers cover gas volume (0.4MPa), Meduced expansion and fragmentation 3.6 Lifers cover gas volume (0.4MPa), Meduced expansion and fragmentation 3.6 Lifers cover gas volume (0.4MPa), Meduce expansion and fragmentation 3.6 Lifers cover gas volume (0.4MPa), Meduce expansion and fragmentation 3.6 Lifers cover gas volume (0.4MPa), Meduce expansion and fragmentation 3.6 Lifers cover gas volume (0.4MPa), Meduce expansion and fragmentation 3.6 Lifers cover gas volume (0.4MPa), Meduce expansion and fragmentation 3.6 Lifers cover gas volume (0.4MPa), Meduce exposion 4.7 Lifers cover gas volume (0.4MPa), Meduce exposion 5.6 Lifers cover gas volume (0.4MPa), Meduce expansion and fragmentation 5.6 Lifers cover gas volume (0.4MPa), Meduce expansion and fragmentation 5.6 Lifers cover gas volume (0.4MPa), Meduce expansion and fragmentation and fragmentati	
150 2 cc 200 31 17 20 4/5 8 5 5 5 5 5 5 5 5	1530 1650 169 170-1800 155 kg 1100-1800 155 kg 1100-1800 155 kg 1100-1800 155 kg 1100-1800 160-1800 170-1800 1800 190-1800 190-1800 190-1800 190-1800 190-1800 190-1800 190-1800 190-1800 190-1800 190-1800 190-1800 190-1800 190-1800 190-1800 190-1800 190-1800 190-1800	380 200 20-230 20-230 20-230 5-15 5-15 5-15 5-15 5-15 5-15 5-15 5-1	20 e/s 30 e/s impact	્રે લ્ લ્	Series of pressure pulses, Max peak 500M crucible broken Yapor explosion of lesser aagnitude than the previous ones. No triggering, Pressure rise tise - 2sec, Condensation tise - 10 sec. Ispra tank facility No explosive interaction, Fuel is cooled down under file boiling. Ispra tank facility No explosive interaction but rapid evaporation. 2.6 Lifes cover gas volume (0.4MPa), Locally high fuel to cool and ratio explosion, fine fragmentation. 2.6 Lifes cover gas volume (0.1MPa), Reduce expansion and fragmentation. 2.6 Lifes cover gas volume (0.1MPa), Reduce expansion and fragmentation. 2.6 Lifes cover gas volume (0.1MPa), Reduce expansion and fragmentation. 2.6 Lifes cover gas volume (0.1MPa), Reduce expansion and fragmentation. 2.6 Lifes cover gas volume (0.1MPa), Reduce expansion and fragmentation. 2.6 Lifes cover gas volume (0.1MPa), Reduce expansion and fragmentation. 2.6 Lifes cover gas volume (0.1MPa), Reduce expansion and fragmentation. 2.6 Lifes cover gas volume (0.1MPa), Reduce expansion. 3.6 Lifes cover gas volume (0.1MPa), Reduce expansion. 3.7 Lifes cover gas volume (0.1MPa), Reduce expansion and fragmentation. 3.8 Lifes cover gas volume (0.1MPa), Reduce expansion. 3.8 Lifes cover gas volume (0.1MPa), Reduce expansion. 3.8 Lifes cover gas volume (0.1MPa), Reduce expansion. 3.9 Lifes cover gas volume (0.1MPa), Reduce expansion. 3.0 Lifes cover gas volume (0.1MPa), Reduce expansion. 3.1 Lifes cover gas volume (0.1MPa), Reduce expansion. 3.0 Lifes cover gas volume (0.1MPa), Reduce expansion. 4.0 Lifes cover gas volume (0.1MPa), Reduce expansion. 5.0 Lifes cover gas volume (0.1MPa), Reduce expansi	
150 14 of 20 14	1650 1650	200 20-230 20-230 20-230 5-15 5-15 5-15 5-15 5-15 5-15 5-15 5-1	30 a/s lepact		Vapor explosion of lesser aagmitude than the previous ones. No triggering, Pressure rise time - 2ser, Condensation time - 10 sec. Ispra tank facility No explosive interaction, inel is cooled down under file boiling. Ispra tank facility No explosive interaction but rapid exaporation. 3.6 Litres cover gas voluee (0.4MPa), Locally high fuel to coolant ratio explosion, fine fragmentation. Intres cover gas voluee (0.4MPa), Reduce expansion and fragmentation. Intres cover gas voluee (0.1MPa), Reduce expansion and fragmentation. Intres cover gas voluee (0.1MPa), Reduced expansion and fragmentation. Put interaction which is a voluee (0.1MPa), Reduced expansion and fragmentation. Put interaction of volume of the properties of the	
1929 2899 200 43 29-230 K,Ap, Ne 20-230 K,Ap, Ne 20-23	1 kg 2850 1200-1800 155 kg 3100-3400 156 kg 3100-3400 156 kg 3100-3400 156 kg 3100-3400 156 kg 3100-3400 1600 kg 3100-3400 1200 kg 3100 1200 kg 3100 12	20-230 20-230 20-230 20-230 5-15 5-15 5-15 5-15 5-15 5-15 6-10-10-10-10-10-10-10-10-10-10-10-10-10-	lepact	44.4.4.4.4.4.4.4.4.4.4.4.4.4.4.4.4.4.4	No triggering, Pressure rise than - Zagr. Condensation than - 10 sec. Ispra tank facility No explosive interaction, fuel is cooled down under file boiling. Ispra tank facility ho explosive interaction but rapid exporation. Is a litres cover gas volume (0.44Fa), Locally high fuel to coolant ratio explosion, fine fragmentation 1.2 or 3.6 litres cover gas volume (0.44Fa), Locally high fuel to coolant ratio explosion, fine fragmentation 2.6 litres cover gas volume (0.44Fa), Solon pressurization 2.6 litres cover gas volume (0.44Fa), Reduced expansion and fragmentation Self-satelating shocks (Mprops64-300 axis), fuel debris finer than 0.03-0.1 amplified Pouring ander, No vapor explosion. Forced dropping ander, 3 experiments, Vapor explosion.	
1300-1800 200 is 20 20 30 30 30 30 30 30	1200-1800 155 kg 3100-3400 155 kg 3100-3400 150-3400 150-3400 100-3400 100-3400 1200 1200 1200 1200 1200 1200 1200 1	20-230 20-230 5-15 5-15 5-15 5-15 5-15 6-10 (10 Pa) es 20(0, 10 Pa) es 50(0, 10 Pa) es 50(0, 10 Pa)	impact	1, 1, 2, 0, 1, 1, 1, 1, 1, 1, 1, 1, 1, 1, 1, 1, 1,	No explosive interaction, tuel is cooled down under file boiling ispra tant facility No explosive interaction but rapid evaporation Ispra tant facility No explosive interaction but rapid evaporation Ispra tant facility Ispra tant faci	
1500-1800 20 kg 20-210 k,kr,the 20-2	1500-1800 15 kg 3100-3400 15 kg 3100-3400 15 kg 3100-3400 100-3400 100-3400 12	20-230 5-15 5-15 5-15 5-15 8-15 8-15 8-15 8-15		2,2,2,5	No explosive interaction but rapid evaporation ispra tank identity 3.6 litres cover gas volume (0.4MP.), Locally high feet to coolant ratio explosion, fine fragmentation 1.2 or 3.6 litres cover gas volume (0.4MP.), Reduced expansion and fragmentation 2.2 litres cover gas volume (0.1MP.), Reduced expansion and fragmentation 3.6 litres cover gas volume (0.1MP.), Reduced expansion and fragmentation 3.6 litres cover gas volume (0.1MP.), Reduced expansion and fragmentation 3.6 litres cover gas volume (0.1MP.), Reduced expansion and fragmentation 3.6 litres cover gas volume (0.1MP.), Reduced expansion and fragmentation 3.6 litres cover gas volume (0.1MP.), Reduced expansion and fragmentation 3.6 litres cover gas volume (0.1MP.), Reduced expansion and fragmentation 3.6 litres cover gas volume (0.1MP.), Reduced expansion 3.7 litres cover gas volume (0.1MP.), Reduced expansion 3.8 litres cover gas volume (0.1MP.), Reduced	
1.2 or 7.5 or	55 kg 3100-3400 55 kg 3100-3400 55 kg 3100-3400 100-3400 660-750 660-750 1200 1200 1200 1200 1200 1200 1200	5-15 5-15 5-15 5-15 85-95 20(0,1MPa) 90(0,1MPa) 70(0,5MPa)	løpact	2.0	3.6 litres cover gas volume (0.4PPa), locally high fuel to coolant ratio explosion, fine fragmentation 1.2 or 3.6 litres cover gas volume (0.4PPa), Slow pressurization 1.2 litres cover gas volume (0.1PPa), Reduced expansion and fragmentation 2.6 litres cover gas volume (0.1PPa), Reduced expansion and fragmentation 2.6 litres cover gas volume (0.1PPa), No containment pressurization 2.6 litres cover gas volume (0.1PPa), No containment pressurization 2.6 litres cover gas volume (0.1PPa), No containment pressurization 2.6 litres cover gas volume (0.1PPa), Reduced exposion 3.6 litres cover gas volume (0.4PPa), Reduced explosion 6. ccd dropping gode, 3 experiments, Vapor explosion	
100-2400 5-15 945	55 kg 3100-3400 55 kg 3100-3400 55 kg 3100-3400 660-750 660-750 1200 1200 1200 1200 1200 1200 1200 12	5-15 5-15 5-15 85-95 20(0.1MPa) 90(0.1MPa) 50(0.1MPa)		-2.0	1.2 or 3.6 lires cover gas volume (0.14-iMPa), Sion pressurization 1.2 litres cover gas volume (0.1MPa), Reduced expansion and fragmentation 2.6 litres cover gas volume (0.1MPa), No containment pressurization Self-sustaining shocks (Uprop.3.00 a/s), fuel debris finer than 0.03-0.1 and Pouring mode, No vapor explosion Forced dropping mode, 3 experiments, Vapor explosion	
1100-1400 5-15 445	55 kg 3100-5400 5100-5400 5100-5400 650 650 1200	5-15 5-15 85-95 20(0.1MPa) 90(0.1MPa) 20(0.1MPa) 50(0.5MPa)			1.2 litres cover gas volume (0.1MPa), Reduced expansion and fragmentation 5.6 litres cover gas volume (0.1MPa), Mo containment presentiation Self-sustaining shocks (Mpropade-200 aks), fuel debris finer than 0.03-0.1 man Pouring ande, Mo vapor explosion forced dropping ande, 2 experiments, Vapor explosion	Millington Millington et al.
11 11 12 12 13 14 14 14 15 14 14 15 14 14	3100-3400 640-720 650-100 1200 1200 1200 1200 1200 1200 1200	5-15 85-95 20(0.1MPa) 90(0.1MPa) 20(0.1MPa) 50(0.5MPa)			2.6 litres cover gas volume (9.1MP2). No containment pressurization 2.6 litrestaining shocks (Mpopse0-300 a/s), tuel debris finer than 0.03-0.1 man Pouring adde, No vapor explosive. Forced dropping adde, 3 experiments, Vapor explosion	Millington et al. et al.
Main	850 850 1200 1200 1200 1200 1200 1200 1200	95-95 20(0.1MPa) 90(0.1MPa) 20(0.1MPa) 50(0.5MPa)			Self-sustaining snocts (Upropside-300 a/s), fuel debris finer than 0.03-0.1 ass Pauring mode, No vapor explosion Forced dropping mode, 3 experiments, Vapor explosion	# # # # # # # # # # # # # # # # # # #
11 11 11 12 12 13 14 14 14 14 14 14 14	850 950-1000 1200 850 1200 1200 1200		a ⊄ ⊄ ⊄ .	;	Pauring mode, No vapor explosion Forced dropping mode, 3 experiments, Vapor explosion	
100 15 litres 2000.18Palair	950-1000 1200 850 1200 1200 1200		⊄ € €	;	Forced dropping ande, 3 experiments, Vapor explosion	i -i -
1200 15 litres 2000. 180	1200 850 1200 1200 1200 1200		€ €	3		: -
111 111	850 1200 1000 1200 950-1000		≪.		Submersion acce, No vapor explosion	
1200 15 litres 20(0.5MPs)air A Subaersion acde, No vapor explosion 1200 15 litres 20(0.5MPs)air A 5 Fouring acde, Yapor explosion 1200 15 litres 20(1.0MPs)air A 5.3-2.5 Fouring acde, No vapor explosion 1200 15 litres 20(1.0MPs)air A 2.3-2.5 Fouring acde, No vapor explosion 1200 15 litres 20(1.0MPs)air A 5.3-2.5 Fouring acde, Yapor explosion 15 litres 20(1.0MPs)air A 5 Fouring acde, Yapor explosion 1200 15 litres 20(1.0MPs)air A 5 Fouring acde, Yapor explosion 15 litres 20(1.0MPs)air A 5 Fouring acde, Vapor explosion 15 litres 20(1.0MPs)air A 5 Fouring acde, Vapor explosion 15 litres 20(1.0MPs)air A 6 Fouring acde, Vapor explosion 15 litres 20(1.0MPs)air A 6 Fouring acde, Long tera vaporization but explosion 15 litres 20(1.0MPs)air A 6 Fouring acde, Long tera vaporization but explosion 15 litres 20(1.0MPs)air A 7 Fouring acde, Vapor explosion 15 litres 20(1.0MPs)air A 7 Fouring acde, Vapor explosion 15 litres 20(1.0MPs)air A 7 Fouring acde, Vapor explosion 15 litres 20(1.0MPs)air A 7 Fouring acde, Vapor explosion 15 litres 20(1.0MPs)air A 7 Fouring acde, Vapor explosion 15 litres 20(1.0MPs)air A 7 Fouring acde, Vapor explosion 15 litres 20(1.0MPs)air A Fouring access 2	1200 1000 1200 950-1000	-	•	6.75	Pouring mode, Long term vaporization but no vapor explosion	
1000 15 litres 90(0.1MPalair A 0.3 500ming ande, Vapor explosion 15 litres 90(0.1MPalair A 0.3-2.5 500mersion ande, Morapor explosion 11 11 11 11 11 11 11	1200		•		Submersion mode, No vapor explosion	: 7
1200 15 litres 2011.0MP2Jair A Submersion ande, No vapor explosion Four interaction Four inter	1200		œ	0.3	Fouring mode, Vapor explosion	; -
130 11 11 11 11 12 12 13 13	050-1000		æ		Submersion mode, No vapor explosion	4
1200 15 little 2 0001.0P2air	1201-001		₹	2.3-2.5	Pouring mode, Long term vaporization but explosive interaction	-
1200 15 litres 9010.1RPalair	1200		≪		Submersion mode, No vapor explosion	-
11 11 11 12 13 14 15 14 15 14 15 15 15	1200		•		Pouring mode, Vapor explosion	<u> </u>
15 11 tes 90 (0.1 Plazist A 20 uring mode, Vapor explosion Henry et 11 tes 90 (0.1 Plazist A 20 uring mode, Vapor explosion Henry et 12 11 tes 90 (0.1 Plazist A 20 uring mode, Vapor explosion Henry et 12 11 tes 90 (0.1 Plazist A 20 uring mode, Vapor explosion Henry et 12 Henry et 13 uring mode, Vapor explosion Henry et 14 uring mode, Vapor explosion Henry et 14 uring mode, Vapor explosion Henry et 15 uring mode, Vapor explosion Henry et Henry et 15 uring mode, Vapor explosion Henry et Henry et 15 uring mode, Vapor explosion Henry et Henry et 15 uring mode, Vapor explosion 15 uring mode, Vapor e	950-1000	-	æ		Submersion, 5 experiments (1 vapor explosion, 3 water ejections)	
1200 15 litres 9000.HPAJair A Submersion, No vapor explosion 850-1200 15 litres 20,50,90 air A Spontameously friggered exp 5, No explosive interactions at elevated system pressure (Pamb.)0.3 NF21 Henry et 850-1200 15 litres 9000.HPAJair A 4.0-4.2 Pouring mode, Vapor explosion but explosive interaction Henry et Pouring mode, Long term vaporization but explosive interaction Henry et Pouring mode, Long term vaporization but explosion Henry et Pouring mode, Long term vaporization but explosion Henry et Pouring mode, Vapor explosion Henry et Henry et Pouring mode, No vapor explosion Henry et Henry et Henry et Henry et Henry et Pouring mode, No vapor explosion Henry et Henry	820		4		Pouring mode, Vapor explosion	
Signature States 20,090 air	1200		∢		Submersion, No vapor explosion	
1000 15 litres 20(0.18Palair A 0.7 Pouring andle Long tera vaporization but explosive interaction Henry et	850-1200		•		Spontaneously triggered exp's, No explosive interactions at elevated system pressure (Pamb)0,3 MPa)	-
15 litres 9010.HPAJAIR	0001		Œ	0.7	Pouring mode, Long term vaporization but explosive interaction	
970-1000 15 litres 904.0MPalair A 4.0-4.2 Pouring ande, Long term vaporization but explosive interaction Henry et l'200 15 litres 900.1MPalair A Fouring ande, Verportagnion Henry et l'Anni	950	•	€		Pouring mode, Vapor explosion	
1200 15 litres 9 CHO.SMPalair A Pouring acode, 4 experiments, No vapor explosion Henry et Fouring acode, 16 vapor explosion Henry et H	920-1000	_	व	4.0-4.2	Pouring made, Long term vaporization but explosive interaction	i =
1200 15 1/tres 9040.5MPa)air A Pouring mode, No vapor explosion Henry et BSO 15 1/tres 5040.1MPa)air A 0.7 Fouring mode, Vapor explosion Henry et BSO 15 1/tres 9040.5MPa)air A Pouring mode, No vapor explosion Henry et Henry et Pouring mode, No vapor explosion	1200		æ		Pouring mode, 4 experiments, No vapor explosion	; -
850 15 litres 50/0.1MPlair A 0.7 Fouring mode, Vapor explosion 850 15 litres 90/0.5MPlair A Pouring mode, No vapor explosion	1200	-	æ		Pauring mode, No vapor explosion	
850 15 litres 90:0.5MPalair A Pouring mode, No vapor explosion	920		Œ	0.7	Fouring mode, Vapor explosion	
	820	_	Œ		Pouring node, No vapor explosion	

6	950					90		TO SECURITY OF THE PROPERTY OF	
2.0 kg	1200		111		. 4	1.0-1.63		forced dropping mode. 3 experiments. No vapor explosion	Henry et al. 1979
2.0 kg	820		ä		⋖			Pouring mode, No vapor explosion	
120 9	1730	٠.	-	impact	æ	23	400	Channel blockage by molten debris	
120 9	1730	353	J12		æ	0.17	200	No fragmentation occurred and no significant pressure	Kottowski 1979
120	1730	293(0.6MP2	~	impact	æ	80			Kottomski 1979
120 g	1730	35312.6HPa	=	1 apact	æ	81			Kottomski 1979
120 9	1730	35310.6HP.	~	Lapact	æ	5	j	is 91 g of the melt participated to the interaction	Kottowski 1979
150 4	0061	293(2,6HP.	=	impact	8	22	ö		
120 9	1730	293(2,6MP.	-	impact	æ	52	65 2.		kottomski 1979
120 g	1730	493(2,6MP)	~	1 apact	œ	-	2.		Kattemski 1979
120	1730	293	air		-	٥.4	70	Shock-tube exp't, No significant reaction	Kottowski 1979
150 g	2100	293(2,6MP,	2	1mpact	æ	S	9		Kottowski 1979
7 10	790	0.013 cu.m 6	air.		aı	2		Very violent and high pressure, Propagation velocity (410-550 a/s) Strong steel vessel	Fry, Robinson
5 4.9	820	0.024 Cu. n 28	air		e n	=		Coherent propagation, Contents of the vessel wereds expelled	Fry, Robinson 1980
10 kg	800	23	Į		20	21		Plate like structure debris, Propagation velocity (267-279 m/s)	Fry, Robinson
S kg	B07	0.024 cu.m 24	zir.		æ	2		Non-transparent wall (No thermal interaction fila)	Fry, Robinson
10 kg	8 04	0.028 cu.# 85	317		æ	~		Coherent propagation through the eixture	Fry, Rubinson
22 49	730-780	3-32	31,		6 0			Hammer impact for triggering (impact energy≃ 186 J), final particle radious=2.1 mm	Hess et al.
5-18 kg	727-1054	.0135 cu. a 13-25	Į.	H=.3338 m	æ				Leanon
puad		16.8 cu.s	, ii		æ	0.81	1.E.=B. 3-		Koopsan et al. 1981
puod		10.8 cu.a	ä		æ	-	1.5.=34.5		Koopman et al. 1981
puod		6.6 cu.m	Ę		œ	3.51	1.6.=20.9		
puod		20.5 cu.m	Ę		œ	1:13	1.E.=1.4-		Koopman et al. 1981
puod		22.3 cu.a	į		. 5 0	1.2	1, 8, =0.9-		
poud		16.8 cu.m	air.		æ	0.72	1.8.=0.6-		1
pood		14.1 cu.n	A1F		•	0.12	1.E.=1.B-		
boud		13.2 cu.m	i.		-	0.63	1. E. =0.4-		Foopsan et al. 1981
pood		2.8 cu.∎	Ę		-	1.62	1, £.=19		Koopaan et al. 1981
puod		2.0 cu.	air			0.72	1.E.=0.7	Mass of LNG in the interaction zone ≈ 390 kg	Koopsan et al. 1981
puod		2.2 cu.a	٦		œ	6.6	1.E.=13.9	1.2 Hass of LNG in the interaction zone = 36-426 kg	Koopsen et al. 1981
2 Kg	900-1200	20 litres 90	air.		æ			Vapor explosions can be initiated by external trigger at the elevated system pressure tout Pamb	_
1.8 kg	1200	0.0068cu. 47,92	air.		æ			Na triggering, Explasion when Tc=47C	_
	2.0 kg 2.		850 15 littres 50(1,00%2 1200 1187 1200 15 littres 50(1,00%2 1730 1730 1730 1730 1730 1730 1730 1730	850 15 litres 50(1.00Pala 850 15 litres 20(0.1MPala 850 15 litres 20(0.1MPala 1730 29(0.5MPala 1730 29(0.5MPala 1730 29(0.5MPala 1730 29(0.5MPala 1730 29(2.6MPala 1730 29(2.6MPala 1730 29(2.6MPala 1730 29(2.6MPala 1730 0.024 cu.a 29 800 0.015 cu.a 6 800 0.024 cu.a 28 800 0.025 cu.a 24 801 0.024 cu.a 28 802 0.025 cu.a 24 804 0.026 cu.a 15 10.8 cu.a 6 6.6 cu.a 15 10.9 cu.a 6 10.9 cu.a 24 80.5 cu.a 13-25 120.6 cu.a 14.1 cu.a 17.0 cu	1200 111tres 2010.100maint 1730 15 11tres 2010.5062air 1730 2331.2.606ai 1840 1950 1850 1950 1850 1950 1950 1950 1950	850 15 litres 200 (JuPalair 1200 231 (Jupalair 231 (Jupa	1300 13 11 11 12 20 13 11 11 12 13 13 13 14 14 15 15 15 15 15 15	1300 15 11 11 12 12 13 13 14 14 14 15 15 15 15 15	1.00 1.11 1.11 1.00

Chamber Latti, Pagi 98 Chamber Latti, Pagi 96 NGRae 198	2 2	841	861	861	961	2 2	20	2 2	900	2 2	2 2	25.	2	2 2	001	pencer et al. 198
Chamberla Chamberla ith McRae	Bird	Bird	Bird	Bird	Bird	Fire	1.5	2		7		McRae of al	Control in parts	material section	Capacac at 1 100	Spencer
No triggering, Mo explosion No explosion without triggering, but explosion with triggering 19 experiments Chamb Coyote serves, 18 ever 15s, 18st 11 conditions and pond temp. Arraitions five types of MPI delayed or early MCRee	Fraction of melt mixed (80.01)	Fraction of melt mixed (13.07)	250 littes cover gas, Fraction of melt mixed (19.92)	Fraction of melt mixed (75.0%), Efficiency independent of the mass of participating melt	Fraction of melt mixed (20.42)	85 Litres cover gas, Fraction of melt mixed (12.5%)	Fraction of melt mixed (3.92)	Fraction of melt mixed (13.5%). Efficiency increase with derreasing water subraction	Fraction of melt mixed (9.03)	Fraction of welt aixed (13,1%)	Fraction of melt mixed (48.2%)	Spill plate below the pipe exit. 8 out of 26 spills produced RPT sir black enuvalent on to 5 sto last	Restricted release mode. Efficiency decrease with increasing submonling Starlar results with HEXAMAGE CONTINUES.	Effi. =0.02-0.06 Free release mode. Rapid bydyssen generation. Frionered interactions 5 more manner.	Corius dropped and water injected on Corius. Alansi no framentation 4 o H2 nemeration	Corium ejection into water, Extensive fragmentation, 18 g H2 generation
	Eff.=1.1	Eff.=3.2	Eff. = 2.3	Eff.=3.0	Eff.=2.8	£46.=1.6		£+f.=4.3		E+f.=3.1	Eff.=2.8		Eff1, =0, 1-0.5	Effi.=0.02-0.08		
															0.23	0.35
an an an an	ھت	.	a	æ	æ	œ.	.20		æ	æ	200	œ,	*	20	æ	au
															_	16 @/5
0.0068cu.m 47 air 0.0068cu.m 10-100 air 5-23 cu.m air 25-40 cu.m air	şeç	5e6	945	MPa) gas	gas	gas	4MPa) yas	945	MPa) gas	945	SKPa)gas	Į.	0 Ar	0. SMPAr	¥	K 2
cu.a 47 cu.a 10-10 u.a cu.a	09	19	8	130	78	99	55(0.	0	130	=	9010.	_	12-10	2-10	66 6	66
1105 810-1200 10-30 > 17	3300	3300	336	3300	3300	3300	3300	3300	3300	3300	3300		2700	2700	2800	2800
4.8 kg 3 kg pond	B kg	24 kg	24 kg	24 kg	24 19	24 kg	24 kg	24 kg	9 kg	24 kg	24 14	pund	0.5 kg	0.5 Kg	2.19 kg	1.94 kg
Cu/Nater Al/Nater Nater/LN6 Jater/LN6	UOZ/Water	U02/Water	U02/Water	UGZ/Water	UO2/Water	U02/Hater	U02/Water	U02/Water	UO2/Water	UO2/Water	UO2/Water	Hater/LN6	Cortus/Nater	Cor sua/Water	Cortue/Water	Corsum/Nater

APPENDIX C. SUMMARY OF COMMENTS ON MAJOR STEAM EXPLOSION PHENOMENA

During the meeting of the Steam Explosion Review Group (SERG), some of the fundamental mechanisms involved in the explosion were discussed. The conclusions of the discussions follow.

The discussions on the fundamental processes were divided into three general categories: (1) initial conditions for the explosion, (2) fuel-coolant mixing and conversion ratio, and (3) slug dynamics. In each area the SERG came to some agreements and identified some areas of differences of opinion. Each category is summarized below.

Initial Conditions

- a) High pressure core-melt sequences may be avoided due to local heating of structure in the upper regions of the reactor pressure vessel (RPV) which may lead to leak before rupture (this same phenomenon may weaken the upper head structure and this possibility, although deemed remote, should be checked).
- b) The amount of the core that is molten at the time of contact between the fuel and coolant is still uncertain -- some consider that the fuel will melt incoherently and drip into the lower plenum in small masses while others conceive of the meltdown process as more coherent resulting in a large molten pool (> 100% molten) before the fuel pours into the lower plenum (see Fig. C.1).

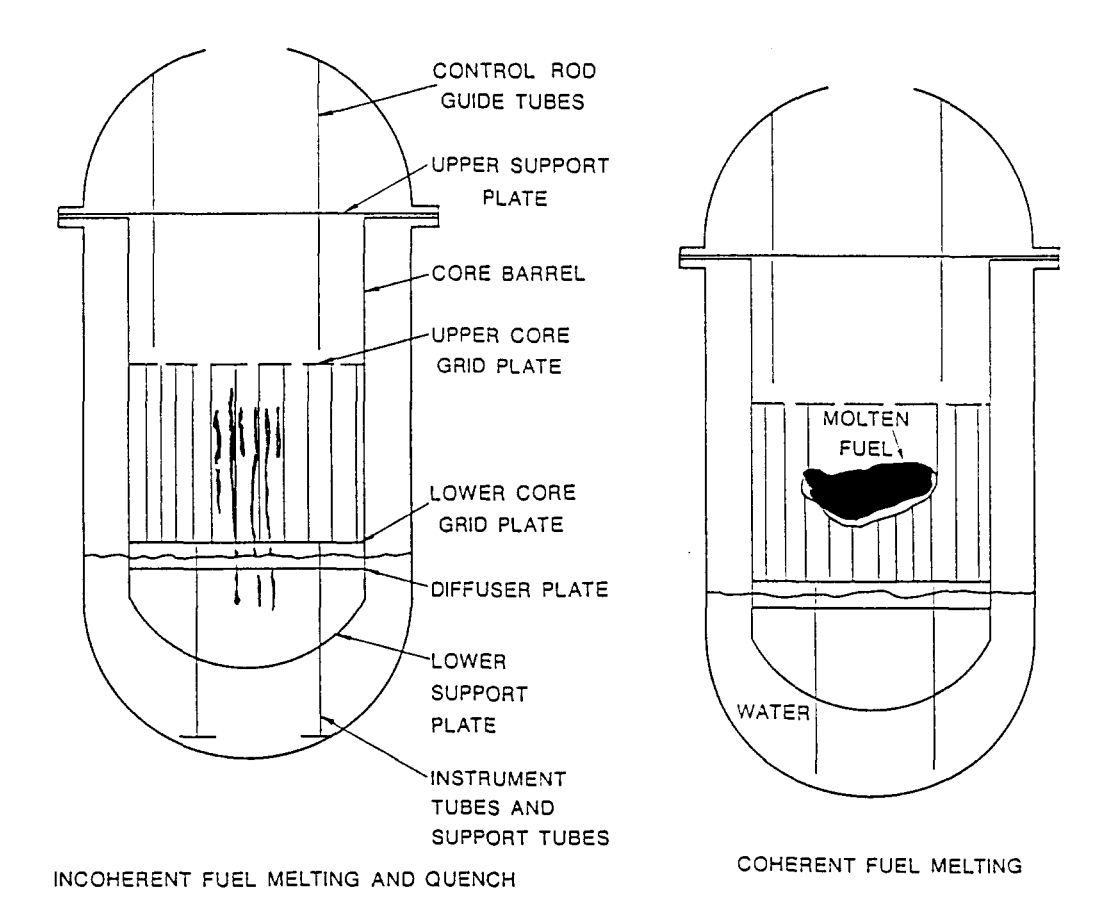
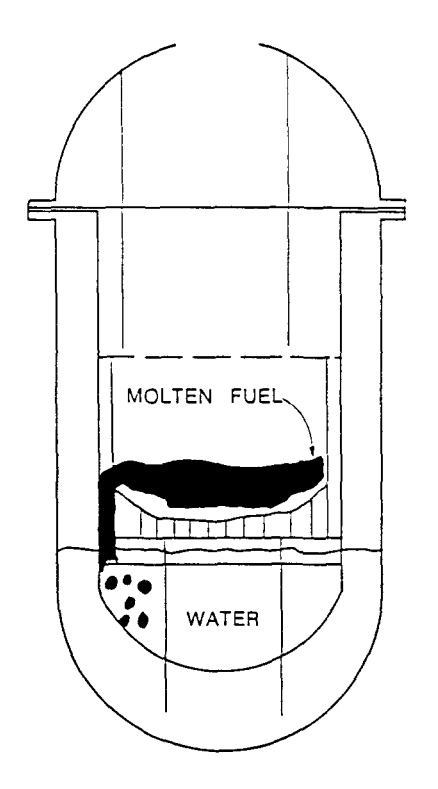
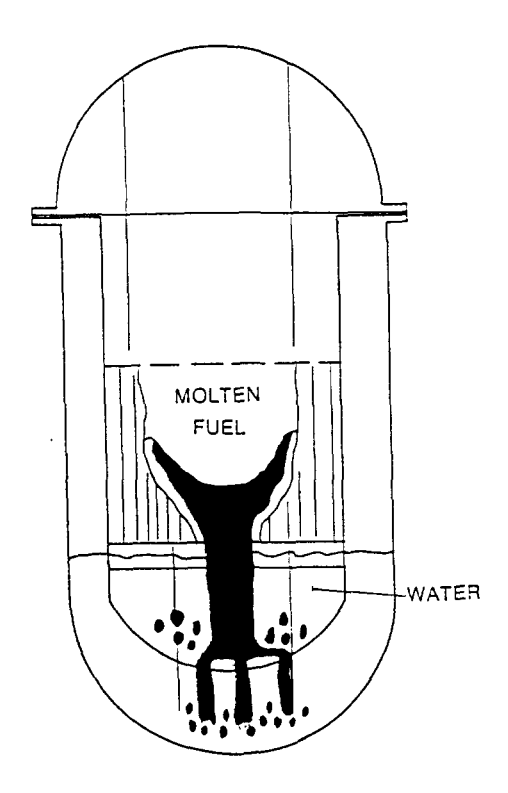


Fig. C.1

c) The temperature of the fuel and its composition at the time of fuel-coolant contact is also uncertain although linked to the possible scenarios in (b) above -- if the meltdown is incoherent, then the probable melt temperature will be between the solidus and liquidus of the melt (U-Zr-O), while if the meltdown is coherent the probable melt temperature will be above the liquidus of the melt (UO $_2$ -ZrO $_2$ -Zr).

d) The size and location of the melt pour stream into the remaining water in the lower plenum of the RPV is also in doubt (see Fig. C.2) -- the pour stream may be centered in the lower





FUEL POURING NEAR EDGE OF CORE

FUEL POURING THROUGH STRUCTURE

Fig. C.2

grid plate or off to the side and may be aided in breakup by the lower internal structure (the lower internal structure may also aid in early triggering of the explosion; neither option has been systematically tested to date).

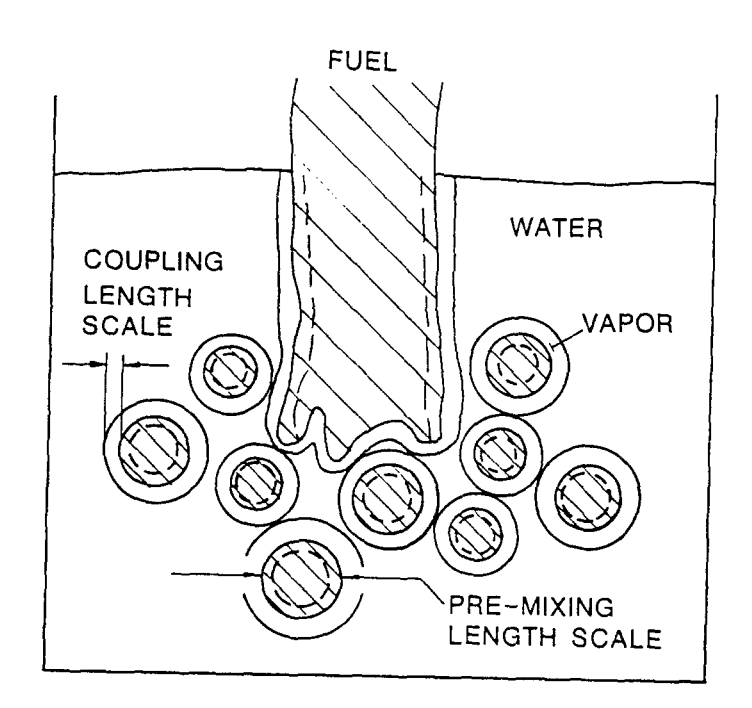
e) The SERG agreed that core meltdown calculations on melt progression in its current state should be viewed with some critical skepticism, and each calculation in its current state should be internally consistent and compared to other consistent sets of calculations.

Fueling Cooling Mixing/Conversion Ratio

- a) In order to aid in understanding of this concept a premixing length scale was defined to be that physical dimension which is determined by the hydrodynamics before the explosion and in turn determines the available exposed surface area of the melt available for interaction with the coolant (see Fig. C.3).
- with the coolant (see Fig. C.3).

 b) The "coupling length scale" was defined as that physical dimension which is determined by the explosion shock wave propagation itself and specifies the depth of melt at the exposed surface area that is rapidly fragmented and quenched -- i.e. the actual mass of melt that "participates" in the explosion (the SERG noted that the subsequent "blast wave" expansion of the explosion could also cause subsequent fragmentation of the fuel but some members felt

- that the rate of this fragmentation was too slow and the size of fragments too large to contribute to the explosion yield).
- c) These concepts were discussed at length and no consensus was reached on how these quantities could be calculated a priori at this time, although some members of the group felt that they could quantitatively bound their values.
- d) Flooding and/or fluidization limits on fuel-coolant mixing and the subsequent explosion seemed to be valid concepts in principle although some members of the SERG had some difficulties with specific models and/or predictions that had been advanced.
- e) Transient jet breakup due to entry hydrodynamics also seemed to be a relevant concept when considering mixing and the explosion, although not all the details of current models have been experimentally examined.



CONCEPTUAL PICTURE OF FUEL-COOLANT MIXING

Fig. C.3

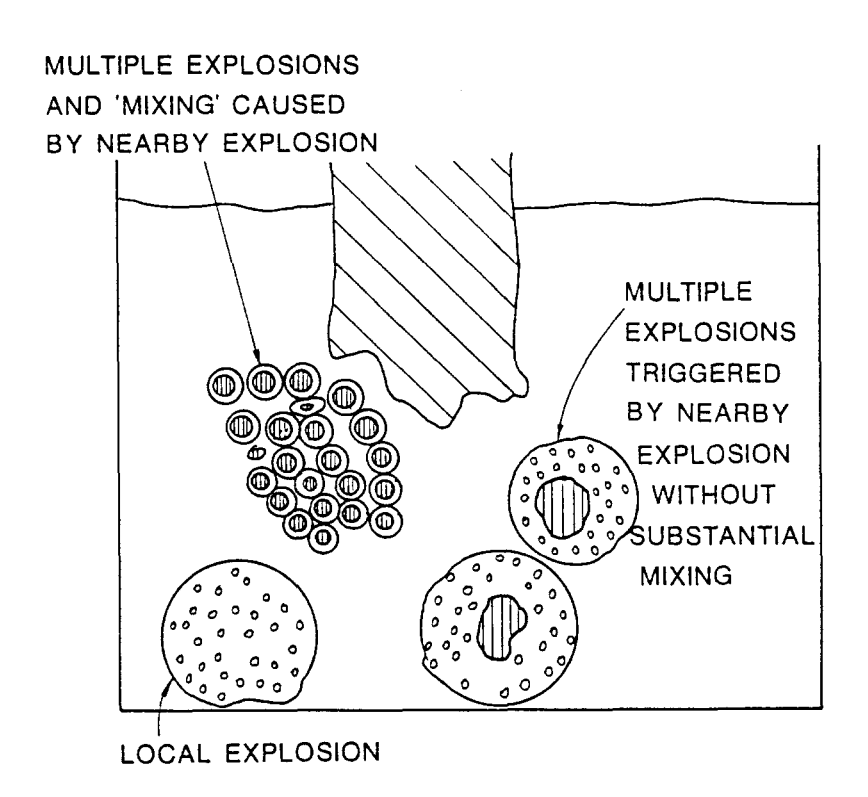
f) Multiple explosions can occur as evidenced by the FITSB experiments at SNL; however, there does not seem to be a consensus on the ramifications of such phenomena in the full scale accident situation -- some members consider multiple explosions to be a concern because one explosion may cause rapid mixing of nearby "unmixed" melt and thereby increase the melt involved, while others consider one explosion to be the trigger of a second explosion of a nearby melt mass and the propagation of the second explosion to be fast enough to "decouple" its fragmentation from the blast wave of the first event (see Fig. C.4).

Slug Dynamics

a) The formation of a slug that transmits the explosion energy to the upper head in the form of slug kinetic energy may take on different compositions -- e.g., a water slug may be formed

in the downcomer region of the RPV while a fuel slug may be formed in the core region (see Fig. C.5). One should consider that these possibilities need not be mutually exclusive depending on the time of the explosion trigger).

- b) Taylor instabilities would be formed at the boundary between the slug and the explosion zone (as originally noted in WASH-1400), and this phenomena would affect the expansion in two ways -- first, the slug would begin to break up and its final kinetic energy would be limited by this process, and second, the liquid from the slug breakup would be entrained into the explosion zone causing energy transfer with it (a cooldown of the explosion zone would occur if coolant is entrained; conversely a heatup of the explosion zone would occur if melt were entrained).
- c) Slug dynamics would be affected by the possible failure of the lower plenum wall of the RPV due to the locally high explosion pressures -- this would reduce the upward slug kinetic energy and has been included in past analyses (Corradini et al., 1981; Berman et al., 1984).
- d) Slug impact with the upper internal structure and the upper support plate in the RPV would absorb some of the kinetic energy of the slug -- Sandia (Berman, 1984) and recent Los Alamos (SERG, 1985) estimates of this energy absorption capability both seem to agree on the upper bound values and this also has been included in the past analyses.



CONCEPTUAL PICTURE OF MULTIPLE EXPLOSIONS

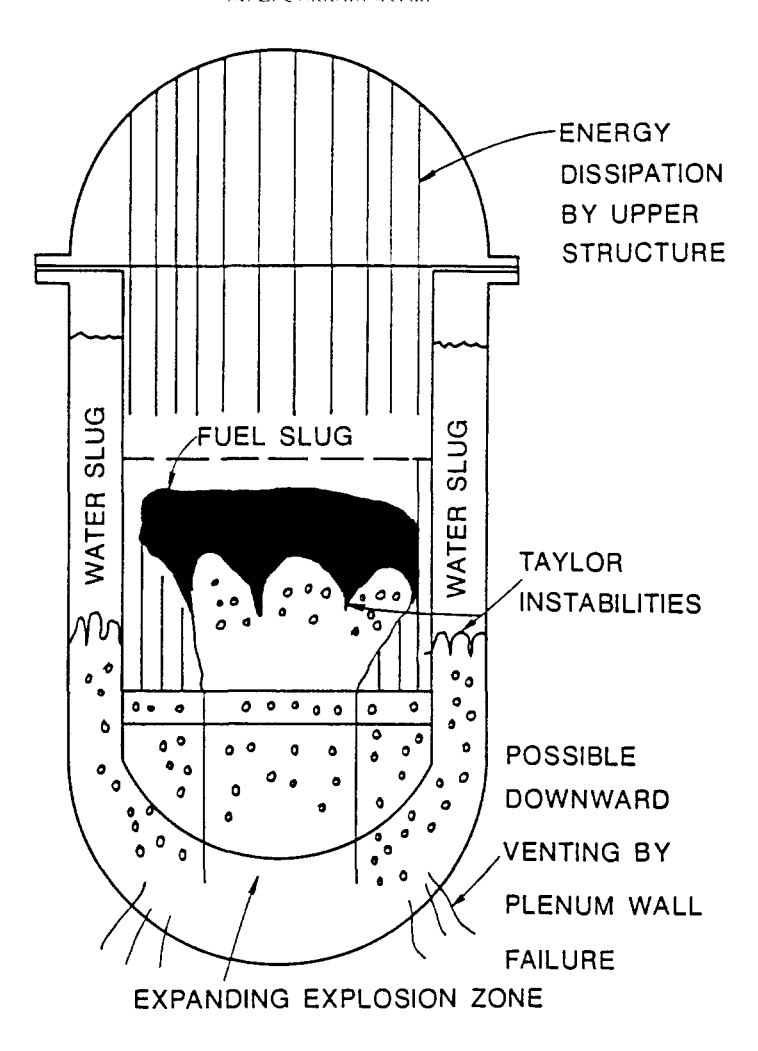


FIGURE C.5 SLUG DYNAMICS PHYSICAL PROCESSES

REFERENCES

Abbey M. J., Asher R. C. and Bradshaw L (1976) The Injection of Sodium into Liquid Stainless Steel: A Report of the Second experiments NA-SS/1, AERE M2771.

Amblard M., Costa J., Syrmalenios P. (1973) Recent JEF and CORRECT 1 Sodium/Fuel Interaction Results. Second Specialist Meeting on Sodium/Fuel Interaction in Fast Reactor, Ispra, Italy,

Amblard P. Syrmalenious, (1972) <u>Les Interactions Combustible - Refrigerant, Etudes Experimentales et Theorique Appliques au cas des Reacteurs a Neutron Rapides Karlsruhe</u>

Amblard M., Costa J., Fabrega S., Lackme C., Syrmalenious P. (1974) Out-of-Pile Studies in France on Sodium-Fuel Interactions $\underline{\sf ANS}$ Safety Research Meeting, LA.

Amblard M. (1976) Preliminary Results on a Contact Between 4 kg $\rm UO_2$ and Liquid Sodium PNC N251 76-12, pp. 545-560.

Amsden A., Ruppel H. M., Hirt C.W. (1976) SALE: A Simplified ALE Computer Program for Fluid Flow at All Speeds Los Alamos Scientific Laboratory Report No. LA-8095.

Anderson R. P., Armstrong D. R (1972) Laboratory Tests of Molten Fuel Coolant Interactions Trans. Am. Nuc. Soc. Vol 15, pp 313-314.

Anderson R. P., Armstrong D. R. (1974) Comparison Between Vapor Explosions Models and Recent Experimental Results AIChE Symposium Series Vol. 70, No. 138, pp. 31-47.

Anderson R. P., Armstrong D. R. (1977) R-22 Vapor Explosions, <u>Annual ASME Winter Mt.: Nuclear</u> Reactor Safety Heat <u>Transfer Section</u>, pp 31-45. Atlanta, GA, Nov. 29 - Dec. 2.

Anderson R. P., Bova, L. (1971) Experimental Investigation of Vapor Explosions in a Molten Salt-Water System. Trans. ANS. Vol. 14 pp. 236.

Anderson R. P., Bova L. (1976) Final Report on the Small-Scale Vapor Explosion Experiments with NaCl- H_2O System. ANL 76-57.

Ando M. (1980) Triggered Fragmentation Experiment at KFK. <u>CSNI Joint Interpretation on</u> Selected FCI Experiments Karlsruhe.

Ando M., Caldarola L. (1982) Triggered Fragmentation Experiments at Karlsruhe. <u>Proceedings of Information Exchange Meeting on Post Accident Debris Cooling Karlsruhe</u>.

Antonakas M. D. (1973) Modele d'Intervation Sodium/Combustible et Application aux Exercises. Proposes par le Crest May.

Apfel R. E. (1971) A Novel Technique for Measuring the Strength of Liquids. J. Acoust. Soc. Am 49(1): part 2, 145.

Arakeri et al. (1975) An Experimental Study on the Thermal Interactions for Molten Tin Dropped into Water. $\underline{\text{UCLA-ENG-7592}}$ (Dec.).

Armstrong D. R. (1970a) Violent Boiling with Molten Fuel and Sodium. ANL-7669

Armstrong D. R. (1970b) Violent Boiling with Molten Fuel and Sodium. ANL-7688.

Armstrong D. R. (1970c) Violent Boiling with Molten Fuel and Sodium. ANL-7705.

Armstrong D. R. (1970d) Out-of-Pile Contacting Studies. ANL-7742.

Armstrong D. R. (1971) Laboratory Experiments on Mechanisms of Fragmentation and Pressure Generation. $\underline{\text{ANL-7887}}$ pp 8.14.

Armstrong D. R. (1972) Laboratory Experiments on Mechanisms of Fragmentation and Pressure Generation. $\underline{\text{ANL-RDP-2}}$ pp 8.31.

Armstrong D. R., Testa F. J. and Raridin D. C. (1971) Interaction of NA with Molten $\rm UO_2$ and Stainless Steel Using a Dropping Mode of Contact. ANL-7890.

Armstrong D. R. et al. (1976) Explosive Interaction of Molten UO_2 and Liquid Sodium. ANL 76-24 (March).

Armstrong D. R. and Anderson R. P. (1976) ANL-RDP 49.

Asher R. C., Bradshaw L., Collett R and Davies D. (1976a) Experimental Work at Harwell on the Injection of Sodium into Liquid Steel. $\underline{\mathsf{AERE}}$ M2770 (Feb.).

Asher R. C., Bullen D. and Davies D. (1776b) Vapor Explosions (Fuel Coolant Interactions) Resulting From the Sub-Surface Injection of Water into Molten Metal: Preliminary Results. <u>AERE M2772</u> (March).

Asher R. C. et al. (1979) The Injection of Liquid Sodium into Stainless Steel: A Report of Further NaSS/4, NaSS/5 and NaSS/6. Fourth CSNI Spec. Mtg. on FCI in Nuclear Reactor Safety, Bournemouth, UK, (April).

Baines M., Board S. J., Buttery N. E. and Hall R. W. (1980) The Hydrodynamics of Large-Scale Fuel-Coolant Interactions. <u>Nuclear Technology</u>, Vol. 49 pp. 27-39. (June).

- Bankoff S. G. and Mikesell R. D. (1959) Bubble Growth Rates in Highly Subcooled Nucleate Boiling. Chem. Eng. Prog. Symp, Series No. 29, pp 95-102.
- Bankoff S. G. and Fauske H. K. (1974) On the Mechanism for Vapor Explosions. <u>Nucl. Sci. Engr.</u> 54, pp. 481-482.
- Bankoff S. G., Jo, J. H. and Ganguli, A. (1976) Mechanisms of Vapor Explosions. CONF-751001, Vol. IV, 1833-1842. Proc. Int. Mtg. on Fast Reactor Safety and Related Physics. Chicago, IL. (5-8 Oct.).
- Bankoff, S. G. and Habib A. (1984) The Application of a User-Friendly Code to Nuclear Thermal Hydraulic Reactor Safety Problems. Nuclear Power Plant Thermal Hydraulics and Operations Topical Meeting, Taipei, Taiwan (Oct.).
- Bankoff S. G. and Han S. H. (1984) An Unsteady One-Dimensional Two-Fluid Model for Fuel-Coolant Mixing in an LWR Meltdown Accident. <u>U.S.-Japan Seminar on Two-Phase Dynamics</u>, Lake Placid, N. Y., (Aug.).
- Beer H. (1969) Heat Transfer in Boiling. Progress of Heat and Mass Transfer 2.
- Berman M. LWR Safety Quarterly. SAND80-1304, Sandia National Laboratories (Jan.-Mar., Apr.-June, July-Sept., Oct.-Dec. 1980); see also SAND81-1216 (Jan.-Mar. 1981); SAND82-0006 (Apr.-Sept. 1981); SAND82-1572 (Oct. 1981-Mar. 1982); (Apr-Sept. 1982); SAND83-1576 (1983); SAND84-1072 (1984); SAND85-1606 (1985).
- Berman M., Swenson D. V. and Wickett A. J. (1984) An Uncertainty Study of PWR Steam Explosions. SAND83-1438, NUREG/CR-3309 (May).
- Bernath L. (1951) Theory of Bubble Formation in Liquids. Ind. Eng. Chem. Vol 44 pp 1310-1313.
- Benz R., Froehlich G. and Unger, U. (1977) Steam-Bubble Collapse Model (SBC Model) to Describe the Course of Fragmentation of Hot, Liquid Melts in Water. <u>ATKEA</u>, Atomkernenergie, Vol. 29, pp 261-265.
- Benz R et al. (1979) Melt Water Interactions in Tank Geometry: Experimental and Theoretical Results. Fourth CSNI Spec. Mtg. on FCI in Nucleal Reactor Safety, Bournemouth, (2-5 April).
- Benz R. and Schriewer J. (1980) Fragmentation of Liquid Drops in Shock Waves, Report Number IKE 2-42, Institute for Nuclear Energy and Energy Systems, University of Stuttgart.
- Bergman S. G. A. and Laufke H. (1979) Recovery Boiler Explosions, The Swedish Steam Users Association, SPC1-Report No. 35.
- Berthoud G. and Scott E. (1979) Multiphase Thermal Detonation for a UO₂-Na system. Fourth CSNI Spec. Mtg. on FCI in Nuclear Reactor Safety, CSNI Report No. 37, Vol. 1, pp. 22-53.
- Bird M. J. and Millington R. A. (1979) Fuel-Coolant Interaction Studies with Water and Thermite Generated Molten Uranium Dioxide. 4th CSNi Spec. Mtg. on FCI in Nuclear Reactor Safety, Bournemouth, UK, (April).
- Bird M. J. (1984) An Experimental Study of Scaling in Core Melt/Water Interactions. PWR/SAWG/P(84)71, <u>22nd National Heat Transfer Conference</u> Niagara Falls, (5-8 August).
- Bjorkquist G. M. (1975) An Experimental Investigation of Fragmentation of Molten Metal in Water, Report No. 31-109-38-2831-4 TR, MIT.
- Bjornard T. A. (1974) An Experimental Investigation of Acoustic Cavitation as a Fragmentation Mechanism of Molten Tin Droplet in Water, Report No. 31-109-38-2831-3, MIT, MITNE-163.
- Bjornard T. A., Rohensow, W. M. and Todreas, N. E. (1974) The Pressure Behavior Accompanying the Fragmentation of Tin in Water. <u>Trans. Am. Nuc. Soc.</u>, Vol. 19, pp. 247-249.
- Board S. J. (1974) A Mechanism for UO₂/Sodium Thermal Interactions. Nucl. Sci. Engr. Vol. 54, No. 2 233.
- Board S. J., Clare, A. J., Duffey, R. B., Hall, R. S., and Poole, D. H. (1971) An Experimental Study of Energy Transfer Processes Relevant to Thermal Explosions. <u>Int. J. Heat Heat Transfer, Vol. 14</u> pp. 1631-1641.

- Board S. J., Duffey R. B., Farmer C. L. and Poole D. H. (1973) The Analysis of Metal-Water Explosions. Nucl. Sci. Eng. 52, pp. 433-438.
- Board S. J., Farmer C. L. and Poole D.H. (1974) Fragmentation in Thermal Explosions. <u>Int. J.</u> Heat Mass Transfer, Vol. 17, pp. 331-339.
- Board S. J. and Hall R. W. (1973) An Explosion Propagation Mechanism. <u>2nd CREST Spec. Mtg. on</u> SFI in Fast Reactors, EUR 5309, Ispra (Nov.).
- Board S. J. and Hall R. W. (1974a) <u>Propagation of Thermal Explosions. 1 Tin/Water</u> Experiments, CEGB Report RD/B/N 2350.
- Board S. J. and Hall R. W. (1974b) <u>Propagation of Thermal Explosions. 2 Theoretical Model</u>, CEGB Report RD/B/N 3249.
- Board, S. J., Hall R. W. and Brown G. E. (1974c) The Role of Spontaneous Nucleation in Thermal Explosions: Freon/Water Experiments, CEGB Report No. RD/B/N 3007.
- Board, S. J., Hall R. W. and Hall R. S. (1975) Detonation of Fuel Coolant Explosions. <u>Nature</u>, Vol. 254, No. 5498, pp. 319-321 (March).
- Board, S. J. and Hall R. W. (1976) Recent Advances in Understanding Large-Scale Vapor Explosions. Third Specialist Meeting on Sodium Fuel Interactions, Tokyo, PNC N251, 76-12, pp. 249-233.
- Bohl W. R. (1982) A Calculational Advance in the Modelling of Fuel-Coolant-Interactions. Proc. of Int'l. ANS/ENS Safety Mtg., Lyon, France (July).
- Bohl W. R. (1986) An Investigation of Steam Explosion Loadings with SIMMER-II, Los Alamos Draft Report (June).
- Bohr N (1923) Zietscrift Physik, Vol. 13, p. 117.
- Borishanskii Z. M. (1956) Zhurn. Tekh. Fiz. Vol. 26, pp. 452; see alsoSov. Phys.-Technical Phys., Vol. 1, pp. 438.
- Bradley R. H. and Witte L. C. (1972) Explosive Interaction of Molten Metals Injected into Water. Nucl. Sci. Eng. Vol. 48, pp 387-396.
- Brauer F. E., Green N. W. and Mesler, R.B. (1968) Metal/Water Explosions. Nucl. Sci. Eng., Vol. 31, pp. 551-554.
- Breton J. P. and Antonakas D. (1976) Model for Fuel-Sodium Interaction Application to the JEF Experiments. \underline{PNC} N $\underline{251}$, 76-12, Vol. 1, pp. 785-817.
- Briggs, A. J. (1976) Experimental Studies of Thermal Interactions at AEE Winfrith. Third Spec. Mtg. on Sodium Fuel Interactions, Tokyo, Japan, PNC N251, 76-12, Vol. 1, pp. 75-96.
- Bruckner, U and Unger H. (1973) Analysis Physiklalischer Vorgange bei Thermodyamischen Mischreaktionen. Universitat Stuttgart, Institut für Kernenergetik, IKE-Bericht No. 6-69.
- Buchanan D. J. (1973) Penetration of Solid Layer by a Liquid Jet. <u>J. Phys. D: Appl. Phys.</u>, Vol. 6, pp. 1762-1771.
- Buchanan D. J. (1974) A Model for Fuel-Coolant Interactions. J. Phys. D: Appl. Phys. Vol. 7, pp. 1441-1457.
- Burger, M.,Carachalios C., Schwalbe W. and Unger H. (Feb. 1983)

 explosion mit Hilfe eines thermischen Detonationsmodells.

 Forschungsvorhaben BMFT 150 371, IKE 2TF-39, University of Stuttgart.
- Burgess, D. S. Murphy, J. N. and Zabetakes M. G. (Feb. 1970) <u>Hazards of LNG Spillage in Marine Transportation</u>. SRC Report No. S-4105, Bureau of Mines, Pittsburgh, PA.
- Burgess D. S., Biordi J., Murphy J. (1972) Hazards of Spillage of LNG into Water, U.S. Bureau of Mines, PMSRC Report No. 4177.

Buxton L. D. and Nelson L. S. (Aug. 1975) <u>Core-Meltdown Experimental Review</u>, SAND 74-0382, Sandia National Laboratories, Chapter 6.

Buxton L. D. and Nelson L. S. (1977) Impulse Initiated Gas Release - A Possible Trigger for Vapor Explosions, <u>Trans. Am. Nuc. Soc.</u> Vol. 26, pp. 398.

Buxton L. D. and Benedick W. B. (Nov. 1979) <u>Steam Explosion Efficiency Studies</u>, SAND79-1399, Sandia National Laboratory.

Buxton L. D. Benedick W. B. and Corradini M. L. (Oct. 1980) <u>Steam Explosion Efficiency Studies: Part II Corium Experiments</u>, NUREG/CR-1746, SAND80-1324, Sandia National Laboratory.

Caldarola L. (1972) A Theoretical Model for the Molten Fuel-Sodium Interaction in a Nuclear Fast Reactor. Nuclear Engineering and Design, 22, pp. 175-211.

Caldarola L and Kastenberg W. E. (1973) A Model for Fuel Fragmentation during Fuel/Coolant Thermal Interactions. I.A.S.R.-R.S.P. Notiz 47 Karlsruhe, West Germany, Nucl. Res. Center.

Caldarola L and Kastenberg W. E. (April 1974) On the Mechanism of Fragmentation during Molten Fuel/Coolant Thermal Interactions. <u>Proceedings of Fast Reactor Safety Meeting</u>, Beverly Hills, CA, pp. 937-954.

Caldarola L (1975) A Theoretical Model with Variable Masses for the Molten Fuel Sodium Interaction in a Fast Reactor. <u>Nucl. Eng. and Des. 34</u>, pp. 181-202.

Carachalios C., Burger M. and Unger H. (1983) A Transient Two-Phase Model to Describe Thermal Detonation based on Hydrodynamic Fragmentation.

Lambridge, Mass., USA, Aug. 28 - Sept. 1.

Carachalios C., Burger M and Unger H. (1985) Triggering and Escalation Behavior of Thermal Detonations. 23rd ASME/AICHE/ANS National Heat Transfer Conf., Denver, Colorado, 6-9 Aug.

Carslaw H. S. and Jaeger J. C. (1959) <u>Conduction of Heat in Solids</u>, 2nd Ed., Clarendon Press, Oxford.

Chamberlain A. T. and Page F. M. (Jan. 1983) An Experimental Examination of the Henry-Fauske Voiding Hypothesis, Dept. of Chemistry, Univ. of Aston, Birmingham.

Chapman D. L. (1889) Phil. Mag. 47, 90.

Cho D. H., Ivins R. O. and Wright R. W. (1971) Pressure Generation by Molten Fuel-Coolant Interactions Under LMFBR Accident Conditions. Proc. Conf., on New Development in Reactor Mathematics and Applications, USAEC Report No. CONF-710302, pp. 25-49.

Cho D. H., Ivins R. O. and Wright R. W. (March 1972) A Rate-Limited Model of Molten-Fuel/Coolant Interactions: Model Development and Preliminary Calculations. ANL-7919.

Cho D. H. and Gunther W. H. (1973) Fragmentation of Molten Materials Dropped into Water. Trans. Am. Nuc. Soc., Vol. 16, pp. 185-186.

Cho D. H., Chen W. L. and Wright R. W. (Aug. 1974) A Parametric Study of Pressure Generation and Sodium-Slug Energy From Molten-Fuel-Coolant Interactions, ANL-8105.

Cho D. H., Gunther W. H. and Armstrong D. R. (Dec. 1974) Fragmentation of Molten Materials Dropped into Water, ANL-8155.

Christiansen J. P. (1973) Numerical Solution of Hydrodynamics by the Method of Point Vortices. <u>J. Comp. Phys.</u>, Vol. 13, pp. 363-379.

Chu C. C. and Corradini M. L. (Nov. 1984) Hydrodynamic Fragmentation of Liquid Droplets. Trans. Amer. Nucl. Soc., Vol. 47, Washington, D. C.

Chu C. C. (May 1986) One-Dimensional Transient Fluid Model for Fuel-Coolant Interactions. Ph.D. Thesis, University of Wisconsin, UWRSR-30.

Chu C. C. and Corradini M. L. (Feb. 1986a) One-Dimensional Transient Model for Fuel-Coolant Fragmentation and Mixing. ANS/ENS Int'l. Thermal Reactor Safety.

Clerici C. et al. (1976) Interactions with Small and Large Sodium and $\rm UO_2$ Mass Ratios, PNC N251, pp. 507-543.

Coddington P (1979) Mechanical Energy Yields and Pressure Volume and Pressure Time Curves for Whole Core Fuel-Coolant Interaction. 4th CSNI Spec. Mtg. on FCI in Nuclear Reactor Safety, Bournemouth, UK, 2-5 April.

Coddington P. and Staniforth M. G. (1980) Calculations on Propagation Vapour Explosions Using the SIMMER Code and Their Relation to the Winfrith Thermir Experiments. <u>CSNI Mtg. on FCI Experiments</u>, Karlsruhe, 2-4 Dec.

Coffield R. D. and Wattelet P. L. (Nov. 1970) Analytical Evaluation of Fuel Failure Propagation for the Fast Flux Test Facility, Report of AEC Contract AT(45-1)-2171, Task Number 1, WARD, Hanford Engineering Laboratories.

Colgate S. A. and Sigurgeirsson T. (1973) Dynamic Mixing of Water and Lava. <u>Nature Vol. 244, pp. 552-555.</u>

Condiff D. W. (1982) Contributions Concerning Quasi-Steady Propagation of Thermal Detonations Through Dispersions of Hot Liquid Fuel in Colder Volatile Liquid Coolants. <u>Int. J. Heat Mass</u> Transfer, Vol. 25, No. 1, pp. 87-98.

Condiff D. W. (Oct. 1983) Thermal Detonation Modeling Analysis of FCI Vapor Explosions: A Critical Review, ANL/RAS 83-39.

Cooper F. and Dienes J. (1978) The Role of Rayleigh-Taylor Instabilities in Fuel-Coolant Interactions. Nuc. Sci. Engr., Vol. 68, pp. 308-321.

Corradini M. L. (1981) Phenomenological Modeling of the Triggering Phase of Small-Scale Steam Explosion Experiments. <u>J. Nuc. Sci. Engr.</u>, Vol. 78, pp. 154-167.

Corradini M. L. (1982) Proposed Model for Fuel-Coolant Mixing During a Core Melt Accident. Proc. Int. Mtg. Thermal Nuclear Reactor Safety, NUREG/EC-0027, Chicago, IL, Aug. 29 - Sept. 2.

Corradini M. L. and Moses G. A. (1983) A Dynamic Model for Fuel-Coolant Mixing. <u>Proc. Int. Mtg. Light Water Reactor Severe Accident Evaluation</u>, Cambridge, MA, Vol. 1, pp. 6.3, American Nuclear Society, Aug. 28 - Sept. 1.

Corradini M. L. and Moses M. L. (1985) Limits to Fuel/Coolant Mixing. <u>Jnl. Nuc. Sci. Engr.</u>, Vol. 90, pp. 19.

Corradini M. L. and Swenson D. V. (June 1981) Probability of Containment Failure Due to Steam Explosions Following a Postulated Core Meltdown in an LWR, Sandia National Laboratories Report, NUREG/CR-2214 or SAND80-2132.

Corradini M. L., Swenson D. V., Woodfin R. L. and Voelker E. L. (1981) An Analysis of Containment Failure by a Steam Explosion Following a Postulated Core Meltdown in a Light Water Reactor. Nuc. Engr. Design, Vol. 66, pp. 287.

Corradini M. L. and Todreas N. E. (1979) Prediction of Minimum UO₂ Particle Size Based on Thermal Stress Initiated Fracture Model. Nuc. Eng. Design, Vol. 53, pp. 105-116.

Corradini M. L. (1982) Analysis and Modelling of Large-Scale Steam Explosion Experiments. <u>Jnl. Nuc. Sci Engr. 82</u>, pp. 429-447.

Corradini M. L. and Oh M. D. et al. (April 1983) Analysis of Molten Fuel Coolant Interaction, UWRSR-9, University of Wisconsin - Madison.

Cronenberg A. W. (1972) A Thermodynamic Model for Molten $\rm UO_2$ -Na Interaction, Pertaining to Fast-Reactor Fuel-Failure Accidents. Appendix a, ANL-7947.

Cronenberg A. W. (1980) Recent Development in the Understanding of Energetic Molten Fuel-Coolant Interactions. <u>Nuclear Safety</u>, Vol. 21, No. 3, pp. 319-337.

Cronenberg A. W. and Benz R. (July 1978) Vapor Explosion Phenomena with Respect to Nuclear Reactor Safety Assessment. NUREG/CR-0245.

Cronenberg A. W., Chawlal T. C. and Fauske H. K. (1974) A Thermal Stress Mechanism for the Fragmentation of Molten UO₂ Upon Contact with Sodium Coolant. <u>Nuc. Eng. Design</u>, Vol. 30, pp. 443-453.

Cronenberg A. W. and Coats R. L. (1976) Solidification Phenomena for UO₂, UC, and UN Relative to Quenching in Sodium Coolant. Nuc. Eng. Design, Vol. 36, pp. 261-272.

Cronenberg A. W. and Fauske H. K. (1974) UO₂ Solidification Phenomena Associated with Rapid Cooling in Liquid Sodium. <u>J. Nuc. Materials</u>, Vol. 52, pp. 24-32.

Cronenberg A. W. and Grolmes M. A. (1974) A Review of Fragmentation Models Relative to Molten UO₂ Breakup When Quenched in Sodium Coolant. ASME Winter Annual Meeting, New York, 17-22 Nov.

Darby K., Pottinger R. C., Rees N.J.M. and Turner R. G. (1972) The Thermal Interactions between Water and Molten Aluminum under Impact Conditions in a Shock Tube. Proceedings of the International Conference on Engineering of Fast Reactor for Safe and Reliable Operation, Karlsruhe, pp. 898-915, 9-13 Oct.

Drescher H. P., Geiser H. and Markett J. (1976) Parametric Investigation of the Steam Explosion in Core-Meltdown Accidents. Atomwirtschaft, pp. 537-539.

Drumheller D. S. (1979) The Initiation of Mlet Fragmentation in Fuel Coolant Interactions. Nuc. Sci. Engr., Vol. 72, pp. 347-356.

Dullforce T. A. (1976) The Influence of Solid Boundaries in Inhibiting Spontaneously Triggering Small-Scale Fuel Coolant Interactions. CLM-P587, Culham Lab.

Dullforce T. A., Buchanan D. J. and Peckover R. S. (1976) Self-Triggering of Small-Scale Fuel-Coolant Interactions: I. Experiments. J. Phys. D: Appl. Phys., Vol. 9, pp. 1295-1303.

Emmons H. W., Chang C. T. and Watson B. C. (1960) Taylor Instabilities of Finite Surface Waves. J. Fluid Mech., Vol. 7, pp. 177-192.

Edwards A. R. (1967) Thermodynamic Limits on the Conversion of Heat to Mechanical Efficiency. FRPMC/RSWP/(67) 146.

Emmons H. W., Chang C. T. and Watson B. C. (1960) Taylor Instabilities of Finite Surface Waves. J. Fluid Mech., Vol. 7, pp. 177-192.

Enger T. and Hartman D. (Sept. 1972) Rapid Phase Transformation During LNG Spillage on Water-Proc. of the 3rd Conf. on Liquefied Natural Gas, Washington, D. C.

Epstein M. (1974) A New Look at the Cause of Thermal Fragmentation. <u>Trans. Am. Nuc. Soc.</u>, Vol. 19, pp. 249.

Epstein M. (1974) Thermal Fragmentation - A Gas Release Phenomena. Nuc. Sci. Engr., Vol 55, pp. 462-467.

Farahat M.M.K., Eggen D. T. and Armstrong D. R. (1974) Pool Boiling in Subcooled Sodium at Atmospheric Pressure. Nuc. Sci. Engr., Vol. 53, pp. 240-253.

Fasoli P. et al. (1973) Results of Thermal Interaction Tests for Various Materials Performed in the Ispra Tank Facility. <u>2nd Spec. Mtg. on Sodium/Fuel Interaction in Fast Reactors</u>, Ispra, Italy, 21-23 Nov.

Fauske H. K. (1973) On the Mechanism of Uranium Dioxide-Sodium Explosive Interactions. <u>Nuc. Sci. Engr.</u>, Vol. 51, pp. 95-101.

Fauske H. K. (1974) Some Aspects of Liquid-Liquids Heat Transfer and Explosive Boiling. Proc. of Fast Reactor Safety Mtg., 992-1005, Beverly Hills, CA, 2-4 Apr.

Fauske H. K. and Epstein M. (Aug 1985) Steam Film Instability and Mixing of Core Melt Jets and Water. ANS Thermal Hydraulic Div. Proc., ASME/AICHE National Heat Transfer Conference, Denver.

Feldbauer G. F. et al. (Nov. 24, 1972) Spills of LNG on Water-Vaporization and Downwind Drift of Combustible Mixtures, Esso Research and Eng. Company, Report EE61E-72.

- Fishlock T. P. (1975) A Computing Module for Molten Fuel/Coolant Interactions in Fast Reactor Sub-assemblies, Rep. R $\overline{1039}$.
- Fishlock T. P. (1979) Calculations on Propagation Vapour Explosions for the Aluminum/Water and UO₂/Sodium Systems. 4th CSNI Mtg. on FCI in Nuclear Reactor Safety, Bournemouth, UK, 2-4 Apr.
- Fletcher D. F. (May 1984) Modelling Transient Energy Release from Molten Fuel Coolant Interaction Debris. Winfrith, United Kindom Atomic Energy authority, AEEW-M2125.
- Fletcher D. F. (June 1984) Modelling the Transient Pressurization During a Molten Fuel Coolant Interaction. Winfrith, United Kindom Atomic Energy Authority, AEEW-M2126.
- Fletcher D. (1985a) A Review of Coarse Mixing Models, UKAEAS Culham Laboratory Report.
- Fletcher D. (1985b) (1985b) Assessment and Development of the Bankoff and Han Coarse Mixing Model, UKAEA Culham Laboratory Report.
- Flory K., Paoli R. and Mesler R. (1969) Molten Metal-Water Explosions. Chem. Eng. Progress, Vol. 65, No. 12, pp. 50-54.
- Flynn, H. G. (1964) Physics of Acoustic Cavitation in Liquids. Physical Acoustics, 1(b), New York: W. P. Mason, Academic Press.
- Fogg G. F. (1977) A Computer Code for the Numerical Solution of the Hick/Menzies Equations for a Fuel-Coolant Interaction, NST/77/21.
- Frohlich G., Muller G. and Unger H (1976) Experiments with Water and Hot Melts of Lead. Non-Equilb. Thermodyn., Vol. 1, No. 2, pp. 91-103.
- Fry C. J. and Robinson C. H. (1979) Experimental Observations of Propagating Thermal Interactions in Metal/Water Systems. 4th CSNI Spec. Mtg. on FCI, Bournemouth, UK, 2-5 Apr.
- Fry C. J. and Robinson C. H. (Jan. 1980a) Propagating Thermal Interactions Between Molten Aluminum and Water, AEEW-R1309, AEE Winfrith.
- Fry C. J. and Robinson C. H. (May 1980b) Results from Selected Experiments Performed in the THERMIR Facility at AEE Winfrith, AEEW M-1778, AEE Winfrith.
- Gettle T. J. (May 15, 1962) Apparatus and Method of Operating a Chemical Recovery Furnace. U.S. pat. 3, 122,421 (Feb. 25, 1964); Can. pat. 641, 338.
- Goldammer H. and Kottowski H. (April 1975) Calculation Model and Code Fuel Coolant Interaction. Working paper for the <u>CSNI Mtg. on "Calculations Models"</u> 28/29.
- Goldammer H.and Kottowski H. (1976) Physical Model and Calculation Code for Fuel Coolant Interactions. PNC N251, 76-12, 2, pp. 839-875.
- Goldammer H. and Kottowski (1976) Theoretical Experiments Investigations of FCI in a Shock Tube Configuration. ANS/ENS, Chicago Conference.
- Goldammer H. and Mehr K. (1977) Final Report on the KAMINA-CODE. BTWB, D-7070, Schwab, Gmund, Under Contract Nr. 737-77-08 SISPP.
- Goldammer H. and Mehr K. (1980) SAMI, a Physical Model and Computer Code for FCI in a LMFBR Subassembly. Nuclear Science and Technology, Ispra, EUR 6635 EN.
- Goldammer H. (1980) Investigations of a Nonuniform Temperature Distribution in the Reactor Mixture of a Thermal Detonation, Final Report, B.T.W.B. Bureau for Technical Advice, P.O. 1303, D-7070, Schwab. Gmund.
- Guest J. N., Turner R. G. and Rees N.J.M. (Jan. 1974) Al/Water Shock Tube Experiments at AWRE Fourness Since January 1972, U.K.A.E.A. Report No. FDR-1-74.
- Gunnerson F. S. and Cronenberg A. W. (1975) A Prediction of the Inert Gas Solubilities in Stoichiometric Molten UO_2 . <u>J. Nuc. Materials</u>, Vol. 58, pp. 311-320.
- Gunnerson F. S. and Cronenberg A. W. (Aug. 1980) Film Boiling and Vapor Explosion Phenomena. Nuclear Technology, Vol. 49, pp. 380-391.

- Gunther F. C. (1951) Photographic Study of Surface Boiling Heat Transfer to Water with Forced Convection. Trans. ASME, Vol. 73, pp. 115-123.
- Hall A. N. (Feb. 1985) A Thermodynamic Model of Energetic Molten Fuel-Coolant Interactions. United Kingdom Atomic Energy Authority Safety and Reliability Diretorate, SRD M 238.
- Hall R. W. and Board S. J. <u>Propagation of Thermal Explosions</u>, Part 3: An Extended Model of <u>Thermal Detonations</u>, Central Electricity Generating Board, Report No. (Dec. 1977).
- Hall R. W. and Board S. J. (1979) The Propagation of Large Scale Thermal Explosions. Int. J. Heat and Mass Transfer, Vol. 22, pp. 1083-1093, Pergamon Press Ltd.
- Hall R. W., Board S. J. and Baines M. (1979) Observations of Tin/Water Thermal Explosions in a Long Tube Geometry: Their Interpretations and Consequences for the Detonation Model. 4th CSNI Spec. Mtg. on FCI, Bournemouth, UK, 2-5 April.
- Hall W. B. (1977) Bubble Growth with Acoustic Loading. Presented at OECD CSNI Mtg., ANL, Argonne, ILL, 8-9 Dec.
- N. A. Halliwell and Pottinger R. C. (1975) Thermal Interaction Experiments with $\rm UO_2$ and Sodium Using Pyrotechnic Heating. Nuc. Engr. Design, Vol. 32, pp. 311-324.
- Harlow F. H. and Ruppel H. M. (Aug. 1981) <u>Propagation of a Liquid-Liquid Explosion</u>. Los Alamos National Laboratory Report, LA-8971-MS, UC-34.
- Henry R. E. et al. (1973) An Experimental Study of Large-Scale Vapor Explosions, <u>Trans. Am. Nuc. Soc.</u>, 17.
- R. E. Henry et al. (April 1974) Large Scale Vapour Explosion. Fast Reactor Safety Mtg., Beverly Hills, CA CONF-740401-PA, pp. 922-934.
- Henry R. E. and Fauske H. K. (1975) Energetics of Vapor Explosions. <u>AICHE-ASME Heat Transfer Conf.</u>, San Francisco, CA, 11-13 Aug.
- Henry R. E., Fauske H. K. and McUmber L. M. (Oct. 1976a) Vapour Explosions and Simulant Fluids. CONF-761001, ANS/ENS, Fast Reactor Safety Mtg., Chicago.
- Henry R. E. et al. (Oct. 1976b) Experiments on Pressure Drive Fuel Compaction with Reactor Materials. CONF-761001, ANS/ENS Mtg. on Fast Reactor Safety, Chicago.
- Henry, R. E. and Fauske H. K. (March 1976c) Nucleation Characteristics in Physical Explosions. Third Specialist Meeting on Sodium-Fuel Interactions in Fast Reactor, Tokyo, Japan.
- Henry. R. E. and Fauske H. K. (May 1979) Nucleation Processes in Large-Scale Vapor Explosions. J. Heat Transfer, Vol. 101, May, pp. 280-287.
- Henry R. E., Hohmann H. and Kottowski H. (1979) The Effects of Pressure on Nacl-H₂O Explosions, <u>4th CSNI Spec. Mtg. on FCI in Nucl. Reactor Safety</u>, Bournemouth, UK, 2-5 April.
- Henry R. E. and Fauske H. K. (1981) Core Melt Progression and the Attainment of a Permanently Coolable State. Proc. Reactor Safety Aspects of Fuel Behavior, Sun Valley, ID, Vol. 2, p. 481, 2-6 Aug.
- Henry R. E. and Fauske H. K. (1981) Required Initial Conditions for Energetic Steam Explosions. ASME_HTD-V19, Washington, DC.
- Hess P. D. and Brondyke K. J. (April 1969) Causes of Molten Aluminum Water Explosions and Their Prevention. Metal Progress, Vol. 95, No. 4, pp. 93-100.
- Hess P. D. et al. (1980) Molten Aluminum/Water Explosions. Light Metals, (C. McMinn Ed.), pp. 387, Proc. of Tech. Sessions Sponsored by TMS Light Metals Comittee at 190th AINE Annual Mtg.
- Hicks E. P. and Menzies D. C. (October 1965) Theoretical Study on the Fast Reactor Maximum Accidents. Proc. of the Conf. on Safety, Fuels, and Core Design in Large Fast Power Reactors, Argonne National Laboratory, Report ANL-7120, 654.
- Higgins H. M. (April 1955) A Study of the Reaction of Metals and Water. USAEC Report No. AECD-3664.

Hillary J. J., Curry P. and Taylor L. R. (1972) Preliminary Experimental Studies of the Interaction of Water with Molten Lead and Molten Salt Mixtures. Proceedings of the International Conference on Engineering of Fast Reactor for Safe and Reliable Operation, Karlsruhe, pp. 852-869.

Hinze J. O. (1948) Critical Speeds and Sizes of Liquid Globules. Appl. Sci. Res. Vol. Al, pp. 273-288.

Hinze J. O. (1948) Forced Deformations of Viscous Liquid Globules. Appl. Sci. Res. Vol. Al, pp. 263-272.

Hohmann H. et al. (1982) Experimental Investigation of Spontaneous and Triggered Vapour Explosions in the Molten Salt/Water System. <u>Int. Mtg. on Thermal Reactor Reactor Safety</u>, Chicago, Aug. 29 - Sept. 2.

Holtbecker H. et al. CREST Mtg. on Fuel-Sodium Interaction at Grenoble.

Holtbecker H. et al. (1973) Results of Thermal Interaction Tests for Various Materials Performed in the Ispra Tank Facility. Proc. of the Second Spec. Mtg. on Sodium-Fuel Interaction in Fast Reactors, Ispra, Italy, 21-23 Nov.

Holtbecker H. et al. (1974) EUR/C-15/733/74.d.

Hoskin N. E. and Morgan K. (Oct. 1972) Studies of Pressure Generation by Water Impact Upon Molten Aluminum With Reference To Fast Reactor Sub-Assembly Accidents. Proc. of Int. Conf. on Eng. of Fast Reactors for Safe and Reliable Operations, Karlsruhe, pp. 870-883.

Hsiao K. H., Cox J. E., Hedgecoxe P. G. and Witte L. C. (1972) Pressurization of a Solidifying Sphere. J. Appl. Mech., Vol. 72, pp. 71-77.

Ivins R. O. (1967) Interactions of Fuel, Cladding and Coolant. ANL-7399, pp. 162.

Ivins R. O. (1969a) Steam Explosion Experiments. ANL-7581, pp. 132.

Ivins R. O. (1969b) Pressure Generation Due to Particle-Water Energy Transfer. ANL-7553, pp. 118-120.

Jackson K. A. and Chalmers B. (1951) Kinetics of Solidifications. Can. J. Phys., Vol. 34, pp. 473-490.

Jacobs H. and Thurnay K. (Oct. 1972) The Calculation of the Pressure History and the Production of Kinetic Energy during a Fuel-Sodium-Interaction by Solving the Exact Thermodynamic Equations. Proc. Conf. Eng. Fast Reactors for Safe and Reliable Operation, Karlsruhe.

Jacobs H. (1975) Prediction of the Pressure Time History due to Fuel Sodium Interaction in a Subassembly. 3rd Int. Conf. Structural Mechanics in Reactor Technology, London.

Jacobs H. (1976) Computational Analysis of Fuel-Sodium Interactions with an Improved Method. CONF-761001, Vol. 3, pp. 926-935, $\underline{Proc.\ Int.\ Mtg.\ on\ Fast\ Reactor\ Safety\ and\ Related\ Physics}$, Chicago, 5-8 Oct.

Jouguet E. (1907) Compt. Rend. 132, 573 (190); 144,415.

Judd A. M. (1970) Calculation of the Thermodynamic Efficiency of Molten-Fuel-Coolant Interactions. <u>Trans. Am. Nuc. Soc.</u>, Vol 13, 369-370.

Judd A. M. (March 1980) The Upper Limit to the Work Done by an MFCI. NII/R/19/79.

Katz D. L. and Spiepcevich (Nov. 1971) LNG/Water Explosions: Cause and Effect. Hydrocarbon, Processing, pp. 240-244.

- Kazimi M. S. (1973) Theoretical Studies of Some Aspects of Molten Fuel-Coolant Thermal Interactions. Science Doctorate Thesis, MIT, Cambridge, MA.
- Kim B. (1985) Heat Transfer and Fluid Flow Aspects of Small-Scale Single Droplet Fuel-Coolant Interactions. PhD Thesis, University of Wisconsin-Madison.
- Kim B. and Corradini M. L. (1984) Recent Film Boiling Calculations: Implication on Fuel-Coolant Interactions. <u>Fifth Int. Meeting on Thermal Nuclear Reactor Safety</u>, Karlsruhe, W. Germany, Vol. 2, pp. 1098-1107.
- Knapp R. B. and Todreas N. E. (1975) Thermal Stress Initiated Fracture as a Fragmentation Mechanism in UO₂-Na Fuel-Coolant Interaction. <u>Nuc. Eng. Design</u>, Vol. 35, pp. 69-76.
- Kondo S., Togo Y. and Iwamura T. (1976) A Simulation Experiment and Analysis on the Effects of Incoherence in Fuel Coolant Interaction. PNC N251, 76-12, 285-305.
- Koopman R. P. et al. (August 1981) Description and Analysis of Burro Series $40-m^3$ LNG Spill Experiments. UCRL-53186.
- Koopman R. P. et al. (1982) Analysis of Burro Series of $40-m^3$ LNG Spill Experiments. <u>J. Hazardous Materials</u>, 6, 43-83.
- Kottowski, H. M., Mol M., Grossi G. and Hohmann H. (Sept. 1979) Experimental Study of the Thermal Interaction Between Molten Reactor Material and Water (Determination of Mechanical Work During a Vapor Explosion). Technical Note No. 1.06.01.79.102, Published by the Commission of European Communities, Joint Research Facility Ispra.
- Krause H. H., Simon R. and Levy A. (Jan. 1973) <u>Final Report on Smelt-Water Explosions to Fourdrinier Kraft bnoard Institute, Inc.</u>, Battelle Columbus Laboratories.
- Ladish R. (1977) Comment on Fragmentation of ${\rm UO}_2$ by Thermal Stress and Pressurization. Nuc. Eng. Design, Vol. 43, pp. 327-328.
- Lawrence R. J. and Mason D. S. (1975) WONDY-IV, A Computer Program for One Dimensional Wave Propagation with Rezoning. SC-RR-710284, Sandia National Laboratory.
- Lazarrus J., Navarre, J. P. and Kottowski H. M. (Nov. 1973) Thermal Interaction Experiments in a Channel Geometry Using Al_2O_3 and Na. Proceedings of Second CSNI Specialist Meeting on Na/Fuel Interactions in Fast Reactors, Ispra, Italy.
- Lemon A. W. (1980) Explosions of Molten Aluminum and Water. Light Metals, (C. McMinn, Ed.), pp. 817, Proc. of Technical Session Sponsored by TMS Light Metals Committee at 190th AIME Annual Meeting.
- Levine H. S. (1971) On the Initiation Mechanism for Explosion During Combustion of Metal Droplet. High Temperature Science, Vol. 3, pp. 237-243.
- Liimatainen R. C. (1964) Study of Magnesium-Water Reaction. ANL-6800, pp. 342-346.
- Long G. (May 1957) Explosions of Molten Aluminum in Water-Cause and Prevention. Metal Progress, Vol. 71, pp. 107-112.
- Ludwig R. M. (May 1980) Report to the API Recovery Boiler Research Subcommittee Mtg., Chicago.
- Martini M. et al (1972) Studies of Preliminary Out-of-Pile Tests Related to Sodium-Fuel Interaction. CREST Spec. Mtg. on SFI, Grenoble.
- Martini M. et al (Nov. 1973) Out-of-Pile Tests on UO₂-Pins. CREST Second Specialist Meeting on Sodium/Fuel Interaction in Fast Reactor, Ispra, Italy.
- McCracken G. M. (1973) Investigations of Explosions Produced by Dropping Liquid Metals into Acqueus Solutions. The Safety Research Bulletin of the Safety and Reliability Directorate, Issue No. 11, UKAEA, SRD/C3/72.
- McRae T. G. (May 1983) Large-Scale Rapid Phase Transition Explosions, UCRL-88683.
- McRae T. G. et al. (1984) Effects of Large- Scale LNG/Water RPT Explosions. ASME Winter Mtg., New Orleans, Louisiana (9-13 Dec.).

Meyer J. F. et al. (1981) Preliminary Assessment of Core Melt Accidents at the Zion and Indian Point Nuclear Power Plants and Strategies for Mitigating Their Effects, Appendix B. NUREG-0850, Vol. 1.

Myer, R. T. and Nelson L. S. (1970). The Role of Nitrogen in the Formation of Micro-bubbles During the Explosive Combustions of Zirconium Droplets in N_2/O_2 Mixtures. High Temperature Science, Vol. 2, pp. 35-57.

Miller R. et al. (June 1964) Report of the SPERT I Destructive Test Program. USAEC Report No. IDO-16883.

Mitchell D. E., Corradini M. L. and Tarbell W. W. (1981) Intermediate Scale Steam Explosion Phenomena: Experiments and Analysis. SAND81-0124, Sandia National Laboratory.

Mitchell D. E. and Evans N. A. (August 1982) The Effect of Water to Fuel Mass Ratio and Geometry on the Behavior of Molten Core-Coolant Interaction at Intermediate Scale. Proc. Int. Mtg. Thermal Nuclear Reactor Safety, Chicago, IL, NUREG/CP-0027.

Mitchell D. E. and Evans N. A. (Feb. 1986) Steam Explosion Experiments at Intermediate Scale: FITSB Series. SAND83-1057, Sandia National Laboratories.

Mizuta H. (June 1973) Notes for Second CREST Sodium Fuel Interaction Mtg. on Comparison of Theoretical Calculation Models, Paris.

Mizuta H. (1974) Fragmentation of UraniumDioxide after Molten UO₂-Na Interaction. <u>Nuc. Sci. Technology</u>, Vol. 11, pp. 480-487.

Morgan K. (1973) TOPAL - A Computer Code for Investigating Metal-Liquid Thermal Interactions in Shock Tube Geometry. Part 1: Theoretical Description. UKARA Report, TRG 24599(R/X).

Mosinger H. (1980) Numerical Experiment on Shock Wave Induced Drop Fragmentation. <u>Nuc. Eng.</u> and Des., 61, pp. 257-264.

Nakanishi E. and Reid R. C. (1971) Liquid Nitrogen Gas-Water Reactions. Chem. Eng. Progress, Vol. 67, No. 12, pp. 36-41.

Nelson H. W. and Norton C. L. (June 3, 1969) Method of Preventing Smelt-Water Explosions. U.S. pat. 3, 447, 895.

Nelson H. W. (Oct. 26, 1971) Preventing Physical Explosions due to the Interaction of Liquid Water and Molten Chemical Compounds. U.S. pat. 3, 615, 175.

Nelson, H. W. (March 1973) A New Theory to Explain Physical Explosions. Presented at Black Liquor Recovery Boiler Advisory Committee Mtg., Atlanta, Georgia (Oct. 11, 1972, Tappi 56(3):121-5.

Nelson L. S. (1965) Explosion of Burning Zirconium Droplets Caused by Nitrogen. <u>Science</u> Vol. 148, pp. 1594-1595.

Nelson L. S. and Buxton L. D. (1977) The Thermal Interactions of Molten LWR Core Materials with Water. Trans. Am. Nuc. Soc., Vol. 26, pp. 397.

Nelson L. S. and Buxton L. D. (1978) Steam Explosion Triggering Phenomena: Stainless Steel and Corium-E Simultants Studies with a Floodable ARC Melting Apparatus. SAND77-0998, NUREG/CR-0122, Sandia National Laboratory.

Nelson. L. S. and Duda P. M. (Sept. 1981) Steam Explosion Experiments with Single Drops of Iron Oxide Melted with CO_2 Laser. SAND81-1346, NUREG/CR-2295, Sandia National Laboratory.

Nelson L. S. and Duda P. M. (1984) Steam Explosion Experiments with Single Drops of Iron Oxide Melted with a $\rm CO_2$ Laser; Part 2. Parametric Studies. SAND82-1105, NUREG/CR-2718, Sandia National Laboratory.

Nelson W and Kennedy E. H. (1956) What Causes Kraft Dissolving Tank Explosions. Paper Trade Journal, Vol. 140, No. 29, pp. 50-56; and Vol. 140, No. 30, pp. 30-32.

von Neumann, J. (1942) Theory of Detonation Waves. OSRD Report 549.

Ochiai M. and Bankoff S. G. (1976) Liquid-Liquid Contact in Vapor Explosion. <u>Proc. ANS/ENS Gas</u> Reactor Safety Mtg., Chicago.

Oh M. D. and Corradini (Nov. 1984) Non-Equilibrium Parametric Steam Explosion Model. Trans. Amer. Nuc. Soc., Vol. 47.

Oh M. D. and Corradini M. L. (1985) A Nonequilibrium Model for Large Scale Vapor Explosions. <u>Proc. of the Third International Conference on Reactor Thermal-Hydraulics</u>, Newport, Rhode Island, (15-18 Oct.)

Padilla A. (1970) Transient Analysis of Fuel-Sodium Interaction. Trans. Am. Nucl. Soc., Vol. 13, pp. 375-376.

Page F. M. (1975) Report on Large-Scale Experiments with Molten Metal and Water at I.M.I. Summerfield July/November, 1975. University of Aston Research Report.

Paoli R. M. and Mesler R. B. (1968) Explosion of Molten Lead in Water. <u>Proceedings of Conference on High Speed Photography</u>, Stockholm.

Patel P. D. and Theofanous T. G. (1978) Fragmentation Requirements for Detonating Thermal Explosions. Nature, Vol. 274, pp. 142-144.

Patel P. D. and Theofanous T. G. (1979) Shock Wave Induced Fragmentation in Liq/Liq and Multiphase System. Second Specialist Meeting on FCI, Argonne National Laboratory.

Peckover R.S. (1977) Optimum Hicks-Menzies Calculations. CFRSWP/MFCIWG/P(77)/103.

Pilch M. (1981) Acceleration Induced Fragmentation of Liquid Drops. Ph.D. Thesis, University of Virginia.

Pilch M. and Young M. F. (May 1987) Preliminary 2-D Calculation of FCI Coarse Mixing, Trigger and Propagation IFCI. Proc. of Severe Fuel Damage Partners Mtg..

Plesset M. S. (1954) On the Stability of Fluid Flow with Spherical Symmetry. <u>J. Appl. Phys.</u>, Vol. 25, pp. 96-98.

Plesset M. S. and Chapman (1971) Collapse of an Initially Spherical Vapor Cavity in the Neighborhood of a Solid Boundary. J. Fluid Mech., Vol. 47, pp. 283-290.

Porteous W. M. and Blander M. (1975) Limits of Superheat and Explosive Boiling of Light Hydrocarbons, Halocarbons, and Hydrocarbon Mixtures. AICHE J., 21, 560.

Porteous W. M. and Reid R. C. (1976) Light Hydrocarbon Vapor Explosions. Che. Eng. Prog. 72(5), 83.

Pottinger R. C., Rees N.J.M. and Turner R. G. (1972) The Thermal Interaction Between Molten Alumina and Liquid Sodium. <u>Proc. of the International Conf. on Eng. of Fast Reactors for Safe and Reliable Operation</u>, Karlsruhe, pp. 839-851, 9-13 Oct.

Puig Szeless (Jan. 1972) CREST Spec. Mtg. on Fuel-Sodium Interaction at Grenoble.

Pugh V. T. and Vaughan G. J. (1975) Hicks-Menzies Calculations. RS-75-N41.

Putten, A. et al. (1976) Interactions on Fuel-Coolant Interaction with the RCN Code. PNC N252, 76-12, 2, pp. 751-783.

Raj P. K., Hagopian J. and Kalelkar A. S. (March 1974) <u>Predictions of Hazards of Spills of Anhydrous Ammonia on Water.</u> Prepared for U.S. Coast Guard, Dept. of Transportation Contract, Report No. AD-779-400.

Reactor Safety Study, WASH-1400, Nuclear Regulatory Commission Report, NUREG-75/0114, Oct. 1975.

Reinecke W. G. and Waldman G. D. (1970) Investigation of Water Drop Disintegration in a Region Behind Strong Shock Waves. <u>Third International Conference on Rain Erosion and Related Phenomena</u>, Hampshire, England.

Robert K. V. (Jan. 1972) Theoretical Calculations of Fuel-Coolant Interactions. CREST Specialist Meeting on Sodium/Fuel Interactions, Grenoble, France.

Rogers C. E., Markant H. P. and Dluehosh H. N. (Feb. 1961) Interactions of Smelt and Water. Tappi 44(2): 146-51.

Sallack J. A. (1955) An Investigation of Explosions in the Soda Smelt Dissolving Operations. Pulp and Paper Magazine of Canada, Vol. 56, pp. 114-118.

Sawata T. et al. (1976) A Parametric Study on Reactor Containment Response to Fuel-Sodium Interaction. PNC N251, 76-12, 2, pp. 681-732.

Schins H. (1973) The Consistent Boiling Model for Fragmentation in Mild Thermal Interaction-Boundary Conditions. Second Specialist Meeting on Fuel/Na Interactions in Fast Reactor, Ispra, pp. 251-269.

Schriewer J., Benz R. and Unger H. (1979) Hydrodynamic Analysis of Shock-Wave Induced Fragmentation in Liquid-Liquid Systems. Fourth CSNI Specialist Meeting on FCI in Nuclear Reactor Safety, Bournmouth, UK.

Schmann U. (Aug. 1982) Steam Explosion - Physical Foundations and Relation to Nuclear Reactor Safety. Karlsruhe Nuclear Research Center Report.

Schwalbe W., Burger M. and Unger H. (1981) Investigations on Shock Waves in Large Scale Vapor Explosions. ASME Winter Annual Mtg., Washington, D. C. 15-20 Nov.

Schwalbe W. (1982) Theoretical Analysis of Thermal Melt-Coolant Reaction Between Large Masses of Melt and Water. Dissertation, Univ. of Stuttgart, Institute for Nuclear Energy and Energy System, Report IKE 2-56.

Seebold O. P. (April 1985) Hicks-Menzies Computer Code. Sandia National Laboratories Memorandum.

Segev A. and Henry R. E. (1978) Thermal and Hydrodynamic Interactions in Shock Tube Configurations. ASME Winter Mtg., San Francisco, CA.

Segev A., Henry R. E. and Bankoff S. G. (1979) Fuel-Coolant Interactions in a Shock-Tube Geometry. Nuclear Technology, Vol. 46, pp. 482-492.

Sharon A. and Bañkoff S. G. (1978a) Propagation of Shock Waves Through a Fuel/Coolant Mixture Part 1: Boundary Layer Stripping. Topics in Two-Phase Heat Transfer and Flow, ASME, pp. 51-68.

Sharon A. and Bankoff S. G. (1978b) Propagation of Shock Waves Through a Fuel/Coolant Mixture Part 2: Taylor Instability. Topics in Two-Phase Heat Transfer and Flow, ASME, pp. 69-76.

Sharon A. and Bankoff S. G. (1981) On the Existence of Steady Supercritical Plane Thermal Detonations. Int. J. Heat Mass Transfer, Vol. 24, No. 10, pp. 1561-1572.

Shick P E. (1976) Personal Communications to Howard S. Gardner, May 6; June 4, 14; July 27; and Aug. 2.

Shick P. E. (Oct. 30, 1980) Concentration-Gradient Trigger Mechanism for Smelt-Water Explosions. Presented at the American Paper Institute Annual Recovery Boiler Committee Mtg. in Chicago.

Shick P. E. and Grace T. M. (Jan. 1982) Review of Smelt-Water Explosions. Project 3473-2, The Institute of Paper Chemistry, Appleton, Wisconsin.

Simpkins P. G. and Bales E. L. (1972) Water-Drop Response to Sudden Acceleration. <u>J. Fluid Mech.</u>, Vol. 55, pp. 629-639.

Smith L. L. (1979) The SIMMER-II Code and Its Applications. Proc. of the Int. Mtg. on Fast Reactor Safety Technology, Seattle, Washington, 12-23 Aug.

Spalding D. B. (1981) A General Purpose Computer Program for Multidimensional One and Two-Phase Flow. J. Mathematics and Computers in Simulation, North Holland Press, 23, 267-276.

Spies T. P. and Fauske H. K. (1973) $U0_2/Na$ Interactions - Recent In- and Out-of-Pile Experiments in the US and Their Interpretation for Fast Reactor Safety Analysis. Proc. of the Second Specialist Meeting on Sodium/Fuel Interaction in Fast Reactor, Ispra, 21-23 Nov.

Spencer B. W. and McUmber L. et al. (1984) Results of Scoping Tests on Corium-Water Thermal Interactions in Ex Vessel Geometry.

Steam Explosion Review Group (Feb. 1985) A Review of Current Understanding of the Potential for Containment Failure Arising from In-Vessel Steam Explosions. Nuclear Regulatory Commission Report, NUREG-1116.

Stevens J. W. and Witte L. C. (1971) Transient Film and Transition Boiling from a Sphere. <u>Int.</u> J. Heat Mass Transfer, Vol. 14, pp. 443-450.

Stevens J. W. and Witte L. C. (1973) Destabilization of Vapor Film Boiling Around Spheres. Int. J. Heat Mass <u>Transfer</u>, Vol. 16, pp. 669-678.

Suzuki K. et al. (1976) An Analysis of Reactor Structural Response to Fuel Sodium Interaction in a Hypothetical Core Disruptive Accident. PNC N251, 76-12, 2, pp. 651-680.

Swenson D. V. and Corradini M. L. (1981) Monte Carlo Analysis of LWR Steam Explosions. SAND81-1092, NUREG/2039, Sandia National Laboratory.

Swift D. L. and Baker L. Jr. (1965) Experimental Studies of the High-Temperature Interaction of Fuel and Cladding Materials with Liquid Sodium. <u>Proceedings of the Conference on Safety, Fuels, and Core Design in Large Fast Power Reactors</u>, ANL-7120, pp. 839.

Swift D. and Pavlik J. (1966) Fuel-Coolant and Cladding-Coolant Interaction Studies. ANL-7125, pp. 187.

Syrmalenious P. (1973) Modele d'interaction thermique entre bioxgde d'Uranium et sodium. Rep. CEA-R-4432.

Taylor G. I. (1950) The Instability of Liquid Surfaces When Accelerated in a Direction Perpendicular to Their Planes. Proc. Roy. Soc. A.201, pp. 192-196.

Teschendorf V. and Wahba A. B. (1976) Molten Fuel-Coolant Interaction During Hypothetical Accidents in Light Water Reactors. Nucl. Technol., 31, pp. 297-305.

Tetzner H. (June 1959) Slag Explosions in Open-Hearth Steelworks. Neve Hutte, Vol. 4, No. 6, p. 352.

Tezuta M. et al. (1973) Analysis of Fuel Sodium Interaction in a Fast Breeder Reactor. Second Spec. Mtg. on Sodium/Fuel Interaction in Fast Reactors, Ispra, 21-23 Nov.

Theofanous T. G., Satio M. and Efthimiadis T. (1979) The Role of Fragmentation in Fuel Coolant Interactions. Fourth CSNI Specialist Meeting on FCI in Nuclear Reactory Safety, Bournemouth UK.

Theofanous T. G. and Saito M. (1982) An Assessment of Class-9 (Core-Melt) Accidents for PWR Dry Containment Systems. Nuclear Eng. Design, Vol. 66, p. 307.

Theofanous T. G. et al. (1987) Probabilistic Analysis of Alpha-Mode Failure in Light Water Reactors, NUREG-5030 Draft Report.

Turnbull D. (1950) Formation of Crystal Nuclei in Liquids Metals. <u>J. Appl. Phy.</u>, Vol. 21, pp. 1022-1028.

Vaughan G. J., Caldarola L. and Todreas N. E. (1976) A Model for Fuel Fragmentation During Molten Fuel/Coolant Thermal Interactions. <u>Proc. ANS/ENS Fast Reac. Safety Mtg.</u>, Chicago, IL.

Vaughan G. J., Lawrence P. M. and Pugh V. T. (1976) ARES, RS/76/N13.

Vaughan G. J. (1977) Analytic Approximation to the Hicks/Menzies Calculation. NST/77/20.

Vaughan G. J. (1979) Some Theoretical Considerations Concerning Molten Fuel Coolant Interaction Debris Size. Fourth Specialist Meeting on FCI in Nuclear Reactor Safety, Bournemouth, UK.

Volmer M. (1945) Kinetik der Phasenbildung, Edwards Bro., Ann Arbor.

Walford F. J. (1969) Transient Heat Transfer from a Hot Nickel Sphere Moving Through Water. Int. J. Heat Mass Transfer, Vol. 12, pp. 1621-1625.

Wallis G. (1981) One-Dimensional Two-Phase Flow, McGraw-Hill Book Company, Inc., New York.

Welser V. C. (1931) Zum Zerfalleines Flossigkeitsstrahles. Z.A.M.M. Vol. 11, p. 136.

Williams D. C. (Oct. 1976) A Critique of the Board-Hall Model for Thermal Detonations in UO₂-Na Systems. Proc. of Amer. Nucl. Soc. Conf. on Fast Reactor Safety, Chicago, IL.

Windquist S. (1986) A Theoretical Model for Steady-State Jet Breakup. M.S. Thesis, University of Wisconsin.

Witte L. C., Cox J. E., Gelabert A. A. and Vyas T. J. (1971) Rapid Quenching of Molten Metals., Univ. Houston Report, ORO-3936-6.

Witte L. C., Vyas T. J. and Gelabert A. A. (1973) Heat Transfer and Fragmentation during Molten Metal/Water Interactions. J. Heat Transfer, Vol. 95, pp. 521-527.

Wright R. W. and Humberstone G. H. (1966) Dispersal and Pressure Generation by Water Impact upon Molten Aluminum. Trans. Am. Nuc. Soc., Vol. 9, No. 1, pp. 305-306.

Yayanos A. A. (April 1970) Equation of State for P-V Isotherms of Water and NaCl Solutions. J. Appl. Physics, 41(5): 2259.

Young M. F. (July 1982) The TEXAS Code for Fuel-Coolant Interaction Analysis. Proc. ANS/ENS Fast Reactor Safety Conference, Lyon, France.

Young, M. (Sept. 1987) IFCI: An Integrated Code for Calculation of AII Phases of FCI, NURE6/CR-5084, SAND87-1048, Sandia National Laboratories.

Zion Probabilistic Safety Study, Commonwealth Edison Co. (December 1980).

Zion/Indian Point Study, NUREG-1016, USNRC (1980).

Zyszkowski W. (1973) On the Mechanism of Heat Transfer at a Strong Accidents in Reactor Core. Reactor Heat Transfer, $\frac{\text{Proc. Int. Mtg.}}{\text{New Mechanism}}$, Karlsruhe, pp. 962, 9-11 Oct.

Zyszkowski W. (1975a) Results of Measurements of Thermal Interaction Between Molten Metal and Water. KfK 2193, Karlsruhe, W. German.

Zyszkowski W. (1975b) Thermal Interaction of Molten Copper with Water. <u>Int J. Heat Mass Transfer</u>, Vol. 18, pp. 271-287.

Zyszkowski W. (1976) On the Transplosion Phenomenon and the Leidenfrost Temperature for the Molten Copper-Water Thermal Interaction. <u>Int. J. Heat Mass Transfer</u>, Vol. 19, pp. 625-633.

Zyszkowski W. (1977) Experimental Investigation of Fuel-Coolant Interaction. Nuclear Technology, Vol. 33, pp. 40-50.